The Identification Of A Novel Mechanism By Which Vincristine Sulphate Causes Painful Peripheral Neuropathy

Old, Liz; Old, Elizabeth

Awarding institution:
King's College London

Title: The Identification Of A Novel Mechanism By Which Vincristine Sulphate Causes Painful Peripheral Neuropathy

Author: Elizabeth Old

The Identification Of A Novel Mechanism By Which Vincristine Sulphate Causes Painful Peripheral Neuropathy

Elizabeth Amy Old

Thesis presented for the degree of

Doctor of Philosophy

at King's College London

Wolfson Centre for Age Related Diseases

King's College London

2013

Abstract

An estimated thirteen million new cancers are diagnosed every year and in many cases patients will be treated with chemotherapeutic agents, either with curative intent or to prolong life and alleviate symptoms. Historically the dose limiting side-effect of these compounds was immune- and myelosupression, however, as our ability to manage these has improved, a secondary dose-limiting side-effect of these compounds has been revealed: neurotoxicity.

Several anti-neoplastics, including the vinca alkaloids, cause a distal, bilateral and symmetrical painful peripheral neuropathy primarily affecting the longest neurons of the extremities. The key symptom of this condition is pain, yet current therapies are ineffective in alleviating this; the average patient rates their pain as a seven out of ten in severity and pain results cessation of treatment in up to 40% of patients.

One of the main pitfalls in the development of analgesics for this condition is that little is understood about the mechanism by which chemotherapy causes neuropathy. Thus, I have aimed to delineate a novel pathway of the mechanism by which vincristine sulphate (VCR) induces painful peripheral neuropathy.

The pathway delineated is based on the observation that there is significant monocyte-macrophage infiltration of the peripheral nerves following VCR administration, in a temporal profile similar to that of the onset of mechanical allodynia (a painful response to normally innocuous stimuli) in the mouse, and that depletion of monocyte/macrophages prior to VCR administration attenuates allodynia. Whilst this depletion is not a viable therapeutic option for

patients, it has led us to investigate of the contribution to the development of pain of the CX_3CR1 receptor, the level of expression of which is the defining characteristic of monocyte/macrophages.

We have established that CX_3CR1 plays a critical role in the development of VCR-neuropathy; mice devoid of CX_3CR1 exhibit a delay in the onset of allodynia and a reduction in VCR-induced nerve infiltration of CX_3CR1^+ monocyte/macrophages. We have demonstrated that this infiltration is likely a result of up-regulation of monocyte adhesion molecules on the endothelial cells lining blood vessels. Furthermore, we suggest that at the blood-nerve interface CX_3CR1^+ monocytes/macrophages are activated by CX_3CL1, endogenously expressed on endothelial cells, promoting the production of reactive oxygen species, which subsequently activate the TRPA1 receptor on sensory neurons.

This work has led to the conclusion that CX_3CR1 antagonists constitute new peripheral targets for the prophylactic treatment of chemotherapy induced painful peripheral neuropathy.

Acknowledgements

First and foremost I'd like to that my primary supervisor, Dr. Marzia Malcangio; without her continued support, enthusiasm and encouragement I would not be here today. I'd also like to thank Dr. Adrian Mogg, my secondary supervisor, and all of the people at Eli-Lilly, especially Dr. Many Sher, that have made it possible for me to complete this PhD.

In addition my sincerest thanks go to Dr. Suchita Nadkarni at the William Harvey Institute who completed the FACS (figure 3.15, 3.16, 3.18, 4.14, 4.15) and ROS production experiments (figure 4.16) for me and to Professor Mauro Perretti for his infinite wisdom of all things immune related!

I must thank several Wolfson CARD members, past and present; Amelia Staniland for teaching me all she knew about mouse behaviour, Clive Gentry for performing a set of intrathecal injections for me (figures 2.13/2.14) and for assessing cold sensitivity in two cohorts of mice (figure 2.6/4.18), John Grist for his excellent perfusions skills and Tom Pitcher for his extra pair of hands when I had more mice than I could cope with and for performing an assessment of mechanical allodynia in the LHVS treated mice (figure 4.5). A huge thank you to Anna Clark for teaching me everything I know in the lab and for her continued and treasured friendship, and to Andrea Ogbonna and Louise Nicol, without whom perfusion parties just wouldn't have been the same. My undying gratitude goes to Viv Cheah and Caroline Abel, whose administrative skills and friendships have held me together for the last four year, to Amanda Ellis, co-creator of windowsill tea, whom I can no longer imagine not having in my life (Amanda that is, not just the tea) and to Lisa Griffiths, who four years down the line is still suggesting soup for lunch. I'd also like to thank all of those who have worked

in the Wolfson during my time here, there are too many of you to name but you have completing this PhD a wonderful experience, I wouldn't change it for the world!

Outside of the lab there are some very important people that I must thank, as without them I wouldn't be sat here; my mum, who is my rock and should be awarded her own PhD for all she has invested in me and this work, and my dad, who is the strongest person I know and has taught me never to give up. I hope I have done you both proud. Thank you to my baby brother Rob for all the times he has listened to be ramble on about random science-y things; I hope my experience has inspired you to take up a career in science rather than caused you to run away screaming. Thank you to Evan for his friendship and support over many years and for putting up with me as his flatmate for a second time; I would have thought he had learnt his lesson the first time around, but he proved me wrong. Thank you to Laura (wifey) for dealing with all my tired and emotional craziness while I've been writing, and to all of the MSC gang, especially Lewis, Alex, Gee, Josh, Sarah, Gary and Jordan for making me laugh when I needed it more than ever, and for providing a much needed distraction.

Table of Contents

List of Figures, Tables and Diagrams

Chapter 1:

Chapter 2:

Chapter 3:

Chapter 4:

Chapter 5:

List of Abbreviations

5HT	5-Hydroxytryptamine
ADAM	A Disintegrin and Metalloprotease Domain
AITC	Allyl Isothiocyanate
ALC	Acetyl-L-Carnitine
ALL	Acute Lymphoblastic Leukaemia
ALS	Amyotrophic Lateral Sclerosis
AMPA	α-Amino-3-Hydroxy-5-Methyl-4-Isoxazolepropionic Acid
ANOVA	Analysis of Variance
AP-2	Adaptor Protein-2
Asp	Asparagine
ASPA	Animals Scientific Procedures Act
ATF-3	Activating Transcription Factor-3
ATP	Adenosine Triphosphate
AUC	Area Under Curve
BBB	Blood Brain Barrier
BDNF	Brain Derived Neurotrophic Factor
BNB	Blood Nerve Barrier
bp	Base Pair
BRET	Bioluminescence Resonance Energy Transfer
BSA	Bovine Serum Albumin
Ca^{2+}	Calcium Ion
CatS	Cathepsin S
CCI	Chronic Constriction Injury
CCR2	C-C Chemokine Receptor 2
CFA	Complete Freud's Adjuvant
CHO	Chinese Hamster Ovary
Cl^-	Chloride Ion
Cl_2BMP	Dichloromethylene-bisphosphonate
CNS	Central Nervous System

COPD	Chronic Obstructive Pulmonary Disease
CREB	cAMP Response Element-Binding Protein
CSF1	Colony Stimulating Factor-1
CVM	Caudal Venterolateral Medulla
Cx	Connexin
Cys	Cysteine
CX_3CL1	CX_3C Chemokine Ligand 1
CX_3CR1	CX_3C Chemokine Receptor 1
DNA	Deoxyribonucleic Acid
dNTP	Deoxyribonucleic Triphosphate
DRG	Dorsal Root Ganglia
EAAT	Excitatory Amino Acid Transporter
EDTA	Ethylenediaminetetraacetic Acid
EGF	Epidermal Growth Factor
EPO	Erythropoietin
EPSC	Excitatory Post-Synaptic Current
EPSP	Excitatory Post-Synaptic Potential
ERK	Extracellular Related Kinase
ESL-1	E-Selectin Ligand-1
FBS	Foetal Bovine Serum
FDA	Food and Drug Administration
FKN	Fractalkine
FLC	Fluorocitrate sulphate
G	Gage
GABA	γ-Aminobutyric Acid
GAPDH	Glyceraldehyde 3-Phosphate Dehydrogenase
G-CSF	Granulocyte Colony Stimulating Factor
GFAP	Glial Fibrillary Acidic Protein
GFP	Green Fluorescent Protein
GI	Gastrointestinal
GLAST	Glutamate Aspartate Transporter
Gln	Glutamine

Glu	Glutamic Acid
GM-CSF	Granulocyte Macrophage Colony Stimulating Factor
GPCR	G-Protein Coupled Receptor
HCAEC	Human Coronary Artery Endothelial Cell
HCN	Hyperpolarisation-activated Cyclic Nucleotide-gated
HIV	Human Immunodeficiency Virus
HRP	Horseradish Peroxidase
HSC	Haematopoietic Stem Cell
HUVEC	Human Umbilical Vein Endothelial Cell
IB4	Isolectin B4
Iba1	Ionized Calcium Binding Adaptor Molecule 1
ICAM-1	Intercellular Adhesion Molecule 1
IFN	Interferon
IgG	Immunoglobulin G
IL	Interleukin
IL-1β	Interleukin 1β
IL-1RA	IL-1 Receptor Antagonist
Ile	Isoleucine
i.p.	Intraperitoneal
IP3	Inositiol Triphosphate
IPSP	Inhibitory Post-Synaptic Potentials
i.t.	Intrathecal
JNK	c-Jun N-terminal Kinase
K^+	Potassium Ion
KA	Kainate
kDa	Kilodalton
KO	Knock-Out
L4	Lumbar 4
L5	Lumbar 5
LCL	Liposome Encapsulated Clodronate
LFA-1	Lymphocyte Function-Associated Antigen 1
LHVS	Morpholinurea-leucine-homophenylalanine-vinyl sulfone-phenyl

LIF	Leukaemia Inhibitory Factor
LPS	Lipopolysaccharide
LTP	Long Term Potentiation
Lys	Lysine
Mg^{2+}	Magnesium Ion
MAPK	Mitogen Activated Protein Kinase
M-CSF	Monocyte Colony Stimulating Factor
M-CFU	Macrophage Colony Forming Unit
MCP-1	Monocyte Chemoattractant Protein 1
Met	Methionine
mGluR	Metabotropic Glutamate Receptor
MHC	Major Histocompatability Complex
MIP-1	Macrophage Inflammatory Protein 1
MMP	Matrix Metalloproteinase
mRNA	Messenger Ribonucleic Acid
Na^{+}	Sodium Ion
NADPH	Nicotinamide Adenine Dinucleotide Phosphate
NF200	Neurofilament 200
NFκB	Nuclear Factor κB
NGF	Nerve Growth Factor
NK	Natural Killer Cells
NMDA	N-Methyl-D-Aspartate
NO	Nitric Oxide
OCT	Optimum Temperature Cutting Medium
PAG	Periaqueductal Gray
PBA	Parabrachial Area
PBMC	Peripheral Blood Mononuclear Cell
PBS	Phosphate Buffered Saline
PCR	Polymerase Chain Reaction
PDGF	Platelet-Derived Growth Factor
PECAM-1	Platelet Endothelial Cell Adhesion Molecule 1
pERK	Phosphorylated Extracellular Signal-Related Kinase

pJNK	Phosphorylated c-Jun N-terminal Kinase
PKA	Protein Kinase A
PKC	Protein Kinase C
PLC	Phospholipase C
PMA	Phorbol 12-Myristate 13-Acetate
PNL	Peripheral Nerve Ligation
PNS	Peripheral Nervous System
pP38	Phosphorylated P38
PPAR	Peroxisome Proliferator-Activated Receptor
PSGL-1	P-Selectin Glycoprotein Ligand-1
PTX	Paclitaxel
PVDF	Polyvinylidene Fluoride
PWL	Paw Withdrawal Latency
PWT	Paw Withdrawal Threshold
RCS	Reactive Carbonyl Species
RM	Repeated Measure
RM-ANOVA	Repeated Measure Analysis of Variance
RNA	Ribonucleic Acid
RNS	Reactive Nitrogen Species
ROS	Reactive Oxygen Species
RVM	Rostral Ventromedial Medulla
SAL	Saline
SEM	Standard Error of the Mean
siRNA	Small Interfering Ribonucleic Acid
SNI	Spared Nerve Injury
SNL	Spinal Nerve Ligation
SNRI	Selective Noradrenalin Reuptake Inhibitor
SP	Substance P
SSRI	Selective Serotonin Reuptake Inhibitor
STAT	Signal Transducer and Activator of Transcription
TACE	Tumour Necrosis Factor-α Converting Enzyme
TAM	Tumour Associated Macrophage

TBS	Tris Buffered Saline
TCA	Tricarboxylic Acid Cycle
TGFβ	Transforming Growth Factor Beta
Thr	Threonine
TLR	Toll Like Receptor
TLR4	Toll Like Receptor 4
TNFα	Tumour Necrosis Factor α
TNFR	Tumour Necrosis Factor Receptor
TrkA	Tropomyosin-Related Kinase A
TRP	Transient Receptor Potential
TRPA1	Transient Receptor Potential Ankyrin 1
TRPV1	Transient Receptor Potential Vanilloid 1
Tyr	Tyrosine
U	Units
UDP	Uridine Triphosphate
Val	Valine
VAMP-3	Vesicle-Associated Membrane Protein 3
VBL	Vinblastine Sulphate
VCAM-1	Vascular Cell Adhesion Protein 1
VCR	Vincristine Sulphate
VEGF	Vascular Endothelial Growth Factor
VGSC	Voltage Gated Sodium Channel
WDR	Wide Dynamic Range
WHO	World Health Organisation
WT	Wild-Type

Published Abstracts

Old EA, Mogg A, Malcangio M (2011). Characterization of spinal glial cell activation in vincristine induced neuropathy. Abcam New Frontiers in Persistent Pain. Paris, France May 2011.

Old EA, Mogg A, Malcangio M (2012). The role of CX_3CR1 in the development of vincristine induced peripheral neuropathy. International Association of the Study of Pain, 14^{th} World Congress on Pain. Milan, Italy August 2012.

Published Papers

Old EA & Malcangio M (2012). Chemokine mediated neuron-glia communication and aberrant signalling in neuropathic pain states. Current Opinion in Pharmacology, 12(1): 67-73.

Old EA, Nadkarni S, Grist J, Gentry C, Bevan S, Kim KW, Mogg AJ, Perretti M, Malcangio M (2013). CX_3CR1-expressing monocyte/macrophage orchestrate the development of chemotherapy-induced neuropathic pain. Under revision. JCI.

Chapter 1:

General Introduction

1. Chemotherapy

Every year, worldwide, an estimated thirteen million new cancers are diagnosed; this number is expected to rise to over twenty million by 2030 (Ferlay et al., 2010). Whilst cancer accounts for approximately thirteen percent of deaths world-wide (Ferlay et al., 2010) in many cases, depending on the type and stage of cancer diagnosed, patients can be treated with chemotherapeutic agents, either with curative intent or to prolong life and alleviate symptoms.

1.1. Chemotherapeutic Agents - Classes & Use

Chemotherapy is the use of a standardised regime of the administration one or more cytotoxic anti-neoplastic compounds to kill cancerous cells. A large variety of anti-neoplastics are used in the clinic, either singly or in combination; the selection of a compound is based on type and stage of cancer. However these drugs can be broadly categorised into four main groups based on their mechanism of action: alkylating agents, anti-metabolics, natural compounds and molecular targeted therapies.

1.1.1. Alkylating Agents

Alkylating agents impair cell function by forming covalent bonds with amino, carboxyl, sulfhydryl and phosphate groups in biologically important molecules, for example in DNA, RNA and proteins; guanine is particularly susceptible to this process. Alkylating agents are sub-classified according to their chemical structure and the mechanism by which the covalent bonds form; the compounds generally fall into one of three classes. Nitrogen mustards, such as cyclophosphamide, have highly reactive metabolites that are especially potent in the hematopoietic system. They are used in the

treatment of leukaemias, lung, testicular and bladder cancers. Nitrosourea compounds (e.g. carmustine) are metabolised into highly lipophilic compounds that can pass freely across membranes, making them ideal for treating brain cancers as they cross the blood brain barrier (BBB). Platinum compounds, such as oxaliplatin, are used to treat many gynaecological cancers and act by causing the formation of DNA cross-links that subsequently inhibit DNA, RNA and protein synthesis.

1.1.2. Anti-Metabolic Agents

Anti-metabolic agents are structurally similar to the endogenous precursors or metabolites of DNA and RNA synthesis; thus they act as competitive inhibitors of key enzymes of this process. They are most active during the S-phase of the cell cycle and are most effective against rapidly growing tumours. Anti-metabolites can be sub-categorised into five main groups based on the endogenous metabolite to which they are similar: folate analogues such as methotrexate are used to treat leukaemia, lymphoma and a variety of solid mass cancers. Purine and adenosine analogues including mercaptopurine and pentostatin (respectively) are also used to treat leukaemias. Pyrimidine analogues for example capecitabine are used to treat breast, colorectal and gastro-intestinal (GI) cancers. Finally substituted ureas, such as hydroxyurea, are used to treat head, neck and gynaecological cancers as well as leukaemia and melanoma.

1.1.3. Natural Compounds

“Natural compounds” encompass a large group of compounds isolated or derived from naturally occurring substances, categorized by their origin. These compounds are pre-dominantly, although not exclusively, used to treat leukaemias; the class includes anti-tumour / cytotoxic antibiotics, e.g.

mitoxantrone, anthracyclines and mitomycin, epipodophyllotoxins which inhibit topoisomerase preventing RNA transcription (e.g. etoposide), microtubule agents such as the vinca alkaloids VCR and vinblastine which bind to tubulin and prevent microtubule polymerisation (thus inhibit mitotic spindle formation) and the taxanes (e.g. docetaxel and paclitaxel [PTX]) which stabilise microtubules and block cells in the mitosis phase of the cell cycle.

1.1.4. Molecular Targeted Therapies

The final class of compounds contains drugs referred to as molecular targeted therapies. This class is, in general, the newest and fastest growing class of anti-neoplastics. These compounds are designed to be more specific that many other anti-cancer agents, targeting molecules highly expressed in cancer cells. They are sub-categorized into two groups: monoclonal antibodies and small-molecule targeted therapies.

Monoclonal antibodies are designed to bind to a specific protein expressed by the cancer cell and either cause it to undergo apoptosis or identify the cell as a target for phagocytes. This family of compounds includes alemtuzumab, which recognises the CD52 antigen expressed on B-lymphocytes and is used for the treatment of B-cell lymphocytic leukaemia, and bevacizumab which binds to vascular endothelial growth factor (VEGF), preventing receptor binding and activation which consequently prevents endothelial cells growth and angiogenesis in tumours which secrete high levels of VEGF (e.g. advanced colorectal cancers). Small-molecule targeted therapies are designed to selectively interact with the predominant signalling pathway in a given cancer; for example imatinib inhibits Bcl-Abl tyrosine kinase present in most cases of myelogenous leukaemia, whilst gefitinib, used for the treatment of non-small cell lung carcinoma, binds to the

ATP-binding site of the EGF receptor, blocking its kinase activity which is associated with cell proliferation and angiogenesis.

1.2. Side-Effects and Their Management

Whilst the type and severity of side-effects occurring as a result of chemotherapy vary between agents, several are common to many classes of drugs. These include anaemia, thrombocytopenia, neutropenia, enterotoxicity and neuropathy/neurotoxicity.

1.2.1. Anaemia

Anaemia is defined as a deficiency in haemoglobin containing erythrocytes and is graded in its severity according to an individual's haemoglobin level. Anaemia can range from mild (level 1; 10-11g/dL) to life threatening (level 4; <6.5g/dL) (Groopman and Itri, 1999) and is a common side effect of both chemotherapy and cancer itself, occurring in between thirty to ninety percent of patients (depending on cancer type and treatment regime) (Knight et al., 2004). In the context of chemotherapy, anaemia primarily occurs as a result of the cytotoxic quality of anti-neoplastic agents which causes the suppression and/or death of rapidly dividing erythropoietic precursors in the bone marrow. Severe anaemia can be life threatening as it can lead to hypoxia and subsequent organ failure, and even mild to moderate anaemia can have a large impact on the quality of life of patients, causing fatigue, dyspnoea, tachycardia and headaches. Anaemia is most prevalent in patients treated with microtubule agents (vinca alkaloids and taxanes); however it can be well managed with red blood cell transfusions, which stabilise haemoglobin levels and restore quality of life (Groopman and Itri, 1999). Whilst transfusion is historically the treatment of choice, it is not without risk, infection and allergic reactions can occur and this has lead to the development of an

alternative therapy; recombinant human erythropoietin (EPO) (Tonia et al., 2012). EPO mimics the action of endogenous erythropoietin, a 34kDa cytokine produced by the kidneys in response to hypoxia that stimulates erythropoiesis in hematopoietic tissues, thus resulting in increased erythrocytes production in the bone marrow (Koury and Bondurant, 1990;Koury et al., 1988).

1.2.2. Thrombocytopenia

Thrombocytopenia is defined as a decrease in platelets, typically a platelet count of less than 150 x 10^9/L; however the condition is rarely symptomatic until a drop below 50 x 10^9/L is seen. A platelet count below 5 x 10^9/L is considered a haematological emergency (Gauer and Braun, 2012)). Thrombocytopenia is caused by either a decrease in platelet production (e.g. as the result of folic acid deficiency) or an increased destruction of platelets. In the context of chemotherapy, thrombocytopenia of varying severities occurs in up to seventy percent of patients (depending of treatment regime), but occurs predominantly following treatment with platinum based alkylating agents (Jardim et al., 2012). Chemotherapy-induced thrombocytopenia in this instance is generally moderate to severe, with the average platelet count of patients dropping to around 20 x 10^9 platelets/L (Kenney and Stack, 2009), and is thought to be caused by the suppression of bone marrow stem cells and the direct destruction of megakaryocytes (Zeuner et al., 2007). Recent evidence suggests sinusoidal injury and splenic sequestration of platelets are also likely to contribute to thrombocytopenia, and supportively, this goes some way to explain the splenomegaly occasionally seen in patients treated with oxaliplatin (Jardim et al., 2012). Typically chemotherapy-induced thrombocytopenia manifests in patients as petechiae and bruising, however in severe cases spontaneous GI, pulmonary or intracranial haemorrhage may occur. In most instances blood platelet levels recover following cessation of treatment with the causative

agent, however when it does not, platelet transfusions are normally sufficient to restore platelet levels (Visentin and Liu, 2007).

1.2.3. Neutropenia

Neutropenia is defined as a decrease in circulating neutrophils (typically below 2000 cells/mm^3 but considered severe below 500 cells/mm^3) and results in an increased susceptibility to infection (Saloustros et al., 2011). Chemotherapeutic agents cause this condition due to their ability to suppress the generation of blood cells, including neutrophils, within the bone marrow due to the rapid turnover of these cells; neutropenia to some degree is often unavoidable. In some cases, as a result of the extended duration and/or severity of neutropenia, patients may develop febrile neutropenia; a temperature in excess of 38^oC occurring as a result of an infection secondary to neutropenia. This side-effect of chemotherapy is tolerated well by most patients; however those who do develop infections as a result are managed with infection-appropriate antibiotics. Patients identified as being at high risk of developing febrile neutropenia, such as those with low neutrophils counts prior to the onset of chemotherapy are given prophylactic granulocyte-colony stimulating factor (G-CSF) which has been demonstrated to decrease the incidents of febrile neutropenia in chemotherapy treated patients by stimulating the survival, proliferation and differentiation of both mature neutrophils and their precursors (Renner et al., 2012).

1.2.4. Enterotoxicity

Also known as GI toxicity, enterotoxicity in a common occurrence in patients treated with a variety of chemotherapeutics and is routinely characterised by diarrhoea, constipation, colitis and nausea/vomiting. These symptoms arise through various mechanisms largely dependent on the

chemotherapeutic used, for example diarrhoea can occur in up to eight percent of patients (Coyle et al., 2013) but is especially common in patients treated with pyrimidine analogues or topoisomerase inhibitors such as irinotecan, as result of acute loss of epithelial cells and damage to the intestinal mucosa (Ikuno et al., 1995), whilst evidence suggests cisplatin, on the other hand, causes diarrhoea as a result of increased gastric emptying (Viana-Cardoso et al., 2011); emerging evidence suggests oxaliplatin induced constipation may arise as a result of damage to or loss of enteric neurons resulting in a decrease in gastric motility (Wafai et al., 2013). Diarrhoea and constipation following chemotherapy have a large impact on the quality of life of patients, however they can generally be well managed with drugs that increase or decrease gastric motility such as opioids (Benson, III et al., 2004) or osmotic salts (Tack, 2011) respectively. Nausea and vomiting as a result of chemotherapy occurs to some degree in an excess of ninety percent of patients (Kris et al., 1985), depending on the agent used, and is hypothesized to occur as a result of activation of abdominal vagal afferents following damage to the GI tract (by the cytotoxic compounds) and subsequent signalling to the emetic centre in the brainstem (Rojas and Slusher, 2012). The neurotransmitters involved in this signalling pathway are understood and accordingly chemotherapy induced nausea/vomiting are generally well managed with 5-HT3 antagonists (e.g. ondansetron), dopamine antagonists (e.g. metaclopramide), corticosteroids (e.g. dexamethasone) and NK1 receptor antagonists (e.g. aprepitant) (Wickham, 2012).

1.2.5. Neuropathy

Chemotherapy induced peripheral neuropathy (CIPN) is a dose-limiting side-effect associated with several classes of anti-neoplastic agents including vinca alkaloids, taxanes and platinum containing compounds; occurring in up to seventy percent of patients (Pachman et al., 2011). Symptoms of CIPN typically start within weeks of the onset of treatment and are predominantly, but not

exclusively, sensory in nature; they include pain, hypersensitivity and loss of sensation (Windebank and Grisold, 2008). Whilst in the majority of patients the prevalence of these symptoms decreases following cessation of treatment, this is not always the case, and there are many incidences where (cancer) treatment has to be halted prematurely as the neuropathy becomes severe. CIPN is discussed in detail below.

2. Physiological and pathophysiological pain signalling

The International Association for the Study of Pain defines pain as "an unpleasant sensory and emotional experience associated with actual or potential tissue damage" (www.iasp-pain.org). Under physiological conditions pain is a vital protective mechanism and persists only for the duration of the nociceptive stimulus or tissue damage; functioning as a warning system against actual or further tissue damage. The fundamental importance of this system becomes apparent when we study those individuals with the rare phenotype of insensitivity to pain, which results is frequent inadvertent self-mutilation and injury throughout life (Cox et al., 2006). Should this system malfunction and the pain experienced outlive the causative stimuli and physiological role it is termed chronic. Generally chronic pain states fall into two broad categories: neuropathic, or inflammatory; whilst these categories are simplistic and imply distinct mechanisms, in reality a wealth of evidence suggests these mechanisms overlap.

2.1. Pain Signalling

Acute (or nociceptive) pain arises as a result of the stimulation of excitation, the 'bare' or 'naked' endings of primary afferent sensory neurons whose cell bodies lie in the dorsal root ganglia (DRG) and mediate the transmission of painful stimuli. Classification of primary afferents is based on the anatomical and electrophysiological characteristics of these neurons, and gives rise to three populations: Aβ fibres, Aδ fibres and C fibres. Aβ fibres are large diameter (>10μm), highly myelinated fibres with fast conduction velocities (30-100msec^{-1}) and low activation thresholds (Millan, 1999). These fibres are predominantly low-threshold mechanoreceptors and respond to non-nociceptive stimuli such as light touch, and are responsible for the transduction of normal tactile sensation. In comparison, Aδ fibres are smaller (2-6μm) and less myelinated than Aβ fibres, thus they have slower conduction velocities (2-30msec^{-1}), and also possess high activating thresholds meaning that, whilst they can convey non-nociceptive sensory information, they are predominantly activated by 'painful' stimuli (Millan, 1999). A fibres can be identified immunohistochemically by their expression of neurofilament 200 (NF200) and whilst both Aδ and Aβ fibres terminate in the deep lamina (III-V) of the dorsal horn of the spinal cord, Aδ also have terminations in the superficial dorsal horn (lamina I and II) (D'Mello and Dickenson, 2008) (see figure 1.1). Finally, C fibres are small diameter (0.4-1.2μm) unmyelinated fibres with low conduction velocities (<2msec^{-1}) and high activating thresholds that respond to noxious stimuli (Lawson, 2002;Millan, 1999;D'Mello and Dickenson, 2008) (see figure 1.1). C fibers are then sub-divided into two populations, peptidergic and non-peptidergic, based on their expression of neuropeptides. Peptidergic C fibres express substance P (SP) (McCarthy and Lawson, 1989) and calcitonin gene-related peptide (CGRP) (Lawson et al., 2002). These fibres express the TrkA receptor (Averill et al., 1995), respond to and are regulated by nerve growth factor (NGF) and project to the lamina I of the dorsal horn (Lewin et al., 1994;McMahon et al., 1995).

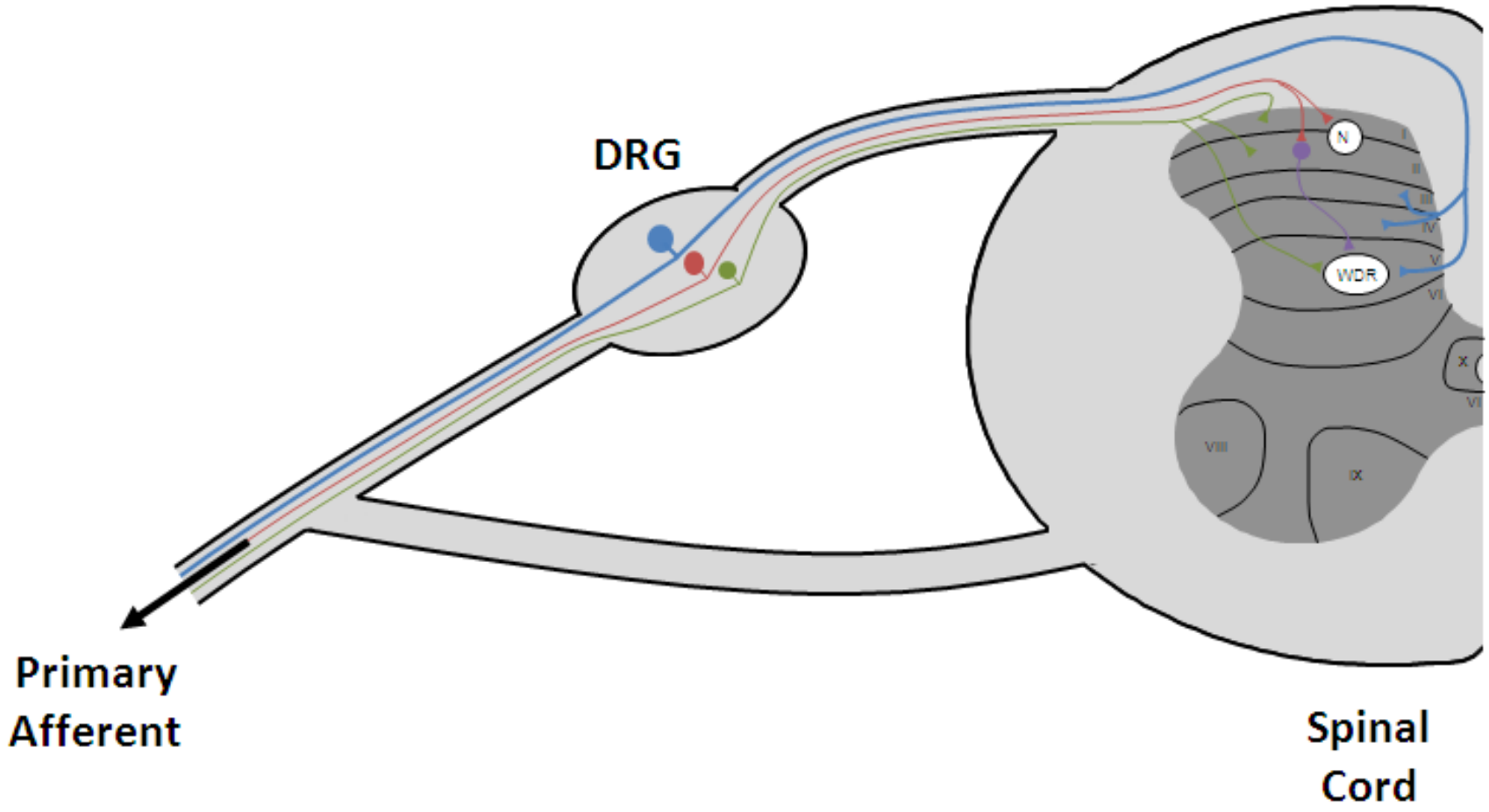

Figure 1.1. Schematic of primary afferent populations and their central terminations. Primary afferent fibers (Aβ [blue], Aδ [green] & C [red]) transmit signals from the periphery, through the dorsal root ganglia (DRG) to the dorsal horn of the spinal cord. Aβ and Aδ fibers have terminations in the deep lamina where they synapse on to wide dynamic range (WDR) neurons. Aδ fibers also have terminations in superficial lamina where along with C fibers they synapse onto nociceptive-specific (N) neurons.

As their name suggest, the non-peptidergic C fibres do not express these neuropeptides and down-regulate TrkA during the early postnatal phase. These fibres terminate in lamina II of the dorsal horn, and are instead characterised by their surface expression of isolectin B4 (IB4) and the purinergic receptor P2X3 (Vulchanova et al., 1998;Bradbury et al., 1998). Primary afferents possess a single axon that bifurcates to give rise to a peripheral and a central branch. The peripheral axon branch innovates peripheral targets, where activation of various receptors or ion channels (e.g. Transient Receptor Potential [TRP] channels) located on nerve terminals, initiates action potentials that are conducted to the CNS via the central branch of the primary afferent.

As hinted to above, the spinal cord is organised into a series of laminae based on the anatomical characteristics of the neurons found there. Laminae I-VI make up the dorsal horn (although laminae VI exists only in the lumbosacral and cervical enlargements) and it is here that Aβ, Aδ and C fibre primary afferents synapse onto second order interneurons or projection neurons; laminae VII-IX make up the ventral horn and are involved predominantly in motor signalling (Rexed, 1952).

The majority of dorsal horn neurons are interneurons with axons that remain in the spinal cord and branches that terminate locally (Todd, 2010). These neurons can be broadly categorized by their excitatory (glutamatergic) or inhibitory (primarily GABA-ergic and/or glycinergic) nature. Interneurons can also be characterised by their responses to varying stimuli. Nociceptive-specific neurons are found predominantly in the superficial laminae and receive input from Aδ and C fibres. Non-nociceptive neurons are found mainly in the deeper laminae, III and IV, and respond to tactile information conveyed to the spinal cord by Aβ fibres (Light et al., 1979). Finally wide dynamic range (WDR) neurons, located primarily in lamina V, receive input from Aβ, Aδ and C fibres and therefore respond to a wide range of stimuli including mechanical, thermal and

chemical stimulation. WDR neurons also exhibit wind-up, a short-lasting form of synaptic plasticity where repetitive stimulation induces an increase in evoked response intensity and prolonged post-discharge (D'Mello and Dickenson, 2008).

Additionally, the dorsal horn contains a range of neurons that form descending projections as well as neurons whose projections ascend to supraspinal sites and a vast number of non-neuronal glial cells. These glial cells (astrocytes and microglia) were initially thought play simply structural and supportive roles, however in the last decade a wealth of evidence has identified a key role for these cells in the modulation of pain signalling under pathophysiological conditions. This is discussed below.

To allow the propagation of an action potential from the primary afferent to the post-synaptic dorsal horn neuron, the electrical activity of the pre-synaptic neuron must be converted to a chemical signal; this activates the post synaptic neuron by activation of specific receptors on the neuron's membrane. In the spinal cord glutamate is the principle mediator of excitatory signalling and is released from the pre-synaptic neuron in both physiological and pathophysiological states; the excitatory effect of glutamate is exerted by the activation of glutamate receptors, predominantly N-methyl-D aspartate (NMDA) and α-amino-3-hydroxy-5-methyl-4-isoxazolepropionic acid (AMPA) receptors, although metabotropic (mGluR) and kainate (KA) receptors (KAR) are also located on the post-synaptic membrane. In the pre-synaptic terminal glutamate is synthesised and packaged into small synaptic vesicles, and released via exocytosis when membrane depolarisation causes an increase in intracellular calcium levels. Glutamate is quickly released from the central terminals of primary afferents following activation of these neurons by noxious stimuli; the excitatory post-synaptic potential (EPSP) resulting from a

single action potential primarily arises a result of this glutamate activating AMPA and KA receptors (Yoshimura and Jessell, 1990;Li et al., 1999). AMPA receptors are ligand-gated cation channels composed of a combination of the subunits GluR1-4; the mRNA for all four subunits has been found in the spinal cord (Furuyama et al., 1993;Henley et al., 1993;Jakowec et al., 1995). The expression of GluR1 and GluR2 is mainly restricted to laminae I and II; GluR3 and GluR4 have a more widespread distribution, with moderate expression in the deep laminae of the dorsal horn and the laminae of the ventral horn and weak expression in the superficial dorsal horn (Nagy et al., 2004). AMPA receptor activation on the other hand results in influx of the cations Na^+ and K^+; Ca^{2+} permeability is dependent on the presence of the GluR2 subunit in the receptor complex, which also determines the susceptibility of the channel to be blocked by polyamines (Hollmann and Heinemann, 1994;Tao, 2012). There are seven NMDA receptor subunits: NR1, NR2A-D and NR3A-B. Receptors are formed of heteromeric complexes of these subunits and require the expression of NR1 and at least one NR2 subunit to be functional (Kew and Kemp, 2005). Under normal physiological conditions the NMDA receptor contributes little to the generation of EPSPs as these receptors are tonically blocked by extracellular Mg^{2+} ions, however if there is repetitive high frequency stimulation of nociceptors, NMDA receptors may become activated as the Mg^{2+} block dissociates due to prolonged depolarization of the membrane (Mayer et al., 1984). Following NMDA receptor activation by glutamate, there is an influx of Ca^{2+} ions which causes depolarisation of the post-synaptic neuron as well as activation of signalling molecules such as calcium/calmodulin dependent kinases, which contributes to long term potentiation and central sensitization (Malinow et al., 1989).

Inhibitory synapses in the dorsal horn are chiefly glycine or GABA-ergic. GABA-ergic neurons are abundant throughout the dorsal horn of the spinal cord, especially within the superficial laminae

(Daniele and Macdermott, 2009;Todd and Sullivan, 1990;Oliva, Jr. et al., 2000), whilst glycinergic neurons are thought to be the predominant inhibitory interneurons of the deeper laminae (Inquimbert et al., 2007;Todd et al., 1996). These neurons evoke inhibitory post-synaptic potentials (IPSPs) via activation of their respective receptors; GABA (γ-Aminobutric Acid) exerts its inhibitory effects via the activation of the ligand-gated ion channel $GABA_A$ or the G-protein coupled $GABA_B$ receptor; glycine activates is own ligand-gated ion channel. Activation of these receptors depresses neuronal activity by hyperpolarisation of the post-synaptic membrane as a result of Cl^- influx or the activation of K^+ channels (leading to K^+ efflux).

Primary afferents, peptidergic C fibres in particular, also express a range of neuropeptides including SP and CGRP that are synthesised as precursors and packaged into large dense core vesicles (Merighi et al., 1991) and cleaved by proteases into active signalling molecules. SP is released from the central terminals of primary afferents following noxious stimulation, both electrical and chemical (capsaicin) (Go and Yaksh, 1987); once released, it exerts its effects via activation of the NK1 receptor, the highest expression of which is in lamina I, where over 75% of nociceptive projection neurons express the NK1 receptor (Cheunsuang and Morris, 2000). These neurons play a key role in transmission of highly noxious stimuli and hyperalgesic responses; specific ablation of NK1 expressing neurons in lamina I results in significant attenuation of responses to these types of stimuli but not to mild noxious stimuli (Mantyh et al., 1997). NK1 receptors are also found on both the peripheral and central terminals of C fibres where their activation regulates the release of neuropeptides (Malcangio and Bowery, 1994;Lever et al., 2003). CGRP exerts its effects by modulating SP release in several ways: enhancing SP release (Oku et al., 1987), blocking SP degradation (Le et al., 1985) and regulating the expression of the NK1 receptor (Seybold et al., 2003). CGRP activates the CGRP receptor, a G-protein coupled receptor (GPCR)

expressed extensively in neurons of the superficial dorsal horn (Ye et al., 1999). Additionally evidence suggests that SP and CGRP are co-released with glutamate from C fibres, with the subsequent receptor activation contributing to prolonged slow depolarizations that aid the removal of the Mg^{2+} block from NMDA receptors, facilitating wind-up in wide dynamic range neurons (Budai and Larson, 1996).

Sensory output from the dorsal horn is relayed to higher processing centres in the brain by ascending pathways, comprised of spinal projection neurons (figure 1.2). Using antero- and retrograde tracing techniques these spinal projections have been extensively mapped; lamina I neurons form the spinoparabrachial tract, projecting supraspinally to high nociceptive processing centres including the parabrachial area (PBA) and the periaqueductal gray (PAG). These brain regions contain neurons that project to the hypothalamus and amygdala, activity in which contributes to the emotional aspects of pain. Lamina I neurons also project to the caudal venterolateral medulla (CVM), the nucleus of the solitary tract and to several nuclei of the thalamus (D'Mello and Dickenson, 2008;Todd, 2010). Approximately eighty percent of lamina I projection neurons are express the NK1 receptor (Todd et al., 2000), and the majority of these neurons project contralaterally (figure 1.2); this is not always the case, however, and there are many neurons that project bilaterally (Spike et al., 2003). Whilst it has been demonstrated that non-NK1 expressing projection neurons respond to noxious stimuli (Todd, 2002) little else is known about them. Projections from deeper laminae, typically IV-VI WDR neurons (and some projections from lamina I) cross the midline of the spinal cord to reach the contralateral white matter and project to the brainstem and thalamus (forming the spinothalamic tract). The spinothalamic tract sends further projections to several nuclei of the cortex, including the primary

and secondary somatosensory, insular, anterior cingulate and prefrontal cortices, collectively referred to as the 'pain matrix' (Tracey and Mantyh, 2007).

These ascending pathways play a critical role in the transmission and modulation of pain in higher brain regions; however a number of descending pathways are also involved in the modulation of nociceptive transmission (figure 1.2). Early studies demonstrated that the electrical stimulation of specific brain regions resulted in analgesia (Reynolds, 1969), suggesting activity in these regions could inhibit nociceptive signalling; however it is now evident that descending pathways can also facilitate nociceptive transmission. The best characterised descending pathway is that connecting the PAG and dorsal horn, which contributes to environmental and opioid analgesia (Heinricher et al., 2009). As shown in figure 1.2 the PAG receives input from the limbic system (amygdala and hypothalamus) as well as the dorsal horn, first projecting to the rostral ventromedial medulla (RVM) which in turn relays the signal to the spinal cord (Tracey and Mantyh, 2007). Electrical stimulation of the RVM is analgesic and inhibits spinal neuron responses to noxious stimuli as does injection of the local anaesthetic lidocaine (Bee and Dickenson, 2007). This suggests that descending projections from the RVM both facilitate and inhibit nociceptive transmission; likely occurring due to the presence of several cell types in this brain region. Three cell types have been characterised in the RVM based on their response to a thermal stimuli: 'on-cells' showed increased discharge, 'off-cells' showed decreased discharge and 'neutral-cells' were unchanged by the stimuli. These cells also differ in their sensitivity to μ-opioids; 'on-cells' are inhibited whilst 'off-cells' become continuously activated (Fields et al., 1983). This pattern of activity suggested that 'on-cells' mediate descending facilitation whilst 'off-cells' mediate descending inhibition. Both 'on-cells' and 'off-cells' project to the dorsal horn where they modulate nociceptive transmission directly by interacting with primary afferents, and indirectly by interacting with excitatory and

inhibitory interneurons and projection neurons (figure 1.2) (Fields et al., 1995), by forming both noradrenergic and serotonergic synapses (Yoshimura and Furue, 2006).

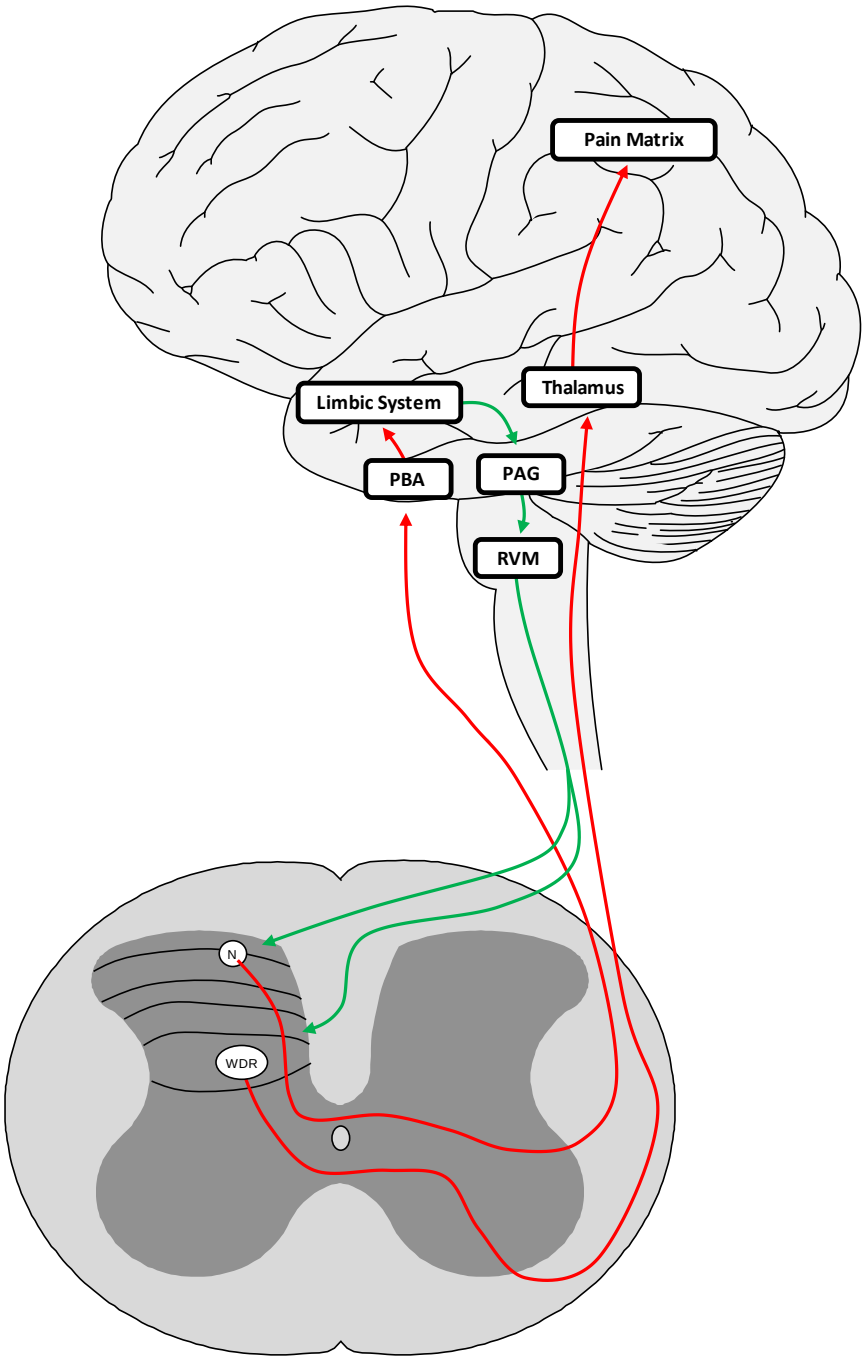

Figure 1.2. Main ascending and descending pathways of nociceptive transmission between the dorsal horn and brain. Ascending pathways are shown in red and include the spinothalamic and spinoparabrachial tracts. Descending pathways are shown in green and include descending input from the PAG via the RVM.

2.2. Chronic Pain

As mentioned above, chronic pain states fall into two categories: neuropathic and inflammatory. In both cases a combination of mechanisms results in enhanced nociceptive transmission due to peripheral and central sensitisation. Whilst variable in its aetiology, chronic pain typically manifests in a similar fashion in human patients and rodent models. It is characterised by the presence of a range of symptoms including sensory loss, spontaneous pain, paraesthesia (spontaneous or evoked abnormal sensation), hyperalgesia (increased sensitivity to noxious stimuli) and allodynia (a painful response to previously innocuous stimuli) (Woolf and Mannion, 1999).

The treatment of chronic pain remains a problem clinically as many patients do not experience sufficient pain relief with classical analgesics. Furthermore, no clear predictors of treatment response have been identified in chronic pain patients (Baron et al., 2010). The difficulty in treating the condition is likely a result of the heterogeneity of the mechanisms underlying the development and maintenance of chronic pain, however some classes of drugs, including the anti-depressant selective serotonin reuptake inhibitors (SSRIs) and opiates have shown efficacy in clinical trials and meta-analyses (Baron et al., 2010;Dworkin et al., 2007;O'Connor and Dworkin, 2009). Regardless of their efficacy these therapeutic approaches are symptomatic and much research is needed to better understand the mechanism by which these pain states are arising so that appropriate treatments can be developed.

2.2.1. Neuropathic Pain

Neuropathic pain is that arising from neuropathy and occurring as a result of a lesion of the nervous system, be that as the result of physical trauma or disease. Typically neuropathy is associated with direct trauma to part of the nervous system, for example it may arise as a result of crushing stretching or severing of a peripheral nerve, or as a result of damage to the CNS such as a spinal cord injury. In addition to these processes, neuropathic pain can arise as a result of the pathogenesis of a disease, for example diabetes mellitus, viral infections and tumour growth are often associated with the development of neuropathy. Furthermore, neuropathy can occur following toxic insult; this may be a direct exposure to specific toxins, for example acrylamide, arsenic or thallium, or a side-effect of pharmacotherapy with neuropathy-causing agents e.g. anti-retrovirals, metronidazole or certain chemotherapeutics (Baron et al., 2010).

2.2.2. Chronic Inflammatory Pain

Inflammation is a complex yet protective response to harmful stimuli elicited by tissue injury or infection that, under physiological conditions, serves to destroy, dilute or provide a barrier against the damaging agent. It is characterized by the development of hyperalgesia (dolor), heat (color), redness (rubor) and swelling (tumor). On a more discrete level it involves a number of biological processes including increased blood flow and dilatation and increased permeability of blood vessels, the exudation of fluid and the migration of leukocytes; pain occurs as a result of the activation of peripheral sensory neurons by pro-nociceptive mediators released from damaged cells or infiltrating immune cells. The first pro-inflammatory mediator to be identified as capable of inducing hyperalgesia was bradykinin (Armstrong et al., 1953); a host of other mediators have since been observed to have a similar effect, they include (but are not limited to) prostaglandins, leukotrienes, chemokines and cytokines. Chronic inflammatory pain is typically associated with

inflammatory diseases, for example rheumatoid or psoriatic arthritis; in these patients the constant presence of these algogenic mediators results in the sensitisation of both the PNS and CNS which results in ongoing pain. Due to our developing understanding of this process a number of successful treatments for chronic inflammatory pain are emerging, targeting peripheral pro-nociceptive inflammatory mediators e.g. tumour necrosis factor-α (TNFα; etanercept / infliximab) and interleukin-1 (IL-1; anakinra). These drugs reduce inflammation-evoked hyperalgesia by reducing nociceptor activation, and also reduce disease progression and immune cell infiltration of the joint, preventing further release of pro-nociceptive mediators (Schaible et al., 2010;Agarwal, 2011;Mertens and Singh, 2009;Breedveld, 2002).

2.2.3. Animal Models

Due to the limitations of studying the mechanisms underlying chronic pain states in humans, a number of animal models have been developed to aid research in this field. Many of the classical models of neuropathic pain involve the surgical injury of a peripheral nerve (see table 1.1.), usually the sciatic nerve or branch thereof. Such injuries induce a sustained pain phenotype in a single hind paw of the rodent, with the contralateral paw acting as an internal control. Likewise, a number of models of inflammatory pain have been developed in order to study the mechanisms by which this normal immune response becomes a persistent pathological condition. These models typically involve the direct administration of an exogenous algogenic compound, either a chemical irritant or an inflammatory mediator (see table 1.2.), that results in the inflammation of the area into which the substance was injected; pain develops as a consequence.

Table 1.1. Surgical models of neuropathy

Model	Surgical Paradigm	Reference
Chronic Constriction Injury (CCI)	Loose ligation of the sciatic nerve.	(Bennett and Xie, 1988)
Partial Nerve Ligation (PNL)	Tight ligation of 1/3-1/2 of the sciatic nerve.	(Seltzer et al., 1990)
Spinal Nerve Ligation (SNL)	Ligation of the L5 and/or L6 spinal nerve	(Kim and Chung, 1992)
Spared Nerve Injury (SNI)	Transection of the tibial and common perineal (but not sural) nerves	(Decosterd and Woolf, 2000)

Table 1.2. Inflammatory models of chronic pain

Model	Inflammatory Agent	Reference
Complete Freud's Adjuvant (CFA)	Mineral oil containing *Mycobacterium tuberculosis*.	(Freund, 1947)
Zymosan	Components of yeast cell wall.	(Piller and Ecker, 1941)
Carrageenan	Extract from seaweed.	(Vinegar et al., 1976)
Formalin	Formalin solution	(Dubuisson and Dennis, 1977)

Whilst use of these models has greatly enhanced our understanding of the mechanisms underlying chronic pain, they display little resemblance to most clinical occurrences; as a result a number of models have been developed that more closely mimic disease states that are associated with the development of chronic pain. As table 1.3 shows, these include models of viral infection, such as post-herpetic neuralgia and HIV-associated neuropathy, models of diabetic neuropathy, models of

bone cancer pain and models of chemotherapy-induced painful peripheral neuropathy induced by the repeated administration of specific chemotherapeutic agents.

Typically the development of chronic pain in these models is assessed behaviourally in terms of alterations in responses to evoked pain, and involves the measurement of reflex flexion withdrawals to noxious stimuli. The majority of pain testing involves the application of mechanical or thermal stimuli to the effected paw where reflex withdrawals are spinally mediated and initiated by the activation of primary nociceptors, and are under descending control from supraspinal structures in the brain stem and midbrain (Fields and Heinricher, 1989). Furthermore the glabrous skin of the underside of the paw provides an area of accessible skin that most closely approximates human skin.

Table 1.3. Disease mimicking models of pain

Model	Disease Initiation	Reference
Bone Cancer Pain	Inoculation of long bones with cancer cell line	(Schwei et al., 1999;Sabino et al., 2002)
Chemotherapy Pain	Intra-peritoneal VCR Intra-peritoneal PTX Intra-peritoneal oxaliplatin/cisplatin	(Aley et al., 1996;Polomano et al., 2001;Deng et al., 2012)
Diabetic Neuropathy	Intra-peritoneal injection of streptozocin	(Wuarin-Bierman et al., 1987;Malcangio and Tomlinson, 1998)
HIV-associated Neuropathy	Application of HIV-1 gp120 to sciatic nerve or intrathecal space	Wallace et al, 2007
Post-herpetic Neuralgia	Infection with varicella-zoster virus	Fleetwood-Walker et al, 1999

First described by von Frey in 1986, the application of graded filaments to the skin is used to measure sensitivity to punctuate mechanical stimuli, and has subsequently been adapted to allow for the average calculation of a fifty percent paw withdrawal threshold (PWT), the force at which when applied to the paw, the paw is withdrawn on half of the occasions tested (Chaplan et al., 1994). Sensitivity to thermal (heat) stimuli is predominantly tested using the Hargreaves' method, developed by Hargreaves and colleagues in 1988 (Hargreaves et al., 1988); a heat source in the form of radiant light is directed at the plantar surface of the hind paw and the latency to withdrawal is recorded. Whilst these two approaches are the most common methods of assessment of pain behaviours in rodent models, several other have been developed and are used

regularly, these include paw-pressure assessment of mechanical sensitivity, hot-plate and tail immersion assessment of thermal sensitivity and cold-plate and acetone tests for assessment of cold sensitivity. It should be noted that these tests do not account for the development of spontaneous pain and results may be confounded by the loss of sensation that can accompany some models.

2.2.4. Mechanisms of Chronic Pain

The development of animal models of neuropathic and chronic inflammatory pain has led to a vast increase in the understanding of the pathogenic mechanisms by which these pain states arise. These can generally be categorised into one of the following, which are discussed below:

1. Peripheral sensitisation and changes in peripheral nerves
2. Central sensitisation and immune responses in the spinal cord
3. Higher centre modulation

2.2.4.1. Peripheral Sensitisation and Changes in Peripheral Nerves

Peripheral sensitisation can be loosely defined as the response of primary afferents to a change in the local environment, which results in a characteristic electrophysiological response in the nociceptor of a reduction in activation threshold and an increase in responsiveness to supra-threshold stimuli (Andrew and Greenspan, 1999;Koltzenburg et al., 1999;Kocher et al., 1987). The usually ordered composition of peripheral nociceptors shows substantial plastic changes following damage or exposure to inflammation. Due to tissue damage there is a dramatic change in the composition of the chemical milieu surrounding primary afferents; a multitude of molecules are released from the damaged cells, infiltrating immune cells and the nerve itself. These molecules include ATP, neurotransmitters (e.g. histamine and 5-hydroxytryptamine [5HT]), peptides (e.g.

substance P [SP], CGRP and bradykinin), neurotrophins (e.g. NGF), chemokines (e.g. CCL2), cytokines (e.g. TNFα and IL-1β) and proteases (e.g. Cathepsin S). Collectively these mediators are referred to as an 'inflammatory soup' and via receptors on the peripheral terminals of primary afferents, they can activate a host of intracellular signalling pathways that can directly alter neuronal conduction properties, induced further mediator release from the neuron or result in post- translational modification of various proteins involved in nociceptive transmission (Campbell and Meyer, 2006;Moalem and Tracey, 2006). There are also many longer-term consequences; following the activation of second messenger pathways there is activation of transcription factors such as ATF-3 (activating transcription factor-3), STAT (signal transducer and activator of transcription) and NFκβ (nuclear factor κβ), which leads to changes in the expression of various proteins. In fact, the upregulation of such transcriptional factors is often used as a unique marker of neuronal damage; ATF-3 activation/expression is induced in the cell body of almost every damaged fibre (Tsujino et al., 2000).

Widespread changes in neuronal gene expression are observed following injury; as shown by micro-array studies, many of these genes encode signalling molecules, receptors and ion channels that are critically involved in the transmission of nociceptive stimuli (Costigan et al., 2002;Kubo et al., 2002;Uno et al., 2002). Whilst early work focused on the role of the damaged fibres and the idea that they become hyper-excitable and generate ectopic action potentials (leading to central sensitisation; (Devor, 2001), there is now a shift towards examining intact fibres as well; the blockade of signal transduction in intact roots, but the administration of local anaesthetic, reduces pain behaviour the spinal nerve ligation model of neuropathic pain (Yoon et al., 1996). Moreover, neuropathic pain like behaviours can be induced in the absence of axonal damage by the local

application of an inflammatory agent (Chacur et al., 2001;Eliav et al., 1999) , indicating that these fibres play a key role in dysfunction nociceptive transmission in these models.

Many of the changes in the conduction properties of nociceptive afferents occur as a result of changes in ion channel expression or activation. Once of the best characterised of these is TRPV1 (Transient Receptor Potential Vanilloid-1); this non-selective cation channel is upregulated in uninjured sensory fibres after nerve injury (Hudson et al., 2001). Furthermore, whilst physiologically expressed in smaller diameter fibres, nerve injury induces *de novo* expression of TRPV1 in large myelinated A-fibres (Hong and Wiley, 2006;Pabbidi et al., 2008) and likely contributes to the development of hyperalgesia, certainly inhibiting TRPV1 activity or decreasing its expression attenuates such pain behaviours in several rodent models of neuropathy (Christoph et al., 2006;Watabiki et al., 2011;Ta et al., 2010). TRPV1 is by far the only ion channel to be altered following injury; the expression of TRPA1 mRNA, a predominantly calcium permeable cation channel, is increased in the uninjured L4 DRG after an L5 spinal nerve ligation, and decreasing this expression by the administration of an antisense oligodeoxynucleotide suppresses injury induced cold allodynia (Obata et al., 2005). The expression of several voltage-gated sodium channels (VGSC) is increased in DRG neurons following injury. Several inflammatory mediators are able to increase the expression and phosphorylation state of the VGSC $Na_v1.8$ that leads to an increase in Na^+ current amplitude and a hyperpolarising shift in voltage dependent activation (Wood et al., 2004). Additionally following nerve injury a change in the spatial distribution of $Na_v1.8$ is seen from the cell body of the DRG to the axonal site of injury (Novakovic et al., 1998), and the antisense knock-down of $Na_v1.8$ attenuates neuropathic behaviour in rodents (Lai et al., 2002). Conversely, however, neuropathic pain develops normally in $Na_v1.8$ null mice (Akopian et al., 1999), arguing against a role for this channel in neuropathic pain states. The $Na_v1.7$ subtype of VGSC is thought to

contribute significantly to inflammatory pain; if this ion channel is selectively knocked out in nociceptors, mice exhibit reduced or completely abolished pain responses to a range of inflammatory mediators (Nassar et al., 2004). In humans, gain of function mutations in the *scn9a* gene (which encodes the $Na_v1.7$ channel protein) lead to altered pain sensitization, for example the hereditary disease early-onset erythromelalgia which is characterized by severe bilateral pain and cutaneous vasodilation (Yang et al., 2004;Dib-Hajj et al., 2005;Dib-Hajj et al., 2007;Drenth and Waxman, 2007). Several HCN (hyperpolarisation-activated cyclic nucleotide-gated) channels, responsible for generating an inward depolarizing current to allow subsequent action potentials, are upregulated following nerve injury. This reduces the refractory period of the neuron and contributes to hyperexcitability; pharmacological blockade of these channels are effective in reducing behavioural hypersensitivity as well as primary afferent ectopic activity (Lee et al., 2005;Emery et al., 2011). Finally, several A-type potassium channels ($K_v4.3$, $K_v3.4$ and $K_v9.1$) that play a critical role in the regulation of neuronal excitability are down-regulated following nerve injury and inflammation, resulting in an overall enhancement of neuronal excitability (Chien et al., 2007;Takeda et al., 2006;Takeda et al., 2008;Tsantoulas et al., 2012).

Changes in ion channel expression are not the only examples of a phenotypic switch in neurons as a response to injury and/or inflammation; a similar phenomenon is seen in regards to neuropeptide expression in peripheral afferents. Physiologically SP expression is confined to a sub-population of small diameter peptidergic neurons; however the expression of SP and its precursor (preprotacykinin) decrease here following injury (Noguchi et al., 1994). This is associated with concomitant *de novo* expression of SP in injured medium and large diameter fibres (Noguchi et al., 1994;Marchand et al., 1994). CGRP and BDNF expression following injury undergo a similar change; physiological expression in small diameter peptidergic DRG neurons is decreased (Verge et

al., 1995;Cho et al., 1998;Michael et al., 1999), whilst *de novo* expression in large diameter neurons is evident (Michael et al., 1999;Cho et al., 1998). Several other neuropeptides show vastly increased expression in primary afferents following injury; these include galanin, cholecystokinin and neuropeptide Y (Verge et al., 1995).

The injury to the nerve or surrounding tissue that ultimately leads to the development of chronic pain triggers a local inflammatory response. This is the body's normal response to tissue damage and consists of two main phases; a pro-inflammatory phase in which there is clearance of pathogens and cellular debris to restore homeostasis, and a pro-resolution phase consisting of local tissue repair and the dampening of the damaging effects of a prolonged pro-inflammatory phase. The cells of the immune system (mast cells, macrophages, neutrophils and T-cells) are recruited to the site of injury due to release of pro-inflammatory mediators released from tissue resident immune cells which are the first to respond to the damage; typically these are tissue resident macrophages, mast cells and Schwann cells. This process is shown schematically in figure 1.3.

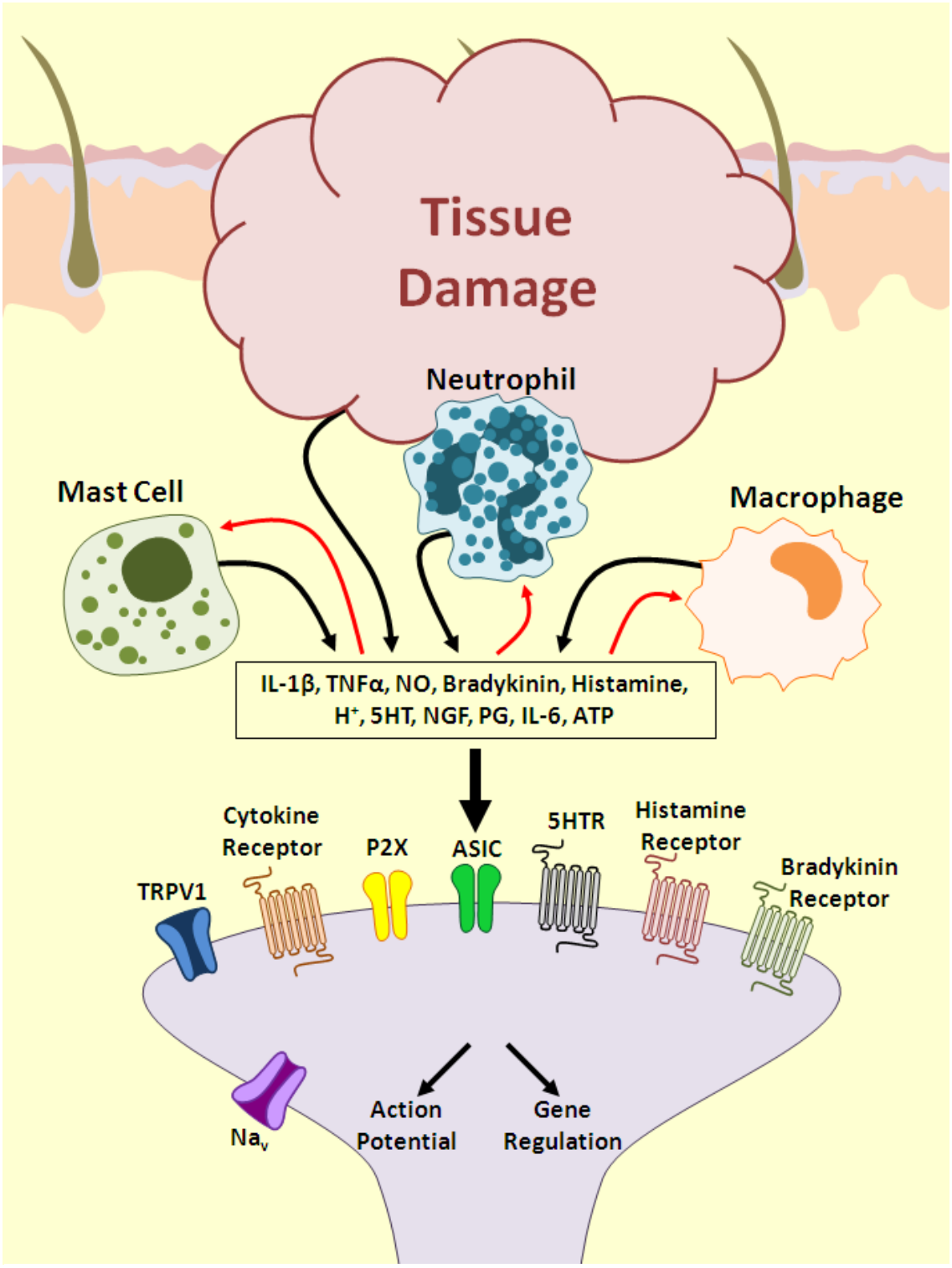

Figure 1.3. Key players in peripheral sensitization. Following tissue damage immune cells (mast cells, neutrophils and macrophages) infiltrate the area and along with the damaged tissue, release a host of pro-nociceptive mediators that are capable of triggering action potentials or altering protein expression in primary afferents. NO - nitric oxide, PG - prostaglandin, NGF - nerve growth factor, ATP - adenosine triphosphate (Adapted from (Marchand et al., 2005).

Schwann cells play a critical role in the inflammatory response to a damaged nerve; the Schwann cells that once myelinated the degenerating axon de-differentiate and taking on a phagocytic phenotype they begin to phagocytose myelin debris; this process of Wallerian degeneration creates a local environment distal to the injury that promotes regeneration (Allodi et al., 2012). During this process Schwann cells synthesis and release a variety of potent inflammatory mediators including IL-1, TNF, IL-6, LIF ATP, prostaglandins and nitric oxide (NO) (Bergsteinsdottir et al., 1991;Murwani et al., 1996;Wagner and Myers, 1996;Bolin et al., 1995;Thacker et al., 2007) that as well as acting directly on the nerve, are able to induce the expression of CCL2 via an MEK-ERK dependent signalling pathways (Perrin et al., 2005;Tofaris et al., 2002;Fischer et al., 2008b) that promotes the recruitment of macrophages; a reduction in CCL2 released from Schwann cells results in a substantial decrease in macrophage recruitment and an amelioration of neuropathic pain behaviours (Fischer et al., 2008a). After peripheral nerve injury tissue resident mast cells become activated and undergo degranulation (Zuo et al., 2003), resulting in the release of a number of pro-inflammatory mediators including histamine, proteases and cytokines (Galli et al., 2005;Thacker et al., 2007) which contribute to the recruitment of immune cells. Histamine itself is pro-nociceptive via the activation of neuronal histamine receptors which are upregulated after nerve injury (Mizumura et al., 2000;Kashiba et al., 1999;Herbert et al., 2001). Prevention of mast cell degranulation by cell stabilization with sodium cromoglycate reduces macrophage and neutrophil infiltration at the site of injury, and attenuates the development of mechanical allodynia in animals with a peripheral nerve injury (Zuo et al., 2003). Similarly blocking the infiltration of neutrophils and macrophages by reducing available circulating cells, using an anti-neutrophil antibody and liposomal clodronate respectively, significantly attenuates behavioural hypersensitivity in models of neuropathic pain (Perkins and Tracey, 2000;Barclay et al., 2007;Liu et al., 2000).

Following tissue injury neutrophils are one of the earliest cell types to infiltrate the affected area, peaking as little as 24 hours after injury (Perkins and Tracey, 2000), and acting as phagocytic cells as well as releasing pro-inflammatory mediators which can activate neurons and recruit macrophages (Witko-Sarsat et al., 2000). Significant neutrophil infiltration is seen in several models of nerve injury (Zuo et al., 2003;Clatworthy et al., 1995;Perkins and Tracey, 2000); current evidence suggests a role for these cells in the development of pain rather than its maintenance, as neutrophil blockade is successful only in preventing the development of hypersensitivity rather than reversing established pain (Perkins and Tracey, 2000). The contribution of macrophages to the development of peripheral sensitization and pain has been examined in several models of neuropathic pain; macrophage infiltration into the nerve occurs as a result of the release of chemoattractant mediators from tissue resident immune cells and neutrophils. An attenuation of pain behaviours has been shown following both the depletion of circulating monocyte/macrophages (Barclay et al., 2007;Liu et al., 2000) and in a mouse with delayed macrophage recruitment, which also demonstrated a retardation of Wallerian degeneration (Myers et al., 1996;Sommer and Schafers, 1998). Following activation these cells increase the synthesis and release of pro-inflammatory mediators including NO, free radical species and cytokines (e.g. TNFα, IL-1β and IL-6) (O'Shea and Murray, 2008;Dale et al., 2008). As well as causing the further recruitment and activation of macrophages, many of these factors are able to act directly on neurons to either trigger nociceptive action potentials or activate pathways that modulate the expression of various proteins such as the ion channels and neuropeptides discussed above.

2.2.4.2. Central Sensitization and Immune Responses in the Spinal Cord

In the spinal cord a variety of plastic changes occur in response to altered nociceptive transmission from the periphery that manifest as enhanced pain signalling. This process, often referred to as central sensitization, includes changes in synaptic strength, activation of glial cells and alterations in protein expression; this is summarised in figure 1.4.

Input from the periphery is transmitted to second order dorsal horn neurons via the excitatory neurotransmitter glutamate. Under physiological conditions glutamate predominantly activates AMPA and KA receptors on the post-synaptic membrane inducing an ion flux that results in depolarisation; the contribution of NMDA receptors in this instance is minimum due to the presence of an Mg^{2+} block that requires repetitive input or slow sustained depolarisation to be removed. Sustained noxious stimuli associated with peripheral tissue injury results in a higher frequency of input to dorsal horn neurons; this results in temporal summation and the release of co-transmitters from the pre-synaptic primary afferent that provide a sufficient stimulus to remove the Mg^{2+} block. Subsequently NMDA receptor activation allows influx of Ca^{2+}, boosting depolarization and activating calcium sensitive intracellular signalling cascades, such as those responsible for phosphorylation of NMDA and AMPA receptors and ion channels, as well as activation of transcription factors that initiates prolonged changes in neuronal excitability; thus NMDA receptors are often considered key mediators of pathological pain (Woolf and Salter, 2000). NR2B, the predominant NMDA subunit in nociceptive pathways, has been suggested as a target for the development analgesics for the treatment of neuropathic pain, and indeed there have been some successes in the use of NR2B antagonists for this condition; NR2B antagonists attenuate pain in animal models (Gogas, 2006), indicating NMDA receptor signalling does play a key role in the pathological changes associated with chronic pain. It has been demonstrated that

sustained noxious input from the periphery can alter membrane expression and subunit composition of AMPA receptors (Tao, 2012); painful stimulation results an increase in the expression of GluA1 at the neuronal membrane but a decrease in GluA2 (Park et al., 2008;Collingridge et al., 2004), resulting in enhanced permeability to Ca^{2+} and facilitating nociceptive plasticity (Hartmann et al., 2004). Potentiating the effects of glutamate is not the only effect of neuropeptides in central sensitisation. The release of SP from the central terminals of primary afferents is enhanced by noxious peripheral stimulation (Go and Yaksh, 1987) which, in turn, leads to increased signalling through its receptor, NK1. The expression of NK1 on lamina I interneurons is substantial (Cheunsuang and Morris, 2000) and the activation of this GPCR enhances the release of peptide neurotransmitters (Malcangio and Bowery, 1994;Lever et al., 2003) which contributes to wind up (Herrero et al., 2000). Additionally, approximately eighty percent of lamina I projection neurons express the NK1 receptor (Todd et al., 2000), and activation here results in an increase of nociceptive signalling to higher brain regions. CGRP, which shows *de novo* expression in the central terminals of medium and large A-fibres following injury, potentiates the effects of SP (Woolf and Wiesenfeld-Hallin, 1986), enhances BDNF release (Buldyrev et al., 2006) and, via activation of post-synaptic CGRP receptors, activates PKA and PKC signalling pathways (Sun et al., 2003) that can alter protein transcription, thus resulting in the altered expression of various ion channels and receptors in dorsal horn neurons. BDNF, following activation of its receptors on neurons enhances NMDA receptor mediated transmission (Kerr et al., 1999) and activates several intracellular signalling pathways, including MAPK (Pezet et al., 2002a), that contributes to altered neuronal protein expression.

Although originally considered to only represent an increase in excitatory synaptic strength and neuronal excitability, it is now understood that central sensitization also consists of loss of

inhibition in the spinal cord (von Hehn et al., 2012). Peripheral nerve injury results in a loss of GABA-ergic currents in the dorsal horn (Janssen et al., 2011) thought to be due to the excitotoxic loss of GABA-ergic interneurons (Scholz et al., 2005); furthermore a reduction in glycinergic inhibitory currents is also observed in the dorsal horn (Moore et al., 2002), again attributed to a loss of inhibitory interneurons (Scholz et al., 2005). Additionally BDNF reduces the expression of the KCC2 ion transporter which results in the reduced inhibitory efficacy of GABA due to an alteration in neuronal anion gradient (Coull et al., 2005;Coull et al., 2003;Miletic and Miletic, 2008), and an increase in nociceptive discharge to higher brain regions is associated with a loss descending inhibitory activity (Viisanen and Pertovaara, 2007;Saade and Jabbur, 2008).

Whilst the neuronal changes occurring the in the CNS following peripheral nerve injury are pronounced, chronic pain states are no long considered to be diseases of purely neuronal origin, and the pro-nociceptive activation of glial cells within the spinal cord is now a hot topic. Glial cells constitute approximately seventy percent of the cells in the brain and spinal cord and consist of microglia (five to ten percent of the glial population) and macroglia (astrocytes and oligodendrocytes) (Vallejo et al., 2010;Milligan et al., 2003); however it is microglia and astrocytes that are of most interest in chronic pain.

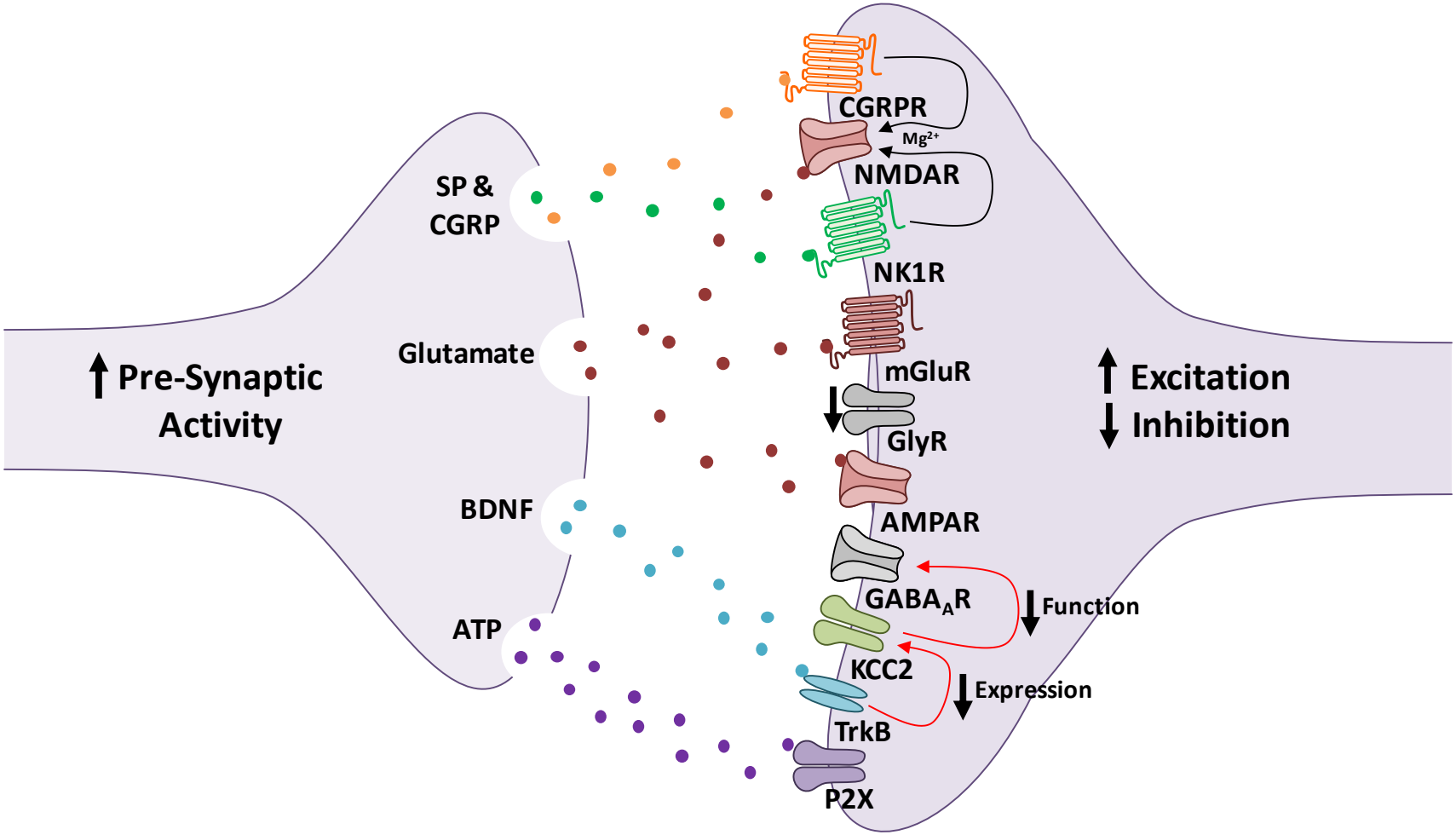

Figure 1.4. Key neuronal players involved in central sensitization. Enhanced pre-synaptic activity and phenotypic switching of primary afferents leads to the release of neurotransmitters and neuropeptides; these activate their specific receptors on the post-synaptic membrane and post-synaptic excitation is enhanced. Activation of TrkB by BDNF decreases KCC2 expression which alters the neuronal anion gradient and reduces the efficacy of GABA; this combined with a reduction in the expression of glycine receptors (GlyR) decreases post-synaptic inhibition.

Microglia are the resident macrophages of the CNS. These cells are of myeloid lineage and invade the CNS during embryogenesis, where they reside physiologically in a 'resting' or 'quiescent' state. Quiescent microglia are characterised by a small soma, expression of receptors for complement components (Fcγ receptor of IgG), low expression of cell surface antigens and the possession of highly motile ramified processes that perform immune surveillance of the surrounding area; it is this that is their main function (Nimmerjahn et al., 2005). In response to injury or insult microglia are rapidly activated, taking on a more amoeboid morphology, altering their expression of a number of cell surface proteins that play a critical role in immune responses, synthesising and releasing inflammatory mediators, and enhancing their proliferative and phagocytic capacity (Davalos et al., 2005;Nimmerjahn et al., 2005;Hanisch and Kettenmann, 2007). This microglial activation, also termed microgliosis, has been documented in a number of models of both inflammatory and neuropathic pain, and is visible immunohistochemically as early as three days after the peripheral injury (Echeverry et al., 2008); however real-time PCR analysis of spinal cord lysates is able to detect changes in the levels of microglial specific mRNA transcripts (e.g. CD11b, TLR4 and CD14) as little as four hours after injury (Tanga et al., 2004). Microgliosis is most abundant in the superficial dorsal horn ipsilateral to the injury in the periphery but is also seen in the ventral horn due to the combination of sensory and motor fibres in the damaged nerve. The temporal profile of microglial activation in the spinal cord following peripheral damage is concomitant with the presence of behavioural hypersensitivity (Zhang et al., 2007;Peters et al., 2007b;Wodarski et al., 2009) and the administration of glial inhibitors attenuate pain in neuropathic models (Clark et al., 2007a;Tawfik et al., 2007), suggesting that microgliosis does indeed contribute to the development of pain. Spinal microglia are activated in a multitude of ways (see figure 1.5) and certainly in models of neuropathic pain it appears that the activating factors arises from an enhanced peripheral drive through primary afferent fibres, as nerve

conduction blockade via the application of local anaesthetic prevents microglial activation (Wen et al., 2007;Hathway et al., 2009;Suter et al., 2009). Microglia possess the receptors for both SP and BDNF (Rasley et al., 2002;Pezet et al., 2002b) that are increasingly released from the central terminals of primary afferents, NMDA and AMPA receptors that are exposed to glutamate released from activated pre-synaptic neurons (McMahon and Malcangio, 2009;Ransohoff and Perry, 2009) and several purinergic receptors, including P2X4 and P2X7 that are substantially upregulated after injury (Tsuda et al., 2003;Chessell et al., 2005). Following peripheral injury the cleavage of CX_3CL1, expressed on neurons in the CNS, is increased; the concentration of the soluble forms of this chemokine in the cerebrospinal fluid of neuropathic animals is considerably higher than that of naive or sham operated animals (Clark et al., 2009). The CX_3CL1 receptor, CX_3CR1, is expressed predominantly on microglia in the brain and spinal cord where it is constitutively expressed and increased by injury (Verge et al., 2004;Milligan et al., 2004;Harrison et al., 1998). Activation of microglial CX_3CR1 is known to be critically involved in the development of neuropathic mechanical allodynia as mice lacking this protein do not develop allodynia following a peripheral nerve injury neither do they show the associated microgliosis (Staniland et al., 2010). Activation of CX_3CR1 results in calcium-dependent activation of P38 MAPK and subsequent release of several pro-nociceptive mediators, including IL-1β, IL-6 and NO (Milligan et al., 2004). Another chemokine, CCL2, has also been hypothesized to activate microglia. Under physiological conditions CCL2 mRNA is almost undetectable in the spinal cord (Zhang et al., 2007;Zhang and De, 2006) (although it is constitutively expressed in DRG neurons (Dansereau et al., 2008)), however following injury CCL2 is upregulated in spinal microglia, astrocytes and small diameter non-peptidergic fibres in the DRG that co-express ATF-3 (Zhang et al., 2007;Dansereau et al., 2008;Abbadie et al., 2003;Ji et al., 2013;Old and Malcangio, 2012). Microglial expression of CCL2's receptor, CCR2, is somewhat debated as recently a CCR2-red fluorescent protein knock-in

mice demonstrated a $CCR2^{+}$ population of cells that did not co-express CX_3CR1 (which is supposedly expressed by all microglia) (Olechowski et al., 2009;Saederup et al., 2010), however increased immunoreactivity for CCR2 has been reported in microglia after injury (Abbadie et al., 2003) and CCL2 does increase microglial immunoreactivity for OX42 (Thacker et al., 2009). As with CX_3CL1, CCR2 contributes to enhanced nociceptive transmission via the release of pro-nociceptive mediators. Furthermore it is able to enhance EPSCs and potentiates NMDA and AMPA currents within the spinal cord (Gao et al., 2009), and additionally may contribute to the development of deregulation of GABA-ergic transmission; co-exposure of DRG neurons to CCL2 and GABA results in a rapid concentration-dependent reduction of GABA-ergic induced inward current (Gosselin et al., 2005;Old and Malcangio, 2012) .In addition, it has been demonstrated that several cytokines, such as those released from activated microglia themselves, can activate microglial cells, thus there may be positive feedback-dependent activation of microglia following injury. For example, the IFNγ receptor (IFNγR) co-localises with microglial markers in the spinal cord following an injury known to increase the expression of IFNγ (Tanga et al., 2005); furthermore it has been demonstrated that IFNγ can activate microglia *in vitro* (Hanisch and Kettenmann, 2007). Additionally, IFNγ induced hypersensitivity and microgliosis can be prevented by the administration of the microglial inhibitor minocycline and $IFN\gamma^{-/-}$ mice do not develop microgliosis following injury (Tsuda et al., 2009).

The predominant intracellular pathway activated in microglia under neuropathic conditions is the MAP kinase pathway, a family of kinase proteins of which there are three members: ERK, P38 and JNK. Activation of both ERK and P38 is seen in microglia following injury; the expression of phosphorylated ERK (pERK) peaks approximately three days after injury (Zhuang et al., 2005) and the inhibition of its signalling pathway attenuates both injury-induced and diabetes-releated

hypersensitivity (Zhuang et al., 2007;Tsuda et al., 2008). The expression of phosphorylated P38 (pP38) also peaks approximately three days after injury and remains elevated for several weeks, and whilst increased pERK can be seen in neurons and astrocytes as well as microglia following injury, pP38 is found solely in microglia (Jin et al., 2003;Tsuda et al., 2004;Clark et al., 2007b). The activation of both ERK and P38 proteins results in the activation of transcription factors that ultimately mediated an up-regulation of several molecules: IL-1, TNF, IL-6, IL-18, NO, CX_3CL1, CCL2, prostaglandins and BDNF (McMahon and Malcangio, 2009); all of which are pro-nociceptive, this process is summarised below in figure 1.5.

Under physiological conditions, astrocytes play a key role in the maintenance of homeostasis in the CNS. Astrocytes are the most abundant glial cell of the CNS; comprising approximately 40-50% of all glia (Aldskogius and Kozlova, 1998;Cahoy et al., 2008) these cells wrap around the soma of neurons and make contact with hundreds of dendrites (Halassa et al., 2007;Haydon, 2001). Due to the close contact between neurons and astrocytes, astrocytes are able to provide support and nourishment to these cells and assist in the regulation of the extracellular environment around synapses (Gao and Ji, 2010b). Astrocytes play an important role in the regulation of extracellular K^+ and Ca^{2+}, control extracellular neurotransmitter concentrations by actively up-taking any excess and assist in the maintenance of the blood brain barrier (BBB) (Cahoy et al., 2008) and provide neurons with a source of anti-oxidants (Pekny and Nilsson, 2005). In this 'active' state astrocytes possess many thin processes, however following activation, such as that occurring in chronic pain states, these cells undergo hypertrophy and increase their expression of several proteins, including glial fibrillary acid protein (GFAP), which is consequently used as a marker of astrocyte activation (Garrison et al., 1994;Vallejo et al., 2010), vimentin and S100β (a calcium binding peptide) (Ridet et al., 1997;Pekny and Nilsson, 2005); these astrocytes are referred to as 'reactive'. As is the case for

microglia, the activation of astrocytes, often referred to as astrogliosis, has been demonstrated in several models of chronic pain (Garrison et al., 1991;Colburn et al., 1999;Sweitzer et al., 1999), and the administration of astrocytic inhibitors, such as fluorocitrate, attenuates pain behaviours in many of these models (Milligan et al., 2003;Watkins et al., 1997;Okada-Ogawa et al., 2009). Furthermore, mice deficient in the astrocytic protein GFAP develop a shorter lasting pain phenotype than wild-type mice and the administration of a GFAP anti-sense mRNA reverses established neuropathic pain (Kim et al., 2009), indicating that this protein, and astrocyte activation, play a critical role in the maintenance of a pain phenotype following injury. Supportively, astrogliosis typically occurs several days after injury and is much longer lasting than microgliosis (Colburn et al., 1999;Tanga et al., 2004;Romero-Sandoval et al., 2008).

Astrocytes can be activated via a multitude of pathways. They possess a number of neurotransmitter receptors including NMDA, mGluR, SP and CGRP receptors (Porter and McCarthy, 1997) that allow them to be activated by increased transmitter release following injury. In fact it has been demonstrated that increased GFAP expression after injury or inflammation requires the NMDA receptor and neuronal activity (Guo et al., 2007;Garrison et al., 1994). Additionally astrocytes express several chemokine and cytokine receptors that can be activated by mediators released from activated microglia; IL-18 released from activated microglial activates the IL-18R on the surface of astrocytes which is upregulated following injury (Miyoshi et al., 2008) and TNFα, also released from microglia, activates astrocytic TNFR in a similar fashion (Gao et al., 2009;Gao et al., 2010b), as does CCL2 via CCR2 (Gao et al., 2009).

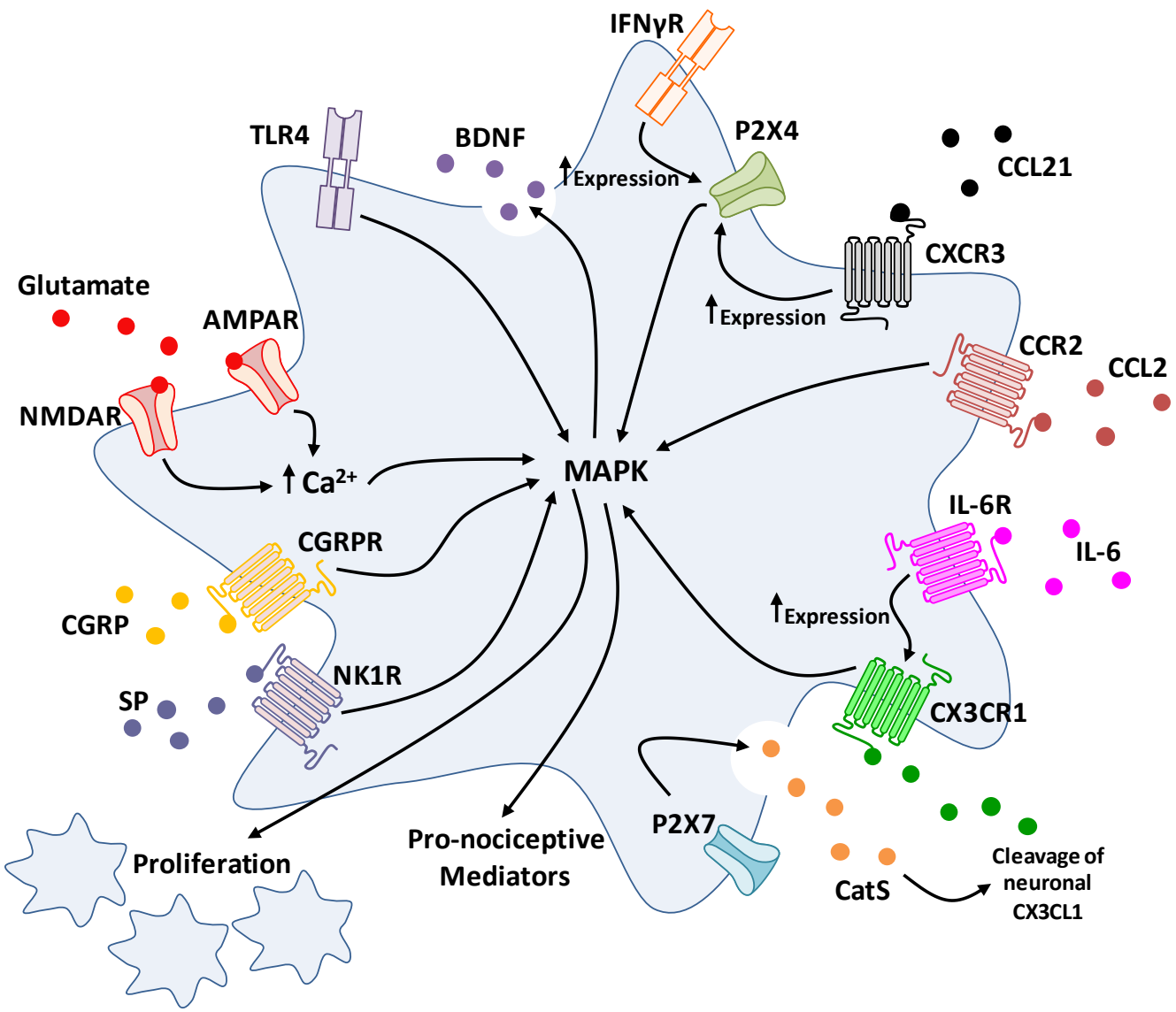

Figure 1.5. Examples of mechanisms of microglial cell activation in models of pain. Activation of the IFNγ and CXCR3 receptors leads to upregulation of the P2X4 ion channel, activation of which results in activation of MAPK signalling pathways that result in the release of pro-nociceptive mediators such as BDNF. Activation of CCR2, TLR4, CGRP and NK1 receptors has similar results. CatS is released from microglial in a P2X7-dependent manner; CatS cleaves neuronal CX_3CL1 which in turn activates CX_3CR1 on the microglial surface, which leads to downstream MAPK signalling. Microglia also possess NMDA and AMPA glutamate receptors which when activated lead to an increase in intracellular calcium levels and subsequent activation of signalling proteins.

Whilst astrocytes undergo many changes following activation, there are two that are likely to be responsible for the contribution of these cells to pain. Following an initial increase after nerve injury, the astrocytic expression of the glutamate transporters GLT1 and GLAST decreases (Sung et al., 2003;Wang et al., 2008;Xin et al., 2009;Tawfik et al., 2008), and as the inhibition of glutamate transporters causes an elevation in spinal extracellular glutamate concentrations (which elicits nociceptive hypersensitivity) (Liaw et al., 2005;Weng et al., 2006), it is reasonable to suggest that this decrease in expression contributes to pain via an increase extracellular concentration of this excitatory neurotransmitter. Additionally, reactive astrocytes express phosphorylated JNK (pJNK) and ERK (pERK) (Zhuang et al., 2006;Gao et al., 2010a;Weyerbacher et al., 2010) that, in a similar fashion to pERK and pP38 in microglia, stimulate the release of a variety of pro-inflammatory mediators via the activation of transcription factors. These mediators include IL-1β which regulates the phosphorylation of the NMDA receptor (Guo et al., 2007;Tsakiri et al., 2008) and increases COX-2 expression in neurons (Samad et al., 2001) and CCL2 which activates CCR2 on neurons (that is upregulated following injury) which increases the frequency of EPSCs and enhances NMDA and AMPA induced inward currents (Gao et al., 2009). JNK signalling in particular dominates pain-astrogliosis research as JNK activation in astrocytes regulates the expression and release of several cytokines and chemokines (Gao and Ji, 2010b). JNK phosphorylation in astrocytes has been demonstrated to increase the expression of COX-2 and iNOS as well as the release of NO, prostaglandin E2 and IL-6 (Falsig et al., 2004) all of which are pro-nociceptive. Increased expression of pJNK in astrocytes is seen in models of both neuropathic and inflammatory pain (Ma and Quirion, 2002;Svensson et al., 2007;Gao et al., 2010a) and its inhibition via the administration of the JNK inhibitors SP600125 or D-JNK1-1 can suppress pain behaviours in models of peripheral nerve injury and diabetes-induced neuropathic pain (Zhuang et al., 2006;Daulhac et al., 2006).

2.2.4.3. Higher Centre Modulation

Sensory output from the dorsal horn is relayed to higher processing centres in the brain by ascending pathways; however there are also a number of descending pathways from these regions that are involved in the modulation of pain transmission, and indeed many of these regions have been shown to contribute to the development and/or maintenance of neuropathic pain.

Despite a wealth of evidence supporting the involvement of cerebral cortical and sub-cortical areas of the brain in humans in pain modulation, relatively few animal studies have attempted to example the role of these regions in chronic pain; however a number of regions have been shown to influence pain modulation in this setting (extensively reviewed in (Saade and Jabbur, 2008)). A transient reduction of thermal hyperalgesia and mechanical and cold allodynia has been demonstrated by blockade of signalling in the ventral orbital area, attributed to a reduction in dopaminergic transmission (Baliki et al., 2003). A similar effect can be observed by altering dopaminergic transmission in the insular cortex; here D1 and D2 receptors play a pro-nociceptive and anti-nociceptive role respectively, via reception of dopaminergic inputs from the amygdala and RVM (Jasmin et al., 2003a;Jasmin et al., 2003b;Ohara et al., 2003;Coffeen et al., 2008). The amygdala itself shows substantial plastic changes in neuropathic models, where amongst other mechanisms, fear reactions regulated in this region can enhance pain through inhibition of descending inhibitory pathways from the locus coeruleus (Viisanen and Pertovaara, 2007;Saade and Jabbur, 2008), which are themselves enhanced by an increase in nociception evoked discharges (Saade and Jabbur, 2008). Although the thalamus does not have descending projections to the brain stem or spinal cord, experimental evidence indicates a role for this brain region in chronic pain; thalamic electrical stimulation produces analgesia in both animals (Dickenson, 1983) and humans (Hosobuchi et al., 1973;Mazars, 1975). Furthermore, electrical stimulation of the

ventral posterolateral nucleus of the thalamus abolishes mechanical allodynia in a rat model of nerve injury without altering the nociceptive thresholds of the contralateral paw (Kupers and Gybels, 1993). One of the most understood descending pathways involved in nociceptive modulation is that of the PAG and RVM. A reduction in descending inhibition from the PAG has been demonstrated in neuropathic animals (Pertovaara et al., 1997), whilst prolonged exposure to noxious stimuli produces nociceptive facilitation in the RVM via an increase in discharge from 'on-cells'; it is thought that an alteration in the ratio of activated 'on' and 'off' cells contributes to hyperalgesia (Morgan et al., 1994;Morgan and Fields, 1994;Saade and Jabbur, 2008). Moreover, inhibition of this facilitation by the injection of lidocaine into the RVM attenuates pain behaviours in neuropathic animals (Pertovaara et al., 1996). Recent animal studies have identified a descending facilitatory projection from the PAG that relays pro-nociceptive signals to the RVM, by enhancing spinal transmission of inputs from the periphery; activation of this system has been associated with the development of hyperalgesia, for example by cholecystokinin (CCK) released from midbrain structures in response to chronic input from nociceptive pathways (Carlson et al., 2007;Heinricher et al., 2004;Tillu et al., 2008;Lovick, 2008). An increase in CCK in the PAG is also thought to contribute to the development of morphine tolerance and its associated development of mechanical allodynia and thermal hyperalgesia (Xie et al., 2005).

3. Chemotherapy induced neuropathy

3.1. Symptoms and Incidence

Chemotherapy-induced neuropathy first came to light in the late 1960's when clinicians observed evidence of neuropathy in leukaemia patients receiving treatment with vinca alkaloids (Sandler et al., 1969). Further study of such patients revealed a loss of the ankle-jerk reflex and paraesthesias (abnormal sensation e.g. tingling) in the fingers and toes that begun following VCR treatment and recovered somewhat with dose reduction (Casey et al., 1973). In the years that followed similar studies identified populations of patients treated with other chemotherapeutic agents, primarily taxanes and platinum containing compounds, which displayed similar symptoms despite their varying anti-neoplastic mechanisms.

One of the most problematic symptoms, with all neuropathy-inducing agents, is pain (Tofthagen, 2010). Two recent studies asked patients to describe the pain they were experiencing; the average patient rated it as a seven out of ten in severity (Dougherty et al., 2004) and assigned 'throbbing, 'sharp', and 'burning' properties to the pain (Dougherty et al., 2007). Pain reporting in chemotherapy-receiving patients is consistent and can occur as early as four days after the first administration of the chemotherapeutic agent (Loprinzi et al., 2011). Pain is described as both spontaneous (Tofthagen, 2010) and occurring as a result of a stimulus, typically cold and mechanical hypersensitivity (Binder et al., 2007). The most prevalent symptoms of chemotherapy-induced painful peripheral neuropathy reported are paraesthesias and dysesthesia (loss of sensation) which occur consistently across varying chemotherapy treatment protocols (Kautio et al., 2011), and can be spontaneous or cold induced (Driessen et al., 2012;Attal et al., 2009). Also commonly reported is a loss of vibratory sensation (Berger et al., 1997), a general reduction in

sensory function in the hands (Kautio et al., 2011), alterations in taste (Strasser et al., 2008), thermal hyperalgesia (Binder et al., 2007), pharyngolarygeal dysesthesia (Argyriou et al., 2013b) and, in patients receiving very high doses of chemotherapeutics, muscle weakness (Tofthagen, 2010). Symptoms are typically experienced in the hands and feet in what is described as a glove and stocking distribution (Dougherty et al., 2007) and commonly extend as far as the wrists and ankles. Additionally this tends to be symmetrical; patients report symptoms of equal severity on the left and right side of the body (Dougherty et al., 2004). Clinically neuropathy is graded based on its severity; the most commonly used scale to score chemotherapy-induced neuropathy is the National Cancer Institute Common Toxicity Criteria (NCI-CTC), which is summarised in the table below.

The incidence of neuropathy occurrence following chemotherapy varies greatly across patient populations and studies, likely due to variation in the drugs themselves and the treatment regimens they are given as part of. Neuropathy resulting from treatment with taxanes has been reported in as few as 35% of patients in a study of patients receiving docetaxel for primary breast cancer (Eckhoff et al., 2011) and as many as 97% of patients in a study of those receiving PTX for the same type of cancer (Tanabe et al., 2013). Chemotherapy-induced neuropathy has been reported in an excess of 85% of patients treated with the platinum-based oxaliplatin for colorectal cancer (Briani et al., 2013), and in a similar number of patients treated with the vinca alkaloid VCR for B cell lymphoma (Kim et al., 2010).

Table 1.4. NIC-CTC neuropathy grading. (Adapted from (Postma and Heimans, 2000))

Scale	Neuropathy - Sensory	Neuropathy - Motor
Grade 0	Normal.	Normal.
Grade 1	Loss of deep tendon reflexes or paraesthesias (including tingling) but not interfering with function	Subjective weakness, no objective findings.
Grade 2	Objective sensory loss or paraesthesias interfering with function but not interfering with activities of daily living.	Mild objective weakness interfering with function but not interfering with activities of daily life.
Grade 3	Sensory loss or paraesthesias interfering with activities of daily living.	Objective weakness interfering with activities of daily live.
Grade 4	Permanent sensory loss that interferes with function.	Paralysis.

It was noted early in the study of this condition that the neurotoxicity associated with chemotherapeutics is dose related and cumulative (Legha, 1986), in fact the dose of chemotherapy received is one of the key factors in predicting the likelihood of a patient developing a neuropathy; patients receiving a high dose per cycle show a greater incidence of neuropathy than low dose receiving patients. For example a prospective study by Postma and colleagues identified neuropathic symptoms in 50% of patients receiving 135mg/m^2/cycle of PTX for ovarian cancer, whilst 100% of patients treated with 250-300mg/m^2/cycle of PTXl for breast cancer experienced neuropathy (Postma et al., 1995). The incidence of neuropathy increases with treatment duration (Augusto et al., 2008) and the number of cycles received. For example a 2004 study of patients being treated for a variety of solid mass tumours found 15% of patients were experiencing neuropathy at the end of a single cycle of chemotherapy, 75% at the end of the

second cycle and 100% of patients experienced some degree of neuropathy by the end of a fourth cycle of their treatment (Dougherty et al., 2004).

In addition to agent and dose, several factors have been suggested to increase the likelihood of a patient developing neuropathy following chemotherapy. Age is a frequently occurring factor in determining the incidence of chemotherapy-induced neuropathy; several studies have reported an increased incidence or increased severity of neuropathy in elderly patients, particularly those over 70 years old (Cen et al., 2012;Johnson et al., 2011).The evidence however, is not conclusive; a recent study by Argyrious and colleagues reported no correlation between age and incidence in their cohort of patients (Argyriou et al., 2013a). The effect of diabetes on incidence is also debated; studies have provided both evidence for (Brunello et al., 2011) and against (Picozzi et al., 2011) an increased incidence of chemotherapy-induced neuropathy in diabetic or hypoglycaemic patients. It has been suggested that malnourishment and hypoalbuminemia, common in cancer patients, may result in patients developing more severe neuropathy than better nourished patients (Arrieta et al., 2010). Several gene polymorphisms have been associated with the development of neuropathy as a result of chemotherapy. These include a greater incidence of a singly nucleotide polymorphism in the *tac1* gene (encoding the tachykinin precursor) in patients with chemotherapy-induced neuropathy compared to non-neuropathic disease matched controls (Won et al., 2012), and a lower incidence in patients with a polymorphism in the *cyb1b1*3* allele which is associated with taxane turnover in the liver. The results of this latter study is supported by evidence of inhibitors of the protein cytochrome p450 (which is involved in drug metabolism) increasing the severity of bortezomib-induced neuropathy (Iwamoto et al., 2010).

Chemotherapy-induced neuropathy is a substantial clinical problem to both oncologists and patients. Neuropathic patients report worse quality of life scores, especially in physical function and pain categories, than non-neuropathic chemotherapy-receiving patients (Kim et al., 2010). In addition, the neuropathy can become severe enough to require dose reduction or complete cessation of treatment, which can directly impact a patient's ability to survive the cancer. Neuropathy has been reported as the dose-limiting side effect in an excess of 70% of people in some patient populations (Postma et al., 1995), and causes treatment to be cessed in between 20% (Briani et al., 2013;Dougherty et al., 2007) and 40% (Bennett et al., 2012) of patients receiving some treatment regimens. In those patients that don't require cessation of treatment and subsequently survive their cancer, symptoms of neuropathy can persist and continue to have an effect on their quality of life. Symptoms of PTXl-induced neuropathy have been reported to persist for as long as 3 years after completion of treatment (Tanabe et al., 2013), VCR neuropathy as long as 4 years after treatment (Dougherty et al., 2007), and a 2009 study of oxaliplatin treated patients calculated the average half life of recovery from the neuropathy was a staggering 6.8 years (Brouwers et al., 2009). Treatment of chemotherapy-induced neuropathy is a critical part of the medical management of cancer patients, current treatment options are discussed below.

3.2. Prevention and Treatment of Chemotherapy Induced Neuropathy

As the mechanism by which chemotherapy-induced neuropathy (discussed below) has not been fully elucidated, the neuropathy itself cannot be treated; rather clinicians aim to manage the most problematic of symptoms, pain. This is primarily done with classical analgesics, however the efficacy in this condition is varied, and a number of patients continue to report pain. In fact the average pain score of patients receiving daily doses of gabapentin, paracetamol, naproxen,

codeine or morphine (in excess of 85mg/day) was three out of ten (Dougherty et al., 2007;Dougherty et al., 2004) and only 75% of patients with bortezomib-induced neuropathy report decreased pain intensity whilst taking control release oxycodone (Cartoni et al., 2012). These statistics are supported by work in rodent models of chemotherapy pain (discussed below) where opioid treatment has mixed results; transiently attenuating some aspects of pain, such as tactile allodynia, in some studies (Park et al., 2013), but not all (Bujalska et al., 2009). However, there does appear to be a higher response rate to opiates in rodents than in humans, but this may be an artefact of the type of pain assessed; whilst rodents are assessed for stimulus induced pain, patients report spontaneous pain.

Gabapentin and pregabalin, traditionally used as anti-epileptics, are used routinely to treat various chronic pain conditions, and chemotherapy-pain is no different. In various rodent models of this condition both gabapentin and pregabalin are able to attenuate established chemotherapy-induced mechanical and cold allodynia (Guindon et al., 2013), however this does not translate fully into the clinic; whilst some patients respond well to this therapy, showing improvement of 1-2 neuropathy grades (Saif et al., 2010), a substantial percentage of patients do not respond, and report post-gabapentin pain scores of four out of ten, no different to placebo treated patients (Vondracek et al., 2009;Rao et al., 2007). Several other anti-epileptic drugs, such as lacosamide, valproate, lamotrigine and oxcarbazepine have shown pain reducing efficacy in animal models of chemotherapy pain (Geis et al., 2011;Rodriguez-Menendez et al., 2008), but their results haven't translated to patients, where these drugs are only partially successful in reducing neuropathy (Rao et al., 2008;Argyriou et al., 2006). SSRI (selective serotonin re-uptake inhibitor), SNRI (selective norepinephrine re-uptake inhibitor) and TCA (tricyclic) anti-depressants fair slightly better; these drugs decrease pain in many (Smith et al., 2013;Katsuyama et al., 2013;Kanbayashi et al., 2013),

although not all (Kautio et al., 2008) patients. Whilst they can have some undesirable side-effects such as nausea and tiredness, patients treated with anti-depressants report increases in quality of life score independent of successful pain management (Kautio et al., 2008).

Trials of several other therapies have been undertaken for the treatment of chemotherapy induced pain with varying results, highlighting the difficulties clinicians face in treating this condition. Several studies have indicated infusions of calcium and magnesium could reduce the incidence of neuropathy in colorectal cancer patients treated with oxaliplatin by half and a recent meta-analysis has supported this; incidence of grade 3 (severe) neuropathy is significantly lower in patients that receive calcium/magnesium infusions than the control group without significant alterations in efficacy of the chemotherapy itself (Gamelin et al., 2004;Wen et al., 2013). On the other hand, whilst initial studies suggested glutathione treatment could prevent a decrease in nerve conduction velocity caused by cisplatin (Hamers et al., 1993) and reduce the incidence of neuropathy in oxaliplatin treated patients (Cascinu et al., 2002), a 2011 Cochrane review found that overall there was insufficient evidence to support a neuroprotective effect of glutathione (Albers et al., 2011). The same review found no neuroprotective effect for vitamin E, which had been observed in some (Pace et al., 2010;Argyriou et al., 2005a), but not all (Afonseca et al., 2013;Kottschade et al., 2011) studies to reduce the incidence and severity of neuropathy occurring as a result of chemotherapy. Additionally, glutamine has been demonstrated to reduce the number of patients requiring chemotherapy dose-reduction as a result of neuropathy (Wang et al., 2007), calcium channel blockers to decrease the incidence of acute neuropathy after oxaliplatin treatment (Tatsushima et al., 2013) and the anti-oxidant N-acetylcysteine to decrease the incidence of oxaliplatin neuropathies of all severities (Lin et al., 2006).

Despite these positive studies, chemotherapy pain patients are still poorly managed due to a lack of drugs with complete efficacy in treating the condition. The above studies look at improvement in the overall incidence of neuropathy, be it a reduction in sensory loss or stimulus induced pain, but patients still complain of spontaneous pain (Dougherty et al., 2004). The underlying problem is that these drugs are primarily treating the symptoms of the neuropathy and are not treating or preventing the neuropathy itself. In order to develop drugs prevent the development of chemotherapy-induced painful peripheral neuropathy, we first need to understand the mechanism by which chemotherapeutic agents cause neuropathy, thus allowing the identification of novel drug targets that allow management of the neuropathy and subsequent pain, without interfering with the anti-neoplastic mechanisms of the chemotherapeutics.

3.3. Modelling Chemotherapy Induced Neuropathy

Patient studies have allowed us to gain some understanding of the pathophysiology occurring as a result of chemotherapy-induced neuropathy. Repeatedly patients report pain and mechanical and cold hypersensitivity and this appears to correlate with electrophysiological abnormalities; symptomatic VCR-neuropathy patients show an abnormal amplitude of sural sensory nerve action potentials and a decrease in sensory nerve conduction velocity which is not seen in patients that don't experience symptoms of neuropathy (Krishnan et al., 2005). This is a common finding across chemotherapeutic regimens (Krarup-Hansen et al., 2007) and has been found to persist, along with pain, beyond the administration of the chemotherapeutic agent (Argyriou et al., 2005b;Ramchandren et al., 2009). Often in patients that do not exhibit a decrease in conduction velocity electrophysiological abnormalities are evident; concentric needle electromyography has demonstrated evidence of denervation of the small muscles in the hand, which is associated with

prolonged mean distal latencies and decreased mean amplitudes of compound muscle action potentials (Pal, 1999). Conversely, nerve conduction and EMG studies have revealed evidence of sensory nerve hyper-excitability which is not reversed by carbamazepine (Pal, 1999;Wilson et al., 2002). The physical properties of the nerves themselves are altered in neuropathic patients; sural nerve biopsies have provided evidence of a loss of large-diameter fibres with both axonal and myelin degeneration (Roelofs et al., 1984). Intraepidermal nerve fibre density is reduced in the distal limbs, where symptoms are most commonly reported (Burakgazi et al., 2011) and ultrasound assessment of the nerves of symptomatic patients has shown enlargement of the nerve at median and ulna entrapment site (Briani et al., 2013).

Whilst this information gives us a starting point, and indicates that chemotherapeutic agents are indeed having a substantial effect on the nervous system, animal models are required to allow the underlying pathology associated with this condition to be studied in detail. Three models are commonly used in the laboratory for such work and are based on four different neuropathy causing agents; PTX, cisplatin or oxaliplatin and VCR. The features of these models are described below and are summarised at the end of the section in table 1.5.

The PTX model of chemotherapy-induced peripheral neuropathy is primarily a rat model and is established by the repeated intraperitoneal administration of PTX. Two dosing regimens are common, both using a dose of between 0.5 and 2mg/kg given either on alternate (Polomano et al., 2001) or consecutive days (Naguib et al., 2012). This results in mechanical and cold allodynia and hypersensitivity, without an effect on motor co-ordination (Polomano et al., 2001). PTX treated rats have decreased sensory nerve conduction velocities (Gilardini et al., 2012;Wozniak et al., 2011), associated with both Aβ and C fibres (Zhang and Tuckett, 2008), a decrease in the

amplitude of sensory compound action potentials (Leandri et al., 2012) and an increase in spontaneous firing of both A and C fibres (Xiao and Bennett, 2008). PTX decreases the density of myelinated fibres and causes myelinated fibre degeneration in the sciatic nerve (Kawashiri et al., 2009), as well as a loss of intraepidermal nerve fibres (Siau et al., 2006). This evidence, gathered approximately four weeks after PTX treatment, indicates neuronal damage; this is supported by an increase ATF3 (a neuronal stress marker) immunoreactivity in the DRG one week after treatment (Jamieson et al., 2007).

Similarly the oxaliplatin and cisplatin models of chemotherapy-induced neuropathy, whilst possible in a mouse, are predominantly studied in the rat. Both oxaliplatin and cisplatin models are comparable to one another in their primary features due to these compounds being of the same class of chemotherapeutic agents. Typically given as a high dose once or twice a week for four weeks (Deng et al., 2012) or as a lower dose daily for up to three weeks (Di Cesare et al., 2012), the platinum compounds produce robust cold and mechanical allodynia without altering responses to heat (Guindon et al., 2013). As shown by electrophysiology studies these animals exhibit a decrease in sensory nerve conduction velocities (Gilardini et al., 2012), a reduction in sensory action potential amplitude (Renn et al., 2011) and spontaneous activity in wide dynamic range neurons (Cata et al., 2008). Oxaliplatin treatment has also been demonstrated to cause neuronal atrophy, increase eccentric nucleoli in DRG neurons (Renn et al., 2011) and reduce intraepidermal nerve fibre density in the skin (fifteen and thirty days after the onset of treatment) (Boyette-Davis and Dougherty, 2011).

VCR can be used to cause chemotherapy-induced neuropathy in both the rat and mouse. In both instances it is administered daily for approximately two weeks (sometimes with a break to divide

treatment into two cycles) at a dose of between 0.1 and 0.5mg/kg/day intraperitoneally (mouse) or intravenously (rat) (Aley et al., 1996;Uceyler et al., 2006). In rodents VCR administration in this fashion causes severe dose-dependent mechanical allodynia and hyperalgesia (Aley et al., 1996;Fukuizumi et al., 2003;Kiguchi et al., 2008b). Thermal hypersensitivity is common (Hansen et al., 2011;Uceyler et al., 2006) but not always present in these animals (Rahn et al., 2007). Similarly to PTX and the platinum-based compounds, VCR treatment is associated with altered electrophysiological properties of sensory nerve fibres. VCR causes a subset (41%) of C-fibres in the saphenous and cutaneous nerves to become hyper-responsive and fire in an irregular pattern with altered action potential timing (Tanner et al., 2003). A and C fibres show increased spontaneous firing (Xiao and Bennett, 2012) and a delayed F wave latency post VCR (Geis et al., 2011). Additionally, it has been demonstrated that VCR causes decreased conduction velocity of (sciatic) sensory nerves (Alimoradi et al., 2012), a decrease in the amplitude of compound action potentials, reduction in myelin thickness and fibre diameter in the sciatic nerve (Callizot et al., 2008) and a reduction in intraepidermal nerve fibre density (three weeks after VCR administration) (Siau et al., 2006). Furthermore, an increase in ATF-3 immunoreactivity in the DRG several weeks after treatment (day 19) has also been reported (Hansen et al., 2011).

Table 1.5. A summary and comparison of the main features of chemotherapy-neuropathy in patients and animal models

Feature	Present in humans	Present in PTX model	Present in platinum models	Present in VCR model
Spontaneous pain	✓	Not Known	Not Known	Not Known
Mechanical hypersensitivity	✓	✓	✓	✓
Thermal hypersensitivity	✓	✘	✘	✓
Cold hypersensitivity	✓	✓	✓	✓
Decreased conduction velocity in sensory nerves	✓	✓	✓	✓
Spontaneous A and/or C fibre firing	Not Known	✓	✓	✓
Reduction in action potential amplitude	✓	✓	✓	✓
Reduction in myelin	✓	✓	Not Known	✓
Reduction in intra-epidermal nerve fibre density	✓	✓	✓	✓
Neuronal atrophy	Not Known	Not Known	✓	Not Known
Increased ATF-3 expression in the DRG	Not Known	✓	Not Known	✓

3.4 The mechanism by which chemotherapeutics cause neuropathy

Whilst chemotherapeutic agents have varying mechanisms of action, the neuropathic symptoms they produce in patients and animal models are similar. As such we can use these animal models to tease out mechanisms by which these agents may be causing the neuropathy independently of their anti-neoplastic effects. When the existing literature is examined several research areas are prevalent and will be discussed here; the endocannabinoid system, ion channels, reactive oxygen species and anti-oxidants, TRP channels and the contribution of the immune system, both peripheral and central.

3.4.1 The endocannabinoid system in chemotherapy-induced neuropathy

The endocannabinoid system has recently emerged as a source for novel analgesics for the treatment of chronic pain (Guindon and Hohmann, 2009;Rahn and Hohmann, 2009). To date the two best studied endocannabinoids are AEA (anandamide) and 2-AG (2-arachidonoylglycerol); both are arachidonic acid metabolites derived from phospholipids of the cell membrane. AEA and 2-AG exert their biological actions by binding to and activating to the G-protein coupled CB1 or CB2 receptors. CB1 receptors are found predominantly within the CNS, within areas of the brain associated with pain processing; these include the PAG, amygdala (Herkenham et al., 1991), thalamus (Matsuda et al., 1993) and DRG (Hohmann and Herkenham, 1999). The CB2 receptor on the other hand is found predominantly in the peripheral immune system (Howlett et al., 2004); however recent evidence has found this receptor to be expressed at low levels on both neurons and non-neuronal cells in the CNS and upregulated in chronic pain states (Beltramo et al., 2006;Wotherspoon et al., 2005) . Agonists of both the CB1 and CB2 receptors are analgesic in models of chronic pain (Yu et al., 2010;Naguib et al., 2008) and antagonists of these receptors can

block this beneficial effect (Tumati et al., 2012;Romero et al., 2013). The synthesis of the endocannabinoids is well characterised; fatty-acid amide hydrolase (FAAH) is the principle catabolic enzyme for AEA (Cravatt et al., 1996), whilst 2-AG is hydrolysed (although not exclusively) by monoacylglycerol lipase (MAGL) (Blankman et al., 2007). Inhibiting the normal function of these enzymes, thus preventing endocannabinoid metabolism, attenuates pain behaviours in neuropathic (Kinsey et al., 2010) and inflammatory (Ghosh et al., 2013;Booker et al., 2012) models of pain.

Due to the clear involvement of the endocannabinoid system in chronic pain signalling, the role of this system in chemotherapy-induced pain has been investigated and the emerging evidence supports a contribution; chemotherapy alters endocannabinoid tone and its correction can attenuate pain. Cisplatin administration reduces AEA levels in the plantar paw skin and intradermal administration of AEA (following cisplatin) can locally attenuate subsequent mechanical hyperalgesia in these animals (Khasabova et al., 2012). Increasing the endogenous levels of AEA and 2-AG available to bind CB1 and CB2 receptors by administration of FAAH or MAGL inhibitors attenuates pain behaviours in cisplatin (Guindon et al., 2013) and VCR (Caprioli et al., 2012) treated rats. This effect is receptor dependent; pre-treatment with a CB1 or CB2 antagonist prevents the anti-nociceptive effects of these inhibitors (Guindon et al., 2013), but has no effect on chemotherapy-induced pain when give alone (Khasabova et al., 2012). Evidence suggests both CB1 and CB2 receptors play a role in the analgesic effect of endocannabinoids in chemotherapy pain; the administration of both CB1 and CB2 agonists can prevent and reverse pain in these models (Naguib et al., 2012;Rahn et al., 2007;Burgos et al., 2012).

So how are the endocannabinoids modulating pain behaviour after chemotherapy treatment? One possible explanation is that the system provides neurons protection from the damaging effects of chemotherapeutic agents. *In vitro* experiments have demonstrated that incubation of DRG neurons with cisplatin causes a reduction in neurite length and that this effect can be blocked by pre-treatment with a CB1 agonist. Furthermore, *in vivo* cisplatin causes the conduction velocities of A-fibres to decrease, and increases TRPV1 and ATF-3 immunoreactivity in the DRG; this can be prevented by concomitant administration of a FAAH inhibitor (Khasabova et al., 2012). There is also evidence to suggest the endocannabinoids modulate pain by suppressing pro-nociceptive activity of non-neuronal cells in the CNS. PTX treatment is associated with an increase in CD11b (microglial marker) and GFAP (astrocytic marker) immunoreactivity in the spinal cord (Burgos et al., 2012;Naguib et al., 2012) that can be attenuated by pre-treatment of animals with the CB2 agonist MDA7. This attenuation is prevented by prior administration of a specific CB2 antagonist, suggesting the effects of MDA7 are via direct activation of CB2 receptors (Naguib et al., 2012). The administration of PTX is associated with enhanced expression of iNOS, IL-1β, IL-6 and TNF-α in spinal glial cells (it is reduced by the glial inhibitor minocycline) that can be prevented by a mixed CB1/2 agonist (Burgos et al., 2012). Crucially the pro-nociceptive effects of cannabinoid modulators do not appear to interfere with the anti-neoplastic actions of chemotherapeutics; concomitant administration of CB1/2 agonists and PTX did not reduce cancer cell death compared to PTX treatment alone (Naguib et al., 2012).

3.4.2 Sodium, Potassium and Calcium in chemotherapy-induced neuropathy

The regulation of ion flux by specific channels is critical for the normal function of the nervous system in terms of both action potential propagation and intracellular signalling. Ion channels play

a key role in determining the excitability of nociceptive neurons, hence altered function leads to aberrant pain signalling such as that occurring in chronic pain states.

Voltage-gated sodium channels (VGSC) are responsible for the propagation of action potentials, including those transmitting painful signals from the periphery to the CNS, which can be demonstrated by the anti-nociceptive effects of sodium channel blocking anaesthetics (Levinson et al., 2012). Moreover, altered expression and function of VGSCs is thought to contribute to neuronal hyperexcitability associated with pain following nerve injury (Docherty and Farmer, 2009). Alterations in the properties of sodium channels have been documented in patients following chemotherapy treatment; patients assessed before and after a single dose of oxaliplatin exhibit altered refractoriness (associated with sodium channel inactivation/activation state) in both sensory and motor axons of the median nerve (Park et al., 2011;Krishnan et al., 2006). As such, sodium channel blockers can be used to attenuate pain in models of chemotherapy pain; they completely reverse both mechanical and cold allodynia in oxaliplatin treated rats (Egashira et al., 2010) and significantly attenuate mechanical hyperalgesia in VCR treated rats (Nozaki-Taguchi et al., 2001). The mechanism by which sodium channels become disregulated following chemotherapy is not known, however in models of nerve injury sodium channel activity can be altered by several cyto/chemokines (Belkouch et al., 2011;Guillouet et al., 2011) the expression of which can be upregulated by chemotherapeutics (Kiguchi et al., 2008a).

Potassium channels are activated by altered membrane potential, allowing efflux of K^+ ions to hyperpolarize the membrane back to its resting potential (Maljevic and Lerche, 2012). During the propagation of the action potential, potassium channels play a key role in nociceptive signalling, and their altered expression has been associated with chronic pain states (Tsantoulas et al.,

2012;Costigan et al., 2010). Whilst evidence for an involvement of these channels in chemotherapy-pain is scarce, it has been reported that cisplatin administration causes membrane depolarization that can be partially prevented with the K_v7 agonist retigabine (Nodera et al., 2011). Additionally pre-treatment with the potassium sparing diuretic amiloride reduces the severity of mechanical and cold hypersensitivity in VCR treated rats (Muthuraman et al., 2008).

Calcium ions have several important functions in the nervous system. Calcium channels are involved in the propagation of action potentials, control of neuronal excitability and neurotransmitter release (Iftinca and Zamponi, 2009). Abnormal calcium homeostasis is thought to significantly contribute to the pain by altering sensory neuron function (Fernyhough and Calcutt, 2010). Increased activity of T-type calcium channels has been associated with neuropathic pain states (Todorovic and Jevtovic-Todorovic, 2007) and their knock-down has been reported to antagonise neuropathic pain (Choi et al., 2007). Ca^{2+} acts as intracellular signalling molecule; it is released from intracellular stores as a response to various stimuli including chemokine receptor signalling or enters the cell via ion channels e.g. NMDA receptors, and its signalling cascades can result in the release of pro-nociceptive mediators from both neuronal and non-neuronal cells (Old and Malcangio, 2012). Modulation of calcium function certainly appears to contributes to chemotherapy-induced pain; patients treated with calcium channel blockers exhibit a reduced incidence of the development of neuropathy (Tatsushima et al., 2013) and the T-type calcium channel antagonist ethosuximide significantly reverses established PTX-hyperalgesia in rats (Flatters and Bennett, 2004). It is likely that chemotherapeutics alter calcium function in terms of both channel activity/neuronal excitability and intracellular signalling, as calcium entry blockers prevent cisplatin-induced decreases in sensory nerve conduction velocities (Hamers et al., 1991) and platinum-containing compounds increase Ca^{2+}/calmodulin dependent protein kinase II

(CaMKII) phosphorylation in the spinal cord, which can be attenuated by a calmodulin inhibitor (Shirahama et al., 2012).

3.4.3 ROS, NOS and anti-oxidants in chemotherapy-induced neuropathy

Reactive oxygen species (ROS) are generated physiologically as a by-product of normal cellular activity; however should an imbalance arise between the production of these species and ability of the system to reduce and detoxify them oxidative stress occurs, and ultimately leads to damage of the cell. Anti-oxidants are able to reduce pain and have beneficial effects on nerve conduction velocities in neuropathic patients (Sima, 2007), indicating oxidative stress may occur in the nervous system of these patients. This is supported by pre-clinical work which has demonstrated an overproduction of ROS in lumbar neurons following spinal cord injury that leads to symptoms of neuropathic pain in the hind paws of rats. Furthermore, this can be attenuated by the administration of ROS scavengers (Gwak et al., 2013).

If the anti-oxidant status of patients is assessed before and after the commencement of chemotherapy significant changes are observed. Chemotherapy decreases total anti-oxidant status and decreases erythrocyte superoxide dismutase and glutathione peroxidase levels, indicative of an increase in ROS (Esfahani et al., 2012). 60% of patients with established PTX or cisplatin neuropathy showed an improvement of at least 2 neuropathy grades after 8 weeks of treatment with the anti-oxidant acetyl-L-carnitine, a naturally occurring amino acid derivative that plays a critical role in the transport of free fatty acids into mitochondria (Rebouche, 2004); patients reported less pain and chemotherapy-induced slowing of sensory nerve conduction velocities was partially reversed (Bianchi et al., 2005). This improvement is also seen in animal models of chemotherapy-pain, where acetyl-L-carnitine is able to prevent or attenuate neuropathic pain

behaviours and electrophysiological changes following PTX (Flatters et al., 2006), oxaliplatin (Pisano et al., 2003) and cisplatin (Ghirardi et al., 2005a;Ghirardi et al., 2005b), without any significant impact on the anti-neoplastic actions of the drugs (Ghirardi et al., 2005a). The administration of antioxidants aims to prevent oxidative stress by shifting the balance of pro- and anti-oxidants to favour the anti. An alternative method is to scavenge excess ROS before it can cause damage, and this is also effective in attenuating chemotherapy pain; the non-specific ROS scavenger PBN reduces both cold and mechanical hypersensitivity occurring as a result of PTX treatment when given as a delayed treatment, and prevented its onset when prophylactically (Fidanboylu et al., 2011).

There are multiple sources of ROS production in nervous tissue, and whilst invading immune cells produce ROS as a mechanism of destroying pathogens, the major source of intracellular ROS is leakage from mitochondria (Schapira and Cooper, 1992). This leakage is likely to be increased following chemotherapy due to mitochondrial dysfunction. Following chemotherapy treatment in rats, nerve fibres exhibit an increase in abnormal, swollen mitochondria (Flatters and Bennett, 2006) and deficits in mitochondrial electron transport chain complexes I and II are observed (Zheng et al., 2011;Zheng et al., 2012). Treatments with compounds that specifically inhibit these mitochondrial complexes dose-dependently attenuate pain behaviours (Joseph and Levine, 2006). Furthermore, if PTX or cisplatin are applied to cultured DRG neurons they cause mitochondrial dysfunction that manifests as a loss of membrane potential, and results in the formation of autophagic vacuoles in the cells (Melli et al., 2008). Peroxynitrite, the product of superoxide and nitric oxide, is increased in the spinal cord following chemotherapy which leads to nitration of GLT-1 and glutamine synthase, rendering them ineffective at clearing glutamate from the synapse. This, in turn, leads to glutamate excitotoxicity. Targeting peroxynitrite formation directly or

indirectly (by reducing nitric oxide production with L-NAME [non-selective NOS inhibitor] or superoxide production with a NADPH oxidase inhibitor) prevents these effects and attenuates PTX-induced mechanical allodynia (Doyle et al., 2012). In the CNS, NOS lies downstream of NMDA receptor activation, thus glutamate excitotoxicity as a result of protein nitration would contribute to a positive feedback mechanism that results in the production of NO, which in turn is available to react with superoxide to form peroxynitrite. Inhibition of this process by antagonism of the NMDA receptor reverses established oxaliplatin-induced mechanical allodynia (Tatsushima et al., 2011). Evidence of oxidation of proteins is also observed in oxaliplatin treated rats as an increase in plasma, spinal cord and peripheral nerve levels of carbonylated protein, a marker of protein oxidation. This oxidative damage can be prevented by the co-administration of antioxidants with the chemotherapeutic, which also attenuates both mechanical and thermal hypersensitivity (Di Cesare et al., 2012).

3.4.4 TRP channels in chemotherapy-induced neuropathy

The TRP family of proteins consists of 28 members sub-divided into 7 sub-families: TRPA, TRPC, TRPML, TRPN, TRPP and TRPV (Clapham et al., 2003;Montell et al., 2002). These channels are widely expressed in a variety of excitable and non-excitable cells within mammalian tissues and mediate flux of cations (Ca^{+}/Na^{+}) across the cell membrane (Ramsey et al., 2006). TRP channels can be activated by a broad range of ligands, including small organic molecules, lipids or productions of lipid metabolism (Ramsey et al., 2006) and even ROS (Andersson et al., 2008). A role for TRP channels in pain transduction was initially suggested based on evidence that indicated that TRPV1 is activated by noxious heat (Caterina et al., 1997), and subsequently several other TRP channels have been found to play a role in the transmission of thermal and pain sensation (Patapoutian et al., 2009). Under chronic and inflammatory pain conditions these channels can be

upregulated (Urano et al., 2012), for example NGF released as a result of inflammation activates p38 in sensory neurons leads to a down-stream increase in TRPV1 expression and transport of this protein to peripheral terminals (Ji et al., 2002). Knock-down or knock-out of TRPs can prevent the development of pain behaviours in animal models of chronic pain (Katsura et al., 2006;Kwan et al., 2006;Caterina et al., 2000;Bolcskei et al., 2005). As such these channels have become the target for the development of novel analgesics, and have had some success in pre-clinical models in chronic and inflammatory pain (Vilceanu et al., 2010;Eid et al., 2008). Additionally, in patients potent TRPV1 agonists, despite initially being noxious, cause desensitisation of the channel which reduces nociceptive transmission and sensitivity to heat (Novakova-Tousova et al., 2007;Simpson et al., 2008).

As in neuropathic pain, there is evidence to suggest a role for TRP channels (specifically TRPA1, TRPV1, TRPV4 and TRPM8) in chemotherapy-pain. Following incubation with cisplatin or oxaliplatin, cultured DRG neurons increase their expression of TRPA1, V1 and M8; a similar increase in TRPA1 and TRPV1 expression is also observed in the trigeminal ganglia of cisplatin treated mice (Ta et al., 2010). In chemotherapy pre-treated cultures, DRG neurons exhibit a dose-dependently reduction in neurite length, an increase in cAMP signal intensity and increased responses to a TRPV1 or TRPA1/M8 agonist (Anand et al., 2010). TRPA1 can be activated by ROS (Andersson et al., 2008) which are produced as a consequence of chemotherapy (see above), and it has been suggested that activation of TRPA1 by chemotherapeutic agents is indirect; indeed the calcium responses induced by oxaliplatin in TRPA1 transfected cells is ablated by a ROS scavenger (Nassini et al., 2011). Furthermore, the pain behaviours occurring as a result of chemotherapy treatment can be attenuated by both the blockade (Nassini et al., 2011;Materazzi et al., 2012;Barriere et al., 2012) and knock-out of TRPA1 (Trevisan et al., 2013). Antagonists of TRPV1

(Chen et al., 2011) and TRPV4 (Materazzi et al., 2012;Chen et al., 2011) are also able to reduced chemotherapy induced pain and TRPV4 knock-out mice exhibit less mechanical hypersensitivity after PTX treatment than wild-types (Alessandri-Haber et al., 2008).

3.4.5 The contribution of non-neuronal cells and cyto/chemokines to chemotherapy-induced neuropathy

As discussed above, neuropathic pain is no longer considered a disease purely of neuronal origin; a substantial body of evidence supports a critical role for non-neuronal cells of both the PNS and CNS in the development and maintenance of chronic pain states, and chemotherapy pain is no exception. In the periphery, following chemotherapy administration, macrophages infiltrate the nerve and DRG where they take on a hypertrophied activated appearance (Jimenez-Andrade et al., 2006;Peters et al., 2007a;Uceyler et al., 2006). Whilst the signal for this infiltration is not yet fully understood, we do know that activated macrophages are capable of releasing a multitude of mediators, such as TNF-α (Niu et al., 2012;Dumitru et al., 2000), that can have a direct effect on sensory neurons (Pollock et al., 2002). Within the spinal cord, chemotherapy administration causes the activation of astrocytes, demonstrated by an increase in the astrocytic marker GFAP (Warwick and Hanani, 2013;Naguib et al., 2012); this is associated with a down regulation of GLAST and GLT-1, proteins involved in the maintenance of glutamate homeostasis by astrocytes, and can be prevented by the systemic administration of minocycline, an inhibitor of cytokine synthesis (Zhang et al., 2012). Spinal astrocyte gap junctions, that allow communication between cells, are likely to contribute to the activation of astrocytes in chemotherapy-pain as blockade with carbenoloxone dose-dependently attenuates mechanical hypersensitivity in a rat model of oxaliplatin-induced neuropathy (Yoon et al., 2013). In some chemotherapy-pain models microgliosis is evident; an increase in OX-42 immunoreactivity in the dorsal horns of the cervical

and lumbar spinal cord sections is observed in PTX treated rats (Ledeboer et al., 2007), and this can be suppressed by the phosphodiesterase and adenosine reuptake inhibitor propentofylline, which also attenuates pain behaviours following daily systemic administration (Sweitzer et al., 2006). In fact in young animals severe gliosis correlates with neuropathic symptoms (Ruiz-Medina et al., 2013).

As in many non-chemotherapy models of chronic pain, several cytokines and chemokines have been identified as possible contributors to pain following chemotherapy. Serum levels of IL-6 are elevated in patients following chemotherapy (Pusztai et al., 2004), especially in those experiencing neuropathic pain symptoms as a result. These patients have higher levels of the interleukin-6 receptor (IL-6R) on $CD14^{+}$ cells and lower serum levels of soluble gp130 (a protein that forms part of the function complex of the IL-6R) than patients with low neuropathy scores (Starkweather, 2010). In animal models this increase in IL-6 expression is also present, and co-localises with macrophage markers in the peripheral nerve and DRG. Local injection of an IL-6 neutralising antibody attenuates pain behaviour (Kiguchi et al., 2008b); in support of this evidence for a role of macrophage derived IL-6 in the development of chemotherapy-induced pain, IL-6 knock-out mice show a reduced incidence of mechanical allodynia following VCR treatment in comparison to wild-type littermate controls (Kiguchi et al., 2008b). Conversely, at low doses IL-6 treatment can prevent the behavioural and electrophysiological abnormalities caused by VCR (Callizot et al., 2008), providing evidence for both pro- and anti-nociceptive effects of this cytokine in chemotherapy-pain. This is in keeping with the literature regarding this molecule; it can be neuroprotective (Akaneya et al., 1995) and in non-chemotherapy models of chronic pain there are reports of attenuation of pain with both treatment with IL-6 (Andriambeloson et al., 2006;Flatters et al., 2004;Flatters et al., 2003) and molecules that inhibit its function (Guptarak et al., 2013;Wei

et al., 2013). It has been reported that levels of TNF-α are unaltered in the spinal cord and brain of PTX treated animals (Zhang et al., 2012;Parvathy and Masocha, 2013). Indeed, patients receiving chemotherapy do not have an increased plasma TNF-α level (Pusztai et al., 2004) and treatment with etanercept, a competitive binder of TNF-α does not reverse established pain; however pre-treatment with this compound can delay the onset of chemotherapy-pain (Park et al., 2013). Following chemotherapy plasma levels of IL-10 are significantly increased, however this is transient (Pusztai et al., 2004) and intrathecal administration of a plasmid that enhances the expression of this anti-inflammatory cytokine prevents is able to reverse established chemotherapy-induced mechanical allodynia (Ledeboer et al., 2007). Spinal levels of the chemokine CCL2 are upregulated following chronic PTX treatment and treatment with a CCR2 (but not CCR1) antagonist can attenuate pain behaviour (cold allodynia), whilst a CCL2 neutralising antibody can suppress chemotherapy-induced activation of microglia (Pevida et al., 2013).

3.4.6 Other contributing factors

Whilst the evidence discussed above constitute the majority of work attempting to determine the mechanism by which chemotherapy causes neuropathy, the use of various inhibitors/antagonists has suggested a great many other pathways may be involved, that don't fit into such neat categories.

Briefly, an increase in the mRNA of the bradykinin B1 receptor is observed in the thalamus and pre-frontal cortex seven days after administration of PTX, and both the administration of B1 or B2 antagonists, or the double knock-out of the B1 and B2 receptors, reduces hyperalgesia in mice treated with this chemotherapeutic agent (Costa et al., 2011) or VCR (Bujalska et al., 2008b). Chronic oxaliplatin therapy has been associated with upregulation of PKCγ in the thalamus and

PAG of rats, and a supraspinally administered specific PKCγ inhibitor reverses hyperalgesia in these animals (Norcini et al., 2009). PKCε and PKA inhibitors are also anti-allodynic (Dina et al., 2001), as are $5HT_3$ antagonists (Whitaker-Azmitia et al., 1995). Alpha-1- and alpha-2-adrenoceptor antagonists are anti-nociceptive and delay the onset of hyperalgesia in a model of VCR-induced neuropathy (Bujalska et al., 2008a), Rho kinase inhibitors improve sural nerve conduction latencies and return sensory thresholds to pre-chemotherapy levels (James et al., 2010), and P38 and ERK inhibition reduce apoptosis of cisplatin-treated DRG neurons (Scuteri et al., 2009).

Despite this wealth of evidence, the precise mechanism by which chemotherapeutic agents cause neuropathy remains elusive, preventing the development of an ideal compound for the prevention of this condition.

4. Thesis Aims

The general aim of the work laid out in this thesis is to delineate the mechanism by which repeated cycles of the anti-neoplastic drug VCR cause pain, and to identify novel therapeutic targets for the treatment of this condition; in particular we hypothesis that infiltrating immune cells significantly contribute to the development of chemotherapy induced pain. The aim of chapter two is to characterise a mouse model of VCR-induced painful peripheral neuropathy and to establish the major changes occurring in both the PNS and CNS. In chapter three changes observed in the PNS are further explored, and the contribution of infiltrating monocyte/macrophages and the CX_3CL1 receptor CX_3CR1 is determined. Chapter four aims to ascertain the contribution CX_3CL1 itself and changes in endothelial adhesion properties make to the development of pain in the model. In summary, the work in this thesis utilises a variety of *in vivo* and *in vitro* techniques such as behavioural assays, immunohistochemistry and western blotting to examine the hypothesis that it is the occurrence of a chain of peripheral non-neuronal changes that instigates the development of chemotherapy-induced painful peripheral neuropathy the occurs following the repeated administration of VCR.

Chapter 2:

Characterisation Of A Mouse Model of Vincristine - Induced Painful Peripheral Neuropathy

1. Introduction

1.1. Vincristine Sulphate: Origin, Clinical Use and Mechanism of Action

Vincristine sulphate (VCR) is a naturally occurring plant alkaloid originally extracted from the leaves of the periwinkle plant, *Catharanthus roseus*. It has been known for its medicinal properties for centuries; extracts from the plant have been used historically to stop haemorrhage, treat scurvy and heal wounds and diabetic ulcers (Gidding et al., 1999). The potent chemotherapeutic nature of this compound was first identified in the late 1950's following a observation by Noble and colleagues that rats treated with an extract of *C.roseus* caused peripheral granulocytopenia and bone marrow suppression (Noble et al., 1958). Additionally Svoboda et al demonstrated anti-leukaemic properties of this extract (Svoboda, 1958), it was able to cure leukaemia and prolong life with an acceptable range of side-effects; this extract was demonstrated to be VCR (Svoboda et al., 1962).

Initial studies in man proved promising (Costa et al., 1962) and VCR was approved by the FDA as Oncovin in 1969. VCR is a widely used and potent anti-neoplastic agent. Its primary use is in the treatment of Hodgkin's and non-Hodgkin's lymphoma and childhood and adult leukaemias such as acute lymphoblastic leukaemia (ALL). The response rate to VCR in the first-line treatment of these diseases is as high as 76-92 % if treatment is completed (Gidding et al., 1999;O'Brien et al., 2013). VCR is also used to treat a variety of solid mass tumours including small cell lung carcinoma (42% first-line response rate) and cervical carcinomas (23% first-line response rate) (Gidding et al., 1999).

The primary mechanism by which VCR inhibits tumour growth is by binding to and stabilising tubulin, resulting in interference with mitotic spindle formation and leading to an inhibition of mitosis (Malawista et al., 1968;Himes et al., 1976;Owellen et al., 1976). It has also been demonstrated that VCR can induce apoptosis of cancerous cells *in vitro* independent of cell cycle phase (Takano et al., 1993;Pittman et al., 1994) and can reduce tumour blood flow resulting in necrosis (Baguley et al., 1991;Hill et al., 1993). It is not yet understood if it is by similar mechanisms that VCR causes neuropathy. As well as forming mitotic spindles, tubulin is also a major component of microtubules which form the cytoskeleton of cells; in neurons these microtubules play a critical role in the axonal transport of survival factors to peripheral nerve terminals, and it has been hypothesised that disruption of this process results in neuronal death. Early evidence has suggested binding of VCR to microtubules causes a reduction in their number (Donoso et al., 1977) as well as disruption of their normally highly organised structure (Topp et al., 2000). Several electrophysiological changes in the peripheral nerves support a role for neuronal damage as the causative factor in the development of pain; following VCR administration rats exhibit a reduction in nerve conduction velocity (Alimoradi et al., 2012) and hyper-responsiveness develops in A and C fibres (Tanner et al., 2003). Furthermore, an increase in the expression of the neuronal stress factor ATF-3 has been observed in the DRG of VCR treated mice (Hansen et al., 2011). However the precise mechanism by which VCR is inducing these changes is not known and using currently available immunohistochemical techniques neuronal damage has not been observed in the very early stages of the development of VCR-induced hypersensitivity. As such some of the focus of the research in this field has shifted to involvement of non-neuronal cells which as now known to significantly contribute to the development of pain in a number of models of neuropathic pain.

1.2. Non-Neuronal Cells in VCR-Induced Neuropathy

As discussed in chapter one there is clear evidence for a role of non-neuronal cells, both centrally and peripherally in the instigation and maintenance of neuropathic pain. Here three key cell types will be discussed (macrophages, microglia and astrocytes) as there is evidence to suggest these cells contribute to VCR-induced hypersensitivity and/or allodynia.

1.2.1. Macrophages

Macrophages are mononuclear phagocytic cells that differentiate from circulating peripheral blood mononuclear cells (PBMCs/monocytes) under steady state conditions to replenish tissue resident cells or in response to inflammation. PBMCs derive from a common myeloid progenitor in the bone marrow that is the precursor of many different cells (figure 2.1) (Mosser and Edwards, 2008).

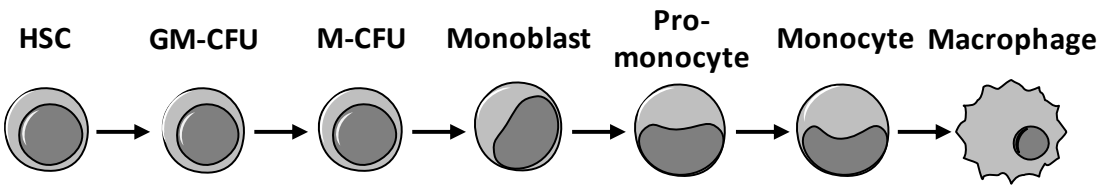

Figure 2.1. Macrophage derivation. Macrophages differentiate from monocytes, which originate in the bone marrow from a common haematopoietic stem cell (HSC) which undergo differentiation steps that commit them to a myeloid and then monocytic lineage via granulocyte/macrophage colony-forming units (GM-CFU) and macrophage colony-forming units (G-CFU). (Adapted from (Mosser and Edwards, 2008)).

Monocytes are a heterogeneous population of cells and as such, so are macrophages; varying size, degree of granularity, nuclear morphology and expression of surface markers (Gordon and Taylor, 2005). Tissue or resident macrophages play a predominantly homeostatic role; these mature cells are involved in immune surveillance. They are involved in the clearance of cellular debris following tissue damage or remodelling, maintaining healthy tissue by removing toxic materials and are able to recruit and activate lymphocytes (and other immune cells) in response to danger signals such as lipopolysaccharide components of bacterial cell walls. Tissue resident macrophages also play an important role in suppressing inflammation mediated by infiltrating inflammatory monocytes, thus restoring tissue homeostasis following injury or infection (Murray and Wynn, 2011). Resident macrophages are crucial for the early detection of tissue damage; however following injury or infection their numbers in tissue are insufficient to mount a full response and monocytes enter the damaged tissue (monocyte/macrophage heterogeneity and infiltration is discussed in detail in chapters three and four). Under physiological conditions, the cellular debris cleared by macrophages is primarily produced by apoptosis results in little or no production of inflammatory mediators (Kono and Rock, 2008), however following trauma or cellular stress, debris is produced by cells undergoing necrotic death. This has a marked effect on the activation state of macrophages as it contains danger signals such as nuclear proteins and cleaved components of the extracellular matrix (Zhang and Mosser, 2008).

Two key macrophage subsets have been described based on their physiology following activation. Classically activated or M1 macrophages are primarily activated through toll-like receptors, PPARγ (peroxisome proliferator-activated receptor γ) signalling and interaction with the cytokines IFNγ (interferon-γ) and TNFα; these cells show enhanced microbicidal activity and increased synthesis and release of pro-inflammatory mediators including nitric oxide (NO), free radical species and

cytokines (e.g. TNFα, IL-1β and IL-6) (Murray and Wynn, 2011;Dale et al., 2008), a result of which is further macrophage activation. Alternatively activated or M2 macrophages on the other hand are predominantly activated by IL-4 or IL-13 and express arginase-1, CD206 and, unsurprisingly, the IL-4 receptor. These cells produce growth factors including TGFβ (transforming growth factor β) and PDGF (platelet-derived growth factor) (Barron and Wynn, 2011) and anti-inflammatory cytokines such as IL-10. They promote wound healing by producing matrix metalloproteinases (MMPs), thus contribute to the production of extracellular matrix components (Kreider et al., 2007) and as such have been referred to as 'wound-healing macrophages' (Mosser and Edwards, 2008).

Current evidence suggests that macrophages contribute to the development of pain behaviours under pathological conditions. The infiltration of monocyte/macrophages into the peripheral nerve following injury is seen in both humans and rodents (Durrenberger et al., 2006;Durrenberger et al., 2004;Lindenlaub and Sommer, 2000;Hu and McLachlan, 2002). Our laboratory has demonstrated that depletion of monocyte/macrophages by administration of liposome clodronate partially attenuates the mechanical and thermal hyperalgesia following peripheral nerve injury for as long as monocyte/macrophages are absent; once cell numbers are restored (examined in the spleen) this effect is lost (Barclay et al., 2007;Liu et al., 2000). Furthermore, the depletion of monocyte/macrophages in the knee joint of mice significantly reduces joint inflammation and the production of pro-inflammatory cytokines (Blom et al., 2004). In both human patients and animal models the peripheral administration of inhibitors of the pro-inflammatory cytokines released by classically activated macrophages attenuates pain (Dahl and Cohen, 2008;Kato et al., 2009;Gabay et al., 2011). Selectively reducing cytokine/chemokine expressing macrophages in the nerve similarly impairs the development of neuropathic pain (Echeverry et al., 2013).

There is evidence for a role of macrophages in models of chemotherapy-induced pain. Following the administration of both VCR or PTX and increase in the number of macrophages in the sciatic nerve and DRG is observed (Jimenez-Andrade et al., 2006;Peters et al., 2007a;Uceyler et al., 2006). These cells take on a hypertrophied activated appearance; an increased in the expression of CD68, a lysosomal protein present in activated macrophages (Holness and Simmons, 1993) has been reported in the sciatic nerve of rats ten days after PTX treatment (Peters et al., 2007a). Furthermore these cells exhibit a hypertrophied and multi-vacuolated appearance (indicative of activated phagocytic macrophages) when compared to the small macrophages present in the nerves of vehicle treated animals (Peters et al., 2007a;Hu and McLachlan, 2002). Whilst it has not yet been possible to assess monocyte/macrophage infiltration in the peripheral nerves of chemotherapy-treated patients, an increased serum level of IL-6 has been reported in patients treated with the agents PTX, 5-fluorouracil and doxorubicin (Pusztai et al., 2004); this cytokine is released from classically activated macrophages (Mosser and Edwards, 2008), and suggests these cells may be activated in chemotherapy-treated patients. Despite this evidence, the signal for macrophage infiltration as a result of chemotherapy has not been elucidated, and the temporal profile of infiltration is not known.

1.2.2. Microglia

Microglia are specialised macrophages of the CNS and constitute between 5-20% of the total glial cell population (depending on the region examined) (Saijo and Glass, 2011). Similarly to macrophages they are of a myeloid lineage; this has been confirmed conclusively by their absence from the CNS in PU.1-null mice (McKercher et al., 1996). PU.1 is a key transcription factor in the control of myeloid cell differentiation (Beers et al., 2006). Recent findings suggest microglia originate from macrophages in the foetal yolk sac that migrate into the CNS early on during

embryonic development (Saijo and Glass, 2011); however there is also evidence from postnatal rodent studies using fluorescently labelled cells that suggest that, at least in the early stages of postnatal development, microglia can differentiate from monocytes entering the CNS from the circulation (Perry et al., 1985). In adult rodents circulating monocytes are able to enter the CNS under conditions where there is disruption to the blood brain barrier (BBB) (King et al., 2009), however evidence obtained from immune-irradiated mice indicate that CNS colonisation by these cells is transient and does not contribute to the resident microglial cell pool (Ajami et al., 2011). The resident microglia population is maintained by proliferation of existing microglia rather than by infiltration of monocytes; thymidine labelling of cells demonstrates that the cells are able to undergo DNA synthesis and divide (Lawson et al., 1992). Regardless, some uncertainty remains in this area.

Under physiological conditions microglia exist in a 'resting' or 'quiescent' state, characterised by a small soma, expression of receptors for complement components (Fcγ receptor of IgG), low expression of cell surface antigens and possession of highly motile ramified processes that perform immune surveillance of the surrounding area (Nimmerjahn et al., 2005); as a result of this function the new terminology of 'surveying' microglia has been suggested (Hanisch and Kettenmann, 2007) as this important function means these cells are far from resting. Several mechanisms by which these cells maintain a quiescent state have been suggested, including interaction of microglial CX_3CR1 with its neuronal ligand CX_3CL1 (Callizot et al., 2008), and inhibitory signalling through the microglial cell surface proteins (typically integrins/lectins) CD172, CD200R and CD45 with their neuronal ligands CD47, CD200 and CD22 respectively (Ransohoff and Cardona, 2010). In response to injury or pathological insult, such as the presence of pathogens or neurotoxic levels of glutamate for example, microglia quickly become activated and proliferate to

expand their population. Activated microglia are morphologically distinct from quiescent cells; they appear more amoeboid, with a hypertrophied cell body and thick retracted processes. Following activation these cells alter their expression of a number of cell surface antigens that play a critical role in immune responses; for example expression of MHC class II is increased allowing the presentation of antigens by microglia. These cells have an enhanced proliferative and phagocytic capacity (McMahon and Malcangio, 2009), and once activated synthesise and secrete a variety of pro-inflammatory mediators into the extra-cellular environment including cytokines (e.g. TNFα and IL-1β), chemokines (e.g. CCL2 and CX_3CL1), reactive oxygen species (ROS) and nitric oxide (NO). Current evidence does suggest that the activation state of microglia is somewhat flexible; different stimuli activating different receptors may result in varied downstream cascades, for example glutamate activating mGLUR2 results in the production of TNFα, whilst activation of P2Y receptors by UDP leads cells to adopt a predominantly phagocytic phenotype (Clark et al., 2012;McMahon and Malcangio, 2009;Calvo and Bennett, 2012;Ellis and Bennett, 2013;Graeber and Christie, 2012;Milligan et al., 2001;Inoue and Tsuda, 2009).

The evidence for a role of microglia (and astrocytes) in the development and maintenance of chronic pain is extensive, has been reviewed umpteen times in the past decade and has been summarised in chapter one (Inoue and Tsuda, 2009;Clark et al., 2012;McMahon and Malcangio, 2009;Calvo and Bennett, 2012;Ellis and Bennett, 2013;Schomberg and Olson, 2012;Vallejo et al., 2010). Briefly, in models of peripheral nerve injury (Colburn et al., 1997;Coyle, 1998;Beggs and Salter, 2007), inflammatory pain (Clark et al., 2007a;Hua et al., 2005) and disease pathology (Tsuda et al., 2008;Wodarski et al., 2009;Clark et al., 2012) there is substantial evidence of microgliosis (the activation and proliferation of microglia) in the dorsal horn of the spinal cord. Inhibiting microgliosis with the glial inhibitor minocycline prevents or attenuate mechanical and thermal

hypersensitivity in these models (Ledeboer et al., 2005;Lin et al., 2007;Raghavendra et al., 2003;Hua et al., 2005) indicating that this process is critical to the development and/or maintenance of hypersensitivity following peripheral nerve damage. The attenuation of hypersensitivity occurring as a result of peripheral nerve damage has also been demonstrated in animals deficient of key microglial proteins, such as CX_3CR1 (Staniland et al., 2010) and by the intrathecal administration of inhibitors of pro-nociceptive mediators released from activated microglia (Clark et al., 2007b).

As with macrophages, there is evidence to support a role for microglia in the development and/or maintenance of chemotherapy-induced pain. Following administration of PTX the immunoreactivity of the microglial marker OX-42 is increased in the dorsal horns of cervical and lumbar spinal cord sections (Ledeboer et al., 2007). This can be suppressed by the phosphodiesterase and adenosine reuptake inhibitor propentofylline, which also attenuates mechanical allodynia following systemic administration (Sweitzer et al., 2006). Additionally chemotherapy-induced mechanical allodynia can be reversed by intrathecal administration of IL-1RA, the receptor antagonist of IL-1β, which is released from microglia following their activation (Ledeboer et al., 2007). However, microgliosis has not been reported in all models of chemotherapy-induced neuropathy and the involvement of microglia in the pathogenesis of this condition remains controversial.

1.2.3. Astrocytes

Astrocytes are the most abundant of the glial cells in the CNS and have traditionally been considered to provide little more than structural and homeostatic support to neurons; however as research in the field has evolved the potential of astrocytes as critical participants in intercellular

communication has been recognised, in fact astrocytes have now been implicated to play a role in almost all processes that occur in the CNS (Volterra and Meldolesi, 2005). Derived from the neuroectoderm, these star shaped cells envelope the many neuronal elements, including synapses, axons and dendrites, with each astrocyte able to make contact with several neurons (Halassa et al., 2007;Haydon, 2001), and have an intimate relationship with the endothelial cells of the blood brain barrier (BBB) (Abbott et al., 2006). Astrocytes play a key role in the maintenance of extracellular K^+ concentrations ($[K^+]_o$); physiological fluctuations in $[K^+]_o$ are normal and occur as a result of neuronal activity, however this must be tightly regulated to prevent a pathological build up of K^+ that could cause hyperexcitability in neurons (Scemes and Spray, 2012). $[K^+]_o$ is regulated by astrocytes via several methods of uptake including various ion channels and transporters (predominantly by Na-K-ATPase pumps or Na-K-Cl co-transporters), or by spatial buffering, a process whereby highly K^+ permeable cells (astrocytes) transfer K^+ ions from regions of high $[K^+]_o$ to regions of low $[K^+]_o$ (Kofuji and Newman, 2004). Astrocytes respond to the accumulation of K^+ that results from increased uptake by altering their metabolism; this can be achieved via several mechanism, for example by enhancing glycolysis by the activation of pyruvate carboxylase (Subbarao et al., 1995). One of the features of astrocytes that allows spatial buffering of K^+ is the presence of gap junctions. Gap junctions are intercellular connections comprising two hemi-channels formed of connexin subunits that allow ions and small molecules to pass between cells. In the adult connexins (Cx) 43 and 30 are the predominant connexins found in astrocytes (Dermietzel et al., 1991;Giaume et al., 1991;Nagy and Rash, 2000); dye coupling experiments have demonstrated that no intercellular communication occurs in Cx43/Cx30 double knock-out mice (Wallraff et al., 2006;Rouach et al., 2008). K^+ regulation is not the only homeostatic mechanism that astrocytes play a key role in; they also play a major role in the regulation of extracellular glutamate levels. The majority of glutamate is released into the extracellular space from neurons

as a neurotransmitter following depolarisation, whilst a small quantity is thought to come from astrocytes themselves; recent evidence has demonstrated glutamate release from astrocytes as a result of both Ca^{2+} dependent and independent mechanisms (Araque et al., 2000;Hamilton and Attwell, 2010;Santello et al., 2011). Glutamate is removed from the extracellular space by excitatory amino acid transporters (EAATs), of which two (GLAST and GLT1) are preferentially expressed on astrocytes (Coulter and Eid, 2012). If for any reason this system fails or its capacity is reduced glutamate excitotoxicity can occur; this phenomenon was first described in retinal neurons by Lucas and Newhouse in 1957 (LUCAS and NEWHOUSE, 1957) and later in CNS neurons by Olney and Sharpe in 1969 (Olney and Sharpe, 1969); it describes the process whereby prolonged activation of glutamate receptors leads to cell death.

The contribution of astrocytes to the development of pain subsequent to peripheral nerve damage has been reviewed in chapter one. Briefly, in terms of pain processing, astrocytes have a clear signalling role, forming the pain triad with neurons and microglia (Scholz and Woolf, 2007). This role is not surprising; astrocytes are considered to be excitatory cells, albeit not in the classical sense that describes the activity of neurons; they can however be activated by internal and external signals and release a variety of factors (Volterra and Meldolesi, 2005). Astrocytes express a large number of neurotransmitter receptors and can themselves release neurotransmitters (e.g. glutamate and ATP) as a consequence of an increase in intracellular calcium concentration (Hansen and Malcangio, 2013). A substantial number of non-neurotransmitter receptors are expressed on the surface of astrocytes; these include cytokine (e.g. TNFR and IL-18R) and chemokine receptors (e.g. CCR2) and purinergic receptors (e.g. P2X7), the substrates for which are all known to be released by neurons and glia in the CNS following injury. Activation of these receptors triggers intracellular signalling cascades such as the activation of PLC-β and subsequent

release of Ca^{2+} from intracellular store via IP3 (inositol triphosphate) and phosphorylation (and activation) of MAPK proteins; these are involved in cell survival, transcriptional regulation and the release of pro-nociceptive/inflammatory mediators (Old and Malcangio, 2012). For example the expression of CCL2 is increased in spinal astrocytes after injury, and following its release in a JNK-dependent fashion, activates the CCR2 receptor on the surface of neurons, where it enhances spontaneous EPSCs and potentiates NMDA- and AMPA-induced currents (Gao et al., 2009). Additionally the expression IL-1β is increased in spinal astrocytes in models of both diabetic neuropathy and peripheral nerve injury (Liao et al., 2011;Weyerbacher et al., 2010); release of this protein and its subsequent activation of IL-1 receptors on the surface of neurons potentiates NMDA-induced currents through phosphorylation of the NMDA receptor (Oka et al., 1993;Weyerbacher et al., 2010). Furthermore, IL-1β can activate microglia, causing downstream phosphorylation of MAPK proteins and consequential release of pro-nociceptive mediators (Okuno et al., 2004). Astrogliosis, the activation of astrocytes, occurs within the spinal cord as a result of injury that leads to the development of a chronic pain state. Typically demonstrated by an increase in the immunoreactivity of glial fibrillary acid protein (GFAP), astrogliosis occurs within days of nerve damage following in models of peripheral nerve injury (Colburn et al., 1997;Chen et al., 2012;Zhang et al., 2011b), inflammatory pain (Gao et al., 2010a;Tenorio et al., 2013) and disease pathology (Zhang et al., 2011a;Bas et al., 2012). As with microglia, inhibition of astrocytic activity is able to reverse mechanical allodynia arising as a result of peripheral nerve injury (Gao and Ji, 2010a) and inflammatory hyperalgesia (Guo et al., 2007) and prevent mechanical allodynia when administered prior to nerve transection (Sweitzer et al., 2001). This evidence indicates that astrocyte activation plays a crucial role in the development and/or maintenance of neuropathic and inflammatory pain. Within the spinal cord, astrogliosis (demonstrated by an increase in GFAP immunoreactivity) is evident within a week of the systemic administration of PTX or VCR (Naguib

et al., 2012;Ji et al., 2013;Kiguchi et al., 2008a). As figure 2.2 illustrates, this is associated with an increase in the expression of the pro-nociceptive mediators CCL2 and TNF (Zhang et al., 2013;Kiguchi et al., 2008a), the post-translational nitration of glutamate transporter proteins which reduces their functional capacity (Doyle et al., 2012) and IL-1β induced phosphorylation of the NMDA receptor (Zhang et al., 2008;Weyerbacher et al., 2010). Furthermore, spinal astrocyte gap junctions are likely to contribute to astrocytic activation in chemotherapy-pain as blockade with carbenoloxone dose-dependently attenuates mechanical hypersensitivity in a rat model of oxaliplatin-induced neuropathy (Yoon et al., 2013). Whilst chemotherapy-induced neuropathy appears to be more heavily associated with astrogliosis than microgliosis, there is still much to learn about the role of this cell type in the development and maintenance of chronic chemotherapy-pain.

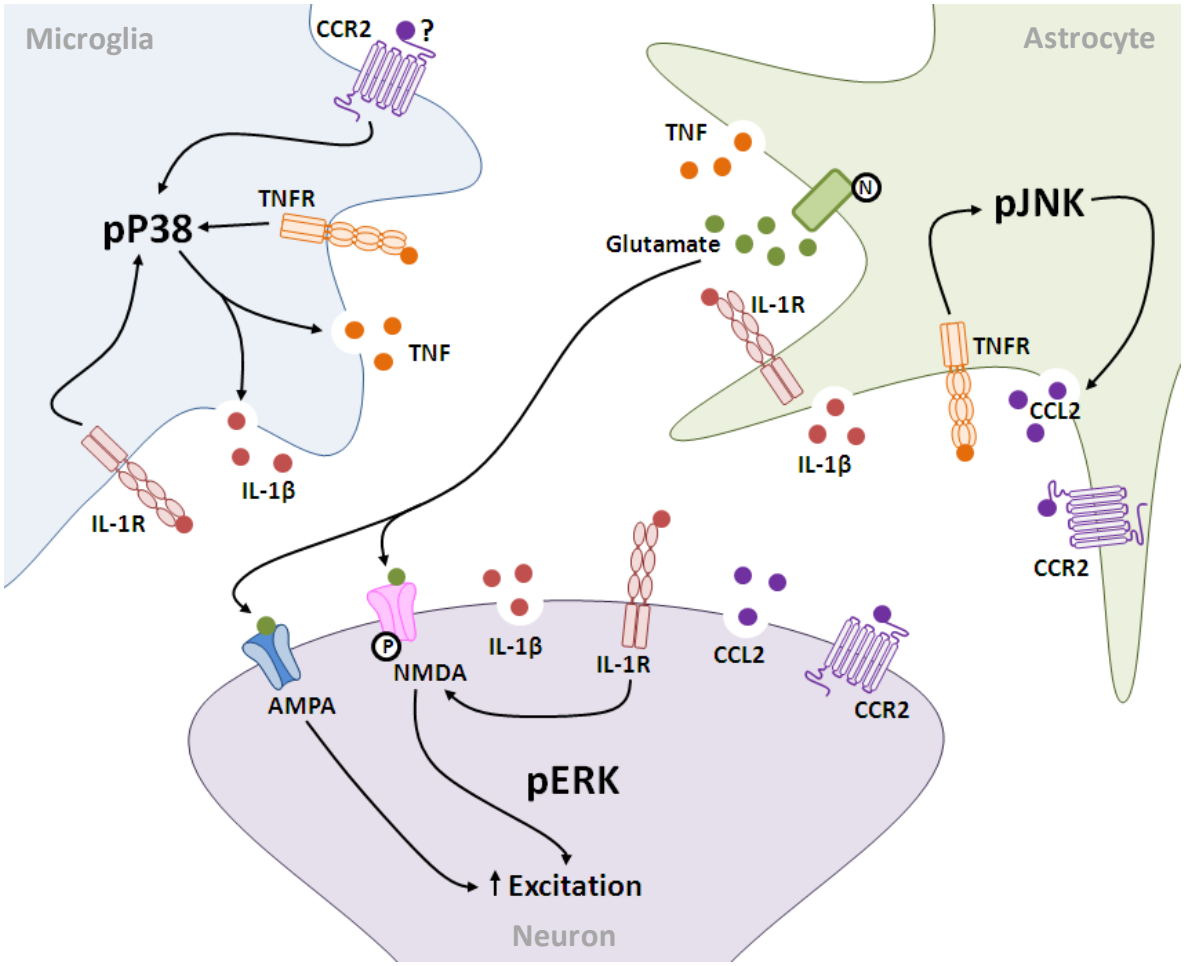

Figure 2.2. Schematic representation of spinal cord changes that contribute to enhanced nociceptive transmission in models of chemotherapy-pain. Activation of spinal glial cells leads to the release of pro-nociceptive cytokines and chemokines which are able to further activate microglia and astrocytes with a positive feedback outcome. Furthermore IL-1 released from astrocytes, microglia and neurons activates the IL-1 receptor on neurons which leads to the down-stream phosphorylation of the NMDA receptor, potentiating excitatory signalling. Additionally post-translational nitration of astrocytic glutamate transporters reduces glutamate scavenging by astrocytes, increasing extracellular glutamate which activates AMPA and NMDA receptors on neurons and further enhances excitatory signalling.

1.3. Chapter aims

Despite a recent increase in research into the treatment of chemotherapy-induced pain, there is still a lack of clinically effective compounds available for treating this condition; the pain experienced by patients undertaking chemotherapy treatment is inadequately managed. It is likely that this stems from a lack of understanding of the underlying mechanism by which the neuropathy occurs. Whilst there is evidence for an involvement of neuronal damage, peripheral immune cell activation and activation of spinal glial cells, the precise mechanism by which VCR causes painful peripheral neuropathy has not yet been elucidated. As a result there is still a lack of viable therapeutic targets for the development of a prophylactic treatment of this dose-limiting side effect. To allow an investigation into this mechanism we must first establish and characterise a model of VCR-induced neuropathy. Here we hypothesise that systemic administration of VCR causes mechanical and cold hypersensitivity and activation of non-neuronal cells in the spinal cord and peripheral nerve. Thus, the aims of this chapter are:

- To examine the temporal profile of the development of mechanical and cold hypersensitivity occurring as a result of systemic VCR administration.
- To examine the cell bodies of sensory neurons in the DRG for evidence of neuronal damage/stress occurring as a result of VCR administration.
- To examine the temporal profile of the activation of non-neuronal cells occurring as a result of VCR administration, both centrally in the dorsal horn or the spinal cord and peripherally in the DRG and trunk of the sciatic.

2. Methods

2.1. Establishing a Mouse Model of VCR-Induced Painful Peripheral Neuropathy

2.1.1. Animals

Unless otherwise stated, all experiments were performed using adult male C57Bl/6 mice (10-14 weeks of age and 22-27g from Harlan UK), in accordance with The Animals Scientific Procedures Act (ASPA) 1986, United Kingdom Home Office regulations and institutional guidelines. Animals were individually housed (to prevent aggressive behaviour) on a 12 hour light / 12 hour dark cycle at 21-22^{o}C, with food and water *ad libitum*.

2.1.2. Drug administration

2.1.2.1. VCR

VCR (Sigma, UK) was dissolved in sterile saline and 0.5mg/kg was injected into the peritoneal cavity (intraperitoneally[i.p.]), using a 30G needle, daily for five days per cycle, for two cycles before treatment was cessed (figure 2.3). This dosing protocol has been used successfully to cause VCR-induced mechanical allodynia in C57Bl/6 mice by Uceyler et al (Uceyler et al., 2006).

2.1.2.2. Fluorocitrate (glial inhibitor)

Fluorocitrate (Sigma, UK) was dissolved in sterile saline and injected intrathecally at 0.1nmol in 5µl. Mice were tightly restrained in a sock and intrathecal injections were performed by lumbar puncture, inserting a 30G 3/8" needle connected to a Hamilton syringe between the L4 and L5 vertebrae. [Performed by Clive Gentry]

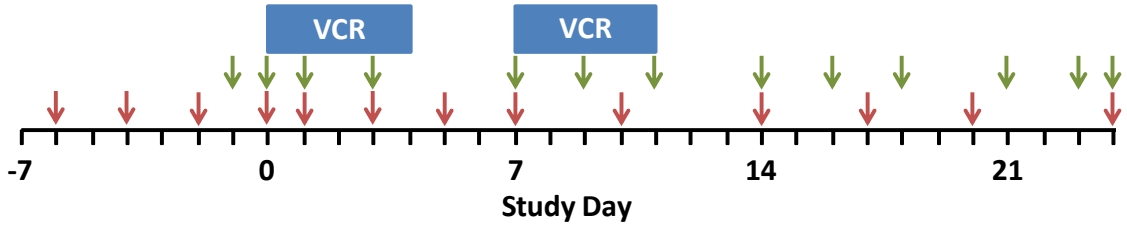

Figure 2.3. Experimental schedule for behavioural assessment and VCR dosing to induce painful peripheral neuropathy. Blue boxes represent cycles of VCR treatment (cycle 1: days 0-4, cycle 2: days 7-11), green arrows represent study days during which cold sensitivity was assessed and red arrows represent study days during which mechanical sensitivity was assessed. Behavioural tests were performed 1 hour after dosing.

2.1.3. Behavioural testing

2.1.3.1. Assessment of Mechanical Sensitivity

Static mechanical withdrawal thresholds were assessed by applying von Frey filaments (Linton Instruments, UK) to the plantar surface of the hind paw. Unrestrained animals were acclimatised in acrylic cubicles (8 x 5 x10cm) above a wire mesh for 60 minutes prior to testing. Calibrated von Frey filaments (flexible nylon fibres of increasing diameter that exert defined levels of force ranging between 0.008 and 1.2g) were applied to the plantar surface of both hind paws of the mouse until the fibre bent, and then held in place for 3 seconds or until the paw was withdrawn in a reflex not associated with movement or grooming. Filaments were applied alternately to the left and right hind paws. A 50% paw withdrawal threshold was calculated using the 'up-down' method (Chaplan et al., 1994) starting with the 0.6g filament. If a positive response was observed, the next lower force hair was applied and if a negative response was observed, the next higher force hair was applied. Responses to four subsequent hairs were assessed according to the up-down sequence. Data are expressed as the average 50% paw withdrawal threshold for both hind paws, in grams, calculated using the method described by Dixon (Dixon, 1980).

2.1.3.2. Assessment of Cold Sensitivity

Cold sensitivity of the hind paws was assessed as described by Gentry et al (Gentry et al., 2010). A cold plate (Ugo-Basile, Milan) was set according to predetermined calibration data, using a surface temperature probe to correlate set temperature with actual surface temperature, and allowed to stabilize at the set temperature for 5 minutes before use. Paw withdrawal latency (PWL) was determined with the actual temperature of the cold plate at 10^{o}C. Mice were lightly restrained with their hind paws free to move. In turn, each hind paw was placed onto the surface of the cold plate and the time taken for the mouse to withdraw each paw noted as the end point. Withdrawal was counted as complete removal of the paw from the surface of the cold plate. A maximum cut-off of 30 seconds was set to prevent tissue damage. Data are expressed as the average withdrawal latencies for both paws in seconds. [Performed by Clive Gentry].

2.1.3.3. Statistical analysis of behavioural data

Statistical analysis of behavioural data was carried out on raw data, using SigmaPlot 12.0 software (Systat Software Inc, UK). Data are shown as mean ± standard error of the mean (SEM) and were analysed using a two-repeated measures analysis of variance (ANOVA) followed by Holm Sidak post-hoc test. A p value of less than 0.05 ($P<0.05$) was considered significant (*), less than 0.01 ($P<0.01$) moderately significant (**) and less than 0.001 ($P<0.001$) highly significant (***).

2.2. Immunohistochemistry

2.2.1. Tissue preparation

Mice, under pentobarbital anaesthesia (Sodium pentobarbital, 200mg/ml; Euthatal; Merial Animal Health, UK), were transcardially perfused with saline (0.9% NaCl [VWR, UK] w/v, 0.1% heparin

sodium [5000units/ml, Leo Laboratories Ltd, UK]), followed by 4% paraformaldehyde in 0.1M phosphate buffer (containing 1.5% picric acid [Sigma, UK]). The lumbosacral spinal cord was exposed by laminectomy and the lumbar enlargement and L3, L4 and L5 DRG excised. The sciatic nerves of the animal were exposed by an anterior to posterior incision along the thigh and 10-20mm segments excised. Tissues were post-fixed for 2 hours in the perfusion fixative and subsequently cryoprotected in 20% sucrose (VWR, UK) in 0.1M phosphate buffer at 4^{o}C for a minimum of 72 hours. Following cryoprotection tissues were embedded in optimum cutting temperature embedding medium (OCT [VWR, UK]) and frozen in liquid nitrogen. Tissue sections were cryostat cut (Bright Instruments, UK) (table 2.1) and thaw-mounted onto glass microscope slides (VWR, UK). Slides were stored in cryoprotectant (PBS containing 20% w/v sucrose [VWR, UK] and 30% v/v ethylene glycol [VWR, UK]) at -20^{o}C until use.

Table 2.1. Thickness and orientation of tissues prepared for immunohistological analysis

Tissue	Thickness	Orientation
Spinal cord	20µm	Transverse
DRG	15 µm	Transverse
Sciatic nerve	15 µm	Longitudinal

2.2.2. Immunohistochemical staining

Slides were washed six times for 5 minutes in 0.1M phosphate buffered saline (PBS)and incubated over night at room temperature with a primary antibody for a specific cell marker (table 2.2) in PBS containing 0.2% TritonX-100 (Sigma, UK) and 0.1% sodium azide (Sigma, UK). Slides were then

washed three times for 5 minutes in PBS and incubated at room temperature, in the dark, with an appropriate secondary antibody (table 2.3) for 2.5-3 hours. Following three further PBS washes slides were cover-slipped with Vectashield mounting media with DAPI (Vector Laboratories, USA) and visualised under a Zeiss Axioplan 2 fluorescent microscope (Zeiss, UK).

Table 2.2. Immunohistochemistry primary antibodies

Primary Antibody	Cellular Marker	Concentration	Supplier
Rabbit anti-activating transcription factor 3 C-19 (ATF3)	N/A	1:500	Santa Cruz Biotechnology Inc, UK
Mouse anti-βIII tubulin	Neurons	1:1000	Promega, UK
Rat anti-mouse F4/80	Monocytes/Macrophages	1:200	AbD Serotec, UK
Rabbit anti-ionized calcium binding adaptor molecule 1 (Iba1)	Microglia	1:1000	WAKO Pure Chemical Industries, Germany
Rabbit anti-glial fibrillary acidic protein (GFAP)	Astrocytes	1:1000	DAKO Cytomation, Denmark

Table 2.3. Immunohistochemistry secondary antibodies

Secondary antibody	Concentration	Supplier
Goat anti-rabbit IgG-conjugated Alexa Fluor 488™	1:1000	Molecular Probes, USA
Goat anti-rabbit IgG-conjugated Alexa Fluor 546™	1:1000	Molecular Probes, USA
Donkey anti-mouse IgG-conjugated Alexa Fluor 546™	1:1000	Molecular Probes, USA
Goat anti-rat IgG-conjugated Alexa Fluor 488™	1:1000	Molecular Probes, USA
Donkey anti-goat IgG-conjugated Alexa Fluor 488™	1:1000	Molecular Probes, USA

2.2.3. Quantification of immunohistochemistry

2.2.3.1. Cell numbers

The number of positive cells for each immunohistochemical marker was determined. Three tissue sections per animal were selected at random with experimental group blinded. Four boxes measuring 100 by 100µm (area $10^4 \mu m^2$) were spaced equally across the superficial laminae of the dorsal horn, for spinal cord sections, or were spaced equally across the tissue for nerve or DRG sections. The number of cells positive for the given marker was counted (with experimenter blind to condition).

2.2.3.2. Fluorescence intensity

Quantitative assessment of immunoreactivity was carried out by determining the immunofluorescence intensity within a fixed area of the superficial dorsal horn. Three L4-L5 spinal cord sections were chosen at random from each animal, with experimental group blinded. Four boxes measuring 100x100µm were spaced equally across the superficial laminae of the dorsal horn. Mean grey intensity each of the boxed areas was determined using Axiovision LE 4.2 software. The background intensity for each tissue section was determined using an area of 50x50µm, and subtracted from the intensity values determined and an average value for immunofluorescence intensity across the superficial dorsal horn was calculated (with experimenter blind to condition).

2.2.3.3. Counts in DRG sections

The number of βIII-tubulin$^+$ cells per section was determined and represents the total number of DRG cells present per section. The total number of ATF3$^+$ cells was then determined and the percentage of ATF3 positive DRG cells calculated (with experimenter blind to condition).

2.2.3.4. Statistical analysis of immunohistochemical data

Statistical analysis of immunohistochemical data was carried out on raw data, using SigmaPlot 12.0 software (Systat Software Inc, UK). For both immunofluorescence intensity and cell numbers an average value was obtained for each animal. A mean value for each experimental group was then calculated, and the groups compared to one another using a one-way analysis of variance (ANOVA) followed by Tukey post-hoc test. Group difference with a P value of less than 0.05 ($P<0.05$) was considered significant. Data shown are mean ± SEM.

3. Results

Mounting evidence indicates that in rodents, as in humans, the repeated systemic administration of the chemotherapeutic agent VCR results in the development of severe mechanical allodynia and cold hypersensitivity. Additionally rodent models have demonstrated that subsequent to VCR treatment macrophages infiltrate the peripheral nerve, the cell bodies of neurons within the DRG up-regulate their expression of the neuronal stress factor ATF3, and glia cells within the dorsal horn of the spinal cord become activated; however the temporal profile of this response is poorly understood. Thus we set out to determine the temporal profile of these responses.

95% of mice survived both cycles of VCR treatment with no significant weight loss (figure 2.4) or signs of ill health. Until tested VCR treated mice were indistinguishable from saline treated control animals; they feed and groom normally and do not display signs of piloerection, excess vocalization or guarding of injection site.

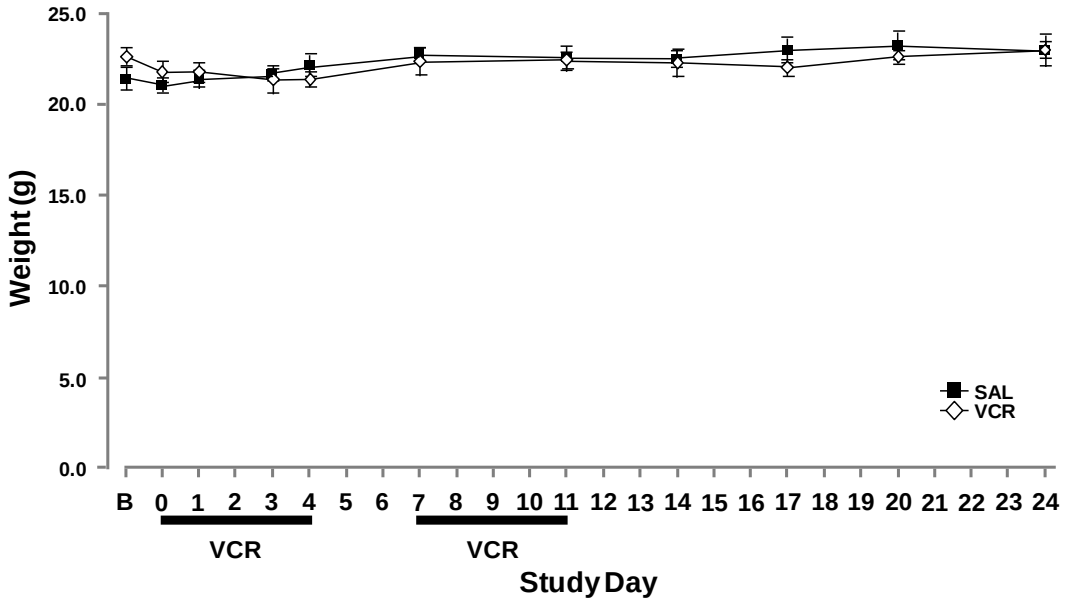

Figure 2.4. Repeated systemic administration of VCR does not cause weight loss in wild-type mice. Repeated *i.p.* VCR (0.5mg/kg/day) administration for two cycles of five days each (0-4 and 7-11; black horizontal bars); total dose approximately 125µg/mouse. Vehicle group received an equal volume of saline. Animals were weighed prior to any dosing or behavioural assessment, and had been in their cages with *ad libitum* access to food and water for a minimum of 20 hours prior to weighing. N=8 per group, data shown are mean ± SEM. No significant difference between saline and VCR treated groups.

3.1. In mice, repeated systemic administration of VCR induces a severe mechanical and moderate cold hypersensitivity that recovers upon cessation of treatment

The administration of VCR (0.5mg/kg *i.p.*) for five consecutive days (days 0-4; first cycle, cumulative dose 2.5mg/kg), followed by a two day pause and then a second cycle of treatment (five consecutive days; 7-11, cumulative dose 5.0mg/kg) was associated with the rapid development of significant and severe hind-paw mechanical hypersensitivity (allodynia), which reached significance twenty-four hours after the first administration of VCR (reduction in PWT of

26.35% ± 13.89 of baseline threshold). The hypersensitivity was well established throughout and following the first cycle of treatment (days 1-4) and was maintained throughout the second cycle (days 5-11; reduction in PWT 98.00% ± 0.21). Mechanical hypersensitivity was sustained at this severity for several days beyond the cessation of treatment (until day 17) before gradually recovering and returning to baseline pre-treatment levels twenty-four days after the first administration (figure 2.5A). Area under the curve analysis of this data reveal a highly significant difference in the allodynia index (mechanical allodynia) of VCR treated mice compared to saline treated controls across the duration of the study, the first cycle of VCR alone, the second cycle of VCR and during the recovery phase; in this analysis a decreased allodynia index value represents a greater degree of allodynia (figure 2.5B).

With a comparable time frame, the administration of two five day cycles of VCR was associated with the development of a moderate hypersensitivity to cold stimuli; a statistically significant decrease in withdrawal latency to a cold stimulus was observed on day 3, after four administrations of VCR (31.27% ± 5.92 reduction of baseline PWL; figure 2.6A). However, area under the curve analysis demonstrates that the reduction in allodynia index (cold allodynia) that is observed over the duration of the study (figure 2.6B; all time) does not occur during the first cycle of VCR treatment (figure 2.6B; first cycle). Cold allodynia resulting from VCR treatment is less severe than the mechanical allodynia observed in these mice and the onset is more gradual; however the maximal difference from baseline was observed at the end of the second cycle of VCR (figure 2.6A; day 11, 60.00% ± 3.97 reduction in PWL). As with mechanical allodynia, a sustained period of cold hypersensitivity was observed, lasting until day 17, before thresholds gradually recovered and returned to vehicle treated levels twenty-four days after the first VCR administration.

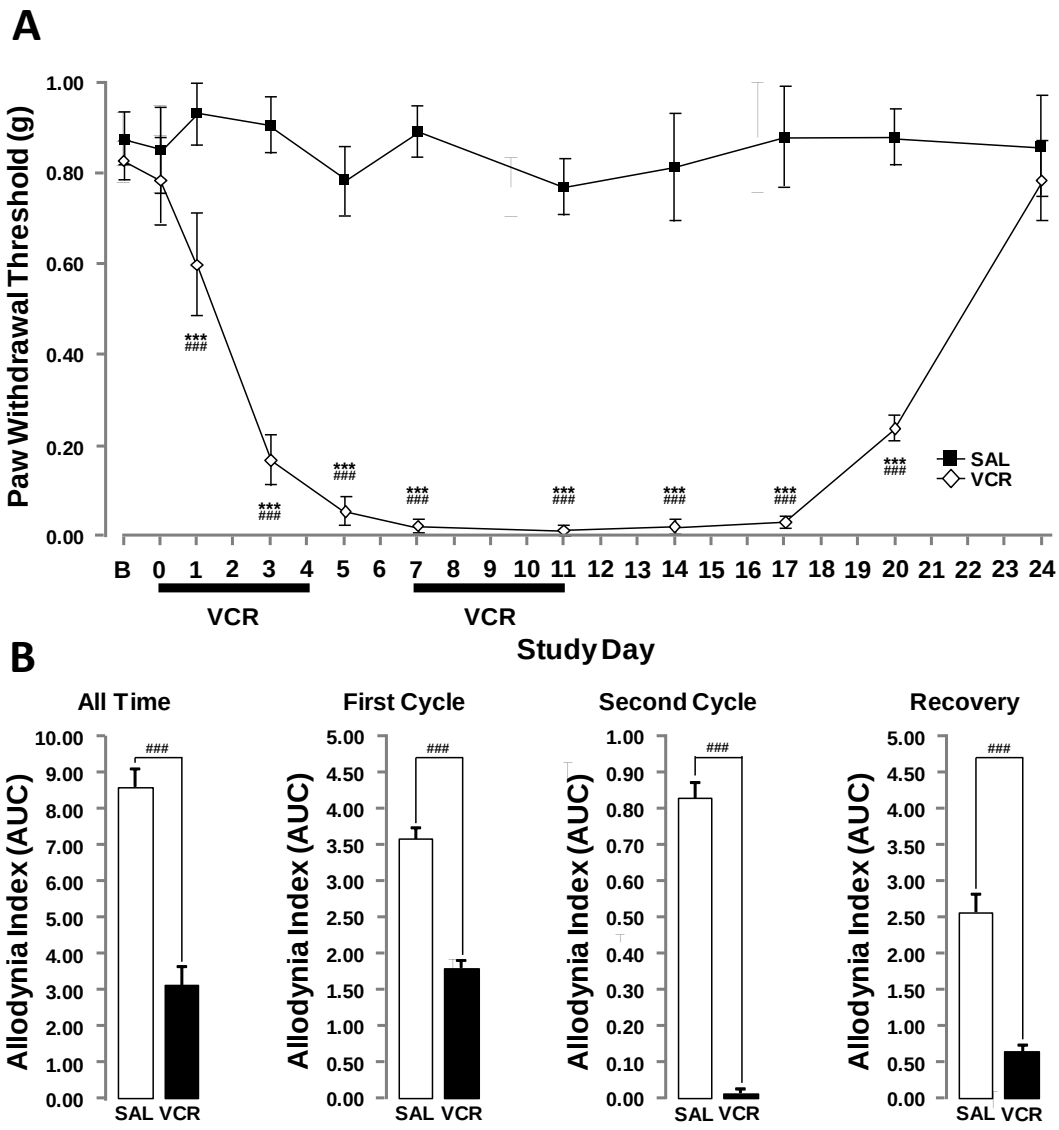

Figure 2.5. Repeated systemic administration of VCR causes severe mechanical allodynia in mice. Development of mechanical allodynia following *i.p.* VCR (0.5mg/kg/day) administration for two cycles of five days each (0-4 and 7-11; black horizontal bars); total dose approximately 125µg/mouse. Vehicle group received an equal volume of saline. **(A)** Time course of the development of mechanical allodynia shown as 50% paw withdrawal threshold (PWT), data shown as mean ± SEM. N=8 per group, ***P<0.001 compared to baseline threshold, ### P<0.001 compared to saline threshold, two-way repeated measures ANOVA with poct-hoc Holm-Sidak test. **(B)** Area under the curve (AUC) analysis showing data expressed as allodynia index where a lower value represent more severe allodynia. All time is the analysis of AUC for baseline-day 24, first cycle baseline-day 4, second cycle day 7-day 11 and recovery day 11-day 24. Data shown are mean ± SEM. N=8 per group, ### P<0.001 compared to saline threshold with Student t-test analysis.

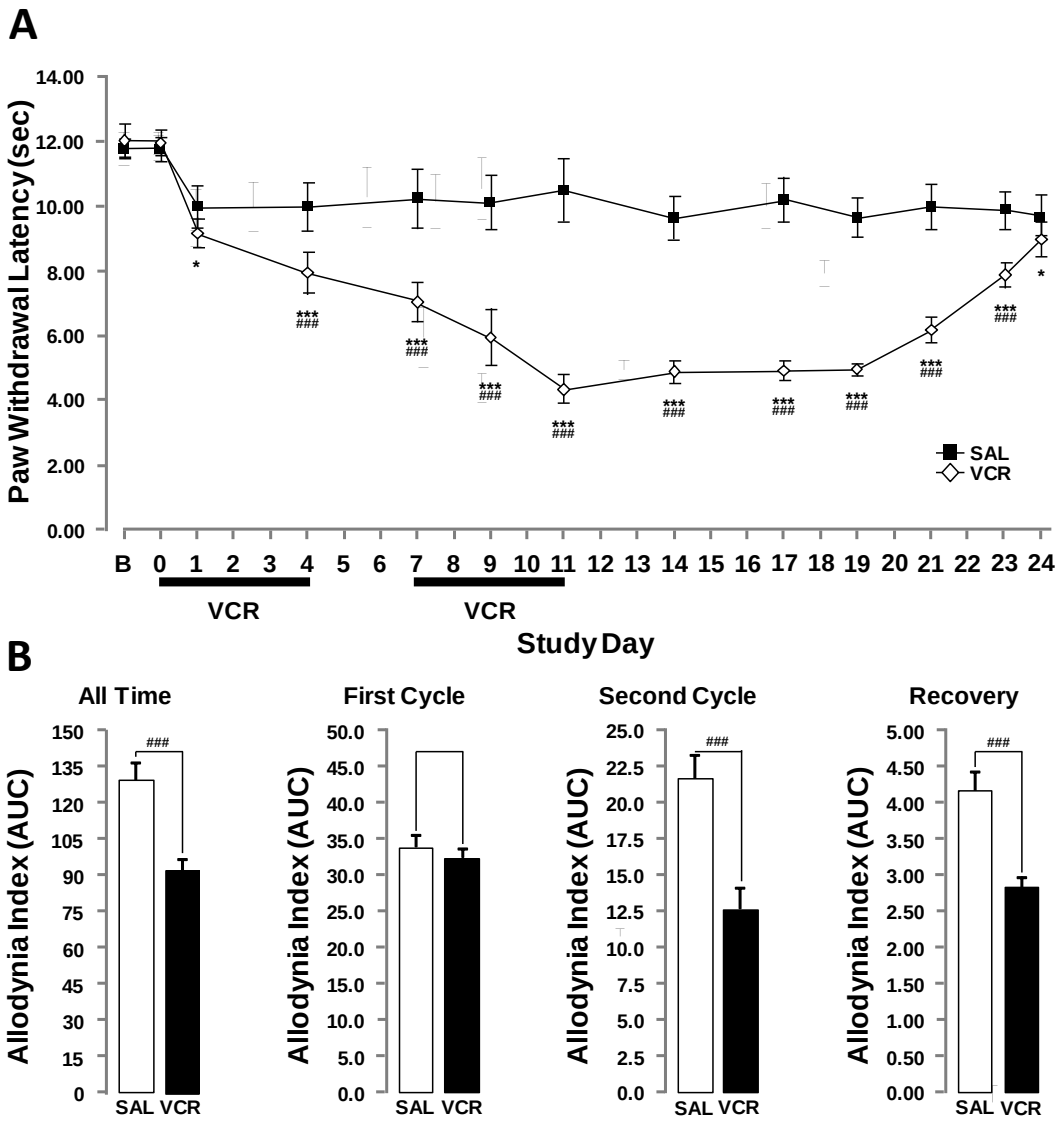

Figure 2.6. Repeated systemic administration of VCR causes moderate cold allodynia in mice. Development of cold allodynia following *i.p.* VCR (0.5mg/kg/day) administration for two cycles of five days each (0-4 and 7-11; black horizontal bars); total dose approximately 125µg/mouse. Vehicle group received an equal volume of saline. **(A)** Time course of the development of cold allodynia shown as paw withdrawal latency (sec; PWL) to a 10^{o}C stimulus, data shown as mean ± SEM. N=8 per group, *P<0.05 and ***P<0.001 compared to baseline threshold, ### P<0.001 compared to saline threshold, two-way repeated measures ANOVA with poct-hoc Holm-Sidak test. **(B)** Area under the curve (AUC) analysis showing data expressed as allodynia index where a lower value represent more severe allodynia. All time is the analysis of AUC for baseline-day 24, first cycle baseline-day 4, second cycle day 7-day 11 and recovery day 11-day 24. Data shown are mean ± SEM. N=8 per group, ### P<0.001 compared to saline threshold with Student t-test analysis.

3.2. Repeated systemic administration of VCR is not associated with a sustained significant increase in the neuronal stress factor ATF3 in the sensory neurons

Direct damage to sensory neurons has been proposed as a mechanism for VCR induced neuropathy; here we assessed the expression of ATF3 in cell bodies of sensory neurons in the lumbar dorsal root ganglia (DRG) following VCR administration. ATF3 is a member of the ATF/CREB family of transcription factors that are activated as part of a range of stress responses (e.g. oxidative stress) (Hai et al., 1999) and inflammatory reactions (Gilchrist et al., 2006) when damage to the cell has occurred; ATF3 is upregulated in several surgical models of peripheral nerve damage and is associated with neuronal damage (Braz et al., 2011;Allchorne et al., 2012).

The representative images in figure 2.7A show $ATF3^+$ cells in the L5 DRG of saline and VCR (day 11) treated mice. Following the completion of the first cycle of VCR (day 4) a slight but significant increase in ATF3 expression was observed in the cell bodies of sensory neurons in the L5 DRG when compared to the DRG of saline treated control animals (percentage of $ATF3^+$ cell bodies: saline 0.71% ± 0.24; day 4 VCR 1.93% ± 0.40; figure 2.7B). A similar increase in ATF3 expression was measured in the L5 DRG of mice that had received two full cycles of VCR (day 11; VCR 1.60% ± 0.42; figure 2.7B), however this increase was not significant.

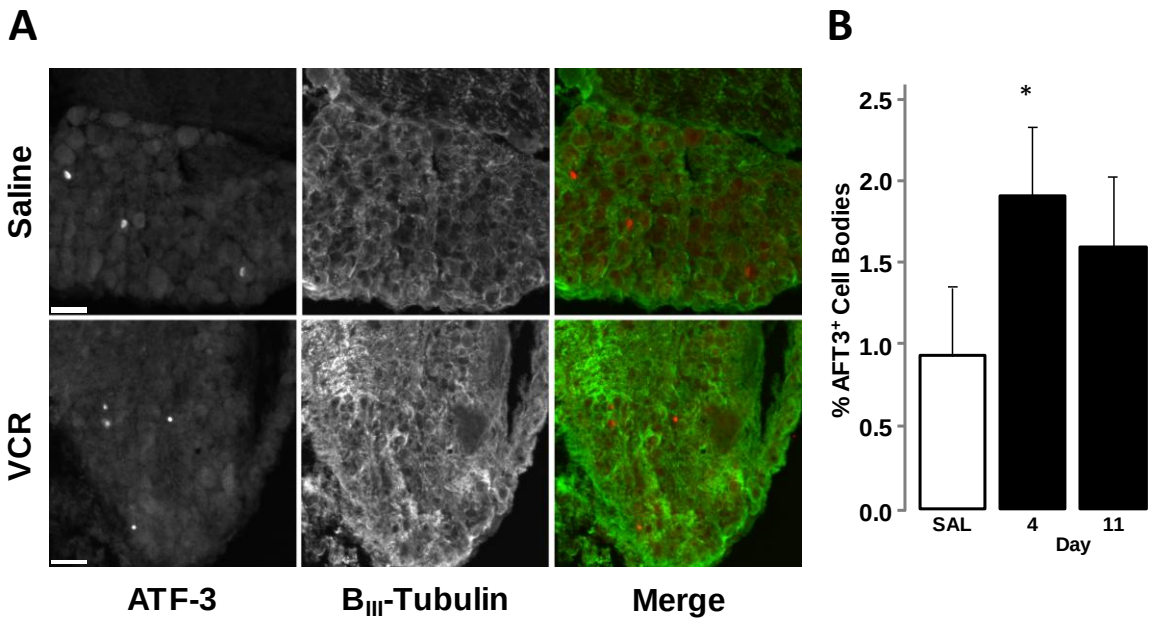

Figure 2.7. Repeated systemic administration of VCR does not cause an increase in ATF3 expression in the lumbar dorsal root ganglia. (A) Representative images showing activating transcription factor 3 (ATF3) expression in L5 dorsal root ganglion (DRG) following vehicle (SAL) or two cycles of VCR (days 0-4, 7-11; 0.5mg/kg/day *i.p.*) where ATF3 is shown in red and Beta-III tubulin (B-III tubulin) is shown in green. Scale bars equal 100 µm. **(B)** Quantification of ATF3 expression in neuronal cell bodies in the DRG, where the number of ATF3 positive cells is given as a percentage of total neuronal cell bodies. Data shown are mean ± SEM and N=4 per group, *P<0.05.

3.3. Repeated systemic administration of VCR is associated with increased monocyte/macrophage infiltration into the sciatic nerve and the lumbar DRG

Using an immunohistochemical approach, we assessed monocyte/macrophage infiltration into both the sciatic nerve and the L5 (lumbar) DRG of the mouse following repeated systemic administration of VCR. This approach was quantitative, with the number of F4/80$^+$ cells in a given area determined and compared across treatment groups and time points.

The representative images in figure 2.8A show F4/80^{+} cells in the sciatic nerve of saline and VCR treated mice. In the sciatic nerve the administration of a five day cycle of VCR (0.5mg/kg i.p.; days 0-4; first cycle), followed by a two day pause and second cycle of treatment (days 7-11) was associated with a significant increase in F4/80^{+} cells, suggestive of monocyte/macrophage infiltration of the peripheral (sciatic) nerve. Specifically, an 83.58% (± 11.48 increase; day 1; figure 2.7A/B) in number of F4/80^{+} cells per $10^{4}\mu m^{2}$ was observed twenty-four hours after the first VCR administration. The number of F4/80^{+} cells continued to increased throughout the first cycle of treatment (100.79% ± 15.97 increase; day 3; figure 2.8A/B), the break between treatment cycles (135.21% ± 6.62 increase; day 5; figure 2.8A/B) and the second cycle of VCR treatment (141.19% ± 25.73 increase; day 11; figure 2.8A/B), peaking at day 14 (186.85% ± 7.21 increase; day 14; figure 2.8A/B) despite cessation of VCR treatment. We then observed F4/80^{+} cell numbers return to baseline pre-treatment values twenty-four days after the first administration concomitantly with recovery of mechanical allodynia.

Similarly, figure 2.9A shows representative images of F4/80^{+} cells in the L5 DRG of saline and VCR treated mice. An increase in F4/80^{+} cells in the L5 DRG was observed following the administration of two cycles of VCR treatment, indicative of monocyte/macrophage infiltration. Specifically, an 11.73% (± 2.32; day 1; figure 2.9A/B) increase in number of F4/80^{+} cell per $10^{4}\mu m^{2}$ in lumbar DRG was observed twenty-four hours after the first administration of systemic VCR, this increase continued throughout the duration of treatment, reaching significance at the end of the first cycle (51.55% ± 3.56 increase; day 4; figure 2.9A/B) and remaining so for the second cycles of VCR (45.22% ± 3.95 increase; day 11; figure 2.9A/B).

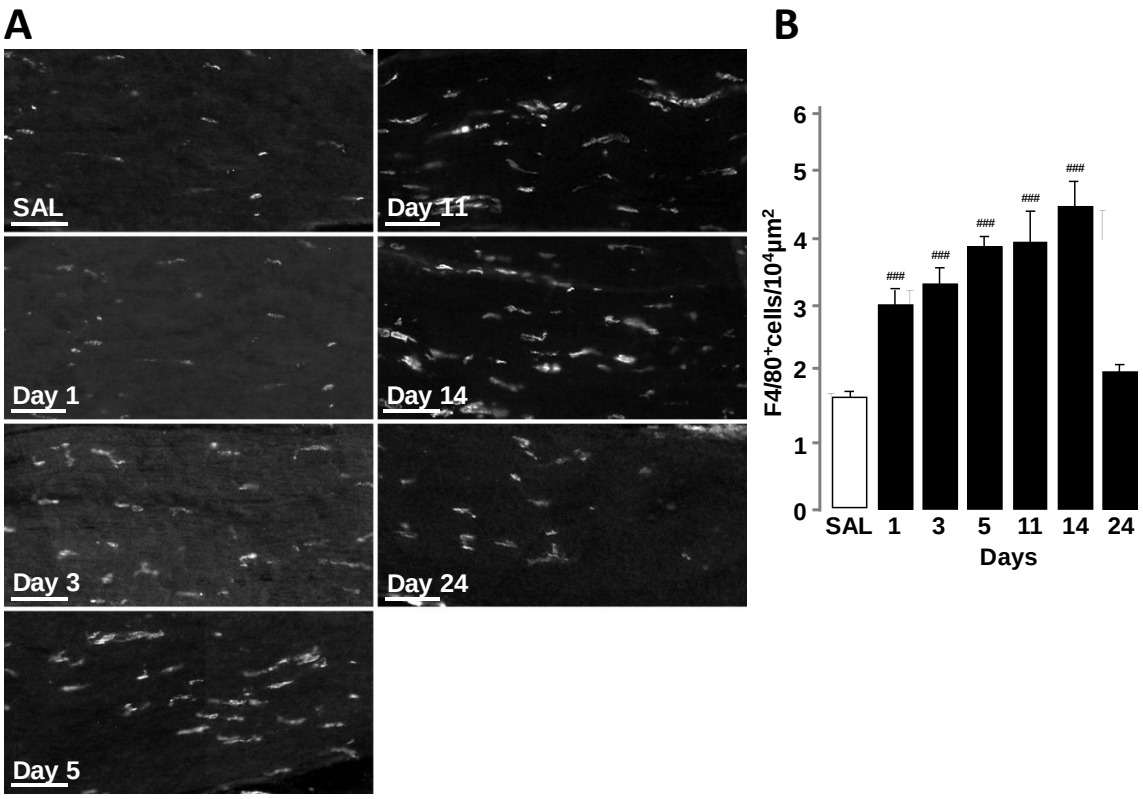

Figure 2.8. Repeated systemic administration of VCR causes macrophage infiltration of the sciatic nerve. **(A)** Representative images showing macrophages in the sciatic nerve following vehicle (SAL) or two cycles of VCR administration (days 0-4, 7-11; 0.5mg/kg/day *i.p.*) where macrophages are visualised as F4/80$^+$ cells. Scale bars equal 100µm. **(B)** Quantification of the number of F4/80$^+$ cells/macrophages in the sciatic nerve, shown as number of F4/80$^+$ cells per $10^4\mu m^2$. Data shown are mean ± SEM and N=4 per group. ### P<0.001 compared to saline threshold, one-way ANOVA with post-hoc Tukey test.

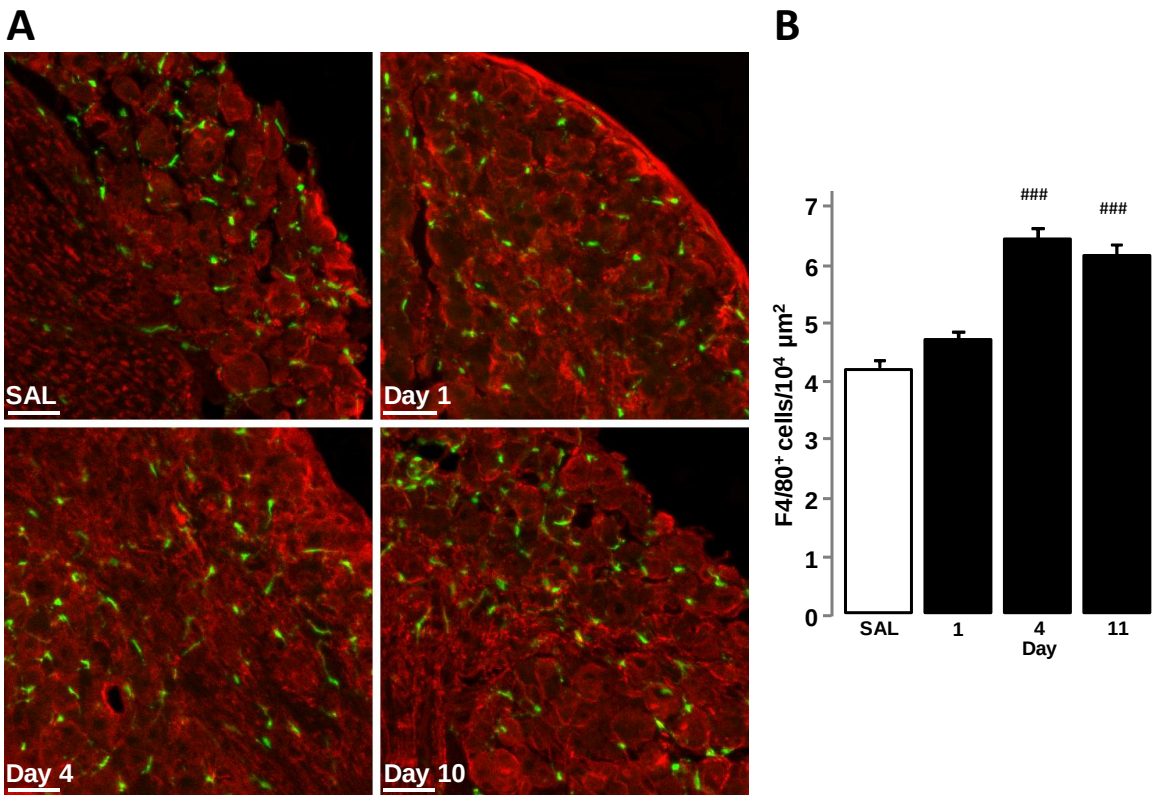

Figure 2.9. Repeated systemic administration of VCR causes macrophage infiltration of the dorsal root ganglia. (A) Representative images showing macrophages in the L5 dorsal root ganglia (DRG) following vehicle (SAL) or two cycles of VCR (days 0-4, 7-11; 0.5mg/kg/day *i.p.*) where macrophages are recognised as F4/80$^+$ cells and shown in green. β_{III}-tubulin, a neuronal marker, is shown in red. Scale bars equal 100µm. **(B)** Quantification of the number of macrophages in the DRG, shown as number of F4/80$^+$ cells per $10^4\mu m^2$. Data shown are mean ± SEM and N=4 per group. ### P<0.001 compared to saline threshold, one-way ANOVA with post-hoc Tukey test.

3.4. Repeated systemic administration of VCR causes astrogliosis but not the microgliosis in the lumbar spinal cord

To test the hypothesis that injury to the peripheral nerve induced by VCR causes activation of glial cells in the dorsal horn of the spinal cord (suggestive of central sensitisation), we next examined this area for changes in glial cells number or activation state, taking an immunohistochemical approach to do so.

The representative images in figure 2.10A (top panels) show $Iba1^+$ cells in the L5 dorsal horn of the spinal cord of saline and VCR (day 11) treated mice; they demonstrate that the repeated systemic administration of VCR was not associated with microgliosis in the dorsal horn of the lumbar spinal cord. No increase in the number of $Iba1^+$ cells in the dorsal horn was observed at any time point examined during and after the first and second cycles of VCR treatment (figure 2.10B). The morphology of microglia within the dorsal horn did not change as a result of VCR treatment; as the high magnification panels (bottom panels) in figure 2.10A show, in both saline and VCR (day 11) treated mice, the microglia in the dorsal horn have a 'quiescent' morphology; they possess a small soma and long branching processes. Furthermore, as the images in figure 2.11A demonstrate, the expression of pP38 does not increase subsequent to VCR treatment; pP38 is frequently used as a marker of microglial cell activation in chronic pain models as it is rapidly activated my several pro-inflammatory mediators. No increase in the number of $pP38^+$ $Iba1^+$ cells in the dorsal horn was observed at any time point examined during and after the first and second cycles of VCR treatment (figure 2.11B)

Despite the lack of microgliosis observed in this model, spinal cord changes were seen following cyclical administration of VCR. Astrogliosis, the change in number and activation state of astrocytes, in the lumbar dorsal horn of the spinal cord was assessed by quantifying the level of immunoreactivity of the astrocytic marker GFAP. The representative images in figure 2.12A show $GFAP^+$ cells in the L5 dorsal horn of the spinal cord of saline and VCR (days 5 and 11) treated mice; they demonstrate that the repeated systemic administration of VCR was associated with an increase in the immunofluorescence of this protein that recovers following the cessation of treatment (day 24). Specifically, the administration of VCR for five consecutive days (days 0-4; first cycle), followed by a two day pause and second cycle of treatment (days 7-11) was associated with an increase GFAP immunoreactivity in the dorsal horn; this increase was significant following one cycle of treatment (96.21% ± 30.11 increase; day 5; figure 2.12B) remained elevated during the second cycle of VCR (114.80% ± 23.68 increase; day 11; figure 2.11B), and for several days beyond the cessation of treatment (82.85% ± 9.00 increase; day 17; figure 2.12B), before gradually recovering and returning to baseline pre-treatment levels concomitantly with mechanical allodynia twenty-four days after the first administration of VCR.

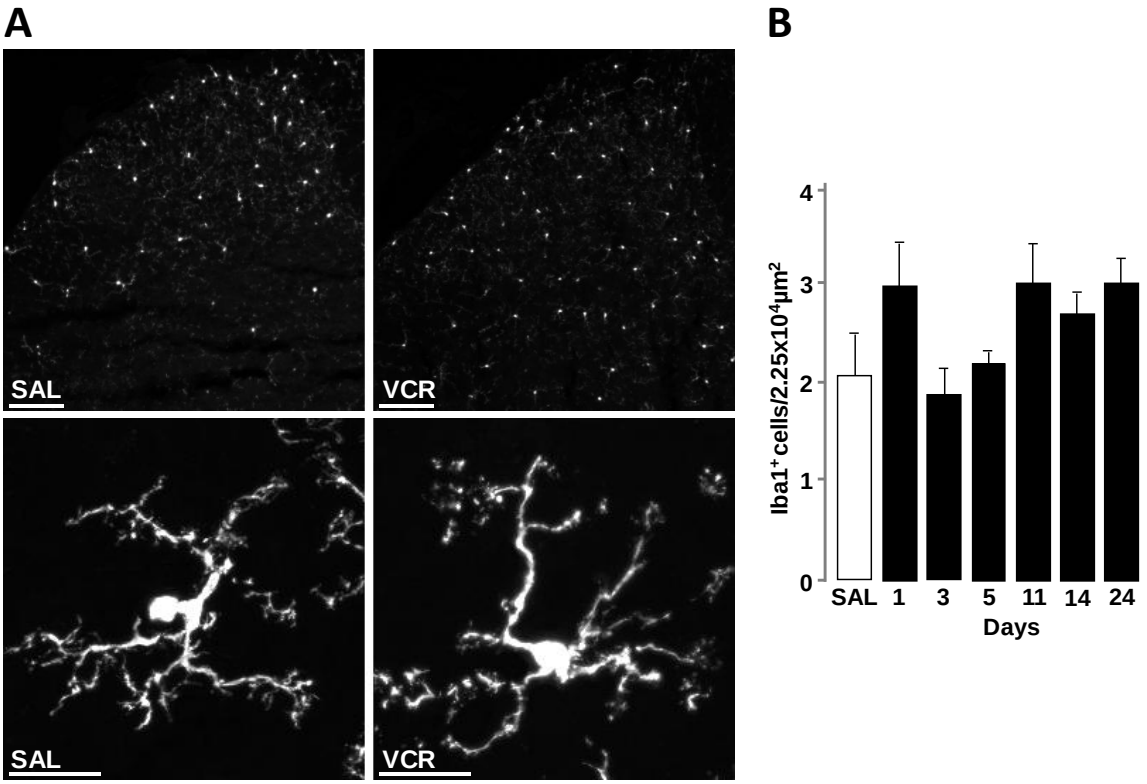

Figure 2.10. Repeated systemic administration of VCR does not cause microgliosis in the dorsal horn of the lumbar spinal cord. (A) Representative images showing microglia in the L5 dorsal horn following vehicle (SAL) or two cycles of VCR (days 0-4, 7-11; 0.5mg/kg/day *i.p.*) where microglia are visualised as Iba1$^+$ cells. Scale bars equal 100µm. **(B)** High magnification images of microglia in the L5 dorsal horn. Scale bars equal to 10µm. **(C)** Quantification of the number of microglia/ Iba1$^+$ cells in the dorsal horn shown as number of Iba1$^+$ cells per 2.25x10^{4}µm^2. Data shown are mean ± SEM and N=4 per group. No significant difference between saline and VCR treated groups (one-way ANOVA with post-hoc Tukey test).

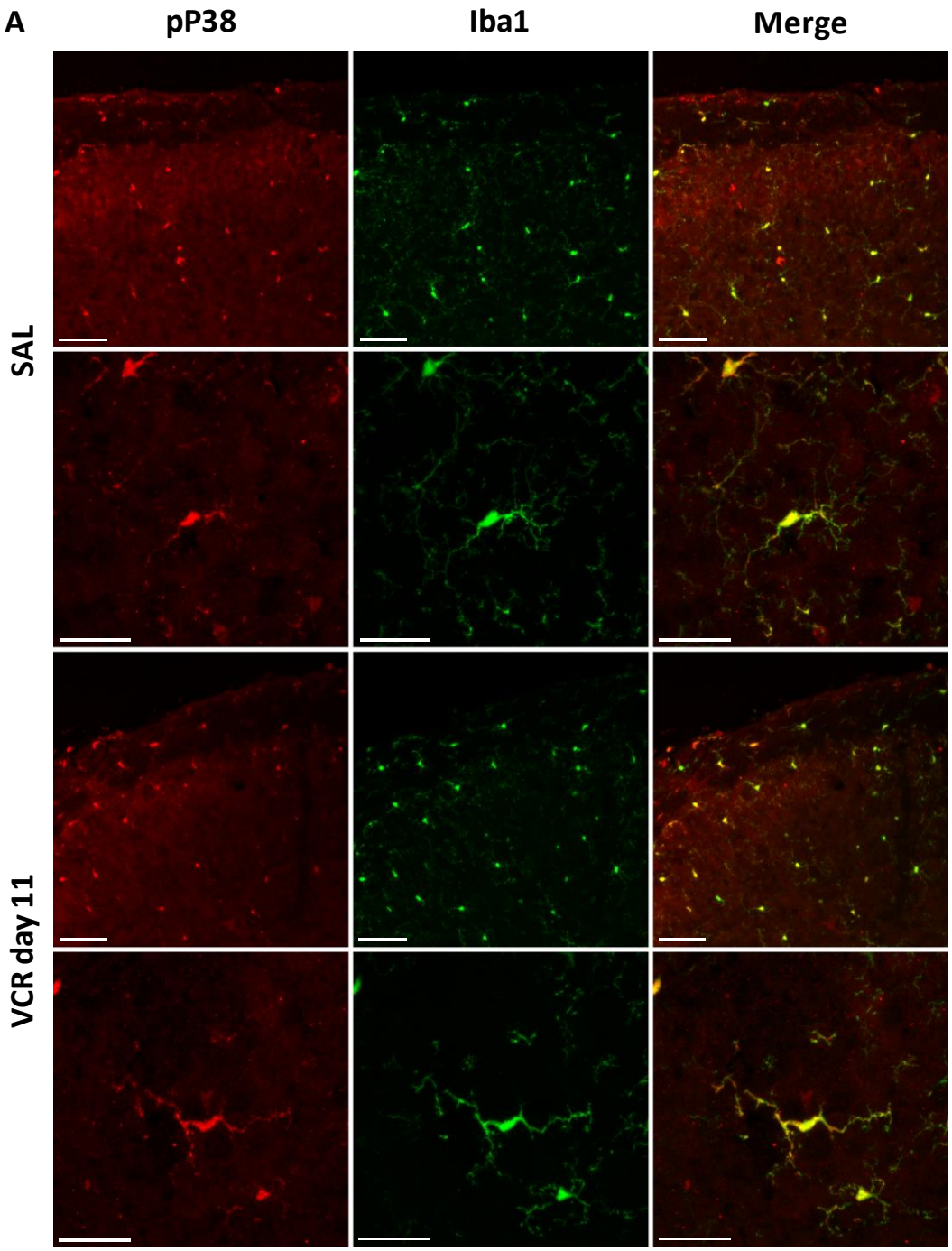

Figure legend on next page.

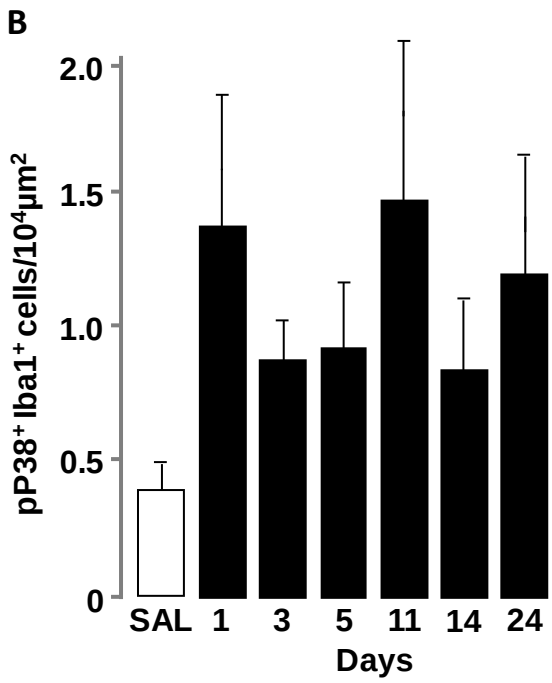

Figure 2.11. pP38 is expressed within microglia in the spinal cord but is not increased by repeated systemic administration of VCR. (A) Representative images showing pP38 expression in the L5 dorsal horn following vehicle (SAL) or two cycles of VCR administration (days 0-4, 7-11; 0.5mg/kg/day *i.p.*). pP38 (red) co-localises exclusively with Iba1 (green), a marker of microglial cells. Scale bars equal 100µm and 10 µm in high magnification images. **(B)** Quantification of the number of $pP38^+$ microglia in the dorsal horn shown as number of $pP38^+$ $Iba1^+$ cells/$10^4\mu m^2$. Data shown are mean ± SEM and N=4 per group. No significant difference between saline and VCR treated groups (one-way ANOVA with post-hoc Tukey test).

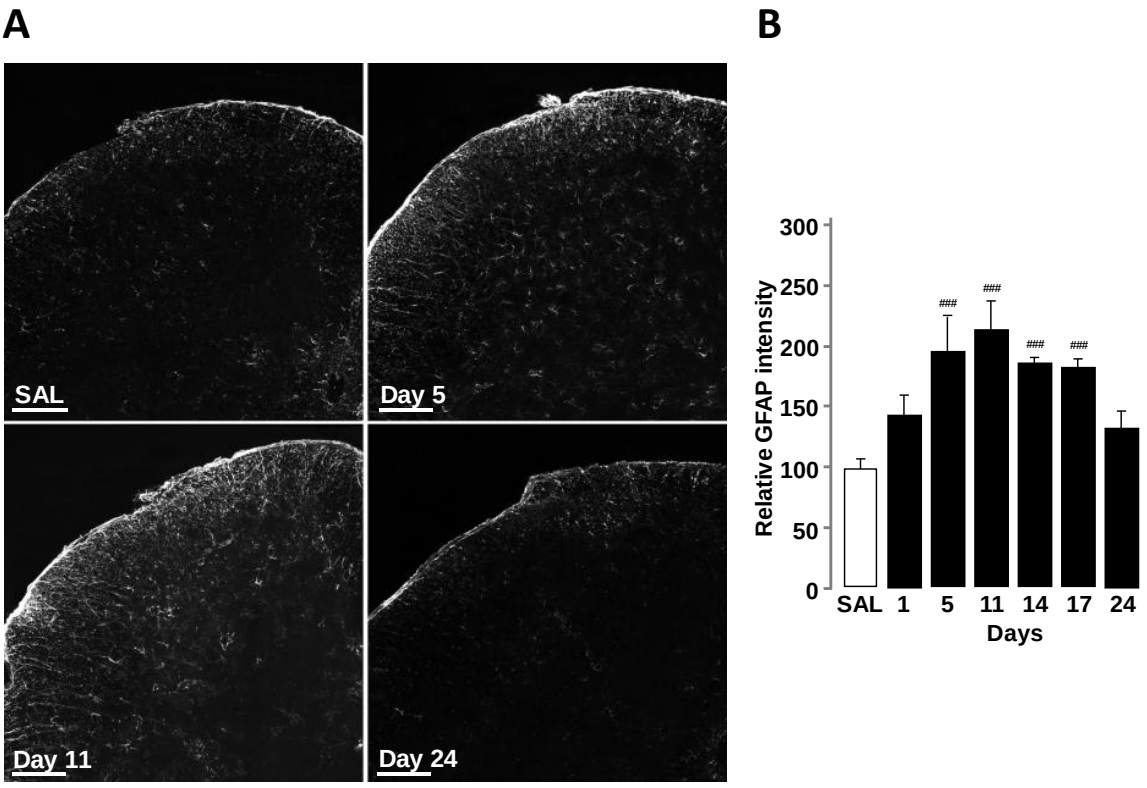

Figure 2.12. Repeated systemic administration of VCR causes astrogliosis in the dorsal horn of the lumbar spinal cord. (A) Representative images showing astrocytes in the L5 dorsal horn following vehicle (SAL) one (day 5) or two cycles (day 11) of VCR administration (days 0-4, 7-11; 0.5mg/kg/day *i.p.*) or following recovery, where astrocytes are visualised as $GFAP^+$ cells. Scale bars equal 100µm. **(B)** Quantification of the intensity of GFAP staining in the dorsal horn shown as relative GFAP intensity (relative to saline treatment) per $10^4\mu m^2$. Data shown are mean ± SEM and N=4 per group. ### P<0.001 compared to saline value with one-way ANOVA with post-hoc Tukey test.

3.5. Astrogliosis is not required for the maintenance of mechanical hypersensitivity following repeated systemic administration of VCR

We then sought to establish the contribution of astrocytes to pain mechanical allodynia in the VCR model of painful peripheral neuropathy by intrathecally injecting fluorocitrate (FLC). FLC is an irreversible inhibitor of aconitase, an enzyme that plays a critical role in the citrate cycle of glia but not neurons (Hassel et al., 1992). In mice that had received the full first cycle of VCR (day 5) the single administration of 0.1nmol FLC in 5µl did not attenuate mechanical allodynia one hour after administration (figure 2.13A +1; figure 2.13b VCR-post). However, as demonstrated by the representative images in figure 2.14A, the single administration of 0.1nmol fluorocitrate in 5µl reversed the increase in GFAP immunoreactivity observed following the full first cycle of VCR, to a level comparable to that of saline treated animals. When this is quantified we show that there is no significant different between the GFAP immunoreactivity of saline treated and VCR-FLC treated animals after FLC administration (SAL-SAL 0% ± 2.19, VCR-FLC 14.97% ± 12.79; figure 2.14B).

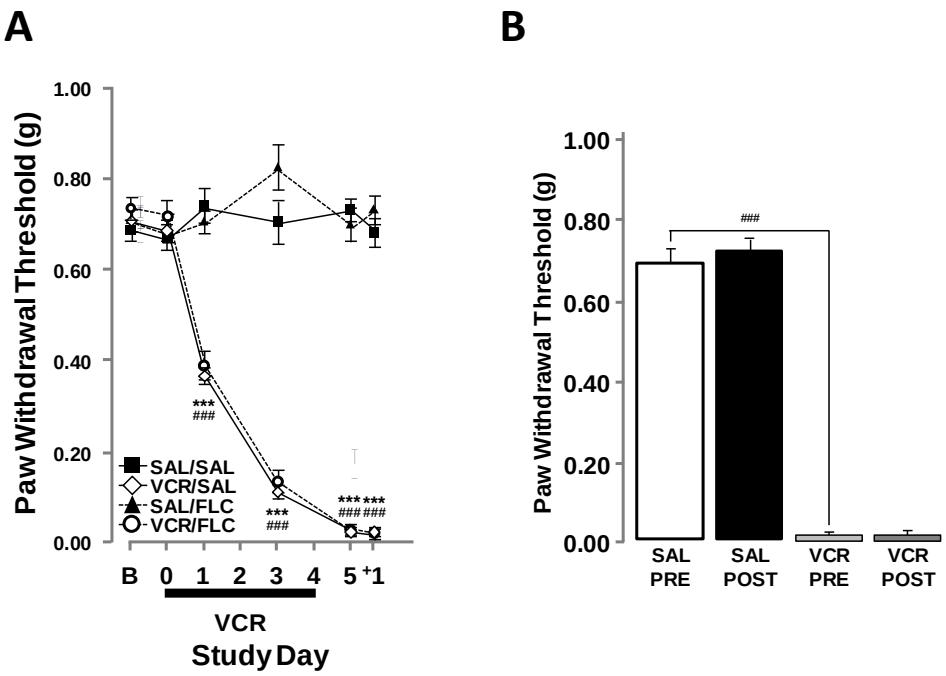

Figure 2.13. Single intrathecal administration of FLC does not attenuate mechanical allodynia in VCR treated mice. Repeated *i.p.* VCR (0.5mg/kg/day) administration for a full cycle of five days each (0-4; black horizontal bar), with or without *i.t.* FLC (0.1nmol in 5µl. Vehicle group received an equal volume of saline. **(A)** Time course of the development of mechanical allodynia shown as 50% paw withdrawal threshold (PWT), data shown as mean ± SEM. N=8, ***P<0.001 compared to baseline threshold, ### P<0.001 compared to saline threshold, two-way repeated measures ANOVA with post-hoc Holm-Sidak test. No significant difference between VCR-SAL and VCR-FLC treated groups. **(B)** VCR produced a significant decrease in PWT compared to saline vehicle, as represented by pre-dose data. This threshold was not altered by FLC administration, as represented by post-dose data. Data shown as mean ± SEM, N=8 per group (Student t-test analysis)

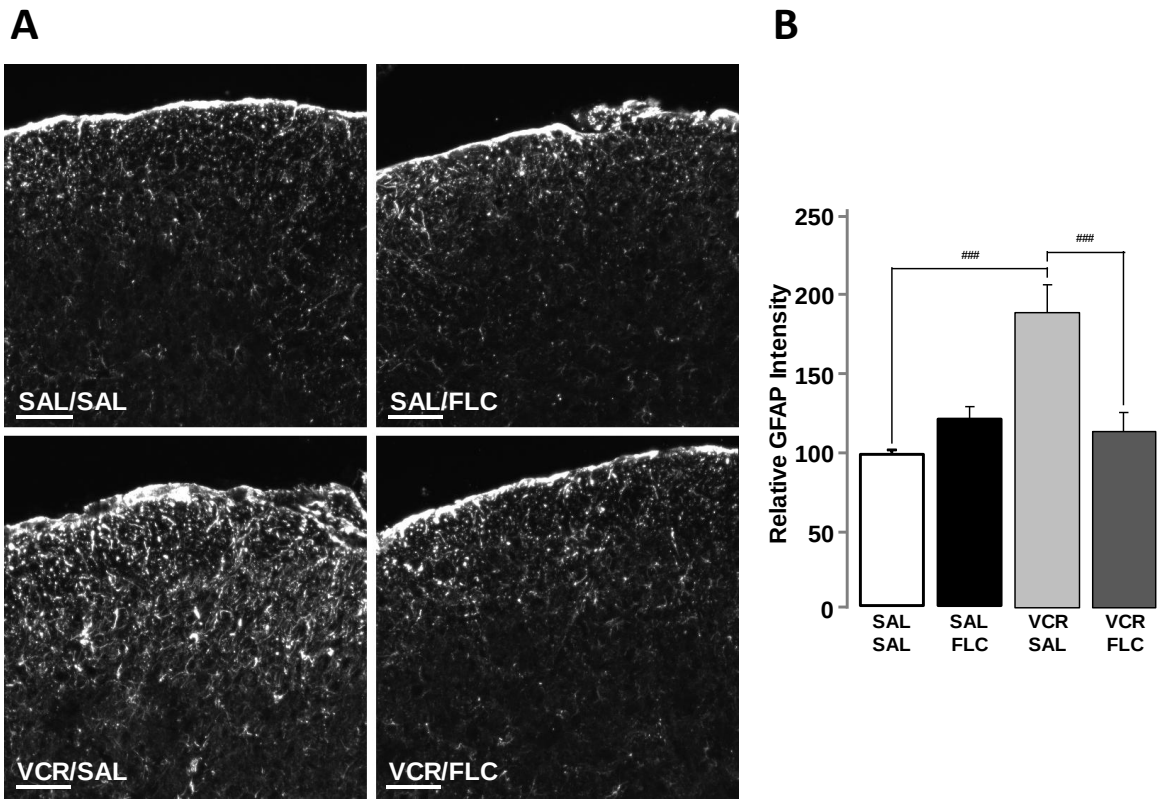

Figure 2.14. VCR-induced astrogliosis in the dorsal horn of the lumbar spinal cord can be suppressed by FLC. (A) Representative images showing astrogliosis in the L5 dorsal horn following vehicle (SAL) or one cycles of VCR administration (0.5mg/kg/day *i.p.*) with (VCR-FLC) or without (VCR-SAL) *i.t.* FLC (0.1nmol in 5µl), where astrocytes are recognised by their expression of GFAP. Scale bars equal 100µm. **(B)** Quantification of the intensity of GFAP staining in the dorsal horn shown as relative GFAP intensity (relative to SAL-SAL) per $10^4 \mu m^2$. Data shown are mean ± SEM and N=4 per group. ### P<0.001 compared to saline threshold, one-way ANOVA with post-hoc Tukey test.

4. Discussion

The introduction and development of chemotherapeutic regimes during the twentieth century has dramatically increased the rate of survival of cancer patients. However these drugs are not without serious side-effects; these stem from the fact that cells with a high turnover, such as those in the bone marrow, are highly susceptible to the toxic effects of chemotherapeutics. The successful management of many of these side-effects, including anaemia, thrombocytopenia and neutropenia has allowed treatment regimens to be advanced but has also exposed a secondary dose-limiting effect: neurotoxicity (Windebank and Grisold, 2008). The symptoms of the chemotherapy-induced neuropathy are predominantly sensory in nature, with patients reporting the most problematic symptom to be pain (Tofthagen, 2010). A number of animal models of chemotherapy pain have been developed in recent years; these exhibit similar sensory abnormalities and symptoms to those observed in patients, specifically a decrease in sensory nerve conduction velocity, mechanical allodynia and cold hypersensitivity. From the evidence obtained from a number of recent studies we know that, at least superficially, the development of VCR-induced neuropathy in rodents is similar to that in man. The neurotoxicity of VCR in both rodent and man is cumulative; symptoms are experienced following multiple doses of this anti-neoplastic agent and become progressively more severe as therapy is continued. Both rodent and man experience a neuropathy that is predominantly sensory and that is associated with altered electrophysiological properties of sensory nerves; the decrease in conduction velocity (Alimoradi et al., 2012;Krishnan et al., 2005) and amplitude of action potentials (Pal, 1999;Callizot et al., 2008) in the sensory neurons of the sciatic nerve.

The development of mechanical allodynia following VCR administration is well documented in the rat; daily intraperitoneal administration of this agent for two weeks causes a rapid decrease in nociceptive threshold. This is dose-dependent and cumulative; higher doses cause a more severe phenotype. Following the cessation of VCR treatment, mechanical allodynia is sustained for several days; nociceptive thresholds return to baseline values approximately three and half weeks after the commencement of the study (Aley et al., 1996). This rat model of chemotherapy-induced mechanical allodynia provides a suitable model for the testing of potential analgesics, due to its large therapeutic window and reproducible results. However, the mouse model of this condition is more appealing for the study of the molecular mechanisms underlying the neuropathy, due to the availability of genetically modified strains. A mouse model of VCR-induced neuropathy has been established in C57Bl/6 mice (Uceyler et al., 2006) however its characterisation is far from complete, hence the need for the current study. Furthermore, despite the wealth of evidence obtained from both human and rodent studies/models, the precise mechanism by which chemotherapeutic agents cause neuropathy remains elusive.

Here, in this chapter, we set out to characterise a mouse model of VCR-induced neuropathy; considering the development of behavioural symptoms of the neuropathy and assessing the temporal profile of non-neuronal cell involvement both peripherally and centrally, as these cells are known to play a key role in the development of pain in a number of models of neuropathy. The principle finding of the work described here is that repeated systemic administration of VCR results in the development of severe and sustained mechanical allodynia and mild cold hypersensitivity. Furthermore, the development of these pain behaviours is associated with changes to non-neuronal cells; specifically macrophage infiltration of the sciatic nerve and DRG and astrogliosis (but not microgliosis) in the dorsal horns of the lumbar spinal cord.

We have demonstrated here that the temporal profile of mechanical allodynia exhibited by mice following VCR administration is actually quite similar to that seen in rats. VCR treated mice develop significant mechanical allodynia within 24 hours of first administration of the drug; by the end of the first cycle of treatment (5 administrations) this allodynia is extremely severe, is sustained throughout a second cycle of VCR and persists for several days after the cessation of treatment before recovery. This temporal profile of allodynia is likely accurate as it is consistent with previous studies of VCR-induced neuropathy in mice, where onset of allodynia is rapid and sustained beyond the cessation of treatment (Uceyler et al., 2006;Hansen et al., 2011;Gauchan et al., 2009;Kiguchi et al., 2008b).

In addition to the development of mechanical allodynia, hypersensitivity to cold is a common complaint in chemotherapy patients (Binder et al., 2007). Here we were able to demonstrate the development of cold hypersensitivity in mice following VCR treatment. Consistent with previous literature (Park et al., 2012;Geis et al., 2011;Thibault et al., 2008), this is not as robust as the development of mechanical allodynia and thresholds are much more varied between animals. Whilst the change in threshold to a cold stimulus is significant for the majority of subsequent studies we have concentrated on mechanical allodynia as a behaviour indication of the development of neuropathy as the data obtained is more consistent that of cold hypersensitivity. It is important to note that whilst the behavioural phenotype observed is severe, no weight loss was evident in VCR treated animals, suggesting this treatment protocol was not overwhelmingly toxic to the animals.

As discussed in chapter one, it has previously been suggested that VCR may cause neuropathy by binding to tubulin and disrupting the normal function of neurons; this hypothesis is supported by

an increase in expression of the neuronal stress factor ATF3 that is reported in models of VCR-induced neuropathy (Hansen et al., 2011). In a study by Hansen et al. a significant increase in ATF3 immunoreactivity (from approximately 5% to 17% of DRG neurons) is reported in the lumbar DRG 19 days after the commencement of VCR treatment. Here we examined ATF3 expression at day 4 (following the completion of the first VCR cycle) and day 11 (at the end of the second cycle) after the commencement of treatment; we observed a small but significant increase in the ATF3 expression of L5 DRG neuronal cell bodies at the earlier time point but not the latter. However, the expression values obtained fall within the previously published values of ATF3 expression in naive or control mice (0.001% (Ogbonna et al., 2013) to 5% (Hansen et al., 2011;Kim and Moalem-Taylor, 2011). To put this increase into perspective, following a severe peripheral nerve injury an increase of approximately 20% is observed in our hands (Ogbonna et al., 2013). It is possible that if tissue was taken at later time points, such as study day 19 or 20 for example, an increase in ATF3 may have been seen in our model, however this seems unlikely, as pain behaviour had reached peak levels by both time points examined, and if a neuronal stress response was the causative factor in this, an ATF3 increase should have been apparent. Further to this, Ja'afer et al recently demonstrated that whilst there is evidence of myelin sheath alterations in the rat sciatic nerve following VCR treatment, there is no axonal loss in the sciatic or tail nerves (Ja'afer et al., 2006); this is consistent with work by Authier et al who reported that whilst there is a decrease in nerve conduction velocity in VCR treated animals, few degenerated fibres are found in the sciatic nerve (Authier et al., 2003). However, the infiltration of the nerve by macrophages is indicative of neuronal damage as these immune cells are recruited to sites of tissue damage; it is possible that the histochemical techniques currently available to use are not sensitive enough to detect the neuronal damage in its earliest stages.

As well as an increase in neuronal ATF3, Hansen et al have also reported an increased number of macrophages in the DRG of VCR animals (Hansen et al., 2011). This was examined at a single time point, but inspired us to assess the temporal profile of macrophage infiltration, and indeed we observe a comparative number of macrophages in the DRG by the end of the treatment protocol. Furthermore, by examining two earlier time points, day 1 (24 hours after the first administration) and day 4 (following a full cycle of VCR), we have established that this increased in macrophage number in the DRG is gradual, unlike the infiltration we see in the peripheral nerve. Analysis of macrophage infiltration of the sciatic nerve has demonstrated that there is a rapid increase in the number of these cells in the nerve just 24 hours after the commencement of treatment. This number continues to rise following subsequent doses of VCR and peaks just after the cessation of treatment, before decreasing back to baseline levels concomitantly with the recovery of the behavioural phenotype. In fact the temporal profiles of mechanical allodynia and macrophage infiltration of the nerve are very similar, and combined with the evidence from previous work in the laboratory, that demonstrates that in a model of peripheral nerve injury depletion of these cells delays the onset of allodynia (Barclay et al., 2007), we hypothesise that these cells play a considerable role in the development of chemotherapy-pain; these experiments are presented in chapter three.

In contrast to the changes in macrophages, the morphology and number of microglia in the dorsal horn of the spinal cord remained unchanged following VCR treatment. This observation, whilst unexpected, is not surprising. Microgliosis in models of chemotherapy pain remains controversial; there is considerable inter-model variation and microgliosis tends to be reported in rat models rather than mouse (Ledeboer et al., 2007). Astrogliosis, on the other hand, was observed; a significant increase in GFAP immunoreactivity was detected five days after the commencement of

treatment (end of cycle one) and this continued to increase during the second cycle of VCR administration, before declining back to baseline levels concomitantly with the recovery of pain related behaviours. This is also consistent with previous studies which have documented astrogliosis at varying time points (Ji et al., 2013;Kiguchi et al., 2008a). Activation of spinal glial cells is indicative of central sensitization, which classically occurs as a result of damage to peripheral nerves, thus the activation of astrocytes in this models provides further, albeit indirect, evidence for neuronal damage in our mice occurring as a result of VCR treatment.

Due to the similarities in the temporal profiles of astrocyte activation and mechanical allodynia, and concomitant recovery of astrogliosis and mechanical hypersensitivity following the cessation of VCR treatment, we hypothesised that astrogliosis might contribute to the maintenance of VCR-induced hypersensitivity. To investigate this we administered a glial inhibitor to mice exhibiting well established VCR-induced mechanical allodynia, to see if this behaviour could be attenuated. It has previously been demonstrated that centrally administered glial inhibitors have efficacy in models of chemotherapy-pain, suggesting glial cells do contribute to the behavioural phenotype observed in these animals. Minocycline, a tetracycline derivative that possesses anti-inflammatory properties, has been reported to preferentially inhibit the function of microglia (rather than astrocyte or neurons) (Tikka and Koistinaho, 2001), but is capable of attenuation of cold hyperalgesia induced by PTX. In these animals significant microgliosis has been demonstrated and this too is attenuated by minocycline (Pevida et al., 2013). Moreover, minocycline is also able to prevent the development of mechanical hypersensitivity in oxaliplatin treated rats (Boyette-Davis and Dougherty, 2011). Propentofylline, a third generation glial inhibitor that decreases both microglial and astrocytic activation (by inhibition of phosphodiesterase cAMP generation) (Tawfik et al., 2008), suppresses spinal glial activation and mechanical allodynia in PTX treated animals.

Here we intrathecally administered FLC; this is a selective inhibitor of the aconitase enzyme found in the tricarboxylic acid cycle (TCA) of glia but not neurons (Hassel et al., 1992). At the time of experimentation a dosing regimen for FLC treatment in mice had not been established and the use of compound in models of chemotherapy pain had not been published. However we have demonstrated that the single intrathecal administration of 1nmol FLC in 10µl suppresses glial activation and reverses hyperalgesia in rat models of chronic pain, with a peak behavioural effect occurring one hour after administration (Clark et al., 2007a). Due to the smaller intrathecal space of mice, we administered 1nmol FLC in 5 µl to mice that had received a full cycle (five administrations; day 5) of VCR. Unfortunately these mice experienced seizures; as a result they were unsuitable for behavioural assessment and we culled in accordance with Home Office Regulations. A reduced dose of FLC (0.1nmol in 5µl) was well tolerated by both saline and VCR treated mice, and it is this dose that was used in the study presented here. We had not previously demonstrated efficacy of FLC at this dose, however, immunohistochemical analysis of the spinal cord following treatment demonstrates that it was able to reverse activation of astrocytes , as demonstrated by a reduced GFAP immunoreactivity of VCR-FLC compared to VCR-SAL treated mice. No behavioural effect was observed; FLC did not attenuate mechanical allodynia in VCR treated mice. Whilst there was initially some concern as to whether this could be attributed to a sub-optimal dose of FLC, Morioka et al have recently demonstrated efficacy in the suppression of astrocytic metabolism at this same dose (Morioka et al., 2012). Thus, these data suggest that whilst cycle administration of VCR is associated with the development of astrogliosis in the dorsal horn of the spinal cord, activation of astrocytes in the spinal cord is not required for the maintenance of mechanical allodynia in these animals. Also, as the development of astrogliosis occurred several days after a reduction in mechanical thresholds was first apparent; our data suggest that the activation of astrocytes do not contribute to the initiation or development of

mechanical allodynia. However as the existing literature shows efficacy of glia inhibitors in PTX and oxaliplatin induced neuropathies (Pevida et al., 2013;Boyette-Davis and Dougherty, 2011), this result may be specific to VCR neuropathy, and suggests that chemotherapeutics with differing anti-neoplastic actions may not cause pathophysiological changes to the nervous system via the same mechanism.

5. Introduction to Chapter 3

In this chapter, we provide evidence for macrophage infiltration of the peripheral nervous system occurring concomitantly with the significant development of pain behaviours in VCR treated mice. Thus, we sought to determine the contribution of these cells to the development of VCR-induced mechanical allodynia. To investigate the hypothesis that macrophage infiltration of the PNS is a critical step in the development of VCR-induced mechanical allodynia, we have not only depleted circulating monocytes (thus preventing the infiltration of macrophages into the nerve), but have also used two genetically altered mouse strains to establish the contribution made by differing populations of macrophages. Macrophages are a heterogeneous population of cells, existing as tissue resident macrophages and differentiating from circulating monocytes upon entry into the tissue following danger signals from the immune system. These experiments are presented in chapter three following an introduction to monocyte/macrophages and CX_3CR1 in the mouse.

Chapter 3:

The Contribution Of The CX_3CR1 Receptor And The Monocyte/Macrophage To Vincristine-Induced Painful Peripheral Neuropathy

1. Introduction

Macrophages were introduced in chapter two as a heterogeneous population of cells that differentiate from circulating monocytes and function as phagocytic cells, involved in the clearance of cellular debris following tissue damage or remodelling. Here we will discuss the origin, heterogeneity and function of these cells in more detail and then focus on one particular chemokine receptor expressed by these cells: CX_3CR1.

1.1. Monocyte / Macrophages; Origin, Function & Heterogeneity

Macrophages (first recognised by Metchnikoff in his 1908 Nobel Prize winning work) can be found in all tissues, and circulate in the blood as monocytes, constituting a significant portion of the peripheral blood mononuclear cells (PBMCs) / leukocytes. Monocytes constitute approximately 10% of circulating leukocytes in man and 4% in the mouse (Auffray et al., 2009), and under steady state conditions do not proliferate. Monocytes can differentiate into inflammatory dendritic cells or macrophages under inflammatory (and sometimes steady-state) conditions (Geissmann et al., 2010;Mosser and Edwards, 2008). They differentiate from committed myeloid progenitors and, as shown by radioisotope labeling of blood and bone marrow cells, are the precursors for macrophages in all tissues. This process is regulated by several growth factors, the most important of which is CSF1 (colony stimulating factor-1; also known as M-CSF). *In vitro* CSF1 stimulates proliferation and differentiation of progenitors (monoblasts, promonoblasts and monocytes) to macrophages. The CSF1 receptor is expressed by all mononuclear phagocytic cells under the control of the transcription factor PU.1 and the CSF-1 protein itself is produced by cells of mesenchymal lineage including endothelial cells, fibroblasts and myoblast; most tissues are able to

produce this protein (Pollard, 2009;Gow et al., 2010;Sweet and Hume, 2003). Additionally macrophages can differentiate from monocytes in the presence of GM-CSF although the phenotype of mice lacking this protein is not as extreme as those lacking either CSF-1 or PU.1 (Pollard, 2009). The full process of macrophage differentiation from bone marrow progenitor is summarised in figure 3.1.

In humans monocytes show substantial morphological heterogeneity but were first identified by their expression of CD14. Subsequent identification of the antigenic marker CD16 allowed two distinct monocyte populations to be determined: $CD14^{+}CD16^{-}$ monocytes, also known as classically activated or inflammatory monocytes, and the alternatively activated or resident $CD14^{+}CD16^{+}$ monocytes, which resemble tissue resident macrophages (Passlick et al., 1989;Ziegler-Heitbrock et al., 1993). *In vitro* transmigration assays have revealed that these cells are able to differentiate into either dendritic cells or macrophages given the appropriate stimulus, although $CD14^{+}CD16^{+}$ monocytes showed a preference for differentiation to dendritic cells and $CD14^{+}CD16^{-}$ monocytes to macrophages (Randolph et al., 2002). Additionally, since their initial identification these two differing populations have been found to have distinct chemokine receptor expression profiles, summarised in table 3.1 (Gordon and Taylor, 2005).

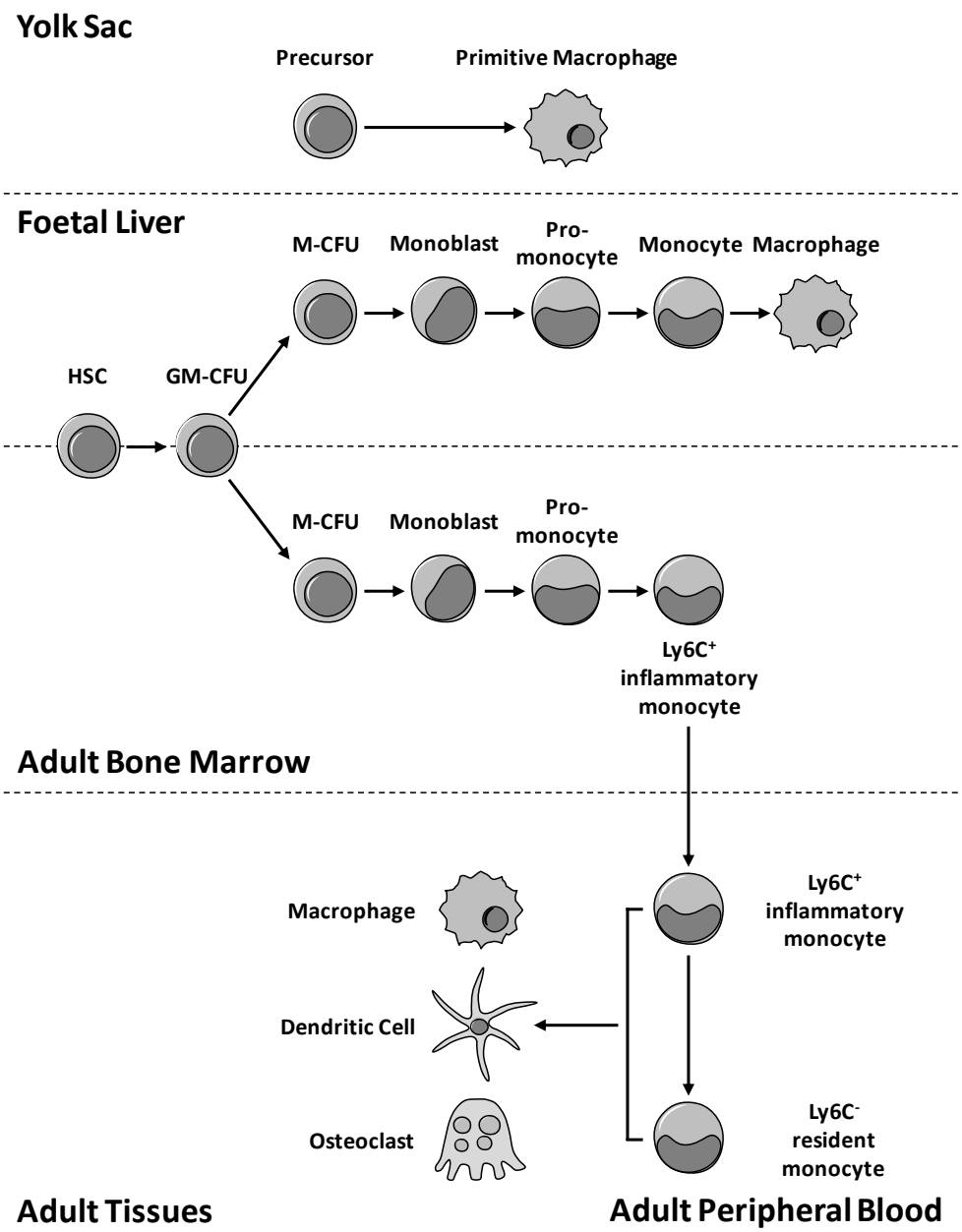

Figure 3.1. The mononuclear phagocytic system development. During development there are cells that derive from the yolk sac that have a macrophage like phenotype, possessing the macrophage marker CD11b. In later developmental stages haematopoiesis in the liver becomes the source of macrophages that bare considerable resemblance to those seen in the adult. As in adults these cells originate from a common haematopoietic stem cell (HSC) which undergoes differentiation steps that commit them to a monocytic lineage via granulocyte/macrophage colony forming units (GM-CFU) and macrophage colony forming units (M-CFU). In adults haematopoiesis occurs in the bone marrow but includes similar steps as in the foetal liver with monocytes migrating into the blood stream where they act as a source of precursors of the replenishment of tissue resident macrophages. (Adapted from Gordon and Taylor, 2005)

Table 3.1. Antigen expression on human monocytes of the two best-characterised subsets. (Adapted from Gordon and Taylor, 2005)

Antigen / Receptor	Expression in Human $CD14^+CD16^+$ 'resident' monocytes	Expression in Human $CD14^+CD16^-$ 'inflammatory' monocytes
CD14	+	+
CD16	+	-
F4/80	Not determined	Not determined
CD11b	+	+
Ly6C	Not determined	Not determined
CX_3CR1	High	Intermediate
CCR2	-	+

As in humans, two phenotypically distinct monocyte populations can be seen in the mouse, albeit based on different antigen expression. In mice monocytes are differentiated from other leukocyte populations by their $F4/80^+CD11b^+$ phenotype and as in humans can also be subdivided according to their expression of the chemokine receptors CX_3CR1 and CCR2, as shown in table 3.2 (Gordon and Taylor, 2005). The expression of these chemokine receptors appears to be critical for the survival and trafficking of monocytes. The role of CX_3CR1 is discussed in detail below but it appears that this receptor is vital for survival of resident $Ly6C^-CX_3CR1^{high}$ monocytes; in CX_3CR1 knock-out mice a lack of CX_3CR1-CX_3CL1 interaction results in a reduction in the number of these monocytes found in the circulation (but no change in inflammatory monocyte numbers) and a decrease in absolute monocyte numbers in these animals (Jung et al., 2000). CCR2 deficiency on the other hand results in retention of $Ly6C^+CX_3CR1^{int}$ monocytes in the bone marrow, indicating that CCR2-CCL2 interaction is required for extravasation of these cells from here (Serbina and Pamer, 2006). In fact CCR2 knock out results in a marked reduction of inflammatory monocyte trafficking in

general; following a thioglycollate inflammatory challenge far fewer cells are recovered from the peritoneum of $CCR2^{-/-}$ mice compared to wild-type controls, and this recruitment deficit is specific to monocyte/macrophages (Kurihara et al., 1997).

Table 3.2. Antigen expression on mouse monocytes of the two best-characterised subsets. (Adapted from Gordon and Taylor, 2005)

Antigen / Receptor	Expression in Mouse 'resident' monocytes	Expression in Mouse 'inflammatory' monocytes
CD14	Not determined	Not determined
CD16	Not determined	Not determined
F4/80	+	+
CD11b	+	+
Ly6C	-	+
CX_3CR1	High	Intermediate
CCR2	-	+

As well as this phenotypic distinction, these subsets of monocytes can also be distinguished functionally using adoptive transfer of GFP-expressing monocytes from a CX_3CR1 knock-in mouse. Geissmann et al determined that $Ly6C^{+}CX_3CR1^{int}CCR2^{+}$ inflammatory monocytes were short lived after adoptive transfer to irradiated wild-type mice, however in models of disease these cells are rapidly recruited to sites of inflammation, whilst $Ly6C^{-}CX_3CR1^{high}CCR2^{-}$ resident monocytes, on the other hand, persisted and could be seen in tissues (Geissmann et al., 2003). As a result of their three key functions (antigen presentation, phagocytosis and immunomodulation) monocyte/macrophages play a critical role in maintaining tissue homeostasis and supporting the adaptive immune response. Examples of resident monocyte/macrophage function are summarised in figure 3.2 below.

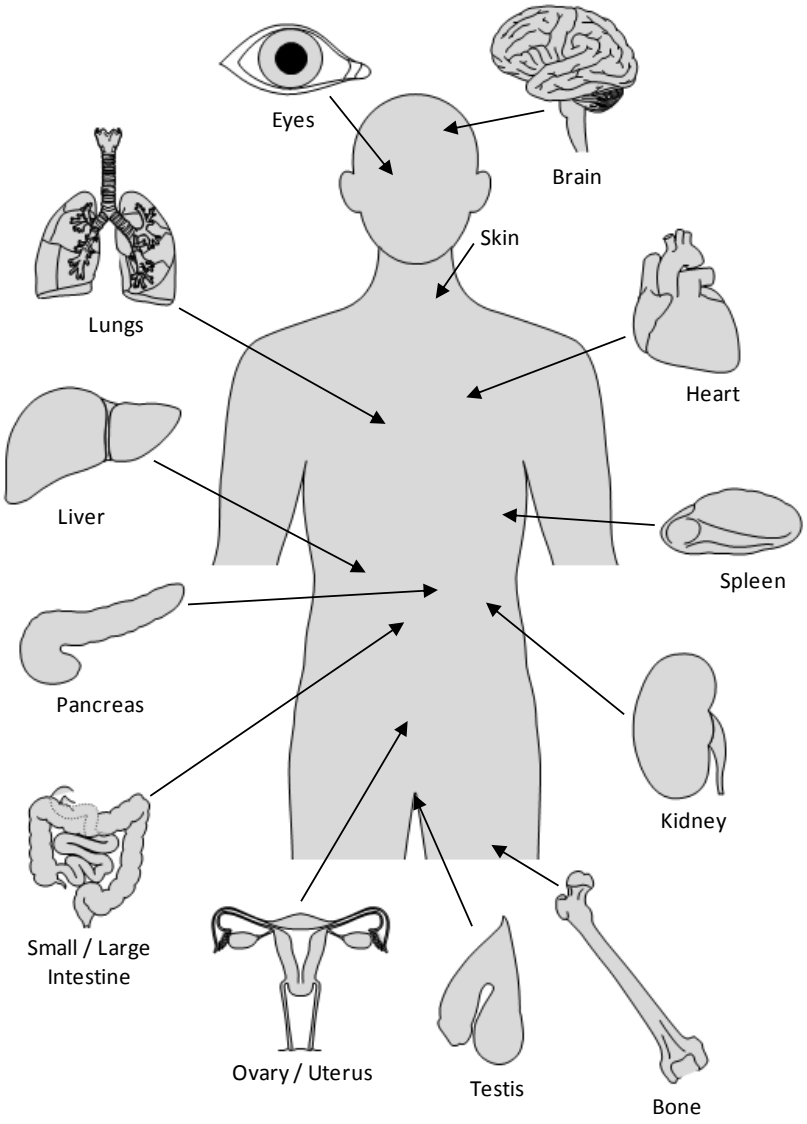

Figure 3.2. Macrophage location and function. Macrophages are found in most tissues where they have specialised functions and sometimes known by specific names. In the brain microglia are involved in neuronal survival, connectivity and repair. In the skin Langerhan cells play an important immune surveillance role and control keratinocyte proliferation and differentiation. In the heart cardiac macrophages are involved in healing and remodelling of cardiac tissue. Splenic macrophages are immune surveyors as are alveolar macrophages in the lungs and crypt macrophages in the small and large intestines. In the liver Kupffer cells clear debris from the blood and contribute to tissue regeneration after injury. Pancreatic macrophages have an important role in islet development whilst in the kidney macrophages are involved in ductal development. In the bone marrow macrophages contribute to erythropoiesis whilst in the rest of the bone osteoclasts are critical for normal bone remodelling. Macrophages found in the eye contribute to vascular remodelling, in the uterus they are involved in cervical ripening and finally in the ovaries and testis macrophages contribute to the production of steroid hormones. Adapted from www.macrophages.com.

Homeostatically monocyte/macrophages ingest waste material, including that arising from the aging of red blood cells (they phagocytically clear approximately 2 x 10^{11} erythrocytes per day) (Mosser and Edwards, 2008) and clean up debris at the side of tissue damage or infection (Geske et al., 2002). In comparison to their polymorphonuclear companions, neutrophils, monocyte/macrophages are relatively long lived. This is clinically very important especially in cancer patients where they provide protection in those at risk of fatal infection following chemotherapy, as they are not depleted as severely as other immune cells by this treatment (Dale et al., 2008). Under physiological conditions tissue resident macrophages survey their local environment and are responsible for mounting a response to invading pathogens. These are detected via their interaction with pattern-recognition receptors on the surface of macrophages, leading subsequently to activation of the cell and the release of various mediators that recruit other cells of the immune system. A key example of this is activation of toll-like receptors (TLRs). TLRs recognise various pathogen related molecules, such as lipopolysaccharide. Ligand-binding to this receptor results in downstream activation of the transcription factor NF-κB and release of pro-inflammatory cytokines and chemokines (Dale et al., 2008) which are able to modulate the immune response by recruiting and activating further immune cells. Importantly resident macrophages phagocytose pathogens and release CCL2 which induces the chemotaxis of inflammatory monocytes. Monocyte/macrophages have a huge capacity for phagocytosis and can internalise almost any antigen which is digested by the fusion of the phagosome with lysosomes. The antigens are then presented on major histocompatability complex (MHC) proteins of class I (predominantly endogenous antigens) or class II (exogenous antigens) and mediate the activation of T-cells (Trombetta and Mellman, 2005). Following their recruitment to inflamed tissues, inflammatory monocyte/macrophages become activated, be it by pro-inflammatory mediators

released from resident monocyte/macrophages or from damaged tissues; they show enhanced microbial activity and begin to secrete high levels of pro-inflammatory mediators themselves.

1.2. Experimental macrophage depletion

Liposomes are artificially prepared lipid vesicles comprised of concentric phospholipid bilayers (figure 3.3), and were first identified by British haematologist Alec Bangham in the early 1960's (Bangham et al., 1962;Horne et al., 1963;Bangham and Horne, 1964). The entrapment of an aqueous compartment by this bilayer allows these vesicles to act as a cross-membrane delivery system for highly hydrophilic molecules dissolved in an aqueous solution; due to the hydrophobicity of the membrane the solutes are unable to readily pass through the lipid membrane, rather they are delivered to their target site by fusion of the lipid bilayer with similar structures, such as those comprising the cell membrane, and consequent release of the contents into the target cell or organelle. Whilst there is ongoing research into specific targeting of liposomes by the introduction of specific surface markers or antibodies, the typically fate of liposomes is to be phagocytosed by mononuclear phagocytes. As a result liposomes offer a valuable tool for targeting compounds to these cells to manipulate their function. A number of liposome encapsulated drugs are already in use, designed to reduce the toxicity of existing formulations; for example liposome-encapsulated doxorubicin (Myocet) has been trialled and approved for the treatment of solid tumours and has been shown to have a longer half-life with less free drug available for tissue distribution than conventional doxorubicin (Mross et al., 2004). Here the specific example of liposome-encapsulated clodronate (LCL) is discussed. Clodronate, also known as dichloromethylene-bisphosphonate (Cl_2BMP) is used extensively in the treatment of

osteolytic bone disease where it exerts anti-bone-resorptive action via cytotoxic effects on osteoclasts (monocyte-derived bone specific macrophages) (Rogers et al., 2000), but has also been reported to have analgesic efficacy independent of this mechanism (Kim et al., 2013). The phagocytosis of LCL by phagocytes results in the development of a phagosome within the cell (figure 3.4A/B), which subsequently fuses with phospholipase containing lysosomes (figure 3.4C/D) which in turn disrupt the phospholipid bilayers of the liposome causing the clodronate, which is dissolved in the aqueous compartments between bilayers, to be released into the cell (figure 3.4E). Clodronate accumulates in the cell (it is strongly hydrophilic and unable to cross the cell membrane) and causes the cell to undergo apoptosis (figure 3.4F/G); the exact mechanism by which this occurs has not yet be unravelled, however the most prevalent suggestion is based upon the mechanism by which non-nitrogen containing bisphosphonates act upon osteoclasts; clodronate is metabolised into a non-hydrolysable methylene-containing analogue of ATP by aminoacetyl-tRNA synthetase enzymes that accumulates in the cell, subsequently triggering apoptosis (figure 3.4E) (Frith et al., 1997;Frith et al., 2001). When administered to non-phagocytic cells *in vitro* LCL has no effect on growth or function of the cells (Claassen et al., 1990). In fact evidence suggest that when administered systemically LCL affects only macrophages and their direct monocyte precursors (Huitinga et al., 1992); despite their phagocytic potential neutrophils appear neither morphologically or functionally affected by LCL (Qian et al., 1994).

Using this method of macrophage depletion, a role for these cells in the pathophysiology of a number of inflammatory and pain-inducing diseases has been established. Depletion of the macrophages in the knee joints of mice by intra-articular injection of LCL before the induction of rheumatoid arthritis significantly reduces osteophyte formation (Blom et al., 2004), joint disruption, joint inflammation and pro-inflammatory cytokine (IL-1β and TNFα) production (van

Lent et al., 1996); blockade of IL-1β and TNFα signalling in arthritis models is anti-hyperalgesic (Sachs et al., 2011). Reduction of circulating monocyte/macrophages reduces infiltration of these cells into the nerve following injury to this tissue; this both reduces thermal hyperalgesia and protects nerve fibres against degeneration, confirming a role for monocyte/macrophages in the development of neuropathy following nerve injury (Liu et al., 2000). Preventing spinal cord infiltration of macrophages following spinal cord injury, by LCL induced depletion preserves fibre myelination, reduces cavity size and encourages enhanced sprouting and behavioural recovery (Popovich et al., 1999). Macrophage depletion prevents infiltration of the nerve by these cells and significantly attenuates disruption of the blood nerve barrier following chronic nerve compression (Gray et al., 2007), reduces nerve-injury induced mechanical hypersensitivity (Barclay et al., 2007) and delays the onset of diabetes induced mechanical allodynia (Mert et al., 2009).

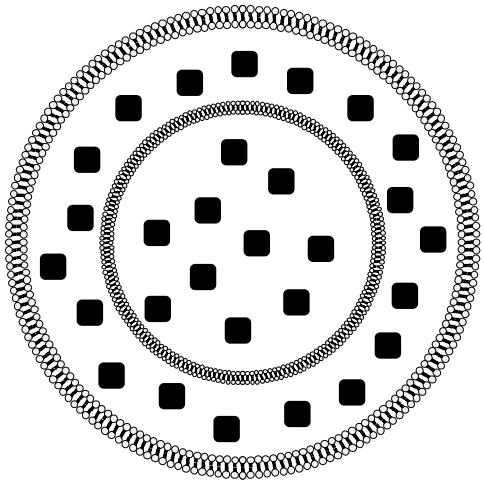

Figure 3.3. Schematic representation of liposome encapsulated clodronate. Concentric phospholipid bilayers encapsulate clodronate (black squares).

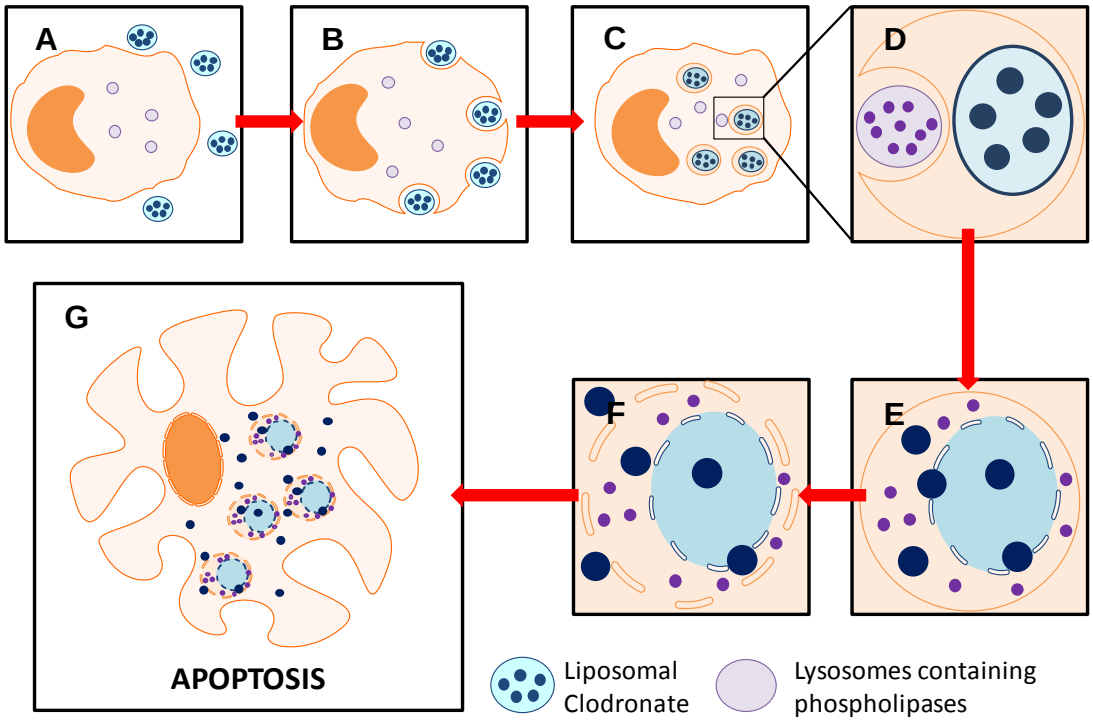

Figure 3.4. Schematic representation of the mechanism of monocyte/macrophage depletion by liposome encapsulated clodronate. The phagocytosis of LCL by phagocytes results in the development of a phagosome within the cell (A/B), which subsequently fuses with phospholipase containing lysosomes (C/D) which in turn disrupt the phospholipid bilayers of the liposome causing the clodronate, which is dissolved in the aqueous compartments between bilayers, to be released into the cell (E). Clodronate accumulates in the cell and causes the cell to undergo apoptosis (F/G).

1.3. CX_3CR1

Chemokines or 'chemoattractant cytokines' are a family of small proteins that obtain their name from their first described function as mediators of leukocyte migration. First discovered in the late 1980's, the chemokines are now a large family of structurally and functionally similar molecules named according to the organisation of cysteine residues on their N-terminal region and are divided into four sub-families: C, CC, CXC and CX_3C. Chemokines with each subclass have a promiscuous relationship with their receptors of which there are over twenty; as a result receptor nomenclature is based on the sub-family of ligands it binds, e.g. CC chemokines bind but CC receptors. The exception to this rule is the interaction between CX_3CL1 and its receptor CX_3CR1 which is a monogamous relationship. The structure, expression and function of CX_3CR1 are discussed here, whilst the protein ligand, CX_3CL1, is discussed in detail in chapter four.

1.3.1. Structure

CX_3CR1 was first identified as the orphan receptor V28, however PCR screens of human PBMCs demonstrated that the amino acid sequence of V28 displayed a number of features also present in several known chemokine receptors, including seven hydrophobic regions, a 20 amino acid region highly conserved in the G-protein coupled receptor super-family and a short sequence in the second cytoplasmic loop which is particularly conserved in the chemokine receptors. In fact 81% of the amino acid sequence of V28 was found to be identical to that of the MIP-1α and MCP-1 receptors (Raport et al., 1995). The genes encoding the chemokine receptors (and their protein ligands) are clustered in the human genome (Maho et al., 1999); CX_3CR1 has been mapped to the 3p21.3 region (Samson et al., 1996;Maho et al., 1999) were it is encoded by a single exon (Raport et al., 1995). Like all of the chemokine receptors, CX_3CR1 is a seven-transmembrane domained G-

protein coupled receptor. The regions of the protein critical for ligand binding by CX_3CR1 have been identified using equilibrium binding analyses of various protein mutants; two acidic amino acid residues, Asp25 located in the N-terminal domain and Glu254 in the third extracellular loop, are crucial for ligand binding; their substitution with alanine abolishes the ligand binding capacity of CX_3CR1. Additionally an N-terminal tyrosine (Tyr14) is implicated in binding affinity as its substitution significantly impacts ligand binding; together this suggests the N-terminal domain and third extracellular loop are involved in ligand binding (Chen et al., 2006). Structural analysis of CX_3CL1 has implicated several positively charged amino acid residues in the chemokine function of this protein (Mizoue et al., 1999;Mizoue et al., 2001;Harrison et al., 2001). Additionally, Chen et al determined the amino acid residues of CX_3CR1 responsible for ligand binding are also essential for the stimulation of receptor mediated cellular responses; mutant receptors with a deficient ligand binding capability failed to induced cellular migration in a CX_3CL1 chemotactic assay . Furthermore, several mutants with unaffected ligand binding showed an unexpected deficit in chemotactic response, suggesting high affinity ligand binding alone is not sufficient for receptor activation (Chen et al., 2006). One of the intracellular consequences of CX_3CL1-induced activation of CX_3CR1 is the phosphorylation of the mitogen-activated protein kinase ERK1/2 (Cambien et al., 2001), which is necessary for CX_3CR1-dependent chemotaxis (Chen et al., 2006); independent mutation of the residues Glu13 and Asp16 in the N-terminal domain and Asp266 in the third extracellular loop results in significant impairment of the ability of CX_3CR1 to induce ERK activation (phosphorylation) which subsequently impairs chemotaxis (Chen et al., 2006), suggesting that these regions necessitate signal transductions as well as ligand binding.

Human genetic studies have identified two CX_3CR1 polymorphisms that are risk factors for coronary artery disease; an isoleucine (Ile) substitution at Val249 (V249I) and a methionine (Met)

substitution at Thr280 (T280M) which are located in the sixth and seventh transmembrane domain respectively (McDermott et al., 2001;Moatti et al., 2001;Ghilardi et al., 2004). Functional analysis of leukocytes possessing CX_3CR1 with these mutations demonstrated that this is a result of a decreased number of CX_3CL1 binding sites and defective chemotactic responses for CX_3CL1, with the T280M mutation contributing to activation independently of binding (Faure et al., 2000;McDermott et al., 2003); however it still unclear whether CX_3CL1 interacts directly with these transmembrane residues.

1.3.2. Expression

Raport et al initially demonstrated using Northern blotting that the expression of V28, now known as CX_3CR1, is highest in the spleen and peripheral blood leukocytes. High levels of expression were also observed in several neural tissues including the medulla (and multiple other brain regions) and the spinal cord. Examination of the RNA from myeloid and lymphoid cell lines found V28 to be highly expressed in THP.1 cells (monocytic cell line) and to a lesser extent U937 (macrophage cell line) and HL60 (myeloid precursor) cells of the myeloid lineage, but not expressed at all in lymphoid cells. Analysis of mRNA from freshly isolated peripheral blood leukocytes demonstrated V28 was expressed mainly by $CD16^+$ natural killer (NK) cells, but the mRNA could also be detected at lower levels in $CD3^+$ T cells (which could be increased with IL-2 treatment), $CD14^+$ monocyte and granulocytes, but barely in $CD19^+$ B cells. When the levels of functional protein was assessed in these cells a slightly different expression pattern was revealed; almost all (92%) of NK cells expressed functional V28 protein, which was expected from the mRNA analysis, however, slightly unexpectedly, the majority (79%) of $CD14^+$ monocytes expressed functional V28. The $CD3^+$ positive T cells found to express functional V28 was predominantly $CD8^+$, although some $CD4^+CD8^+$ T cells expressed V28. The expression of the V28 functional protein in $CD19^+$ B cells was equal to that of

the mRNA expression, in that its expression was barely detected. Conversely, unlike mRNA, virtually no V28 protein was detected in granulocytes (Raport et al., 1995). The expression of CX_3CR1 in T-cells was examined in more detail by Foussat and colleagues several years later. Using a series of flow cytometry studies they demonstrated that approximately 8% of $CD4^+$ and 14% of $CD8^+$ T-cells express CX_3CR1 on their surface, the majority of which were $CD45RO^+$ memory T-cells; however there were some $CD8^+$ cytotoxic and $CD4^+$ helper T-cells that expressed this protein. They observed that $CD8^+$ T-cells expressed CX_3CR1 under both resting and activated states, whilst $CD4^+$ helper T-cells expressed the protein only when activated. The CX_3CR1 protein is functional in these cells; CX_3CL1 causes migration of $CD8^+$ memory, $CD8^+$ cytotoxic and $CD4^+$ memory T-cells via the induction of either transient or sustained actin polymerization (Foussat et al., 2000).

The rat homologue of CX_3CR1, RBS-11 was identified in the late 1990's based on its sequence homology to V28. Radio-ligand binding analysis confirmed highly specific binding of this receptor to CX_3CL1 with no competitive binding by other chemokines. Analysis of mRNA expression found RBS-11 to be relatively abundant in the brain; expression of RBS-11 mRNA in cultured primary microglia was ten-fold higher than that of whole brain samples suggesting the signal seen in these samples was from microglial RBS-11 mRNA. FACS analysis of cortical microglia demonstrated that these cells express the RBS-11 protein on their surface as well as the mRNA; this was confirmed to be functional as treatment of these cells with CX_3CL1 induced calcium mobilization and chemotaxis that could be blocked with an anti-RBS-11 antibody (Harrison et al., 1994).

The development of a transgenic mouse by Jung et al, in which the CX_3CR1 gene was mutated to contain a green fluorescent protein (GFP) reporter gene, allowed the pattern of CX_3CR1 expression in the mouse to be analysed in depth. Reverse transcription PCR analysis of these mice

demonstrated the presence of chimeric transcripts in CX_3CR1-GFP mice and the absence of wild-type transcripts in $CX_3CR1^{gfp/gfp}$ mice; thus heterozygous mice ($CX_3CR1^{+/gfp}$) expressed both the GFP reporter and functional CX_3CR1, whilst homozygous CX_3XR1-GFP mice ($CX_3CR1^{gfp/gfp}$) expressed only the GFP reporter and no functional CX_3CR1 protein. Using the heterozygous mice Jung et al were able to use FACS analysis to determine which murine cell populations express CX_3CR1; this protein was confirmed to be functional by demonstrating that these cells were able to bind a CX_3CL1 fusion protein that could easily be visualised (NTN-Fc). In accordance with data collect from human peripheral blood cells, murine blood contained a population of monocytes ($CD11b^+$ $Gr1^{low}$) that expressed CX_3CR1, as did approximately 5-30% of NK cells in the mouse; these could be found in the peripheral blood as well as lymphoid and non-lymphoid organs such as the liver. B-lymphocytes, on the other hand, were CX_3CR1 negative. In contrast to human data, murine T-lymphocytes, both resting and active, were CX_3CR1 negative. Other peripheral blood cells of myeloid lineage (eosinophils and $CD11b^+$ $Gr1^{high}$ neutrophils) did not express functional CX_3CR1; however some neutrophils expressed low levels of GFP, attributed to residual expression from the CX_3CR1 positive granulocyte-macrophage colony forming precursor from which these cells derive. Jung et al also characterised the expression of CX_3CR1 on dendritic cells and found this protein to be expressed on $CD8\alpha^-$ (myeloid) and $CD8\alpha^+$ (lymphoid) dendritic cells as well as $CD11c^{low}$ $F4/80^+$ cutaneous Langerhans cells. Similar to data collected on the expression of CX_3CR1 in the rat, microglial cells in the mouse CNS were positive for CX_3CR1 but the protein was not seen in astrocytes or oligodendrocytes (Jung et al., 2000). More recently it has been suggested that CX_3CR1 is also expressed on $GFAP^+$ satellite glial cells in the DRG based on the observation that in an inflammatory model pain (carrageenan) there is an increase in satellite cell activation in the DRG in comparison to control, that could be attenuated by treatment with either the glial inhibitor FLC or an antibody against CX_3CR1. However protein expression of CX_3CR1 in the DRG is not shown

by this group (immunohistochemically or otherwise) (Souza et al., 2013) and it may be possible to attribute the effect of the CX_3CR1 antibody to the suppression of CX_3CL1-CX_3CR1 signalling in macrophages in the DRG, which are known to express CX_3CR1. Additionally, Yang et al have demonstrated that both the CX_3CR1 protein and mRNA are present in endothelial cells (human coronary artery endothelial cells [HCAECs] and human umbilical vein endothelial cells [HUVECs]); the protein appears functional as treatment of these cells with soluble CX_3CL1 results in an increase in adhesion molecule (ICAM-1) expression shown to be dependent on a CX_3CL1-CX_3CR1 interaction; this increase in ICAM-1 was attenuated in cells transfected with a CX_3CR1-interferring RNA that knocked down the expression of CX_3CR1. These cells were, however, in an *in vitro* setting and the expression of CX_3CR1 in endothelial cells was not confirmed *in vivo* (Yang et al., 2007).

Furthermore there is evidence to suggest pathophysiological changes may alter the expression profile of CX_3CR1. In a rat model of temporomandibular joint inflammation Wang et al demonstrate CX_3CR1 expression in $NeuN^+$ (neurons) and $GFAP^+$ (astrocytes) cells in the trigeminal nucleus caudalis, a subdivision of the trigeminal nucleus of the medulla, that receives pain information conveyed from the ipsilateral face. The activation of these receptors by CX_3CL1 increases GFAP immunoreactivity, suggestive of astrocyte activation, and exacerbates pain in these animals (Wang et al., 2012). Double immunofluorescence labelling of coronary arteries from patients with atherosclerotic plaques/lesions with antibodies against CX_3CR1 and smooth muscle actin has demonstrated that CX_3CR1 is expressed by smooth muscle cells in the lesions of these patients, which were often adjacent to CX_3CL1 positive cells. Coupled with the observation that cultured smooth muscle cells undergo chemotaxis to CX_3CL1 it is suggested that CX_3CR1 is functional in these cells (Lucas et al., 2003). This data supports previous work by Wong et al, who have reported co-localization of CX_3CR1 with a smooth muscle cell marker (α-smooth muscle actin)

in the coronary arteries taken from patients with diabetes mellitus and atherosclerosis (Wong et al., 2002). It has been demonstrated that CX_3CR1 is expressed by several kinds of cancer cells including renal carcinoma cells (Yao et al., 2013), pancreatic ductal adenocarcinoma cells (Zhao et al., 2012) and non-small cell lung cancer cells (Mauri et al., 2012), as well as in astrocytoma, oligodendroglioma and glioblastoma cells, to name just a few. In these cells it is thought that the receptor may contribute to cell migration and metastasis (Yao et al., 2013;Zhao et al., 2012), leading some to hypothesis that high CX_3CR1 expression may be a marker of poor prognosis (Xu et al., 2012); CX_3CR1 positivity is significantly associated with stage and number of metastatic sites (Mauri et al., 2012).

1.3.3. Function and contribution to disease

1.3.3.1. Peripheral Physiological Functions of CX_3CR1

The development of CX_3CR1 functional knock-out mice has allowed the function of this receptor to be extensively evaluated. One of these (described above in terms of its use to evaluate the expression of CX_3CR1) is an mouse containing GFP reporter in which mice of the homozygous phenotype $CX_3CR1^{gfp/gfp}$ do not possess functional CX_3CR1. Jung et al compared the CX_3CR1^{+} cell populations from the chimeric $CX_3CR1^{+/gfp}$ to the GFP^{+} populations of the $CX_3CR1^{gfp/gfp}$ mouse and found that none of these were absent or significantly altered in the absence of functional CX_3CR1 (Jung et al., 2000). However a later paper by the same group has since reported that expression of functional CX_3CR1 is critical for the survival of $Gr1^{low}CX_3CR1^{high}$ monocytes; the absence of CX_3CR1-CX_3CL1 interaction results in a specific reduction in the number of circulating $Gr1^{low}$ CX_3CR1^{high} monocytes (but no change in $Gr1^{high}$ CX_3CR1^{low} monocyte numbers) and a decrease in absolute monocyte numbers in these animals. Adoptive transfer of $CX_3CR1^{+/gfp}$ monocytes into CX_3CR1

knock-out animals restored monocyte number, whilst the same process using $CX_3CR1^{gfp/gfp}$ monocytes could not, suggesting impaired survival of these cells. Enforced expression of the anti-apoptotic factor Bcl2 was able to rescue monocyte numbers in $CX_3CR1^{gfp/gfp}$ mice; a pronounced increase in $Gr1^{low}$ CX_3CR1^{high} monocytes was demonstrated and it was suggested that CX_3CR1-CX_3CL1 interaction promotes activation of Bcl2, preventing apoptosis. This was confirmed with a series of experiments using cultured monocytes in which addition of CX_3CL1 to the media could prevent cell death induced by serum starvation; the effect of CX_3CL1 was blocked by treatment of the monocytes with pertussis toxin which blocks Gα signalling associated with CX_3CR1 (Landsman et al., 2009).

So CX_3CR1 function is critical to the survival of CX_3CR1^{high} cells, but what other functions does it have? In circulating monocytes the key function of CX_3CR1 appears to be its role in adhesion of these cells to the endothelium. The adhesive property of monocytes provided by CX_3CR1 was established early on. In their 1997 paper, Imai et al demonstrate rapid immobilization of V28 (CX_3CR1) transfected cells on glass plates coated with a FKN-SEAP fusion protein (CX_3CL1 fused with the secreted form of placental alkaline phosphatase that allows chemokines to retain their binding capacity whilst allowing quantitative determination of specific binding), but not to plates coated with SEAP lacking FKN (fractalkine/CX_3CL1). The adhesion was stable and not affected by depletion of divalent cations. The adherence also occurred in cells in which calcium mobilization after CX_3CL1 treatment did not occur despite transfection with V28, suggesting that adherence via CX_3CR1 does not require an intracellular calcium response (Imai et al., 1997). To create a more physiological setting, Fong et al added the element of shear stress to similar experiments and observed that despite this additional factor, immobilised CX_3CL1 still rapidly captured leukocytes without rolling. They also demonstrated that if a mixed population of PBMCs was subjected to this

assay approximately 62.5% of the captured cells were $CD14^+$ monocytes and another 30% were $CD8^+$ T-cells, which is to be expected given our understanding of CX_3CR1 expression in human leukocytes. Finally, they confirmed the observation made by Imai and colleagues that this adherence occurs independently of calcium mobilization (Fong et al., 1998). Later Haskell et al used chimeras of the mucin stalk of CX_3CL1 and the soluble receptor binding domains of other chemokines to demonstrate that the adhesive property of the CX_3CR1-CX_3CL1 interaction occurs as a result of the specific conformation of CX_3CL1, as opposed to the presence of a chemokine with a mucin stalk tethering the soluble domain to a cell membrane (Haskell et al., 2000). Interestingly, the presence of this chemokine domain alone is not sufficient to induce adhesion, repetition of FKN-SEAP experiments using fusions of SEAP to individual domains of CX_3CL1 determined that, whilst monocytes adhere efficiently to immobilised FKN-SEAP, they could not adhere to a version of the fusion protein containing only the mucin stalk (mucin-SEAP) or only the chemokine domain (CX_3C-SEAP) (Goda et al., 2000). Despite evidence to suggest that the interaction between CX_3CL1 and its receptor is alone enough to cause monocyte adherence, the contribution of integrins should not be overlooked. In fact it is likely that CX_3CL1-CX_3CR1 interactions impacts integrins mediated monocyte adhesion. Monocytes are able to adhere to the endothelial layer by interaction with the integrins VCAM-1 and ICAM-1, but the addition of soluble CX_3CL1 (chemokine domain) and subsequent activation of CX_3CR1 greatly enhance adherence via these integrins (Goda et al., 2000).

Using intravital microscopy Auffray et al have shown that $Gr1^{low}CX_3CR1^{high}$ monocytes constitutively exhibit a crawling type of motility which is not seen with CX_3CR1^{int} cells under steady state conditions. In CX_3CR1-deficient mice the number of crawling monocytes is reduced by approximately two thirds; it's possible to suggest that this crawling behaviour is conveyed, at least

in part, by the intrinsic adhesion function of CX_3CR1, along-side a significant contribution by β2-integrins and LFA-1. The patrolling monocytes provide immune surveillance of the endothelium and surrounding tissues; in response to tissue damage they quickly extravasate and invade the affected tissue providing an early inflammatory immune response to the damage by releasing TNFα and IL-1β, contributing to the recruitment of $Gr1^{high}CX_3CR1^{int}$ cells (Auffray et al., 2007).

The evidence presented above demonstrates that CX_3CR1 is critically involved in the adhesion of CX_3CR1^{high} monocytes to the endothelium, occurring independently of receptor activation. Following adhesion, monocytes transmigrate across the endothelium to infiltrate the underlying tissue. This process is also heavily dependent on CX_3CR1 and three key regions of the receptor have been identified. Firstly, a NPX(2-3)Y sequence (asparagine-proline-X(2-3)-tyrosine where X represents leucine, isoleucine & valine) in the seventh transmembrane domain is required for ligand binding. Secondly, serine residues within the intracellular C-terminus contribute to receptor trafficking. Finally, and most critically for transmigration, a DRY (asparate-arginine-tyrosine) sequence in the second intracellular loop is required for the activation of the receptor and G-protein that leads to calcium mobilization; mutation of these regions results in a receptor that is unable to induce transmigration of the monocyte (Schwarz et al., 2010). It is likely that this transmigration is induced by polymerization of actin filaments, which has been observed in migrating dendritic cells following a CX_3CL1 stimulus (Dichmann et al., 2001); actin reorganization is a prerequisite for leukocyte migration after a chemokine stimulus and can be inhibited by the addition of pertussis toxin which blocks Gi signalling (Tenscher et al., 1997;Aspinall et al., 2010). Indeed CX_3CR1 mediated migration can be inhibited by blocking Gi signalling, and requires cleavage of membrane bound CX_3CL1 by ADAM10 or ADAM17, to produce a soluble chemokine

domain that is able to activate intracellular signalling pathways downstream of CX_3CR1 (Schwarz et al., 2010).

As well as providing a mechanism by which monocytes can adhere to and migrate into the endothelium to provide immune surveillance of surrounding tissues, CX_3CR1 can recruit NK cells in a similar fashion (El-Shazly et al., 2013), and also promotes the development of dendritic cells under steady state conditions. Expression of CX_3CR1 is a marker of myeloid monocyte/dendritic cell precursors, and whilst it has been demonstrated that deficiency of CX_3CR1 does not result in an obvious deficiency in dendritic cell differentiation (Jung et al., 2000), the results of a series of adoptive transfer experiments performed by Lyszkiewicz et al indicate that CX_3CR1 signalling promotes dendritic cell differentiation under physiological conditions, and that progenitors that are deficient of CX_3CR1 perform poorly at giving rise to dendritic cells in comparison to wild-type progenitors (Lyszkiewicz et al., 2011). Additionally there is evidence to support a role for CX_3CR1 in the maintenance of bone homeostasis through the regulation of osteoblasts and osteoclasts. Osteoclasts are a type of specific tissue resident macrophage that express CX_3CR1 as a result of their differentiation from circulating monocytes; they are involved in the demineralization and breakdown of bone. CX_3CR1-deficient mice exhibit a decrease in osteoclast number resulting in deregulation of bone homeostasis that leads to an increase in bone formation rate and bone volume (Koizumi et al., 2009).

1.3.3.2. Central Physiological Functions of CX_3CR1

Within the brain CX_3CR1 is exclusively expressed in microglia, where its interaction with CX_3CL1 contributes to the suppression of an inflammatory state in these cells; CX_3CL1 is able to limit the release of pro-inflammatory mediators, reducing production of NO and TNFα (Mizuno et al., 2003;Lyons et al., 2009). This would suggest the CX_3CR1-CX_3CL1 interaction is protective and there is certainly *in vivo* evidence to support this. It has been demonstrated that in the brain the CX_3CR1-CX_3CL1 interaction is neuroprotective; CX_3CR1-deficient mice show enhanced neuronal loss in a model of both amyotrophic lateral sclerosis when compared to wild-type littermate controls; a similar effect has been shown in a model of Parkinson's disease (Cardona et al., 2006). Additionally when this model of Parkinson's disease was established in wild-type mice an increase in CX_3CR1 protein was seen and associated with microgliosis and parkinsonian-like behaviours that could be reverse with treatment with an anti-CX_3CR1 antibody (Shan et al., 2011). Likewise, in a model of experimental auto-immune uveitis (inflammation within the eye) $CX_3CR1^{-/-}$ animals show increased disease severity and neuronal loss suggesting a neuroprotective role for this receptor. This effect was partially attributed to an inability of monocytes to fully transmigrate, causing clustering of semi-differentiated cells (Dagkalis et al., 2009); this is not surprising considering all we have learnt regarding the role of CX_3CR1 in leukocyte extravasation. Furthermore a protective role for this interaction can be deduced from studies of age-related retinal disease; Seidler et al observed that in human monocytes CX_3CR1 expression decreases with age (Seidler et al., 2010) and a lack of CX_3CR1 in mice is associated with enhanced accumulation of hypertrophied microglia in the sub-retinal space (Combadiere et al., 2007;Chinnery et al., 2012;Raoul et al., 2008), that contribute to the development of age-related macular degeneration (Combadiere et al., 2007). This suggests that the CX_3CR1-CX_3CL1 interaction may contribute to the maintenance of a resting morphology in these cells; however this research is still controversial and enhanced retinal degeneration in

CX_3CR1 knock-out mice is not seen by all groups (Luhmann et al., 2013b;Luhmann et al., 2013a). A possible mechanism for the neuroprotective effect of CX_3CR1 is the induction of neurogenesis or long term potentiation (LTP) both of which are important in learning and memory; young CX_3CR1 knock-out mice display motor learning deficits and impaired associative and spatial memory associated with decreased hippocampal neurogenesis and alterations in the induction of LTP (Rogers et al., 2011). CX_3CL1 enhances hippocampal NMDA receptor function, via the activation of adenosine receptor type A2 (A2AR) and the release of D-serine from glia, which increases NMDA-field excitatory post-synaptic potentials (Scianni et al., 2013). Conversely a neurotoxic effect of CX_3CR1-CX_3CL1 signalling has also been proposed following the observations that CX_3CR1-deficiency correlates with reduced ischemic damage in a model of stroke; $CX_3CR1^{-/-}$ mice show enhanced functional recovery and a reduction in infarct size and pro-inflammatory mediator expression in comparison to wild-type controls (Denes et al., 2008). However it is possible that this effect is a result of reduced leukocyte infiltration and subsequent release of pro-inflammatory mediators as opposed to a direct neurotoxic effect; these mice do indeed appear to have fewer apoptotic and infiltrating leukocytes in the lesion (Denes et al., 2008). Additionally a similarly neurotoxic effect for CX_3CR1 has been demonstrated in a model of spinal cord injury where deficient CX_3CR1 signalling promotes recovery by limiting the recruitment and activation of $Ly6C^-$ CX_3CR1^{high} monocytes, which would otherwise synthesise and release a host of inflammatory cytokines and oxidative metabolites which impede recovery (Donnelly et al., 2011).

1.3.3.3. Pathophysiological Functions of CX_3CR1

1.3.3.3.1. Cardiovascular Disease

Physiological CX_3CR1-CX_3CL1 signalling is certainly a necessity; survival of immune surveying monocytes depends on it and in its absence show reduced survival to a number of infections including herpes simplex virus (Boivin et al., 2012) and vaccinia virus (Bonduelle et al., 2012), and demonstrate reduced bacterial clearance (Ishida et al., 2008b). However, it has also become evident that aberrant CX_3CR1-CX_3CL1 signalling can contribute significantly to the pathogenesis of a number of chronic diseases, perhaps unsurprising given the role of this protein pair in immune and inflammatory processes. Early examination of patients with polymorphisms of the gene encoding CX_3CR1 identified a reduced risk of atherosclerosis in those with alterations that resulted in the expression of a receptor with a reduced binding capacity (Moatti et al., 2001;McDermott et al., 2001). Following an inflammatory stimuli endothelial cells up-regulate their expression of CX_3CL1, promoting enhanced CX_3CR1^{high} monocyte transmigration (Harrison et al., 1999). As these cells differentiate into macrophages in the tissue they begin to accumulate lipids and release chemokines that lead to further immune cell recruitment. Interestingly, as discussed previously, under atherosclerotic conditions smooth muscle cells being to express CX_3CR1, leading to their recruitment to the developing lesion due to the chemotactic effects of CX_3CL1 (Lucas et al., 2003;Wong et al., 2002). The contribution of $CX_3CR1/L1$ to the pathogenesis of cardiovascular disease is significant; an increased number of CX_3CR1^{high} monocytes alone is sufficient to act as a predictor of plaque rupture (Ikejima et al., 2010), and, as to be expected from the human polymorphisms, mice deficient in CX_3CR1 show a decreased prevalence of atherosclerosis (Lesnik et al., 2003). In fact these mice show an 83% decrease in arteriolar leukocyte adhesion (Rius et al., 2013). Indeed CX_3CR1 appears to contribute to the pathology of several diseases based on its role in leukocyte migration. Patients with coronary artery disease have increased plasma levels of

soluble CX_3CL1 and an increased number of circulating CX_3CR1^+ PBMCs, due to an expansion of the $CX_3CR1^+CD8^+$ T-cell subset; this is associated with enhanced chemotaxis and adhesion of leukocytes and is treated with aggressive statin therapy, which decreases both CX_3CR1 and CX_3CR1 expression in these patients (Damas et al., 2005).

1.3.3.3.2. Wound Healing

Normal wound healing is heavily dependent in the infiltration of immune cells to the site of injury; here they play a key role in the phagocytosis of pathogens and support angiogenesis. In CX_3CR1 deficient animals there is a delay or decrease in myeloid recruitment to the injury site. This is accompanied by a reduced magnitude of neovascularisation and an inability to maintain new vessels, likely due to a reduction in macrophage TGF-β and VEGF release and reduced deposition of α-smooth muscle actin and collagen (Ishida et al., 2008a). The overall effect of this is a pro-longed temporal profile of wound healing (Clover et al., 2011;Khan et al., 2013); these effects can all be reversed and normal wound healing restored by the adoptive transfer of wildtype (CX_3CR1-expressing) macrophages (Ishida et al., 2008a).

1.3.3.3.3. Kidney Disease

CX_3CL1 expression is elevated in the endothelium of the nephritic/fibrotic kidney and is associated with enhanced infiltration of CX_3CR1^+ leukocytes (Feng et al., 1999;Oh et al., 2008). These cells contribute to the developing pathology occurring in this disease state; blockade of CX_3CR1-mediated leukocyte infiltration by the administration of an anti-CX_3CR1 antibody dramatically debilitates leukocyte infiltration and is functionally protective; reducing renal pathology and increasing renal function (Oh et al., 2008;Feng et al., 1999). This protective effect of CX_3CR1

signalling deficiency is also demonstrated in the CX_3CR1 knock-out which shows both a reduction in monocyte recruitment and injury severity in a model of ischemic kidney injury, which can be reversed by the adoptive transfer of CX_3CR1-expressing monocytes (Li et al., 2008), and a reduction in renal inflammation and fibrosis in a model of diabetes-induced kidney damage (Song et al., 2013).

1.3.3.3.3. Arthritis

Similarly enhanced CX_3CR1^{high} monocyte migration is seen in models of arthritis; high levels of CX_3CR1^{high} monocytes are seen in the synovium of rheumatoid arthritis patients (Yano et al., 2007), as is the upregulation of CX_3CL1 (Ruth et al., 2001). Systemic treatment with an anti-CX_3CL1 antibody, that blocks CX_3CR1-CX_3CL1 interaction, reduces disease severity and immune cell infiltration in animal models of this condition (Nanki et al., 2004). CX_3CR1-deficient mice demonstrate a similar reduction in disease severity and clinical score in comparison to wild-type mice (Tarrant et al., 2012). Furthermore, intrathecal administration of an antibody against CX_3CR1 is able to suppress the activation of spinal microglia that is frequently seen in arthritis models (Clark et al., 2012), concomitantly with delaying the onset of both mechanical allodynia and thermal hypersensitivity, suggesting a role for CX_3CR1/CX_3CL1 in pain modulation (Sun et al., 2007).

1.3.3.3.4. Chronic Pain

Current evidence indicates that CX_3CR1 contributes significantly to pain processing in a number of chronic pain conditions through a microglial mechanism. As discussed in chapter two, microglia are specialised macrophages of the CNS. These cells are CX_3CR1^{+} and in a similar way to the

CX_3CR1^+ monocytes of the periphery, they play an immune surveillance role under physiological conditions and are believed to maintain this phenotype via interactions between CX_3CR1 and CX_3CL1 (Saijo and Glass, 2011). This changes, however, when microglia detect an immune challenge, be it injury or infection; microglia take on an 'activated' phenotype, becoming hypertrophied and retracting their processes, as well as altering their expression of cell surface proteins to allow antigen presentation, undergoing proliferation and synthesizing and secreting a number of pro-inflammatory mediators.

Several models of chronic pain show evidence for microglial activation. For example Zhuang et al have demonstrated that following spinal nerve ligation, a marked reduction in paw withdrawal threshold is seen that is associated with microgliosis and enhanced expression of CX_3CR1 in the ipsilateral dorsal horn of the spinal cord (Zhuang et al., 2007). Additionally we have previously shown in our laboratory that microgliosis occurs subsequent to partial ligation of the sciatic nerve and induction of peripheral inflammation that is, again, associated with the development of thermal and mechanical hypersensitivity (Staniland et al., 2010). The interaction between CX_3CR1 and CX_3CL1 is critical for these responses. Mice deficient in CX_3CR1 do not develop thermal hyperalgesia and/or mechanical allodynia in these models, and show reduced microgliosis and activation of the P38 MAPK (Staniland et al., 2010). Likewise both the behavioural and microglial responses to peripheral nerve injury can be attenuated by the intrathecal administration of a CX_3CR1 neutralizing antibody (Zhuang et al., 2007;Milligan et al., 2004;Milligan et al., 2005a), whereas activation of CX_3CR1 by administration of soluble CX_3CL1 has the opposing effect (Zhuang et al., 2007;Milligan et al., 2005a;Milligan et al., 2004). The same effect is true for the development of bone cancer pain; the development of pain in animals with experimental bone cancer occurs concurrently with microgliosis and an increase in the expression of microglial

CX_3CR1 and pP38; the onset of this can be significantly delayed by the intrathecal administration of a CX_3CR1 neutralizing antibody (Hu et al., 2012) despite a lack of efficacy in suppressing bone pathology (Yin et al., 2010).

1.4. Chapter aims

The evidence presented above clearly establishes a role for CX_3CR1 in the development and/or maintenance of chronic pain and in the pathogenesis of peripheral diseases, in which migrating leukocytes make a substantial contribution. Data presented in chapter two confirms that there is indeed macrophage infiltration of the peripheral nerve following the induction of chemotherapy-induced neuropathy; however what has not yet been demonstrated is the contribution to pain made by peripheral CX_3CR1 and its mediation of leukocyte transmigration into the nerve. Here we hypothesise that nerve infiltrating monocyte/macrophages contribute significantly to the generation of a pain phenotype in our model of VCR-induced pain and that this process is CX_3CR1 dependent; thus, the aims of this chapter are:

- To determine the significance of macrophage infiltration in this model; do these cells contribute to the pain phenotype?
- To characterise the population of macrophages that infiltrates the nerve in model of chemotherapy pain and to determine if the population phenotype is altered by VCR treatment.

2. Methods

2.1. Animals

Unless otherwise stated, all experiments were performed using adult male C57Bl/6 mice (22-27g; 10-14 weeks from Harlan UK or bred in house), in accordance with The Animals Scientific Procedures Act (ASPA) 1986, United Kingdom Home Office regulations and institutional guidelines. Animals were individually housed (to prevent aggressive behaviour) on a 12 hour light / 12 hour dark cycle at 21-22^{o}C, with food and water *ad libitum*.

2.1.1. Generation and breeding of CX_3CR1-GFP mice

The original CX_3CR1-GFP mice were created by the manipulation of the murine CX_3CR1 locus by targeted replacement of the gene with cDNA encoding EGFP. In the mutant locus the *egfp* gene replaces the first 390bp of the second *cx3cr1* exon encoding the N-terminus. Genomic fragments flanking the *cx3cr1* gene were used to construct a *cx3cr1* targeting vector. Following homologous recombination and isolation of cell clones that harboured the expected replacement of *cx3cr1* with *egfp*, the *loxP* site-flanked *neo* gene was excised and the targeting cell clones were injected into blastocysts to generate chimeric mice. Germ line transmission of the mutant allele yielded heterozygous mutants, $CX_3CR1^{+/gfp}$. These animals were cross-breed to generate $CX_3CR1^{gfp/gfp}$ mice, which were subsequently, in our hands, bred with wildtype C57Bl/6 mice to generate experimental heterozygous mice that possessed both CX_3CR1-GFP and functional CX_3CR1 protein (Jung et al., 2000). Litters were weaned at 21 days and group housed (up to 5 per cage) in single

sex cages. Both male and female animals were used for behavioural studies from eight weeks old, at which time they were singly housed and allowed to acclimatise to their new cage for one week.

2.1.2. Generation of CX_3CR1-/- mice

The original CX_3CR1 knock-out mice (Taconic, USA) were created by the insertion of a neomycin resistance cassette into the wild-type *cx3cr1* gene, causing an interruption of the transcription of the gene. Two homologous recombinants were identified by southern blot and microinjected into C57Bl/6 blastocysts. Chimeric mice were then mated with wildtype C57Bl/6 mice to produce heterozygous mice which were then backcrossed three times on the C57Bl/6 background (Combadiere et al., 2003). These transgenic mice were backcrossed a further ten times with C57Bl/6 mice (Harlan, UK) to obtain heterozygous breeding pairs. These breeding pairs were used to obtain litters for experimental use with a heterozygous (+/-): homozygous knockout (-/-): homozygous wildtype (+/+) ratio of 2:1:1. Litters were weaned at 21 days and group housed (up to 5 per cage) in single sex cages. Animals were used for behavioural studies from ten weeks old, at which time they were singly housed and allowed to acclimatise to their new cage for one week. Both male and female animals were used, with wild-type littermates serving as a control.

2.1.3. Macrophage depletion

Prior to VCR treatment, the circulating monocyte/macrophage population was depleted as described previously (Barclay et al., 2007;Van and Sanders, 1994). Liposome-encapsulated clodronate (LCL; 10µl/g of a 5mg/ml solution [Rooijen, Netherlands]) or control liposome-encapsulated PBS was administered to mice on two occasions, three and one days before the

commencement of VCR treatment, via injection into the peritoneal cavity with a 30G needle. This schedule is shown diagrammatically in figure 3.5 below.

2.1.4. Vincristine induced painful peripheral neuropathy

VCR-neuropathy was induced as described previously described by Sommer et al (Uceyler et al., 2006). Vincristine sulphate (VCR [Sigma, UK]) was dissolved in sterile saline (0.9% NaCl [VWR, UK]) and 0.5mg/kg was injected into the peritoneal cavity (intraperitoneally [*i.p.*]), using a 30G needle, daily for five days per cycle, for up to 2 cycles, shown below in figure 3.5.

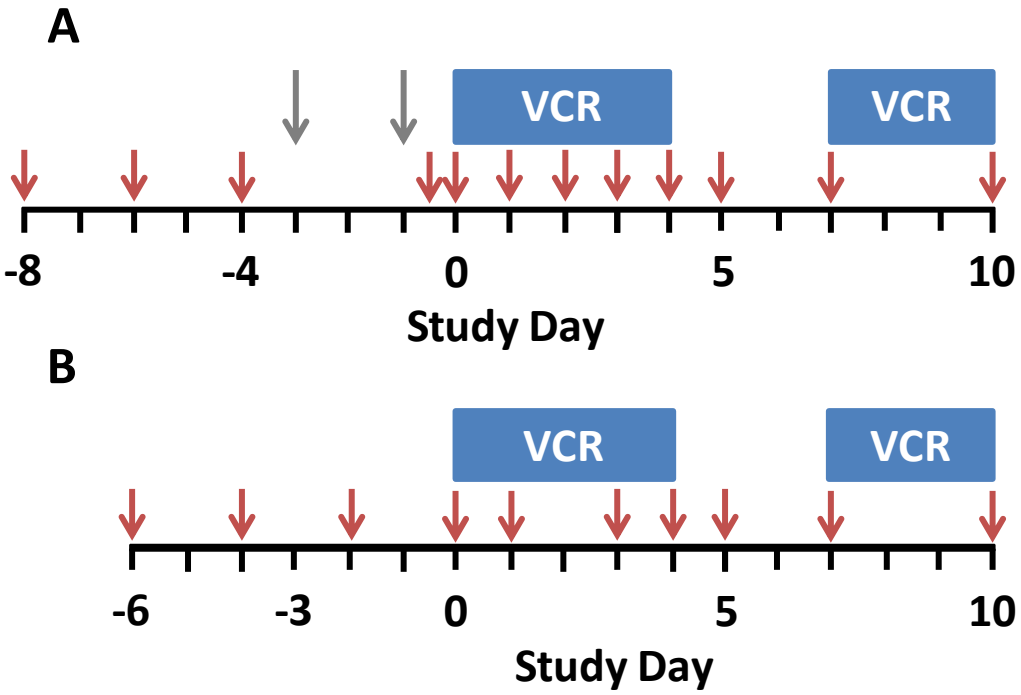

Figure 3.5.: Experimental schedule for behavioural assessment and VCR (and LCL) dosing. (A) Macrophage depletion study: blue boxes represent cycles of VCR treatment, the grey arrows represent LCL dosing and red arrows represent study days during which mechanical sensitivity was assessed. **(B)** $CX_3CR1^{-/-}$ study: blue boxes represent cycles of VCR treatment and red arrows represent study days during which mechanical sensitivity was assessed. Behavioural tests were performed approximately 1 hour after dosing.

2.2. Behavioural testing

2.2.1. Assessment of mechanical sensitivity

Static mechanical withdrawal thresholds were assessed as previous described in chapter two. Data are expressed as 50% paw withdrawal threshold, in grams, calculated using the method described by Dixon (Dixon, 1980).

2.2.2. Statistical analysis of behavioural data

Statistical analysis behavioural data was carried out on raw data, using SigmaPlot 12.0 software (Systat Software Inc, UK). Data are shown as mean ± standard error of the mean (SEM) and analysed by two way repeated measures analysis of variance (ANOVA) followed by Tukey post-hoc test. A p value of less than 0.05 ($P<0.05$) was considered significant (*), less than 0.01 ($P<0.01$) moderately significant (**) and less than 0.001 ($P<0.001$) highly significant (***).

2.3. Genotyping

2.3.1. Ear biopsy

Transgenic mice were identified by individual ear marks made by taking a 1.5mm punch biopsy (Harvard Apparatus, UK) from the ear. The punch biopsies were performed when the mice were 10-21 days of age and the samples were collected in individual 0.5ml Eppendorf tubes (Starlab, UK) to provide DNA samples for genotyping.

2.3.2. DNA extraction

Each ear biopsy was incubated with 30µl of ear lysis buffer (67mM Tris [Sigma, UK], 16mM $(NH_4)_2SO_4$ [Sigma, UK], 6.7mM $MgCl_2$ [Sigma, UK], 0.2% v/v TritonX-100 [Sigma, UK], 0.1% v/v β-mercaptoethanol [Sigma, UK], 0.4mg/ml Proteinase K [VWR, UK] in dH_2O) for 60 minutes at 55^oC followed by 5 minutes at 95^oC. Samples were then vortexed for 30 seconds and centrifuged at 12,000g for 1 minute, with the resulting supernatant containing the DNA used for PCR.

2.3.3. CX_3CR1-GFP PCR

A single PCR reaction was performed for each DNA sample. A PCR reaction master mix was made consisting of 2mM $MgCl_2$ (Promega, UK), 20% (v/v) 5x reaction buffer (Promega, UK), 300µM dNTP (Promega, UK), 50 units/ml Taq DNA polymerase (Promega, UK) and 1µM oligonucleotide primers (Sigma, uk). The forward wild-type and GFP and reverse oligonucleotide primers had the sequences 5'CAACAGGGTTCCAAGCAAG 3', 5' GGACAGGAAGATGGTTCCAA 3' and 5'TGGTGCAGATGAACTTCAGG 3' respectively. Each reaction consisted of 2µl of 1:10 diluted DNA and 23µl of PCR master mix. The PCR reaction was performed in a TC412 Flexigene thermal cycle (Techne, UK) with an initial denaturation step of 94^oC for 5 minutes, followed by 35 cycles with denaturation at 94^oC for 30 seconds, annealing at 60^oC for 30 seconds and polymerisation at 72^oC for 30 seconds. This was then followed by a final extension step at 72^oC for 5 minutes. The expected sizes of the end products were 438bp for the wild-type cx3cr1 gene and 569bp for the *cx3cr1-gfp* gene.

2.3.4. $CX_3CR1^{-/-}$ PCR

A separate wildtype and knockout PCR reaction was performed for each DNA sample. A PCR reaction master mix was made for each allele (wild-type and knock-out) consisting of 1.5mM $MgCl_2$ (Promega, UK), 20% (v/v) 5x reaction buffer (Promega, UK), 0.2mM dNTP (Promega, UK), 50 units/ml Taq DNA polymerase (Promega, UK),0.1µM antisense oligonucleotide primer and 0.1µM wild-type or knock-out oligonucleotide primer (Sigma, UK). The antisense, wild-type and knock-out oligonucleotide primers had the sequences 5' TGGGGTGACGCCACTAAGA 3', 5' GGCCTGTTATTTGGGCGACAT 3' and 5' GACCGCTTCCTCGTGCTTTA 3' respectively. Each reaction consisted of 1.5µl DNA and 18.5µl of PCR master mix. The PCR reaction was performed in a TC412 Flexigene thermal cycle (Techne, UK) with an initial denaturation step of 96^{o}C for 3 minutes, followed by 25 cycles with a denaturation at 94^{o}C for 30 seconds, annealing at 60^{o}C for 30 seconds and polymerisation at 72^{o}C for 30 seconds. This was then followed by a final extension step at 72^{o}C for 10 minutes. The expected sizes of the end products were 440bp for the wild-type *cx3cr1* gene and 600bp for the knock-out *cx3cr1* gene.

2.3.5. Gel electrophoresis and band visualisation

To visualise the PCR products a gel electrophoresis was performed. Post- PCR samples were loaded onto, and run down, a 2% agarose gel containing 100µg/ml ethidium bromide (Sigma, UK), at 100V for 25 minutes using a Power Pac 200 (BioRad, UK). A 1kb DNA ladder (Promega, UK) was also run down each gel to allow for the sizes of the products to be easily determined. The gels were viewed using a GeneGenius system (Syngene, UK) and images collected using the GeneSnap programme (Syngene, UK). All samples from experimental and breeding animals underwent a repeat analysis to reduce the likelihood of both false positive and false negative results.

2.4. Immunohistochemistry

2.4.1. Tissue preparation

Tissue for immunohistochemical staining was prepared as described in chapter two.

2.4.2. Immunohistochemical staining

Slides were washed six times for 5 minutes in 0.1M PBS and incubated over night at room temperature with a primary antibody for a specific cell marker (table 3.3) in PBS containing 0.2% TritonX-100 (Sigma, UK) and 0.1% sodium azide (Sigma, UK). Slides were then washed three times for 5 minutes in PBS and incubated at room temperature, in the dark, with an appropriate secondary antibody (table 3.4) for 2.5-3 hours. Following three further PBS washes slides were cover-slipped with Vectashield mounting media with DAPI (Vector Laboratories, USA) and visualised under a Zeiss Axioplan 2 fluorescent microscope (Zeiss, UK).

Table 3.3: Immunohistochemistry primary antibodies

Primary Antibody	Cellular Marker	Concentration	Supplier
Rabbit anti-ionized calcium binding adaptor molecule 1 (Iba1)	Microglia	1:1000	WAKO Pure Chemical Industries, Germany
Rabbit anti-glial fibrillary acidic protein (GFAP)	Astrocytes	1:1000	DAKO Cytomation, Denmark
Rat anti-mouse F4/80	Monocytes/Macrophages	1:200	AbD Serotec, UK
Mouse anti-NeuN	Neurons	1:100	Chemicon, UK
Mouse anti-βIII-tubulin	Neuronal β-tubulin	1:1000	Promega, UK
Goat anti-CD31	Endothelial cells	1:100	R & D Systems Ltd, UK

Table 3.4: Immunohistochemistry secondary antibodies

Secondary Antibody	Concentration	Supplier
Goat anti-rabbit IgG-conjugated Alexa Fluor 488™	1:1000	Molecular Probes, USA
Goat anti-rabbit IgG-conjugated Alexa Fluor 546™	1:1000	Molecular Probes, USA
Donkey anti-mouse IgG-conjugated Alexa Fluor 488™	1:1000	Molecular Probes, USA
Donkey anti-mouse IgG-conjugated Alexa Fluor 546™	1:1000	Molecular Probes, USA
Donkey anti-goat IgG-conjugated Alexa Fluor 546™	1:1000	Molecular Probes, USA
Goat anti-rat IgG-conjugated Alexa Fluor 488™	1:1000	Molecular Probes, USA
Goat anti-rat IgG-conjugated Alexa Fluor 546™	1:1000	Molecular Probes, USA

2.4.3. Quantification of immunohistochemistry

2.4.3.1. Fluorescence intensity

Quantitative assessment of immunoreactivity was carried out by determining the immunofluorescence intensity within a fixed area of the superficial dorsal horn. Three L4-L5 spinal cord sections were chosen at random from each animal, with experimental group blinded. Four boxes measuring $10^4 \mu m^2$ were spaced equally across the superficial laminae of the dorsal horn. Mean grey intensity each of the boxed areas was determined using Axiovision LE 4.2 software (Zeiss, UK). The background intensity for each tissue section was determined using an area of $10^4 \mu m^2$, and subtracted from the intensity values determined. An average value for immunofluorescence intensity across the superficial dorsal horn was then calculated.

2.4.3.2. Cell numbers

The number of positive cells for each immunohistochemical marker was determined. Three tissue sections per animal were selected at random with experimental group blinded. Four boxes

measuring $10^4 \mu m^2$ were spaced equally across the superficial laminae of the dorsal horn, for spinal cord sections, or were spaced equally across the tissue for nerve sections. The number of cells positive for the given marker was counted.

2.4.3.3. Statistical analysis of immunohistochemical data

Statistical analysis for immunohistochemistry was carried out on raw data, using SigmaPlot 12.0 software (Systat Software Inc, UK). For both immunofluorescence intensity and cell numbers and average value was obtained for each animal. A mean value for each experimental group was then calculated, and the groups compared to one another using a one-way analysis of variance (ANOVA) followed by Tukey post-hoc test. Group difference with a P value of less than 0.05 ($P<0.05$) was considered significant.

2.5. Monocyte/Macrophage Harvest

Monocyte/macrophage infiltration of the peritoneal cavity was encouraged by the instigation of sterile inflammation, by injection of 1ml of 2% polyacrylamide bio-gel beads (Bio-Rad, UK) into the peritoneal cavity four days prior to harvest. To harvest the cells, animals were first euthanised by exposure to increasing concentrations of CO_2 until breathing cessed. A small incision was made along the midline of the abdomen and the skin manually retracted. A syringe connected to a 20G 3/8" needle was then used to inject 5ml of cold harvest media (sterile PBS [Sigma, UK], 3mM EDTA [Sigma, UK]) into the peritoneal cavity of the mouse, and the abdomen lightly massaged to allow movement of the fluid. Using the same syringe and needle the fluid was aspirated, moving the needle away from the viscera to cause tenting of the peritoneal wall to prevent visceral damage. The peritoneal exudate was filtered through 75µm nylon mesh filters (BD Falcon, UK) and a second

peritoneal wash performed. The exudates were centrifuged at 400g for 10 minutes and resuspended in antibody solution for FACs analysis (see below).

2.6. Flow Cytometry Analysis

All antibodies were obtained from eBioscience (Hatfield, UK). Monocyte/macrophages from $CX_3CR1^{+/+}$ mice were stained with FITC-conjugated Gr-1 (clone RB6-8C5) and APC-conjugated F4/80 (clone BM8) antibodies, and monocyte/macrophages from $CX_3CR1_{gfp/+}$ mice with APC-conjugated Gr-1. Cells were incubated on ice for 30 minutes then washed twice with PBS containing 1.5% BSA (Sigma, UK) and re-suspended before analysis on a BD FACS calibur flow cytometer (Becton Dickenson, UK). [Performed by Dr Suchita Nadkarni].

3. Results

As discussed in chapter one, repeated systemic administration of VCR causes monocyte/macrophage infiltration of the peripheral (sciatic) nerve with a temporal profile similar to that of the onset of mechanical hypersensitivity. Here we have performed a series of experiments to elucidate the role these cells play in the development of VCR induced painful peripheral neuropathy, and whether or not they constitute a viable target for analgesic development.

3.1. Pre-treatment with liposome encapsulated clodronate prevents the development of mechanical hypersensitivity and monocyte/macrophage infiltration of the sciatic nerve that occurs following repeated systemic administration of VCR

To determine the contribution made by monocyte/macrophages to the development of VCR-induced mechanical allodynia, these cells were depleted by administration of two doses of liposome encapsulated clodronate (LCL) prior to VCR dosing; this alone had no effect on the mechanical thresholds of mice, which remained at baseline levels subsequent to treatment (figure 3.6A; LCL-SAL mice). As described previously, in chapter two, the administration of VCR (0.5mg/kg *i.p.*) for five consecutive days (days 0-4; first cycle, cumulative dose 2.5mg/kg), followed by a two day pause and second subsequent cycle of treatment (days 7-11, cumulative dose 5.0mg/kg) was associated with significant and severe hind-paw mechanical hypersensitivity (allodynia) in PBS-VCR treated mice. In LCL pre-treated mice, however, the onset of VCR induced mechanical allodynia was significantly delayed, with the thresholds remaining at baseline levels (LCL-VCR), during the first cycle of VCR treatment (figure 3.6A). This is most apparent when an area under curve (AUC)

analysis is completed (figure 3.6B); a significant difference is seen in the allodynia index between PBS-VCR and PBS-SAL treated animals, however the difference between LCL-VCR and LCL-SAL treated animals is much smaller in comparison (figure 3.6B; decrease in allodynia index calculated from area under curve; PBS-VCR 57% ± 3.3, LCL-VCR 3% ± 3.2%). Allodynia index of VCR treated mice is significantly reduced by pre-treatment with LCL. Interestingly, as the representative images in figure 3.7A demonstrate, immunohistochemical analysis of sciatic nerves taken from LCL-VCR treated animals at the end of this first VCR cycle, demonstrate that monocyte/macrophage levels at this time are comparable to that of control tissue (day 4; figure 3.7A/B); no increase in the number of F4/80^{+} cells is observed. This suggests that the VCR-induced infiltration of these cells that usually occurs has not happen, consistent with the circulating population of monocyte/macrophages having been depleted with the LCL; thus not being available to infiltrate.

Following a second cycle of VCR, as expected, PBS-VCR treated mice maintained severe mechanical hypersensitivity which recovered several days following the cessation of treatment. At this time the mechanical thresholds of LCL-VCR treated mice began to decline, reaching levels comparable to PBS-VCR mice following the commencement of the second cycle of VCR treatment (figure 3.6; LCL-VCR) and became indistinguishable from PBS-VCR mice throughout the second cycle and recovery period, as demonstrated by AUC analysis (figure 3.6B). Sciatic nerve tissue samples were taken for immunohistochemical analysis at the end of the second VCR cycle, and it was observed that the number of F4/80^{+} cells present in the tissue of LCL pre-treated animals (LCL-VCR) had increased to a level comparable to PBS-VCR treated mice (figure 3.7C/D), indicating that monocyte/macrophages had infiltrated the nerve.

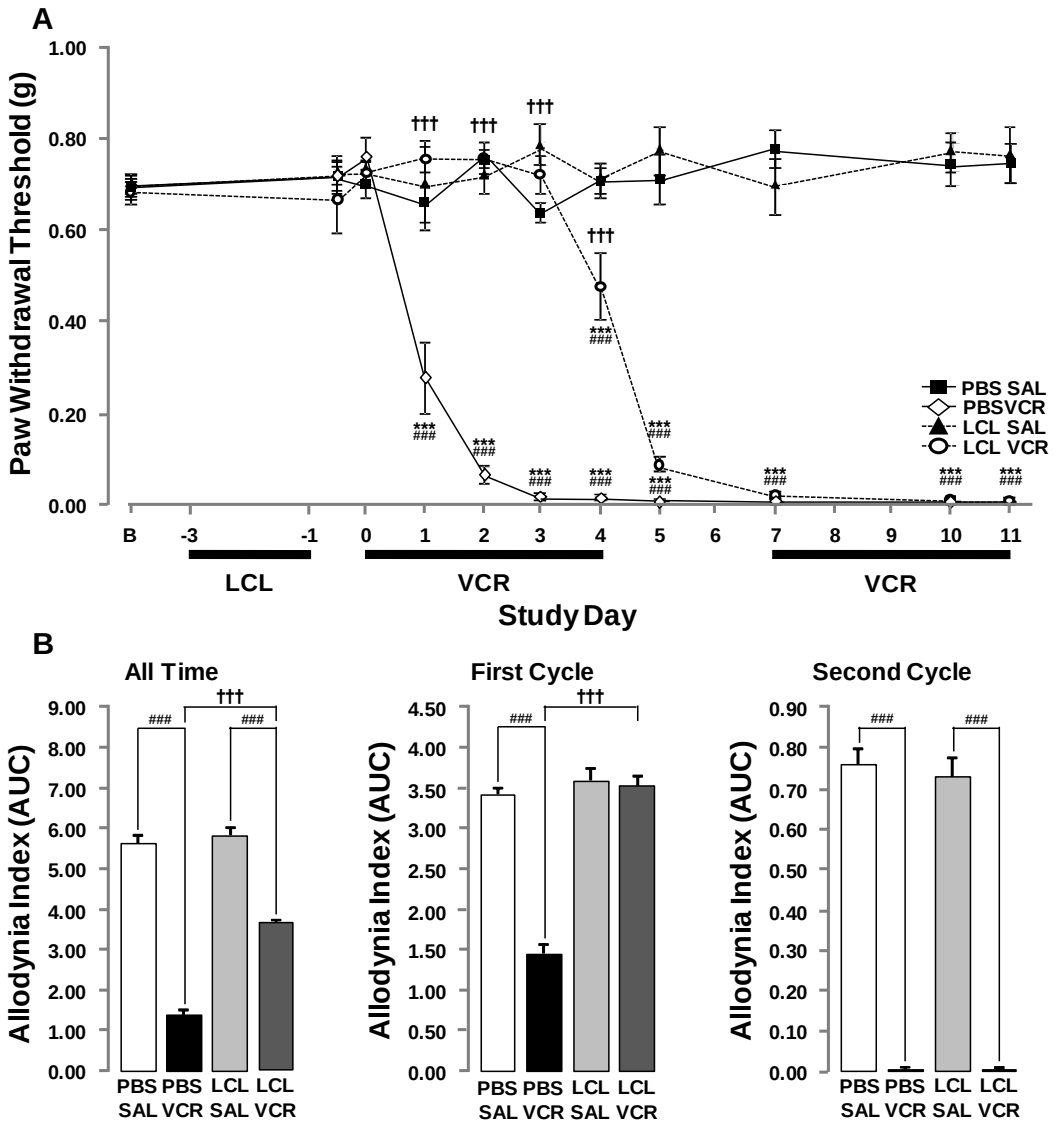

Figure 3.6. Pre-treatment with LCL delays the onset of mechanical allodynia induced by repeated systemic administration of VCR. Development of mechanical allodynia in mice pre-treated with either liposome encapsulated clodronate (10µl/g of a 5mg/ml solution [Rooijen, Netherlands]) or PBS control, with or without *i.p.* VCR (0.5mg/kg/day; 0-4 and 7-11; black horizontal bars) **(A)** Temporal profile of mechanical allodynia development shown as 50% PWT, data shown as mean ± SEM. N=8 per group, ***P<0.001 compared to baseline threshold, ### P<0.001 compared to saline threshold, ††† P<0.001 LCL-VCR threshold compared to PBS-VCR threshold, two-way RM ANOVA with post-hoc Holm-Sidak test. **(B)** Area under the curve (AUC) analysis with data expressed as allodynia index where a lower value represent more severe allodynia. All time = day 0-day 24, first cycle= day 0- 4, second cycle = 7-11, recovery = 11-24. Data shown are mean ± SEM. N=8 per group, ### P<0.001 compared to saline index, ††† P<0.001 LCL-VCR compared to PBS-VCR index with one way ANOVA and post-hoc Holm-Sidak.

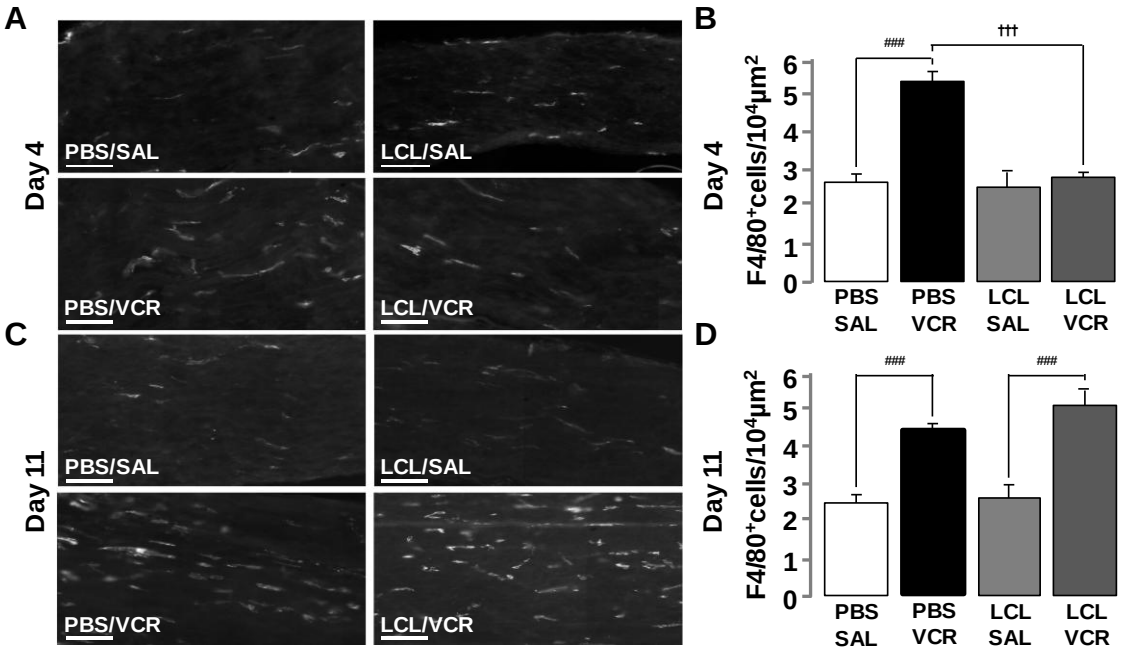

Figure 3.7. Pre-treatment with LCL delays the onset of macrophage infiltration of the sciatic nerve induced by repeated systemic administration of VCR. (A/C) Representative images showing macrophages in the sciatic nerve following vehicle (SAL) or one (A; day 4) or two (B; day 11) cycles of VCR (0.5mg/kg/day *i.p.*) with (LCL) or without (PBS) liposome clondronate pre-treatment, where macrophages are visualised by their expression of F4/80. Scale bars equal 100µm. **(B/D)** Quantification of the number of macrophages in the sciatic nerve, shown as number of $F4/80^{+}$ cells per $10^{4}\mu m^{2}$. Data shown are mean ± SEM and N=4 per group. *** P<0.001 compared to saline, ###P<0.001 compared to PBS-VCR, one-way ANOVA with post-hoc Tukey test.

3.2. No difference in the severity of VCR induced mechanical allodynia is seen between male and female mice

The study described above suggests that the monocyte/macrophages invading the nerve following systemic VCR administration play a critical role in the generation of mechanical allodynia. In the mouse, as in the human, monocyte/macrophages show substantial heterogeneity and whilst LCL is an exceptionally useful tool in studying these cells as a whole population, it its mechanism of

depletion does not allow one to use it to target specific subpopulations of monocyte/macrophages. One of the key differences between the two most well characterised populations of monocyte/macrophages in the mouse is the level of expression of the chemokine receptor CX_3CR1; by using mice in which this protein has been genetically modified we can study the role of CX_3CR1 expressing monocyte/macrophages and the receptor itself in VCR-induced neuropathy to see if a mechanism for the involvement of these cells can be teased out. Here we made use of two CX_3CR1 modified mouse strains. The first of these is a GFP knock-in mouse in which the addition of an *egfp* reporter gene in the second exon of the CX_3CR1 gene causes the expression of CX_3CR1 tagged with GFP; this allows CX_3CR1^+ cells to be easily visualised. Secondly we used a CX_3CR1 knock-out mouse that lacked functional CX_3CR1 protein, this is discussed further below.

The initial characterization we performed of the mouse model of VCR-induced painful peripheral neuropathy was carried out on male mice; however to allow for larger group sizes in colony bred mice it would be ideal to use both male and female mice. Recent evidence has suggested a difference in the development of pain phenotypes between sexes in mouse models of chronic pain states (recently reviewed in (Bartley and Fillingim, 2013)). Falk et al have demonstrated earlier onset of pain related behaviours in female mice compared to males in a model of bone cancer pain (Falk et al., 2013); consistently Sorge et al have presented evidence for a sex difference in the occurrence of LPS-induced mechanical allodynia, with only male mice developing a pain phenotype. However this does seem to be a spinal cord specific response as this difference was only seen with intrathecally and not intracrainally or subcutaneously administered LPS (Sorge et al., 2011). This sex difference has not been noted in our laboratory previously (unpublished data), however to determine whether or not sex would be an influencing factor in the development of

VCR-induced mechanical allodynia, we assessed the mechanical thresholds of both male and female wild-type mice. As shown by figure 3.8A repeated systemic administration of VCR results in the rapid development of severe persistent mechanical allodynia in both male and female wild-type C57Bl/6 mice. The mechanical thresholds of all mice are significantly reduced ($P<0.001$) from 24 hours (day 1) after the first dose of VCR and remain so for all further time points assesses. Furthermore, area under curve (AUC) analysis (figure 3.8B) demonstrates that there is no significant difference (or even trend) between the mechanical thresholds of male and female mice; an equal reduction in threshold due to VCR treatment is seen overall and in both VCR cycles individually. This data is indicative of a lack of sex variation in the development of VCR-induced painful peripheral neuropathy, thus we have used both male and female mice in subsequent studies.

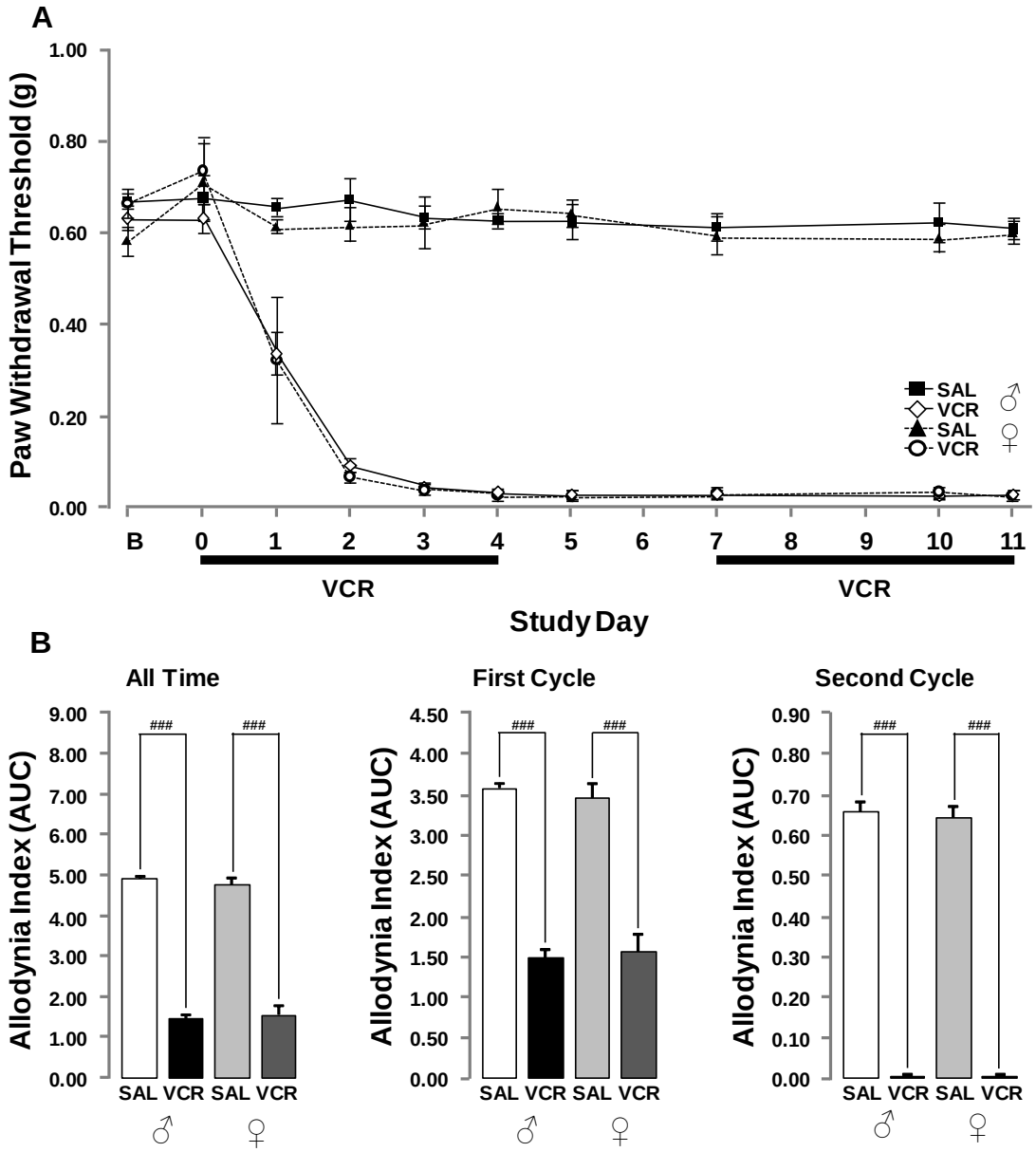

Figure 3.8. No difference in VCR-induced mechanical allodynia is seen between male and female mice. Development of mechanical allodynia following *i.p.* VCR (0.5mg/kg/day) administration for two cycles of five days each (0-4 and 7-11; black horizontal bars). Vehicle group received an equal volume of saline. **(A)** Time course of the development of mechanical allodynia shown as 50% paw withdrawal threshold (PWT), data shown as mean ± SEM. N=8 per group, two-way repeated measures ANOVA with post-hoc Holm-Sidak test. **(B)** Area under the curve (AUC) analysis showing data expressed as allodynia index where a lower value represent more severe allodynia. All time = BL-day 24, first cycle = BL-day 4, second cycle = day 7-11 Data shown are mean ± SEM. N=8 per group, ### P<0.001 compared to saline threshold with one way ANOVA and post-hoc Holm-Sidak test.

3.3. Use of a transgenic mouse expressing GFP tagged CX_3CR1 demonstrates that early infiltrating monocyte/macrophages are CX_3CR1 positive

We next set out to phenotype the monocyte/macrophages infiltrating the peripheral nerve following VCR administration. To do this we used a CX_3CR1-GFP expressing mouse in which all CX_3CR1^+ cells are also GFP^+. The mice used in these experiments were heterozygous for GFP tagged CX_3CR1 ($CX_3CR1^{+/gfp}$); at this stage we did not wish to determine the role of CX_3CR1 in the infiltration of monocyte/macrophages into the nerve and its effect on mechanical allodynia, and it has been demonstrated by Jung et al that due to the nature of the genetic modification homozygous mice ($CX_3CR1^{gfp/gfp}$) are a functional knock-out of CX_3CR1; the presence of the *egfp* gene in both alleles of the CX_3CR1 gene prevents the transcription and translation of any functional protein.

Prior to all experiments, mice were genotyped to confirm expression of wild-type CX_3CR1 protein and CX_3CR1-GFP protein. As figure 3.9, demonstrates wildtype mice ($CX_3CR1^{+/+}$) express a single transcript of approximately 440bp and homozygous GFP ($CX_3CR1^{gfp/gfp}$) mice express a single, larger transcript of approximately 570bp, whilst heterozygous $CX_3CR1^{+/gfp}$ mice express one wild-type (440bp) and one GFP transcript (570bp). Genotyping was performed twice (to remove false positives) and only heterozygous mice were selected for experimentation.

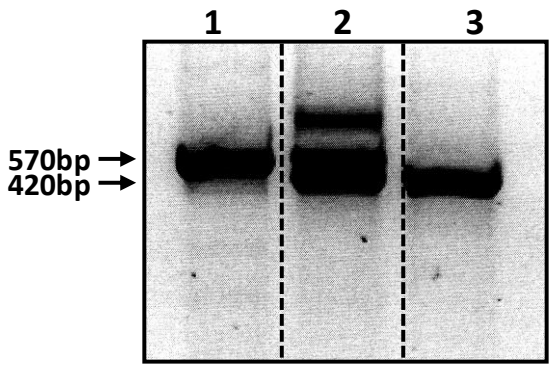

Figure 3.9. Genotyping electrophoresis of PCR samples from CX_3CR1-GFP mice. Representative image of agarose gel following electrophoresis of PCR products with homozygous knock-in mice (lane 1) yielding a 570bp product, wild-type mice (lane 3) yielding a 440bp product, and heterozygous mice yielding both (lane 2).

We then conducted a series of immunohistochemical studies in naïve $CX_3CR1^{+/gfp}$ mice to confirm that the expression of CX_3CR1-GFP was restricted to myeloid cells as previous literature predicts (Jung et al., 2000). Figure 3.10 shows representative high magnification images demonstrating expression of CX_3CR1-GFP in the spinal cord. Here, CX_3CR1-GFP co-localised exclusively with the microglial marker Iba1 (figure 3.10; top three panels); no co-localization with the astrocytic marker GFAP (figure 3.10; middle panels) or neuronal marker NeuN (figure 3.10; bottom panels) was observed. In a similar fashion, in the DRG CX_3CR1-GFP was only observed to co-localise with the macrophage marker F4/80 (figure 3.11; third row); no co-localization with the neuronal marker β_{III}-tubulin (figure 3.11; top row), satellite cell marker GFAP (figure 3.11; second row) or endothelial cell marker CD31 (figure 3.11; bottom row) was observed. Finally in the trunk of the sciatic nerve CX_3CR1-GFP was observed only to co-localise with the macrophage marker F4/80 (figure 3.12; third row); no co-localization was observed with the neuronal marker β_{III}-tubulin (figure 3.11; top row), satellite cell marker GFAP (figure 3.11; second row) or endothelial cell marker CD31 (figure 3.11; bottom row).

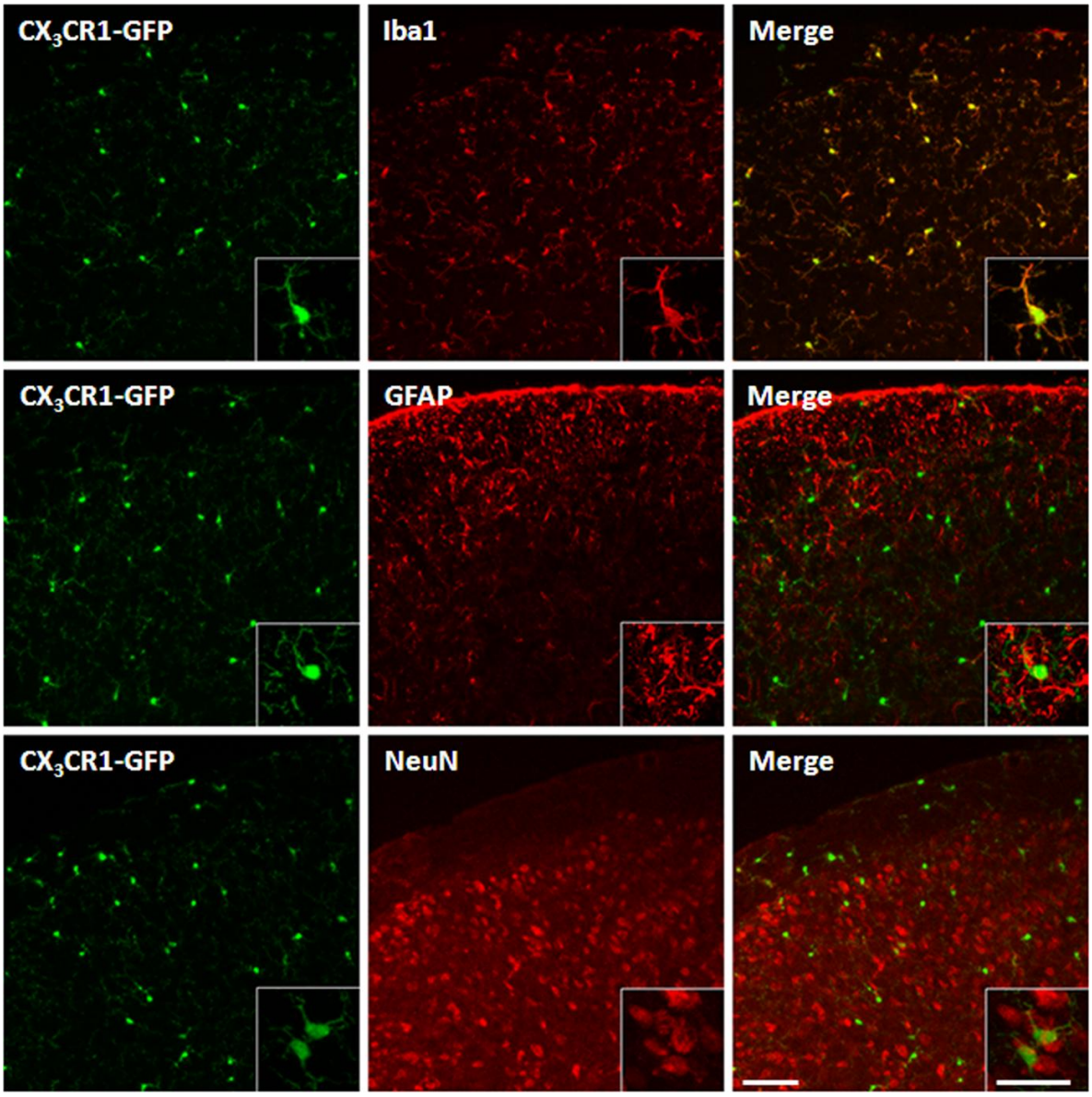

Figure 3.10. In the spinal cord CX_3CR1-GFP is only expressed in Iba1$^+$ cells. Representative low and high magnification images demonstrating expression of CX_3CR1-GFP in the dorsal horn of the (L5) spinal cord. CX_3CR1-GFP (green) co-localises with Iba1 (red), but not with GFAP (red) or NeuN (red). Scale bars equal to 50µm and 20µm in low and high magnification images respectively.

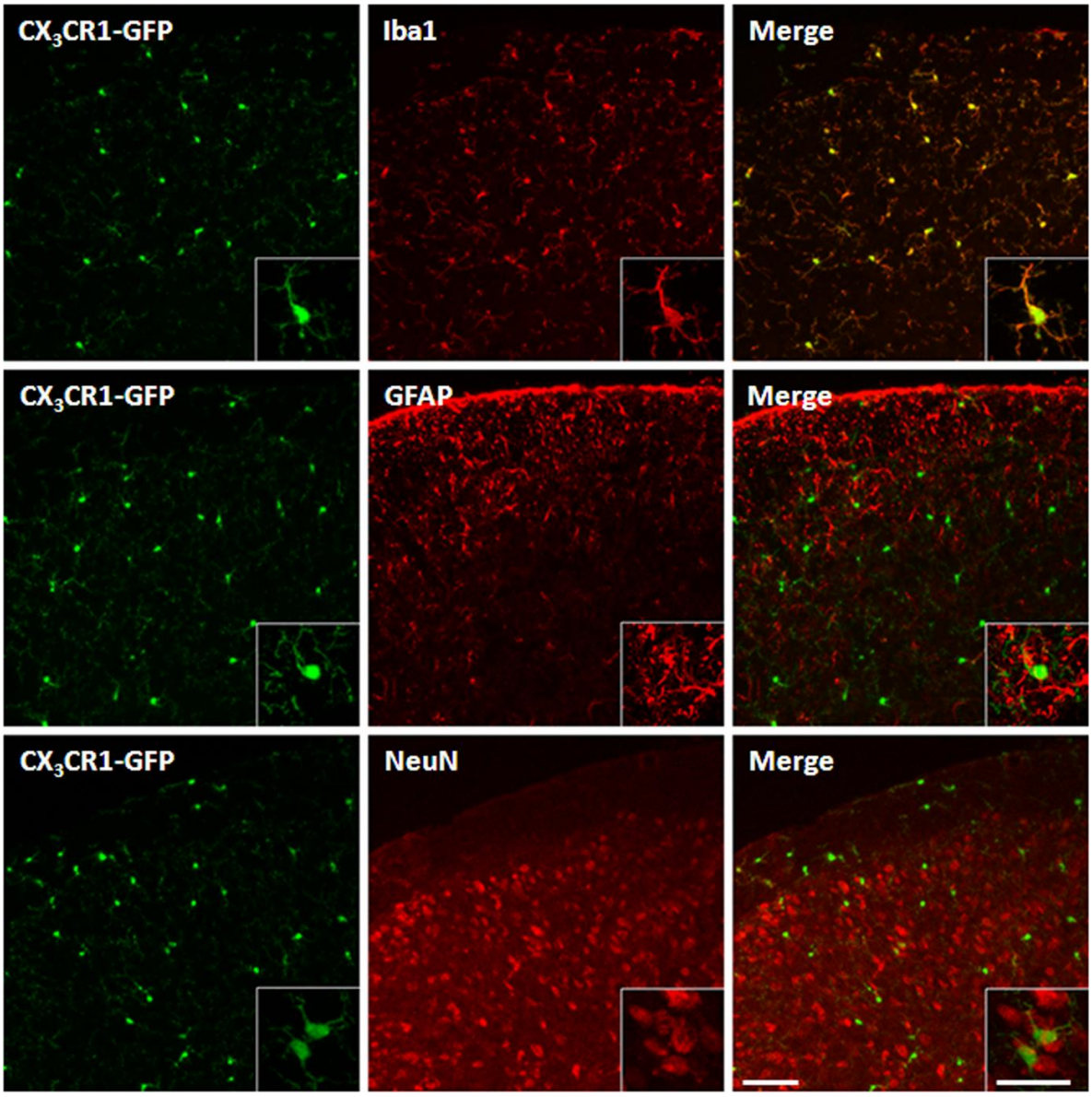

Figure 3.11. In the DRG CX_3CR1-GFP is expressed in F4/80$^+$ cells. Representative low and high magnification images demonstrating expression of CX_3CR1-GFP in the L5 DRG. CX_3CR1-GFP (green) co-localises with F4/80 (red), but not with β_{III}-tubulin (red), GFAP (red) or CD31 (red). Scale bars equal to 50µm and 20µm in low and high magnification images respectively.

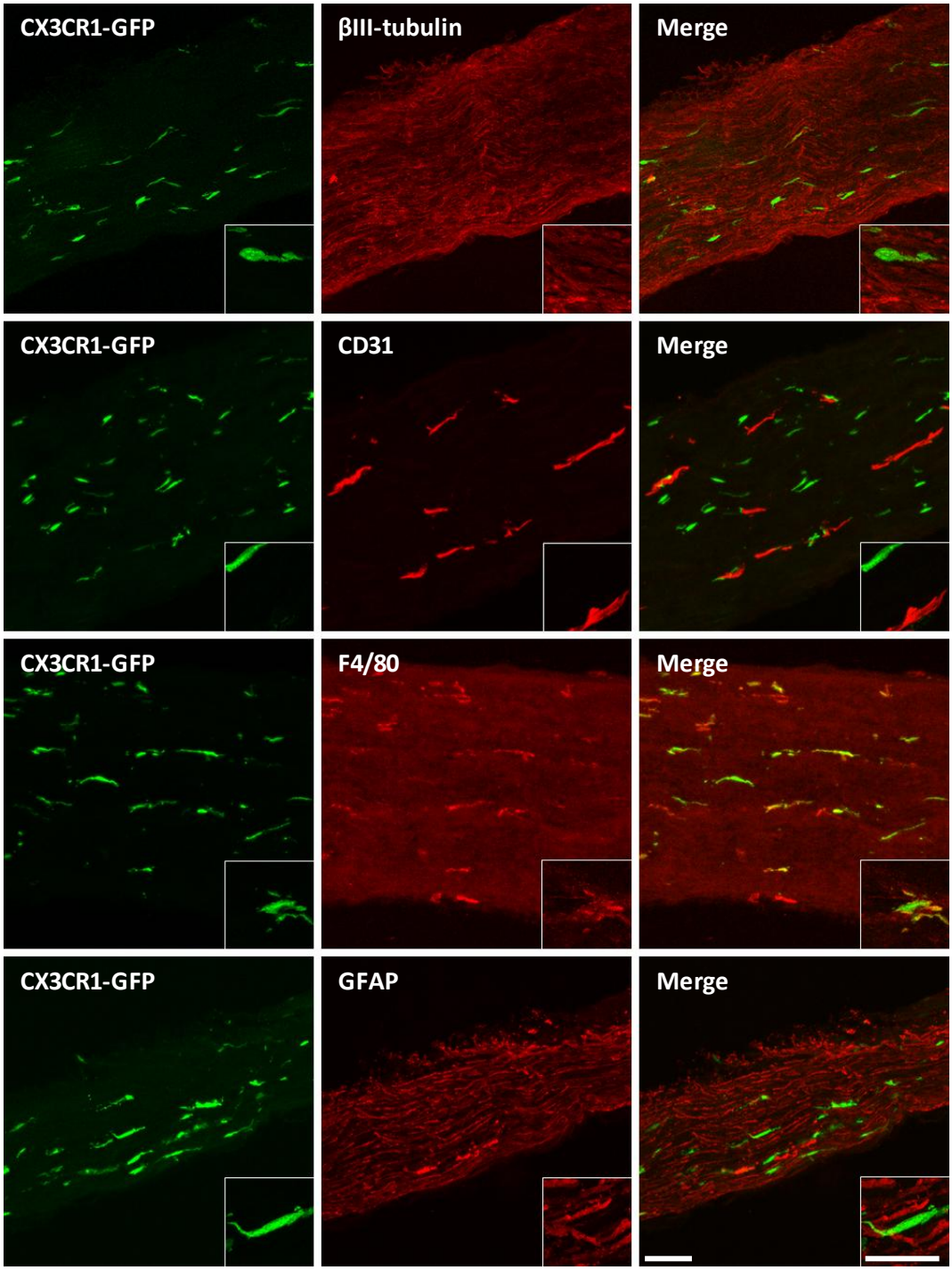

Figure 3.12. In the nerve trunk CX_3CR1-GFP is expressed in F4/80$^+$ cells. Representative low and high magnification images demonstrating expression of CX_3CR1-GFP in the sciatic nerve. CX_3CR1-GFP (green) co-localises with F4/80 (red), but not with β_{III}-tubulin (red), GFAP (red) or CD31 (red). Scale bars equal to 50μm and 20μm in low and high magnification images respectively.

Whilst previous assessment of the migration patterns of $CX_3CR1^{+/gfp}$ monocyte/macrophages has suggested that the function of CX_3CR1 is not affected in heterozygous mice, we have provided evidence that suggests the development of pain in our model is monocyte/macrophage sensitive. Thus we first assessed the mechanical thresholds in $CX_3CR1^{+/gfp}$ mice to ensure the expression of GFP was not influencing the function of these cells in terms of their involvement in the development of VCR-induced mechanical allodynia. As our previous data has suggested, the repeated systemic administration of VCR was associated with the development of severe and sustained hind-paw mechanical allodynia in CX_3CR1-GFP mice (figure 3.13A); mechanical thresholds and allodynia indices (AUC analysis; figure 3.13B) were comparable to those of all previously tested wild-type mice (see figure 2.4 in chapter two and figure 3.8. above), as was the maximum reduction in thresholds ($CX_3CR1^{gfp/+}$ 97.63% ± 0.55, $CX_3CR1^{+/+}$ 98.00% ± 0.21 reduction in PWT).

As mentioned above, mouse monocytes can be categorised into two distinct populations based on their expression of CX_3CR1. The first of these is a population of $Ly6C^-CX_3CR1^{high}$ resident cells which are long lived and have the primary function of surveying their local environment for signs of danger; the second is a population of $Ly6C^+CX_3CR1^{int}$ "classical" inflammatory monocytes that are comparably short lived and are rapidly recruited to sites of inflammation (Auffray et al., 2007;Geissmann et al., 2003;Yona et al., 2013). Due to this patrolling/surveying nature of the $Ly6C^-CX_3CR1^{high}$ monocytes it is likely that these cells comprise the myeloid infiltrate seen in the sciatic nerve following systemic VCR administration.

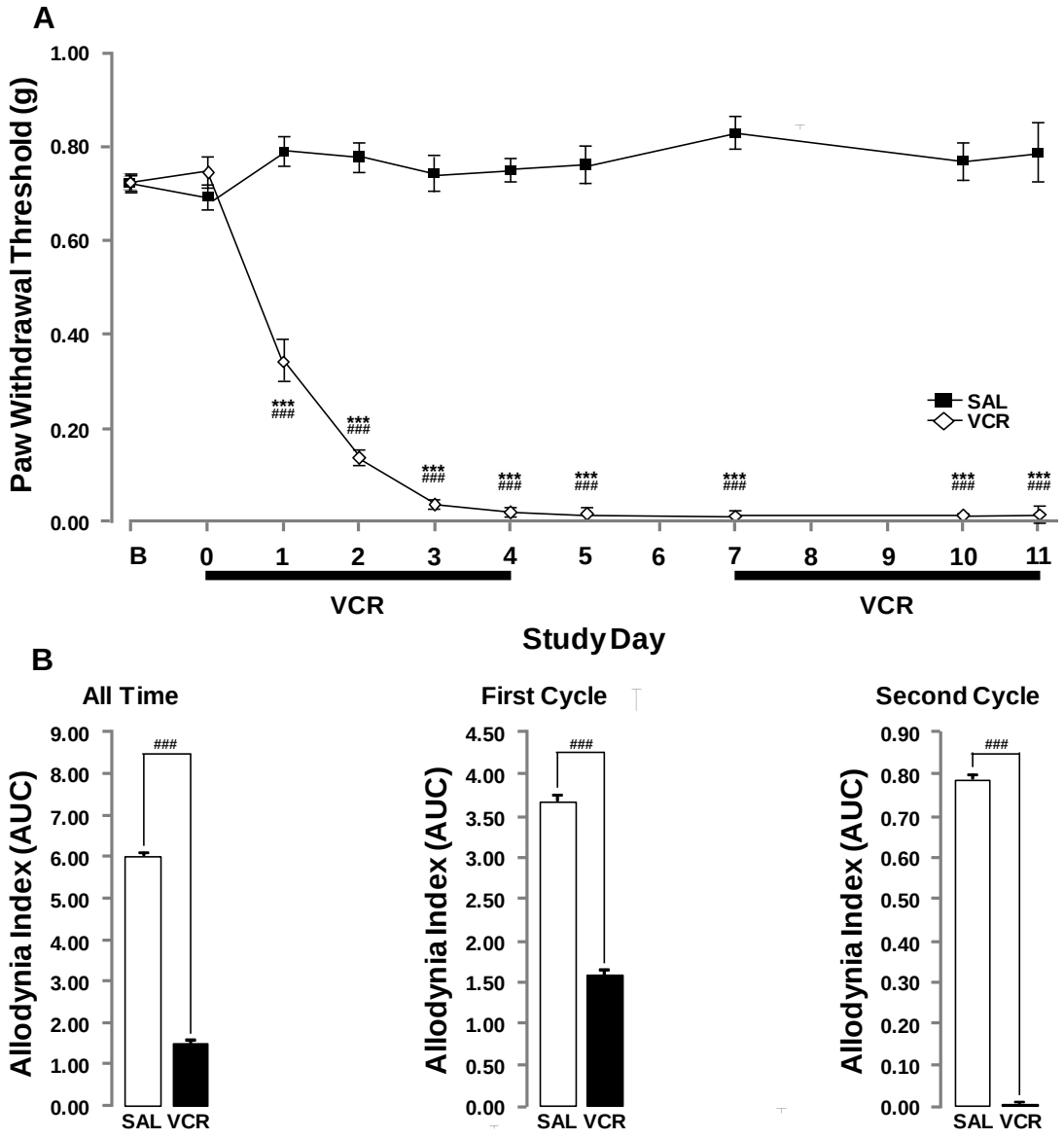

Figure 3.13. Heterozygous CX_3CR1-GFP expressing mice develop severe sustained mechanical allodynia following VCR treatment. Development of mechanical allodynia following *i.p.* VCR (0.5mg/kg/day) administration for two cycles (days 0-4 and 7-11; black horizontal bars). Vehicle group received an equal volume of saline. **(A)** Time course of the development of mechanical allodynia shown as 50% paw withdrawal threshold (PWT), data shown as mean ± SEM. N=8 per group, ***P<0.001 compared to baseline threshold, ### P<0.001 compared to saline threshold, two-way repeated measures ANOVA with post-hoc Holm-Sidak test. **(B)** Area under the curve (AUC) analysis showing data expressed as allodynia index where a lower value represent more severe allodynia. All time = BL-day 11, first cycle = BL-day 4, second cycle = day 7-11 Data shown are mean ± SEM. N=8 per group, ### P<0.001 compared to saline threshold with Student t-test.

Using mice expressing CX_3CR1-GFP we tested this hypothesis that the infiltrating cells were CX_3CR1^+. The analysis of CX_3CR1-expressing cells in the sciatic nerves of $CX_3CR1^{+/gfp}$ revealed that both GFP^+ (CX_3CR1^+) and $F4/80^+$ (monocyte/macrophage) cells were present in enhanced numbers following VCR treatment compared to their vehicle treated counterparts (figure 3.14A/B). Specifically the number of monocyte/macrophages ($F4/80^+$ cells) was elevated 24 hours after the first administration of VCR (figure 3.14B; day 1) and remained so for the duration of VCR treatment (day 4 end of first cycle and day 10 end of second cycle); consistent with the analysis of $F4/80^+$ cells in wild-type mice described in chapter two (figure 2.7). More interestingly the number of GFP^+ (CX_3CR1^+) cells concomitantly peaked 24 hours after the first administration of VCR (figure 3.14B; day 1), was slightly reduced at the end of the first cycle of treatment (figure 3.14B; day 4) and was significantly lower (than day 1) by the end of the second cycle of chemotherapy (figure 3.14B; day 11). These data indicate that CX_3CR1^+ monocyte/macrophages infiltrate and populate the peripheral nerve immediately after the commencement of and during the first cycle of VCR treatment but are less numerous thereafter.

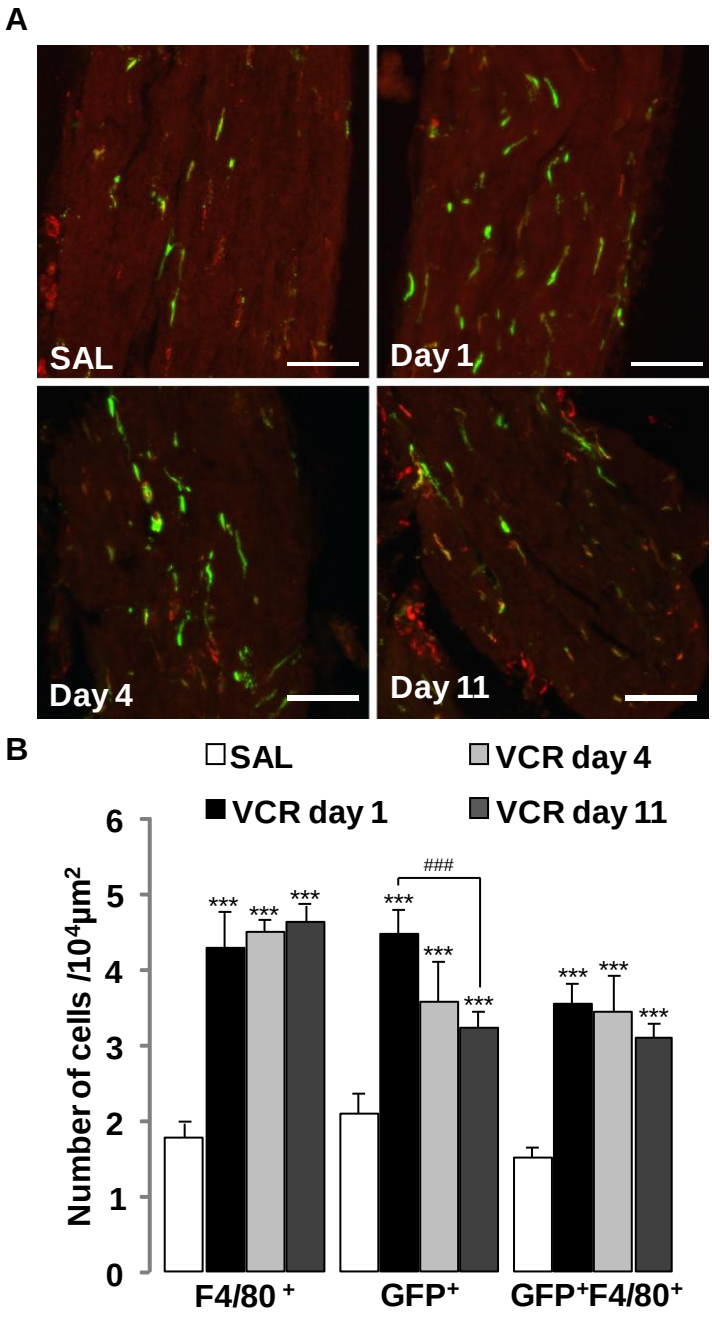

Figure 3.14. VCR administration induces infiltration of CX_3CR1^+ monocyte/macrophage into the nerve. (A) Representative images showing $F4/80^+$ (red) and GFP^+ / CX_3CR1^+ (green) cell infiltration into the sciatic nerve in vehicle (SAL) and VCR (day 1/4/11) treated animals (VCR *i.p.* 0.5mg/kg; days 0-4 and 7-11). Scale bars equal 100µm. **(B)** Quantification of the number of $F4/80^+$ or GFP^+ cells per $10^4\mu m^2$. Data shown are mean ± SEM and N=4per group. *** P<0.001 compared to saline, ###P<0.001 compared to day 1, one-way ANOVA with post-hoc Tukey test.

To further analyse, by FACS, the effect of VCR on the trafficking and/or phenotype of monocyte/macrophages, a peritoneal lavage was performed to collect these cells from the peritoneal cavity of $CX_3CR1^{gfp/+}$ mice following a single cycle of VCR. Intraperitoneal administration of VCR caused a notable increase in the total number of monocyte/macrophages infiltrating the peritoneal cavity (figure 3.15; saline: 4.5 ± 0.5 $x10^6$ cells, VCR: 9.9 ±1.6 $x10^6$ cells).

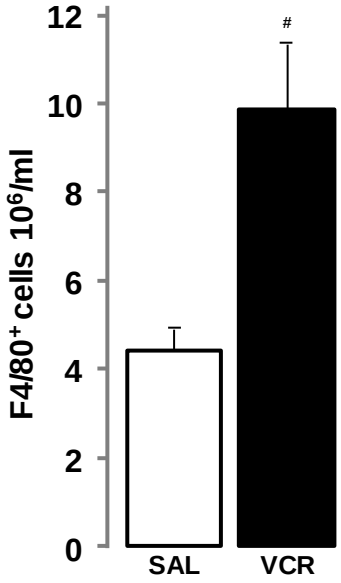

Figure 3.15. VCR administration increases the number of monocyte/macrophages infiltrating the peritoneal cavity. Counts of $F4/80^+$ cells in the fluid recovered from peritoneal lavage of saline (SAL) and VCR treated (VCR) mice (VCR *i.p.* 0.5mg/kg; days 0-4). Data shown are mean ± SEM and N=3 per group. #P<0.05 compared to saline with post-hoc Student t-test.

Interestingly FACS analysis of these cells demonstrated that not only was there this increase in cell infiltration, the cells that infiltrated underwent a phenotypic shift as a result of VCR treatment. Figure 3.16A/B shows typical FACS plots obtained from these experiments, as the quantification shows (figure 3.16C/D) in both $CX_3CR1^{+/+}$ and $CX_3CR1^{+/gfp}$ saline treated animals the majority (97% and 87% respectively) of cells are Gr-1^- (thus $Ly6C^-$ monocyte/macrophages). Analysis of these cells from the $CX_3CR1^{+/gfp}$ mouse shows they do indeed express GFP (CX_3CR1), suggesting that these cells are likely to be the $Ly6C^-CX_3CR1^{high}$ cells considered 'resident' monocyte/macrophages. In $CX_3CR1^{+/+}$ mice there is a shift towards a larger proportion of the cells being Gr-1^+ ($Ly6C^+$) following VCR treatment; suggesting a shift towards a $Ly6C^+CX_3CR1^{int}$ monocyte/macrophages population (considered inflammatory). This shift was also evident when this experiment was repeated using $CX_3CR1^{+/gfp}$ mice.

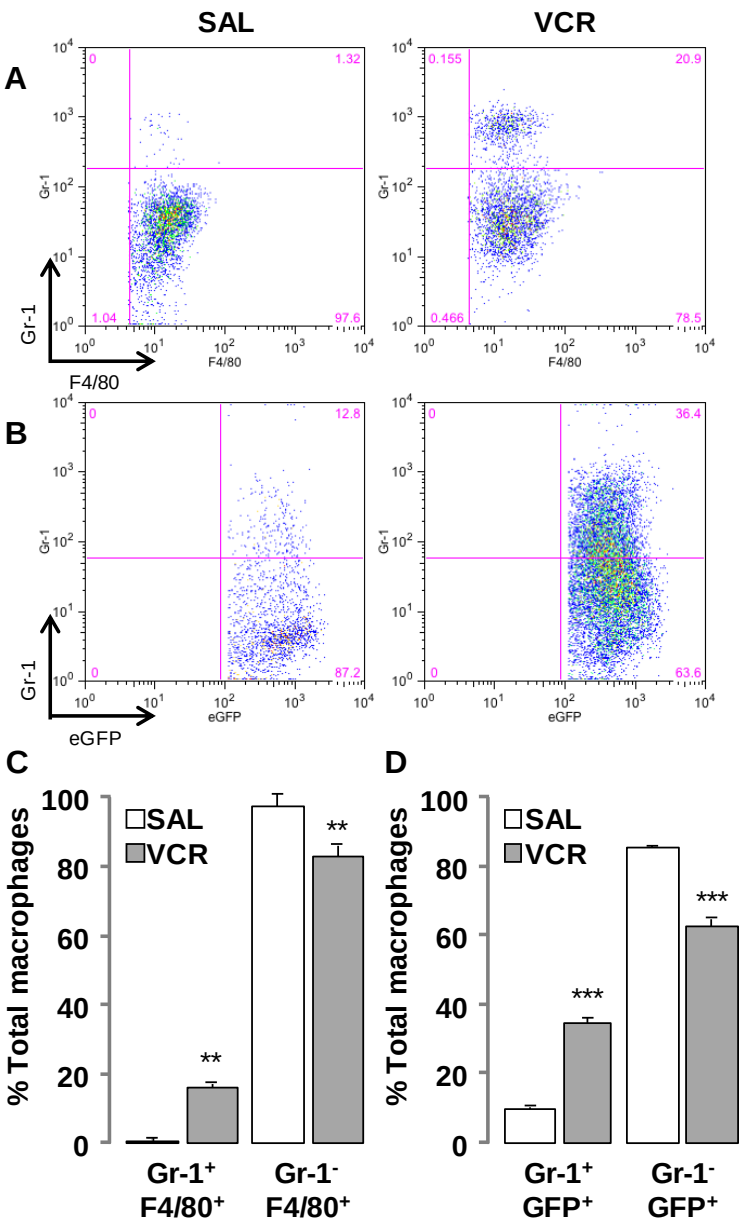

Figure 3.16. FACS analysis of peritoneal monocyte/macrophages shows a phenotypic shift following VCR treatment. (A/B) Representative dot-plot / FACS plots analysis of Gr-1 and F4/80 or GFP expression in vehicle (SAL) and VCR treated mice (VCR *i.p.* 0.5mg/kg; days 0-4). **(C)** Cumulative data of relative percentage of Gr-1^{+} and Gr-1^{-} cells in the F4/80^{+} population in $CX_3CR1^{+/+}$ mice. Data shown are mean ± SEM and N=3 per group. **P<0.01 compared to saline treated with post-hoc Student t-test. **(D)** Cumulative data of relative percentage of Gr-1^{+} and Gr-1^{-} cells in the GFP^{+} population in $CX_3CR1^{+/gfp}$ mice. Data shown are mean± SEM and N=3 per group. ***P<0.001 compared to saline treated with post-hoc Student t-test.

3.4. The CX_3CR1 receptor is critical for the development of VCR-induced mechanical hypersensitivity

These last studies have demonstrated that the majority of infiltrating monocyte/macrophages express CX_3CR1 to some degree, especially in the early stages of this chemotherapy-pain model, where infiltrating cells are likely to be patrolling/resident $Ly6C^-CX_3CR1^{high}$ monocyte/macrophages. It is well established that CX_3CR1 expression is vital for the survival of this population of cells and that its function as an adhesion molecule means that it plays a critical role in migration of cells from the blood into tissues. As data obtained from our liposome clodronate study has suggested that the infiltration of monocyte/macrophages into the nerve is a crucial step in the development of chemotherapy-induced mechanical allodynia, this receptor (CX_3CR1) constitutes an attractive candidate as a target for therapeutic intervention in this condition. As such, we went on to evaluate the importance of this receptor in the development of VCR-induced mechanical allodynia. The role of CX_3CR1 was elucidated using a second transgenic mouse tool; a CX_3CR1 knock-out ($CX_3CR1^{-/-}$). These animals completely lack functional CX_3CR1 due to the insertion of a neomycin cassette that results in disrupted transcription of the protein, as shown by the presence of a smaller PCR product (figure 3.17). Additionally we assessed monocyte/macrophage numbers in CX_3CR1 knock-out and wild-type mice by stimulating peritoneal cavity infiltration of monocyte/macrophages by the intraperitoneal administration of sterile bio-gel beads; the peritoneal cavity of wild-type ($CX_3CR1^{+/+}$) contained approximately 14×10^6 cells/ml. The number of cells obtained from the peritoneal cavity of CX_3CR1 knock-out was significantly lower (9.5×10^6 cells/ml), as demonstrated by figure 3.18.

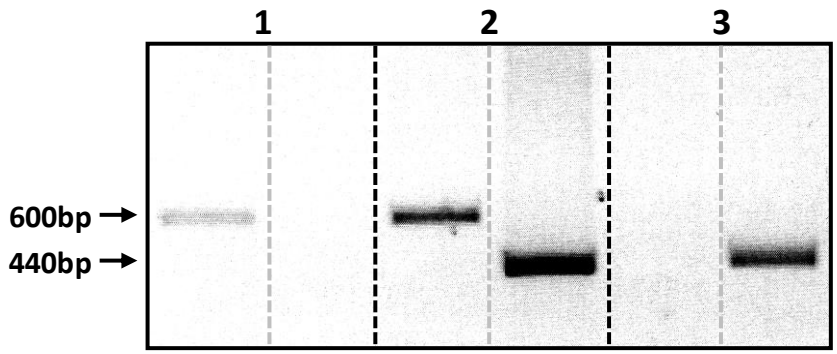

Figure 3.17. Genotyping electrophoresis of PCR samples from CX_3CR1 knock-out and wild-type mice. Representative pictograph of agarose gel following electrophoresis of PCR products with homozygous knock-out mice (lane 1) yielding a 600bp product, wild-type mice (lane 3) yielding a 440bp product, and heterozygous (lane 2) mice yielding both.

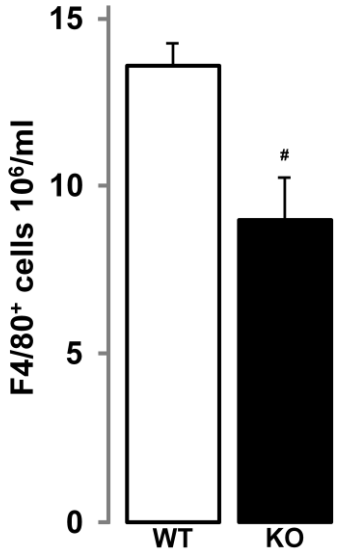

Figure 3.18. Fewer $F4/80^+$ cells are present in the $CX_3CR1^{-/-}$ mice. Counts of $F4/80^+$ monocyte/macrophages in the fluid obtained from the peritoneal cavity of $CX_3CR1^{+/+}$ (WT) and $CX_3CR1^{-/-}$ (KO) mice under sterile inflammatory conditions. Data shown are mean ± SEM and N=3 per group. #P<0.05 compared to WT with post-hoc Student t-test

We first evaluated the development of VCR-induced mechanical allodynia in $CX_3CR1^{-/-}$ mice compared to wildtype littermate controls ($CX_3CR1^{+/+}$). As figure 3.19A demonstrates, in contrast to $CX_3CR1^{+/+}$ mice, the thresholds of $CX_3CR1^{-/-}$ mice remained unchanged (at baseline levels) for the duration of the first VCR cycle (until day 4). Area under curve analysis (figure 3.19B) for the first cycle shows a dramatic difference in allodynia index between VCR treated $CX_3CR1^{+/+}$ and $CX_3CR1^{-/-}$ mice. Interestingly, following the first cycle of treatment and during the second the paw withdrawal thresholds of $CX_3CR1^{-/-}$ mice fall to a level comparable to that of $CX_3CR1^{+/+}$ mice (day 7: $CX_3CR1^{+/+}$ 98.00% ± 0.37, $CX_3CR1^{-/-}$ 96.89% ± 0.49 reduction in PWT). Indeed, the area under curve analysis for the second cycle of treatment (figure 3.19B) confirms that there is no significant difference in allodynia index between $CX_3CR1^{+/+}$ and $CX_3CR1^{-/-}$ mice at this time. Thus this data suggests that CX_3CR1-deficiency delays the onset of mechanical hypersensitivity following repeated systemic VCR administration.

In a similar fashion to the study performed in LCL pre-treated animals, we then performed immunohistochemical analysis of the sciatic nerve of VCR treated $CX_3CR1^{+/+}$ and $CX_3CR1^{-/-}$ mice. This revealed that the number of $F4/80^+$ cells (monocyte/macrophages) in the nerve of $CX_3CR1^{-/-}$ mice had remained unchanged following the first cycle of VCR (day 4; figure 3.20A/B), in contrast to the increased number of monocyte/macrophage seen in the nerve of wildtype ($CX_3CR1^{+/+}$) mice. However, by the end of the second VCR cycle (day 11) the number of $F4/80^+$ cells (monocyte/macrophages) in the sciatic nerves of $CX_3CR1^{-/-}$ mice had increased to a level significantly higher than that of saline treated mice, although still lower than in VCR treated $CX_3CR1^{+/+}$ mice (figure 3.20C/D).

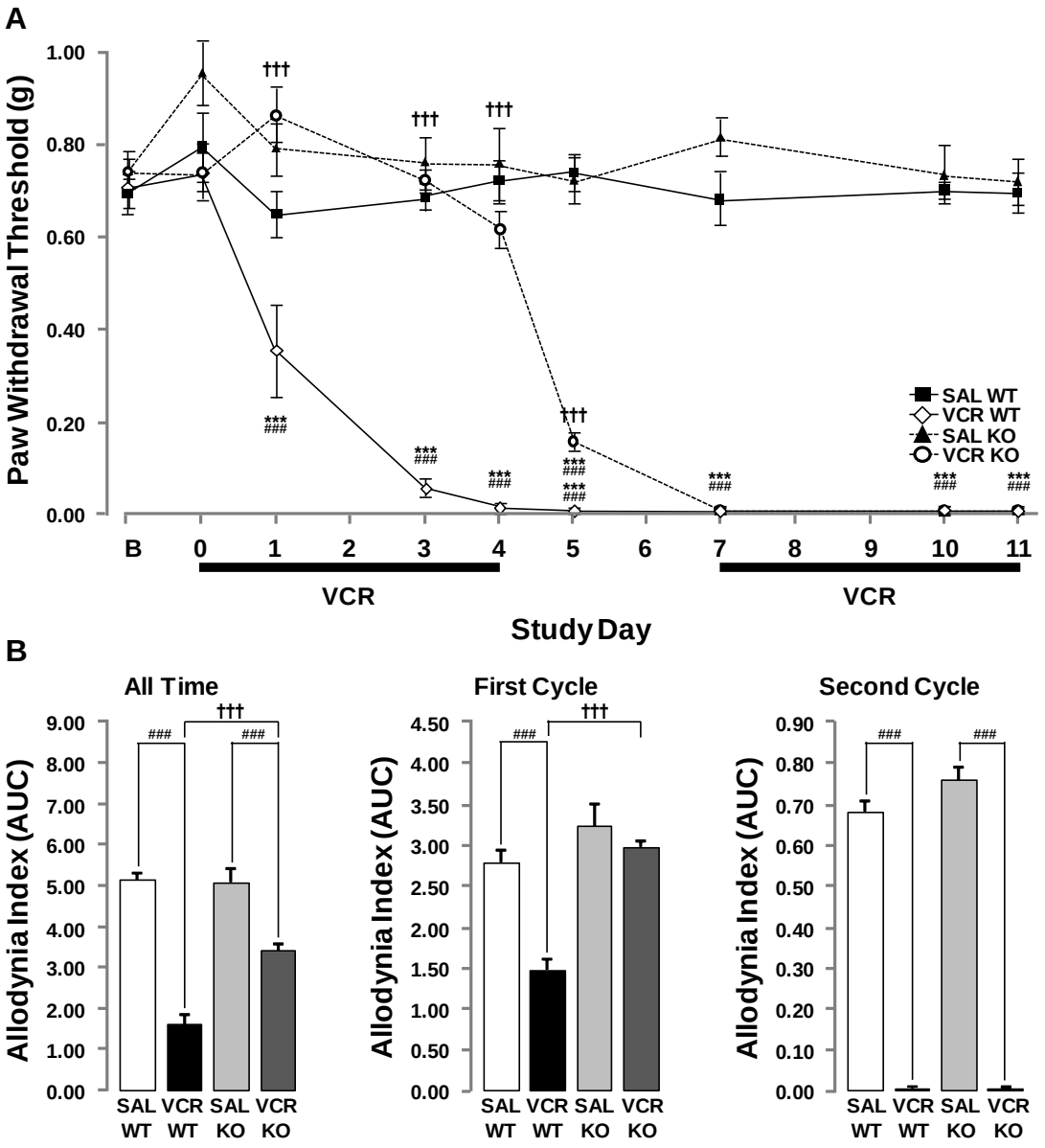

Figure 3.19. CX_3CR1-deficiency delays the onset of mechanical allodynia induced by repeated systemic administration of VCR. Development of mechanical allodynia in $CX_3CR1^{-/-}$ (KO) mice or $CX_3CR1^{+/+}$ (WT) control receiving *i.p.* VCR (0.5mg/kg/day; days 0-4 and 7-11; black horizontal bars) or equal volume of vehicle (SAL). **(A)** Temporal profile of mechanical allodynia development shown as 50% PWT, data shown as mean ± SEM. N=8 per group, ***P<0.001 compared to baseline threshold, ### P<0.001 compared to saline threshold, ††† P<0.001 compared to wild-type threshold, two-way RM ANOVA with post-hoc Holm-Sidak test. **(B)** Area under the curve (AUC) analysis data expressed as allodynia index where a lower value represent more severe allodynia. All time = BL-day 24, first cycle= BL-day 4, second cycle = 7-11, recovery = 11-24. Data shown are mean ± SEM. N=8 per group, ### P<0.001 compared to saline index, ††† P<0.001 LCL-VCR compared to WT-VCR index with one way ANOVA and post-hoc Holm-Sidak.

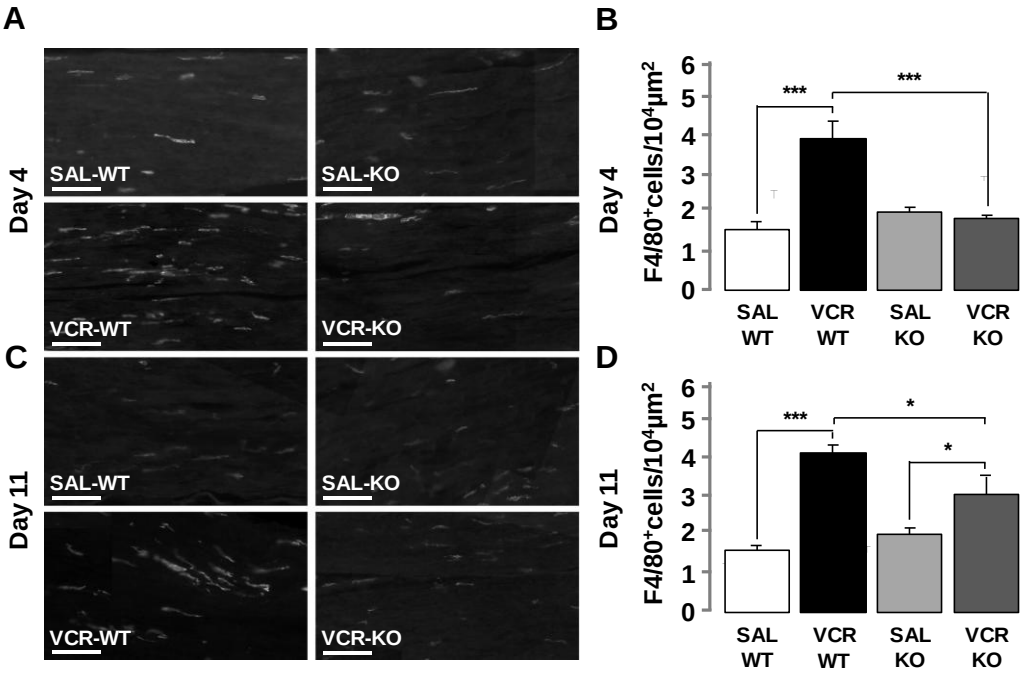

Figure 3.20. CX_3CR1-deficiency delays the onset of macrophage infiltration of the sciatic nerve induced by repeated systemic administration of VCR. (A/C) Representative images showing macrophages in the sciatic nerve following vehicle (SAL) or one (day 4) or two cycles (day 11) of VCR treatment (0.5mg/kg/day *i.p;* days 0-4 and 7-11.) in $CX_3CR1^{+/+}$ (WT) and $CX_3CR1^{-/-}$ (KO) mice, where macrophages are visualised by their expression of F4/80. Scale bars equal 100µm. **(B/D)** Quantification of the number of macrophages in the sciatic nerve, shown as number of $F4/80^+$ cells per $10^4\mu m^2$. Data shown are mean ± SEM and N=4 per group. *P<0.05, *** P<0.001 compared to saline or WT-VCR, one-way ANOVA with post-hoc Tukey test.

3.5. CX_3CR1 deficiency does not influence spinal glial activation following repeated systemic administration of VCR

As well as being expressed on monocyte/macrophages in the periphery, CX_3CR1 is expressed exclusively on microglia in the central nervous system, where its interaction with CX_3CL1 contributes to the maintenance of homeostasis by limiting the release of pro-inflammatory mediators (Mizuno et al., 2003;Lyons et al., 2009). Under pathophysiological conditions the expression of CX_3CR1 in microglia is enhanced and its activation contributes to enhanced nociceptive signalling (Zhuang et al., 2007;Staniland et al., 2010). Whilst we have previously established that the repeated systemic administration of VCR does not induce microgliosis in the spinal cord (chapter two figure 2.9), it was important for us to determine whether central changes in microglia could contribute to the phenotype we have observed in the CX_3CR1 knock-out mouse following VCR administration. As shown previously, $CX_3CR1^{+/+}$ mice exhibited no increase in the number of microglia ($Iba1^+$ cells) in the dorsal horn of the spinal cord following repeated VCR administration (figure 3.21A/B; WT SAL/WT VCR) at either the end of the first cycle of treatment (day 4) or the second (day 11). Furthermore, as the high magnification inserts in figure 3.21A demonstrate, these cells did not exhibit a change in morphology associated with activation. In addition, no difference in the number or morphology of microglia in $CX_3CR1^{-/-}$ mice was observed in either saline or VCR treated mice irrespective of VCR cycle (figure 3.21A/B; KO SAL/KO VCR) and no distinction could be seen between $CX_3CR1^{+/+}$ and $CX_3CR1^{-/-}$ microglia.

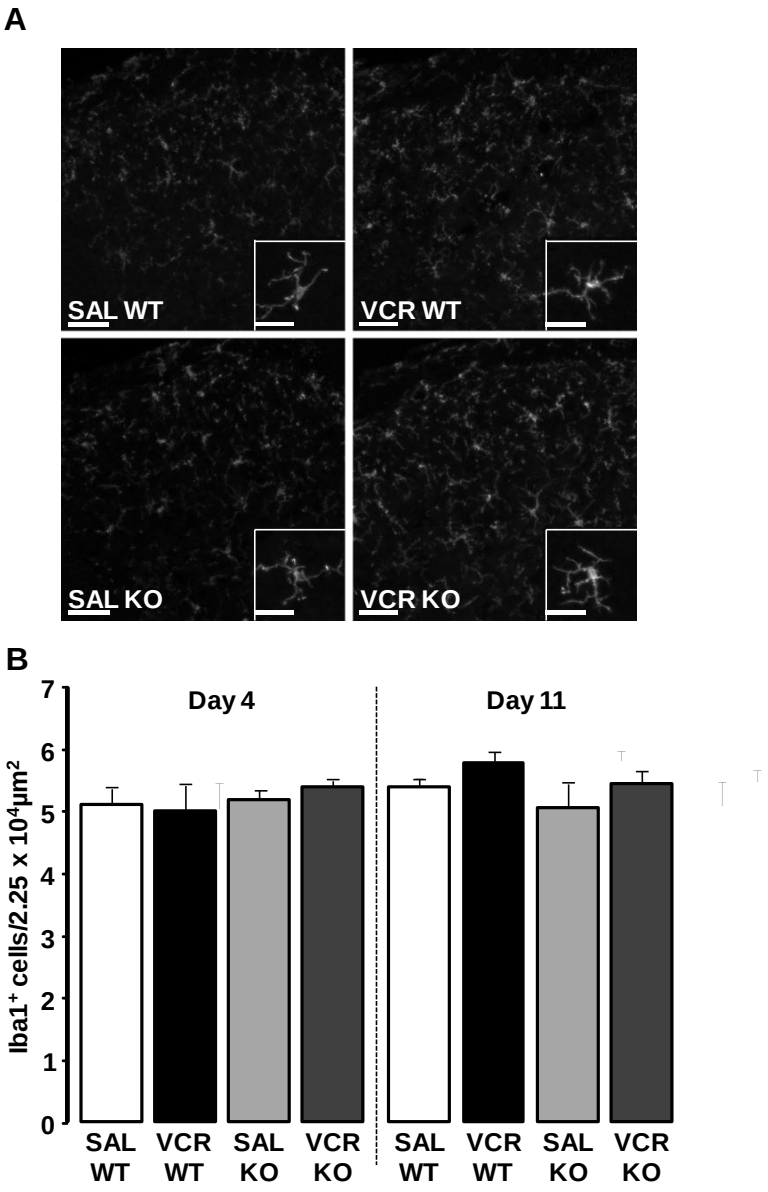

Figure 3.21. Microgliosis does not occur in the spinal cord of $CX_3CR1^{+/+}$ or $CX_3CR1^{-/-}$ mice following repeated systemic administration of VCR. (A) Representative images showing low and high magnification images of microglia in the dorsal horn of the spinal cord following administration of vehicle (SAL) or one (day 4) or two cycles (day 11) of VCR (0.5mg/kg/day *i.p.*; days 0-4 and 7-11) in $CX_3CR1^{+/+}$ (WT) and $CX_3CR1^{-/-}$ (KO) mice, where microglia are visualised by their expression of Iba1. Scale bars equal 100µm and 20 µm in inserts. **(B)** Quantification of the number of microglia in the dorsal horn of the spinal cord, shown as number of $F4/80^+$ cells per 2.25 x $10^4\mu m^2$. Data shown are mean ± SEM and N=4 per group. No significant difference seen with one-way ANOVA with post-hoc Tukey test.

As shown previously $CX_3CR1^{+/+}$ mice developed significant astrogliosis following VCR treatment, as demonstrated by an increase in GFAP immunoreactivity in the dorsal horn of the spinal cord (figure 3.22A/B; WT SAL/WT VCR). Interestingly no difference was observed in the development of astrogliosis between $CX_3CR1^{+/+}$ and $CX_3CR1^{-/-}$ mice; $CX_3CR1^{-/-}$ mice exhibited astrogliosis (increased GFAP immunoreactivity) equivalent to that of $CX_3CR1^{+/+}$ mice at both the end of the first cycle of chemotherapy (day 4) and at the end of the second cycle (day 11). This is in line with the lack of effect of FLC in wild-type mice; taken together these data suggest the CX_3CR1-deficiency does not influence spinal cord glia in this model.

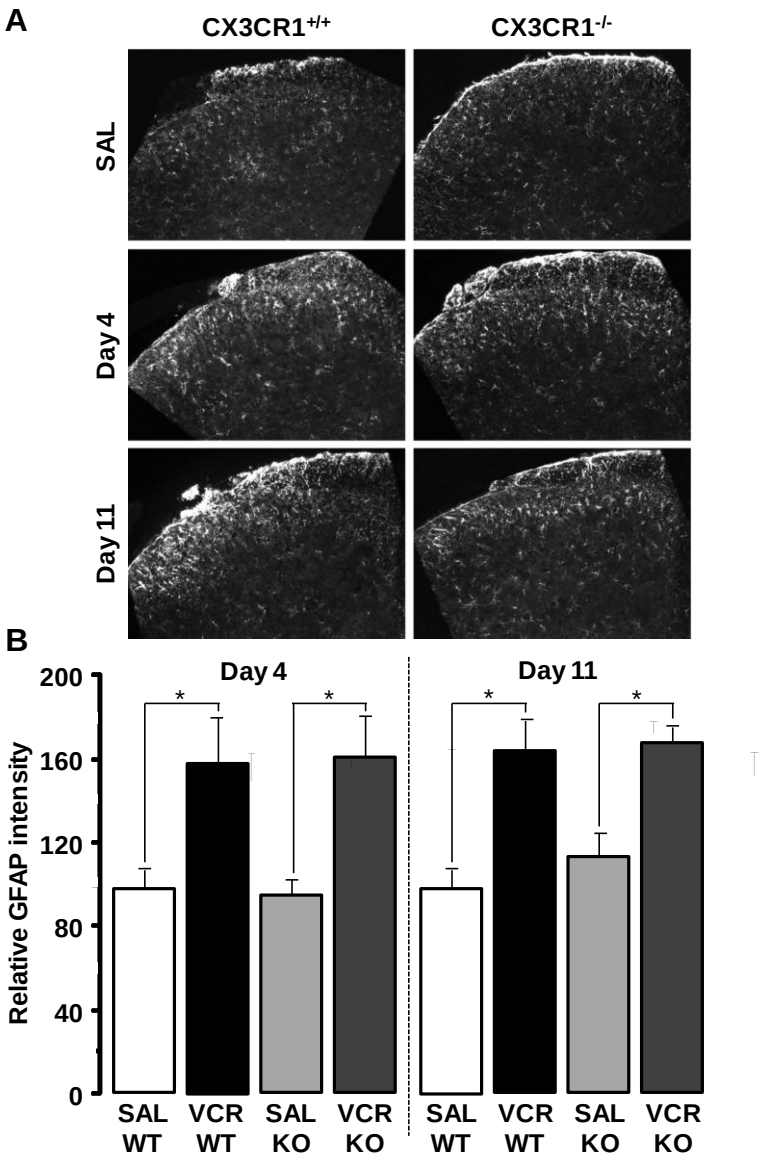

Figure 3.22. Astrogliosis occurs equally in the spinal cord of $CX_3CR1^{+/+}$ and $CX_3CR1^{-/-}$ mice following repeated systemic administration of VCR. (A) Representative images showing astrocytes in the dorsal horn of the spinal cord following administration of vehicle (SAL) or one (day 4) or two cycles (day 11) of VCR (0.5mg/kg/day *i.p.*; days 0-4 and 7-11) in $CX_3CR1^{+/+}$ (WT) and $CX_3CR1^{-/-}$ (KO) mice, where astrocytes are visualised by their expression of GFAP. Scale bars equal 100µm and 20 µm in inserts. **(B)** Quantification of the intensity of GFAP staining in the dorsal horn shown as relative GFAP intensity (relative to saline treatment) per $10^4\mu m^2$. Data shown are mean ± SEM and N=4 per group. * $P<0.05$ compared to saline value with one-way ANOVA with post-hoc Tukey test.

4. Discussion

In chapter two we demonstrated that following repeated systemic administration of VCR there is an increase in the number of F4/80^{+} cells in the trunk of the sciatic nerve, indicative of macrophage infiltration. Furthermore, the temporal profile of the infiltration we observed was similar to that of the development of mechanical allodynia in these mice. This data is synergistic to previous work by both the Mantyh and Sommer laboratories who have demonstrated macrophage infiltration of the sciatic nerve and lumbar DRG following chemotherapy, where they take on a hypertrophied activated morphology (Peters et al., 2007a;Jimenez-Andrade et al., 2006;Uceyler et al., 2006). It has been hypothesised that macrophages contribute to the development of chemotherapy-pain through the release of pro-nociceptive mediators; the expression of IL-6 is increased in macrophages in the sciatic nerves of mice as a consequence of chemotherapy treatment and local administration of an IL-6 neutralising antibody attenuates VCR-induced mechanical allodynia (Kiguchi et al., 2008b). However, unlike in models of surgical nerve injury and diabetic neuropathy, the contribution of macrophages to the development of pain has not been fully elucidated. Thus, here in this chapter we set out to characterise the nerve infiltrating monocyte/macrophages present in VCR treated mice, and to determine the contribution these cells make to the development of VCR-induced mechanical allodynia. To achieve this we utilised three tools; liposome encapsulated clodronate (LCL) induced depletion of monocyte/macrophages, a CX_3CR1-GFP reporter mouse and a $CX_3CR1^{-/-}$ mouse.

The principle finding of this set of experiments is that monocyte/macrophages contribute significantly to the development of pain following administration of VCR; depletion of these cells prevents the onset of the mechanical allodynia normally observed in this model. Additionally the

evidence we have gathered suggests that the mechanism by which these cells are pro-nociceptive is CX_3CR1 dependent; when phenotypically characterised it is apparent that a significant portion of these cells are CX_3CR1 expressing and, in a similar temporal profile to monocyte/macrophage depleted animals, mice deficient in CX_3CR1 experience a delay in the onset of VCR-induced mechanical allodynia in comparison to wild-types.

The depletion of monocyte/macrophages by the systemic administration of liposome LCL had no effect on the baseline paw withdrawal thresholds of wild-type C57Bl/6 mice and no reduction in the number of tissue resident macrophages counted in these animals. This is to be expected; LCL was administered systemically but is unable to cross the blood nerve barrier (BNB), thus it is phagocytosed by, and depletes only circulating monocyte/macrophages. LCL reduces the number of monocyte/macrophages available to migrate into tissues rather than decreasing pre-existing tissue resident cells. The rapid onset of a severe and sustained mechanical hypersensitivity previously observed in VCR-treated mice was, interestingly, not present in LCL pre-treated animals. In these animals paw withdrawal thresholds remained at a level comparable to both baseline and vehicle animals for the first cycle of VCR chemotherapy, before declining to reach a level comparable to PBS-VCR treated mice by the start of the second cycle of treatment. When the sciatic nerves of these animals are examined immunohistochemically, we observed that infiltration of monocyte/macrophages into the sciatic nerve of LCL pre-treated mice is absent at a time point when these animals do not experience mechanical allodynia (day 4), but it is present at a later time point when the animals display severe mechanical hypersensitivity (day 11). These data indicate that monocyte/macrophage infiltration into the peripheral nerve is associated with the development of mechanical allodynia; mice that do not exhibit mechanical allodynia do not display an increased number of monocyte/macrophages in the sciatic nerve. Additionally these data

appear to indicate that the effect of macrophage depletion on the development of mechanical allodynia is transient; however we must consider the repopulation capacity of these cells. Our laboratory has shown previously that the systemic administration of LCL is associated with a reduction of splenic macrophages of approximately 90%, but that this is not permanent; 8 days after the administration of LCL this cell population has recovered fully (Barclay et al., 2007). Indeed this idea is well supported; following LCL-induced depletion of Kupffer macrophages in the liver, repopulation begin within a week and given that bone marrow precursors are unaffected, due to the inability of the liposomes to migrate into tissue, depleted cells are ultimately replaced (Van and van Kesteren-Hendrikx, 2002). Furthermore, the temporal profile of the attenuation of mechanical allodynia observed in our model of chemotherapy pain is comparable to that previously reported by ourselves (Barclay et al., 2007) and others (Liu et al., 2000).

Whilst LCL induced depletion of monocyte/macrophages is a useful tool experimentally, it is not an attractive therapeutic option. Not only is the depletion transient but these cells play an important role in the immune system and are critical for the maintenance of homeostasis in relation to detecting and responding to infection; thus depletion of the cell population as a whole would leave patients immune suppressed and vulnerable to infection.

In the mouse, as in the human, monocyte/macrophages show substantial heterogeneity, and it is possible that a similar reduction in hyperalgesia could be achieved by the suppression of only a single subpopulation, whilst maintaining an effective immune response. In order to assess this as a viable therapeutic option, our pro-nociceptive nerve infiltrating monocyte/macrophages must first be characterised. One of the key differences between the two most well characterised phenotypes of monocyte/macrophages in the mouse is the level of expression of the chemokine receptor

CX_3CR1. This receptor is expressed highly in $Ly6C^-$ resident monocyte/macrophages ($Ly6C^-CX_3CR1^{high}$) but is expressed at a lower level in $Ly6C^+$ inflammatory monocytes/macrophages ($Ly6C^+CX_3CR1^{int}$). We hypothesised that the cells infiltrating the nerve early on in the development of VCR-neuropathy were $Ly6C^-CX_3CR1^{high}$ monocyte/macrophages, and evaluated the expression of CX_3CR1 in monocyte/macrophages of VCR-treated mice. This was achieved by utilizing a genetically modified mouse, in which an *egfp* reporter gene had been inserted into the second exon of the *cx3cr1* gene, resulting in the expression of functional GFP tagged CX_3CR1 in heterozygous mice ($CX_3CR1^{+/gfp}$).

To enable these experiments we obtained homozygous CX_3CR1-GFP mice and breed them with wild-type mice to produce heterozygous ($CX_3CR1^{+/gfp}$) offspring. We had previously characterised the VCR model of chemotherapy-pain only in male mice, however to enhance the number of offspring from these breeding pairs that could be used experimentally, we performed a comparative study of male and female wild-type mice; assessing development of mechanical allodynia in VCR treated animals to determine whether or not sex was an influencing factor. In contrast to some previous work which has demonstrated a sex difference in the development of neuropathic pain following the induction of bone cancer (Falk et al., 2013) and chronic inflammatory pain arising as the result of LPS administration (Sorge et al., 2011), no difference was seen in the paw withdrawal thresholds of male and female mice at any stage during the development or maintenance of VCR-induced mechanical allodynia. Thus in subsequent experiments both male and female mice were used.

Whilst the current literature suggests that the function of CX_3CR1 is unaffected in CX_3CR1-GFP mice, the evidence we have gathered so far suggest the development of mechanical allodynia in

our model is dependent on a normal infiltration capacity of monocyte/macrophages. We, therefore, assessed the development of mechanical hypersensitivity in CX_3CR1-GFP heterozygous mice and have demonstrated that these mice do indeed develop mechanical hypersensitivity/allodynia to the same degree as wild-type mice. We then set out the test the hypothesis that the majority of infiltrating monocyte/macrophages are CX_3CR1^+ (thus GFP^+). Sciatic nerve sections were taken at various time points from VCR treated $CX_3CR1^{+/gfp}$ mice. At all of these time points mice had a significant reduction in their paw withdrawal thresholds indicative of mechanical hypersensitivity. Immunohistochemical analysis of these nerve sections demonstrated that significant infiltration of $F4/80^+$ cells (monocyte/macrophages) occurs concurrently to an increase in CX_3CR1-GFP^+ cells, suggesting that these infiltrating cells are CX_3CR1^+ monocyte/macrophages. Interestingly, whilst this increased number of $F4/80^+$ cells remains consistently elevated, a gradual decrease in CX_3CR1-GFP^+ cells is seen over the course of the two cycles of VCR. On first glance, this suggests that at later time points the infiltrating cells may be CX_3CR1^- (GFP^-), however it is likely an artefact of the earlier infiltrating monocytes settling in the tissue and differentiating fully into macrophages following their migrating and activation, which causes them to decrease their expression of CX_3CR1 (Yona et al., 2013). We have provided evidence further to support the idea that VCR induces monocyte/macrophage infiltration of peripheral tissues; systemically administered VCR induces infiltration of these cells into the peritoneal cavity.

Our data demonstrate that in saline treated wild-type mice the majority of monocyte/macrophages extracted from the peritoneal cavity are $Gr\text{-}1^-$ 'resident' monocyte/macrophages. The same conclusion was drawn following the examination of monocyte/macrophages extracted from the peritoneal cavity of $CX_3CR1^{+/gfp}$ mice. Following a

single cycle of VCR, however the ratio of Gr-1$^-$ to Gr-1$^+$ monocyte/macrophages in both wild-type and $CX_3CR1^{+/gfp}$ shifted; whilst the Gr-1$^-$ population still dominated in both, a substantial increase in the proportion of Gr-1$^+$ cells was seen (approximately 20%) in both genotypes. This represents a shift towards a Ly6C$^+$ 'inflammatory' phenotype and this observation leads us thus to suggest that monocyte/macrophages infiltrating the nerve may be able to produce pro-inflammatory mediators which can activate neurons and evoke pain. We will return to this idea and investigate it further in chapter four.

The data obtained from the experiments conducted with CX_3CR1-GFP expressing mice indicates that the majority of infiltrating monocyte/macrophages express CX_3CR1 to some degree. Unfortunately we are currently unable to distinguish between Ly6C$^-$$CX_3CR1^{high}$ and Ly6C$^+$$CX_3CR1^{int}$ monocyte/macrophages with the tools currently available to us. Both populations of cells express CX_3CR1, however they differ in their level of expression of this protein; this is high and intermediate respectively (as opposed to high verses low) and it is not possible to visually differentiate the two populations. Fortunately the expression of CX_3CR1 is crucial for the survival of only one of the population's cells, and this distinction can be utilised to distinguish the populations and their contribution to the development of VCR-induced mechanical allodynia. Expression of functional CX_3CR1 is critical for the survival of Gr1^{low}CX_3CR1^{high} (Ly6C$^-$$CX_3CR1^{high}$) monocytes; the absence of CX_3CR1-CX_3CL1 interaction results in a specific reduction in the number of circulating Gr1^{low} CX_3CR1^{high} monocytes and a decrease in absolute monocyte numbers in these animals. This is via a Gα-Bcl2 dependent mechanism; forced expression of the anti-apoptotic factor Bcl2 rescues monocyte numbers in CX_3CR1 deficient mice and a pronounced increase in Gr1^{low}CX_3CR1^{high} monocytes is observed, indicating that CX_3CR1-CX_3CL1 interaction promotes activation of Bcl2, preventing apoptosis. Additionally the pro-survival effect of CX_3CR1-CX_3CL1 is

blocked by treatment of the monocytes with pertussis toxin which blocks Gα signalling associated with CX_3CR1 (Landsman et al., 2009). Due to the necessity of the CX_3CR1-CX_3CL1 interaction for the survival of $Ly6C^-CX_3CR1^{high}$ monocyte/macrophages $CX_3CR1^{-/-}$ mice lack this population of cells. Thus these CX_3CR1 knock-out mice provided us with a tool with which we can examine the specific role of $Ly6C^-CX_3CR1^{high}$ monocyte/macrophages in the development of VCR-induced mechanical allodynia.

CX_3CR1 wild-type ($CX_3CR1^{+/+}$) mice rapidly develop a severe and persistent mechanical hypersensitivity as a result of VCR treatment. Fascinatingly, in a pattern comparable to that of LCL-VCR treated animals, this does not occur in $CX_3CR1^{-/-}$ animals. In these animals paw withdrawal thresholds remains consistently at levels comparable to both baseline and vehicle treated animals for the first cycle of VCR chemotherapy. As this cycle nears completion, the mechanical thresholds of $CX_3CR1^{-/-}$ animals begin to decline, reaching a level comparable to that of $CX_3CR1^{+/+}$ mice by the start of the second cycle of treatment; as with LCL-VCR and PBS-VCR treated mice, $CX_3CR1^{+/+}$ and $CX_3CR^{-/-}$ show an equal decline in allodynia index during the second cycle of VCR chemotherapy. These data suggest that $Ly6C^-CX_3CR1^{high}$ monocyte/macrophages make a significant contribution to the development of mechanical allodynia occurring subsequent to VCR treatment; when these cells are absent the onset of mechanical allodynia is substantially delayed. Indeed an increase in the number of monocyte/macrophages infiltrating the nerve is not observed in following a single cycle of VCR treatment in CX_3CR1 knock-out mice, when these mice do not exhibit mechanical allodynia. In the nerves of these and vehicle treated CX_3CR1 knockout mice a small population of monocyte/macrophages is present in the nerve. At present we do not possess the tools to fully characterise this remaining population, however it is possible that the population of $Ly6C^+CX_3CR1^{int}$ monocyte/macrophages that express CCR2 compensate for the lack of patrolling

monocyte/macrophages in $CX_3CR1^{-/-}$ animals, and take on an immune surveillance role. Perhaps unsurprisingly as the mechanical thresholds of $CX_3CR1^{-/-}$ mice decline during the end of the first cycle and for the duration of the second cycles of treatment, monocyte/macrophages began to infiltrate the sciatic nerve, and a significantly higher number of these cells is observed in the nerve in VCR treated knock-out mice compared to their vehicle treated counterparts at the end of the second cycle of treatment. Again, whilst we do not currently possess the tools to precisely determine the phenotype of these infiltrating cells, they are likely to be $Ly6C^{+}CX_3CR1^{int}CCR2^{+}$ inflammatory monocyte/macrophages as the survival of this population of cells is not influenced by CX_3CR1-deficiency (Landsman et al., 2009).

We also provide data that indicates, as in wild-type mice, CX_3CR1 knock-out mice develop astrogliosis, but not microgliosis, following systemic administration of VCR. Astrogliosis is present in knock-out animals in the absence of mechanical allodynia, and occurs despite removal of a key peripheral component that likely drives central glial activation this process. Thus it possible to suggest that astrocytic activation is not occurring as a result of neuronal activation by pro-nociceptive mediators from monocyte/macrophages; rather it is an indication of direct activation of sensory neurons by VCR via a mechanism not yet determined. However, as we've shown in chapter two, suppression of glial activation by the aconitase inhibitor FLC is not sufficient to attenuate mechanical allodynia in the VCR-neuropathy model so the contribution made to the development of a pain state by astrocytes in this condition is still unknown.

5. Introduction to Chapter 4

In this chapter, we provide evidence that demonstrates that the infiltration of monocyte/macrophages of the peripheral nerve that occurs as a consequence of systemic VCR administration is a critical step in the development of VCR-induced mechanical allodynia. Additionally we have demonstrated that the majority of these infiltrating cells are CX_3CR1^+, and that the rapid development of mechanical hypersensitivity after the administration of VCR requires the expression of this receptor and the presence of circulating $Ly6C^-CX_3CR1^{high}$ monocyte/macrophages. Thus CX_3CR1 is an attractive target for a novel therapeutic intervention for the treatment of chemotherapy induced pain. Next we must ask the question, if CX_3CR1 is so critical for the development of pain in these circumstances, what role is its ligand CX_3CL1 playing? In the next set of experiments we set out to test the hypothesis that CX_3CL1 contributes to the development of VCR induced mechanical allodynia by activating monocyte/macrophages via CX_3CR1, causing these cells to produce pro-nociceptive mediators that have the capacity to activate neurons. To do this we have utilised a CX_3CL1-mCherry reporter mouse and have established an *in vitro* assay to assess the expression of CX_3CL1 in the endothelium. We have also used a primary macrophage culture system to determine the effect of CX_3CL1-CX_3CR1 interaction on the production of pro-nociceptive mediators by these cells. These experiments are presented in chapter four following an introduction to CX_3CL1 and the adhesion properties of endothelial cells.

Chapter 4:

The Contribution Of Endothelial CX_3CL1 And TRPA1 To Vincristine-Induced Painful Peripheral Neuropathy

1. Introduction

Chapter three introduced the protein CX_3CR1; a chemokine receptor expressed on the surface of cells of a myeloid linage, which plays an important role in the transmigration of these cells into tissue. Here we will discuss this receptors ligand, CX_3CL1 and the endothelial cells on which it is expressed, and then the TRPA1 receptor which is found on the axons and terminals of primary afferent neurons.

1.1. CX_3CL1

As we mentioned previously in chapter three, chemokines are a family of proteins critically involved in the migration of leukocytes. CX_3CL1, also known as fractalkine (FKN), is no exception to this; as determined by structure (see figure 4.1), it is the only member of the CX_3C family of chemokines and was first described by Bazan et al as a potent attracter of T-cells and monocytes (Bazan et al., 1997). The protein can exist in two forms, each of which mediates distinct biological actions: a membrane tethered protein and a soluble chemokine domain (Bazan et al., 1997). Membrane bound CX_3CL1 serves as an adhesion protein, promoting the firm adhesion of leukocytes without the activation of integrins (Fong et al., 1998), whilst soluble CX_3CL1 is a potent chemoattractant for monocytes, NK cells, T cells and B cells (Imai et al., 1997;Corcione et al., 2009).

1.1.1. Structure

In 1997 two groups independently described a novel chemokine that differed from those previously described (of the C, CC and CXC families), as it possessed a unique cysteine motif in its

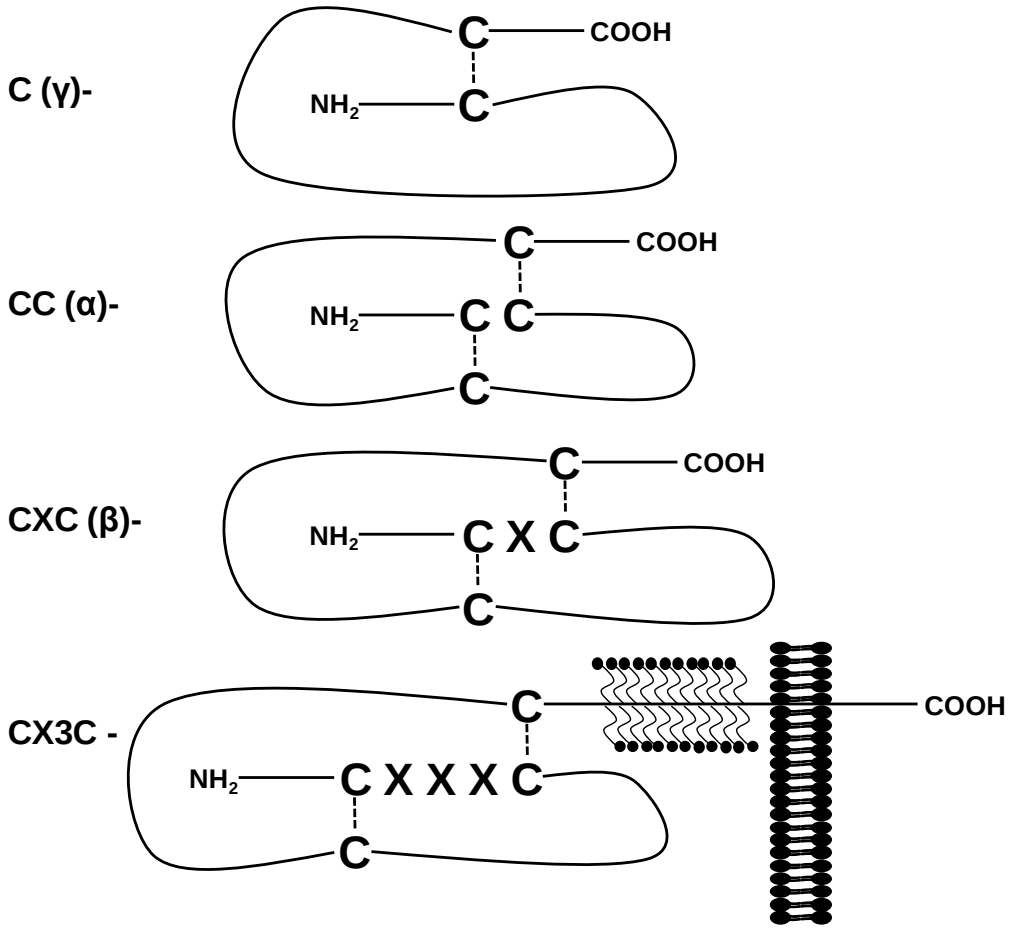

Figure 4.1. Classification of chemokines according to the organization of N-terminal cysteine residues.

chemokine domain: Cys-X-X-X-Cys (CX_3C). This new chemokine was identified from sequence analysis of a cDNA library of the murine choroid plexus; a specific sequence clone, pT1, had a sequence quite similar to that of MCP-1 (CCL2) and was named neurotactin (Pan et al., 1997). The 1194 base pair *neurotactin* gene was localised to chromosome 16q and encodes a 397 amino acid protein with several key regions. The first of these is the chemokine domain; made up of amino acids 23-92, alignment analysis of this region showed remarkable homology to the chemokine domain of many known chemokines, with the exception of the CX_3C region. Based on this observation neurotactin is now known as CX_3CL1 (Bazan et al., 1997;Pan et al., 1997). The precise

structure of this chemokine domain is now well established; the N-terminal region contains 7 amino acids residues prior to the first cysteine residue (Cys-8), the sequence of which does not seem to be of much relevance to function (with the exception of Lys-7, see below). Following Cys-8 is a long loop, a three stranded anti-parallel β sheet (residues 24-51) and a tightly packed C-terminal α–helix (residues 56-67) (Mizoue et al., 1999); this forms a globular protein domain of approximately 3nm in diameter that is maintained by two disulphide bridges (Fong et al., 1998). Secondly, CX_3CL1 possesses a stalk segment of approximately 26nm in length (comprised of 241 amino acid residues) (Fong et al., 2000), that database comparison has identified as a mucin-like chain, defined by extensive *O*-glycosylation of serine and threonine residues in short tandem repeats of varying length (Imai et al., 1997;Fong et al., 1998). CX_3CL1 possesses a juxtamembranous dibasic arginine motif (Thr-Arg-Arg-Gln) believed to be the primary site of cleavage, and finally this protein possesses an uninterrupted stretch of 18 hydrophobic residues that form a transmembrane link to a 37 amino acid intracellular tail (Bazan et al., 1997;Pan et al., 1997).

As has been done with the receptor, CX_3CR1, mutational analysis of CX_3CL1 has identified which of these regions are the most critical for function. For example Harrison et al, using mutation of the length of the mucin-like stalk, have demonstrated that the affinity and efficacy of chemokine domain binging is independent of stalk length (Harrison et al., 2001). Cells possessing the entire mucin-line domain are more efficient at capturing leukocytes than cells possessing the chemokine domain alone (Fong et al., 2000), however it is possible that is as a result of the increased length of the protein rather than a function of the mucin-like stalk itself, as the adhesive function of CX_3CL1 is retained at full capacity when the mucin-like stalk is replaced with E-selectin (Fong et al., 2000). Additionally, CX_3CL1 with mutations of basic residues in the chemokine domain and glycosylation

consensus sequence display reduced binding potency (although those that bound retained receptor activating capabilities). Residues Lys-7 and Arg-47 were found to be of particular importance in this respect (required for receptor binding); mutation of these residues renders the protein ineffective at both binding and stimulating chemotaxis (Harrison et al., 2001). Furthermore, there is remarkable cross-species conservation in the CX_3CL1 protein; significant sequence homology is observed between all of the key domains of this protein when the sequence of the rat protein is compared to that of mice and humans, as table 4.1 below demonstrates (Nishiyori et al., 1998).

Table 4.1. Sequence homology of rat, mouse and human CX_3CL1 amino acid sequence

Rat sequence compared to…	**Mouse sequence**	**Human sequence**
Total protein	85.5% homology	66.1% homology
Chemokine domain	85.5% homology	82.7% homology
Mucin-like domain	79.9% homology	53.9% homology
Transmembrane domain	100% homology	100% homology
Intracellular domain	100% homology	91.9% homology

1.1.2. Expression

The *in vivo* expression pattern of CX_3CL1 is generally considered to be less well defined than that of the ligand's receptor, CX_3CR1 (Kim et al., 2011). Pan et al originally described *cx3cl1* gene expression to be most abundant in the brain and heart, but it was present in all other tissues tested, with the exception of peripheral blood leukocytes; expression in endothelial cells was found to be constitutive and enhanced by exposure to LPS, whilst in the brain

immunohistochemical analysis demonstrated localization of CX_3CL1 to capillary walls and microglia. Expression here was also increased by exposure to LPS and in a model of multiple sclerosis (Pan et al., 1997). However, more recently it has been determined, using *in situ* hybridization and immunohistochemical analysis, that neurons are in fact the principle CX_3CL1 expressing cells of the CNS, and microglia and endothelial cells in the brain actually show little or no expression of this protein or its mRNA (Hughes et al., 2002;Nishiyori et al., 1998;Tarozzo et al., 2003). Additionally, Schwaeble et al reported that CX_3CL1 mRNA is not increased in mouse model of multiple sclerosis (Schwaeble et al., 1998). These data supported the *in vitro* evidence provided by Maciejewski-Lenoir and colleagues; they reported that CX_3CL1 mRNA was not expressed by microglia (either constitutively or cytokine/toxin induced) but was constitutively expressed by both hypothalamic and cortical neurons (but was not increased by cytokine or toxic insult). Additionally low levels of CX_3CL1 mRNA were found in astrocytes, but this was robustly increased following exposure of these cells to the cytokines IL-1β or TNFα (Maciejewski-Lenoir et al., 1999). Consistently, Hughes et al have demonstrated minimal expression of CX_3CL1 in a small subset of astrocytes associated with blood vessels and pia mater in the dorsal hippocampus, thalamic and cortical regions that is significantly upregulated in the late stages of prion infection, but is not associated with an increase in neuronal CX_3CL1 (Hughes et al., 2002). More detailed analysis of CX_3CL1 expression in the brain reveals that expression varies between brain regions and indicates that discrete subsets of neurons expression the *cx3cr1* gene (Feng et al., 1999). Tarozzo et al used semi-quantitative PCR analysis to demonstrate high levels of CX_3CL1 mRNA expression in the cortex, hippocampus and striatum, intermediate expression within the olfactory bulb, thalamus, hypothalamus and brainstem and low levels of expression in the cerebellum. The results of a series of *in situ* hybridization studies confirmed this expression profile, as did immunohistochemical analysis; the protein was present in these locations, not just mRNA, and the

expression is, as expected, neuronal (Tarozzo et al., 2003). Furthermore, immunohistochemical studies have recently demonstrated localization of cytoplasmic glutamate containing vesicles within CX_3CL1 positive neurons, suggesting CX_3CL1 is expressed in excitatory glutamatergic neurons (Tong et al., 2000). In the spinal cord both CX_3CL1 immunoreactivity and mRNA expression are observed in spinal neurons and afferents from DRG neurons under physiological conditions, and this is not altered by the induction of a chronic pain state (Verge et al., 2004;Lindia et al., 2005).

The evidence for endothelial expression of CX_3CL1 presented by Pan et al does appear to be well supported, and indeed endothelial and epithelial cells are likely the predominant CX_3CL1-expressing cells in the periphery. In cardiac tissues CX_3CL1 is localised to cells surrounding the luminal side of coronary vessels and the endocardium lining of the ventricle chambers (Harrison et al., 1999). CX_3CL1 is also found within endothelial cells of the blood vessels in the dermis of normal human skin and in Langerhan cells of the epidermis (Papadopoulos et al., 2000;Papadopoulos et al., 1999). In small intestinal and colonic tissues, CX_3CL1 mRNA is expressed in epithelial cells; CX_3CL1 expressed by intestinal epithelial and endothelial cells is significantly upregulated during the active phase of Crohn's disease and can be upregulated in these cells by exposure to pro-inflammatory cytokines (Muehlhoefer et al., 2000).

Any controversy in the expression profile of CX_3CL1 has been quashed by the recent development of a CX_3CL1 reporter mouse. The CX_3CL1 reporter mouse was generated by Kim et al, who utilised BAC transgene generation to produce mice possessing a fluorescent reporter gene embedded in the *cx3cl1* gene, thus expressing a CX_3CL1 protein that was mCherry tagged. These mice demonstrate that CX_3CL1 (mCherry) expression in the brain almost exclusively co-localises with the

neuronal marker NeuN, and confirmed that in the steady state there is abundant expression in the hippocampus, striatum and cortex (primarily cortical layer II). Additionally, Kim et al demonstrated CX_3CL1 expression in neurons of the spinal cord (but not in $CGRP^+$ cell bodies of the DRG). Expression of CX_3CL1 in these mice is completely restricted to non-hematopoietic cells. Peripherally CX_3CL1-mCherry can be found on both alveolar and bronchial epithelial cells in the lung, tubular epithelial cells and glomeruli in the kidney and mucus secreting goblet cells of the epithelial layer in the intestinal lamina propria (Kim et al., 2011). Interestingly, within many cells CX_3CL1 appears to be present in two distinct cellular compartments, being expressed diffusely on the plasma membrane as well as in a punctuate juxtanuclear compartment. CX_3CL1 exists in equilibrium between these compartments, being actively recycled as required. The juxtanuclear compartment shares features with recycling endosomes; CX_3CL1 expressed here co-localises with VAMP-3 and syntaxin-13, the luminal pH is approximately 6.3 and addition of brefeldin-A causes the compartment to collapse (Liu et al., 2005). The cytoplasmic tail of CX_3CL1 is recognised as the region of the protein critical for facilitating the internalization of the protein; two adaptor protein-2 (AP-2) binding motifs are found here and their mutation results in decreased CX_3CL1 internalization. The process of internalization is both dynamin and clathrin dependent; inhibition of the function of these proteins by the addition of targeted siRNAs prevents CX_3CL1 endocytosis (Huang et al., 2009). Endosomal recycling of CX_3CL1 occurs constitutively and has been hypothesised to serve three main purposes: providing a mechanism by which the protein can be rapidly down-regulated, protecting pre-synthesised CX_3CL1 from degradation and to expose CX_3CL1 to intracellular ADAMs (a disintegrin and metalloproteases domain; enzymes responsible for the cleavage of CX_3CL1), allowing intracellular cleavage and accumulation of CX_3CL1 to allow accelerated exocytosis of the chemokine domain to enhance chemotaxis (Liu et al., 2005;Huang et al., 2009). Additionally, the majority of CX_3CL1 located at the plasma membrane is clustered; BRET

analysis demonstrates that CX_3CL1 is able to behave as an aggregating protein which enhances the proteins ability to capture leukocytes, as well as allowing the establishment of a gradient for chemotaxis (Hermand et al., 2008;Proudfoot et al., 2003). Aggregation of chemokines for this purpose is quite normal; however whilst most soluble chemokines accomplish this by binding sulphated glycosaminoglycans in the extracellular matrix and on the surface of endothelial cells, the clustering behaviour of CX_3CL1 is unique in that it is the transmembrane domain of the protein that is critical for the process (Proudfoot et al., 2003). Whilst the precise sequence responsible is not known, knowledge of the clustering behaviours of other proteins that aggregating via a transmembrane domain suggests a combination of a glycine motif, leucine zipper and/or a phenylalanine dimer interface are likely responsible (Hermand et al., 2008).

1.1.3. Cleavage/Shedding

CX_3CL1 exists and functions as both a membrane bound and soluble chemokine (likely in several forms due to cleavage by different proteases), with the latter being produced by the enzymatic cleavage of the chemokine domain of the former by the metalloproteases ADAM10 and ADAM17 and the cysteine protease Cathepsin S (Clark et al., 2011).

Cathepsin S (CatS) is a lysosomal enzyme of the papain family of cysteine proteases and was first purified from bovine lymph nodes (Turnsek et al., 1975) as a single chain molecule with a molecular weight of approximately 24kDa (Kirschke et al., 1986). CatS falls into the endopeptidase family of proteases as it catalyses the hydrolysis of peptide bonds within a polypeptide chain (as opposed to exopeptidases which cleave at the N or C terminus of the polypeptide) and is expressed by epithelial cells (Beers et al., 2005) as well as by antigen presenting cells including macrophages and microglia, where its secretion is enhanced by a number of pro-inflammatory

mediators including cytokines (Liuzzo et al., 1999a;Liuzzo et al., 1999b) and is likely P2X7 dependent (Clark et al., 2010). CatS has been strongly implicated in antigen presentation, however this is by no means its only function and several pieces of evidence have been presented to suggest CatS is responsible, at least in part, for the cleavage of neuronal CX_3CL1 in the spinal cord. Our laboratory has previously observed that the intrathecal administration of both CatS and soluble CX_3CL1 are similarly pro-nociceptive, and that a CX_3CL1 neutralizing antibody is able to prevent the development of mechanical hyperalgesia and microgliosis induced by CatS (Clark et al., 2009;Clark et al., 2007b).

The shedding of soluble CX_3CL1 from endothelial and epithelial cells is both constitutive and inducible, and the metalloproteases ADAM-10 (a disintegrin and metalloproteases domain-10) and ADAM-17 (a disintegrin and metalloproteases domain-17, also known as TACE; tumor necrosis factor-α converting enzyme) play a key role in this process. Constitutive shedding of the soluble chemokine domain of CX_3CL1 has been demonstrated to be predominantly ADAM-10 dependent; an inhibitor of both ADAM-10 and ADAM-17 blocks both inducible and constitutive shedding/cleavage of soluble CX_3CL1 *in vitro*, however a preferential ADAM-10 inhibitor reduced constitutive shedding only. Additionally, over-expression of ADAM-10 in endothelial cells enhances constitutive cleavage, which is believed to play a role in the regulation of leukocyte recruitment adhesion under steady state conditions, as specific ADAM-10 inhibition results in increased monocyte adhesion and prevents de-adhesion of bound cells (Hundhausen et al., 2003;Hundhausen et al., 2007). Inducible shedding, on the other hand, is thought to be ADAM-17 dependent. Inducible shedding generally refers to the enhanced shedding of soluble CX_3CL1 observed following incubation of CX_3CL1 expressing cells with the phorbol ester PMA, which has been repeatedly demonstrated to increase the soluble CX_3CL1 content of the media of treated

cells. In a similar fashion to the experiments used to determine ADAM-10 as the metalloproteinase responsible for constitutive cleavage, the use of ADAM-17 specific inhibitors has demonstrated this protease to be able to reduce inducible shedding only and no PMA induced shedding occurs in CX_3CL1 transfected ADAM-17/TACE$^{-/-}$ cells. Additionally, it is thought that the activity of ADAM-17 is dependent on the presence of divalent cations, as the addition of EDTA to cell media decreases CX_3CL1 shedding (Garton et al., 2001;Tsou et al., 2001). Interestingly, it also seems that ADAM-10 and ADAM-17 may cleave CX_3CL1 at different locations; ADAM-10 cleaves CX_3CL1 at a dibasic juxtamembrane sequence (Thr-Arg-Arg-Gln) (Bazan et al., 1997), however mutation of the arginine residues to alanine has no effect on PMA induced shedding of CX_3CL1; the CX_3CL1 cleavage site of CatS has not yet been determined and it's likely that soluble CX_3CL1 exists in several forms (Garton et al., 2001;Tsou et al., 2001). It should be noted that ADAM-10 and ADAM-17 are able to cleave proteins other than CX_3CL1, TNFα for example, however a full review of ADAM-10/17 activity is beyond the scope of this introduction.

1.1.4. Function and Contribution to Disease

The majority of functions of CX_3CL1 are discussed in chapter three in terms of the function of CX_3CL1-CX_3CR1 interactions; membrane bound (full length) CX_3CL1 is primarily responsible for the capture and adhesion of leukocytes, while soluble (cleaved) CX_3CL1 establishes a chemotactic gradient and activates leukocytes via CX_3CR1. Additionally, the interaction between CX_3CL1 and CX_3CR1 is critical for the survival of CX_3CR1^{high} monocytes via the activation of the anti-apoptotic factor Bcl2. The contribution made by this receptor-ligand interaction to a number of pathologies has also been discussed, thus here only the involvement of CX_3CL1 in inflammation and pain are discussed here due to their association with cell infiltration and pain related to the data presented.

1.1.4.1. Inflammation

Inflammation is a complex protective response to harmful stimuli elicited by injury or infection that serves to destroy, dilute or provide a barrier against the damaging agent. It is characterised by the development of hyperalgesia (dolor), heat (color), redness (rubor) and swelling (tumor). On a more discrete level it involves a number of biological processes including increased blood flow and dilatation and increased permeability of blood vessels, the exudation of fluid and the migration of leukocytes. The process of acute inflammation is typically initiated by cells present in the affected tissue, such as tissue resident macrophages or dendritic cells that, when activated, release a host of pro-inflammatory mediators such as cytokines, chemokines, bradykinin, histamine and NO that contribute to the development of the characteristic biological responses. Chemokines, or chemoattractant cytokines, as their name suggests act as a chemoattractant for infiltrating leukocytes, in particular monocyte/macrophages.

Like other chemokines, CX_3CL1 acts as a chemoattractant during inflammation, but also plays a key role in the process by which recruited cells transmigrate into inflamed tissues (see below). With CX_3CL1 playing such a vital role in recruitment of cells critically involved in the inflammatory process, it is of no surprise that CX_3CL1 has been suggested to contribute to a variety of inflammatory conditions. In fact upregulation of CX_3CL1, be it the mRNA or actual protein, has been observed in inflammatory conditions affecting almost all organs of the body: in the endometrial foci of endometriosis patients (Bellelis et al., 2013), in the lung fibroblasts of chronic obstructive pulmonary disease (COPD) patients (Dagouassat et al., 2013), in the conjunctiva in a rodent model of toxic ocular surface inflammation (Denoyer et al., 2012), in the plasma and tissues of animals experiencing septic shock (Raspe et al., 2013), in the serum of patients with acute pancreatitis (Uchida et al., 2013), in synovial fibroblasts of rheumatoid arthritis (RA) patients

(Jones et al., 2013) and in atheroma and smooth muscle cells of patients and rodents with arthrosclerosis (Gan et al., 2013;Lucas et al., 2003). Indeed tissue specific changes in CX_3CL1 mRNA expression have been suggested as a diagnostic marker for diseases associated with chronic inflammation (Mehta et al., 2012). CX_3CL1 largely contributes to inflammation and pathogenesis by recruiting monocyte/macrophages which in turn release a host of inflammatory mediators; as mentioned previously coronary artery disease patients with increased plasma levels of CX_3CL1 have elevated numbers of CX_3CR1^+ cells and therapies that reduce this (increase in of CX_3CR1^+ cells) are effective at treating the condition (Damas et al., 2005). Furthermore, the blockade of CX_3CR1^+ cell recruitment in a model of renal failure dramatically reduces fibrosis and increases function (Feng et al., 1999;Oh et al., 2008). Monocyte/macrophages are by no means the only cell type influenced by $CX_3CL1/R1$ under inflammatory conditions; in patients with allergic asthma and rhinitis soluble CX_3CL1 levels are increased and notably contribute to the recruitment of $CD4^+$ T-lymphocytes (Rimaniol et al., 2003). Furthermore both CX_3CL1 and CX_3CR1 have been detected on a variety of cell types (including monocyte/macrophages, T-helper cells and dendritic cells) within the joints of rheumatoid arthritis patients (D'Haese et al., 2010;D'Haese et al., 2012).

This wealth of evidence for a pro-inflammatory and pro-pathogenic action of CX_3CL1 suggests compounds blocking both the synthesis and release of CX_3CL1 or its signalling via CX_3CR1 are likely to be advantageous in the treatment of many chronic inflammatory conditions; indeed this certainly seems to be the case as CX_3CR1 knock-out animals show reduced pathology in models of inflammatory diseases. For example $CX_3CR1^{-/-}$ mice show reduced atherosclerotic plaque formation compared to $CX_3CR1^{+/+}$ controls (Lesnik et al., 2003). Furthermore, administration of an anti-CX_3CL1 or anti-CX_3CR1 antibody attenuates leukocyte adhesion to inflamed endothelial cells or atherosclerotic lesions (Schulz et al., 2007).

1.1.4.2. Pain

If we examine CX_3CL1 in the context of pain, we find it to be pro-nociceptive; intrathecal administration of soluble CX_3CL1 causes mechanical allodynia and thermal hypersensitivity (Sun et al., 2013;Clark et al., 2007b;Milligan et al., 2004;Milligan et al., 2005a). Similarly injection of CX_3CL1 in the PAG region of the brain, an area of that plays a key role in the descending modulation of pain, is also pro-nociceptive (Chen et al,. 2007). The administration of an anti-CX_3CL1 antibody attenuates the pain behaviours of both neuropathic and arthritic animals (Clark et al., 2007b;Clark et al., 2012). The central expression of CX_3CL1 is substantially upregulated in models of arthritis (Yang et al., 2012), in some cases *de novo* expression in astrocytes is observed (Lindia et al., 2005), and compounds that are able to reduce CX_3CL1 expression are analgesic (Yang et al., 2012). As the above mentioned anti-CX_3CL1 antibodies are given intrathecally, in these instances it is neuronal CX_3CL1 in the CNS that is contributing to pain; we can also determine that it is soluble rather than membrane bound CX_3CL1 that is pro-nociceptive as the intrathecal administration of the irreversible CatS inhibitor LHVS attenuates pain to a similar degree as an anti-CX_3CL1 antibody (Clark et al., 2012;Clark et al., 2007b). As expected from the expression profile of CX_3CR1, CX_3CL1 does not have a direct affect on neurons (Zhuang et al., 2007), instead following its liberation from neurons, CX_3CL1 induces nociceptive behaviours via activation of the CX_3CR1 receptor on microglia, stimulating the activation of p38 MAPK-mediated pathways (this release is assumed based on the anti-nociceptive effects of blockers of CX_3CL1 signalling) (Clark et al., 2007b;Zhuang et al., 2007) and the release of a variety of pro-nociceptive mediators, including IL-1β, IL-6 and NO (Milligan et al., 2005b), that are able to sensitise neurons e.g. the induction of a hyper-responsive state in wide dynamic range neurons in the spinal cord (Owolabi and Saab, 2006).

Conversely, Holmes et al have demonstrated an anti-nociceptive effect of CX_3CL1 in the periphery; pre-injury intraneural injection of CX_3CL1 attenuated neuropathic pain related behaviours in a spared nerve injury model, and CX_3CR1 knock-out mice were reported to show more pronounced allodynia than wild-types in the same model (Holmes et al., 2008); however these observations were made at a single time point and used a considerably higher dose than is required in the spinal cord to cause hypersensitivity (400ng vs 30ng (Holmes et al., 2008;Clark et al., 2007b)). This data might suggest a striking difference between the relationship between CX_3CL1 and pain centrally and peripherally, however evidence from a recent human study suggests the contribution of CX_3CL1 to pain may not be solely a central effect; unstable angina pectoris, partially defined as experiencing ischemic chest pain, is associated with elevated serum levels of CX_3CL1 (Yao et al., 2011). So what is responsible for this pronounced difference? In a recent review from our laboratory, we suggested this may be the result of a mouse strain variation; it has previously been demonstrated that mouse strains vary in their sensitivity to pain, and in fact the specific strain used by Holmes and colleagues (Balb/c) has been shown to have a significantly lower microglial response to CNS injury than C57Bl/6 mice typically used (Clark et al., 2011;Mogil et al., 1999a;Mogil et al., 1999b;Kigerl et al., 2006).

Whilst considering the suitability of CX_3CL1 and CX_3CR1 as targets for the development of analgesics it is important to consider the protective effects of the interaction between these two proteins; in the brain CX_3CL1-CX_3CR1 interaction certainly seems to be neuroprotective in models of both amyotrophic lateral sclerosis (ALS) and Parkinson's disease (Cardona et al., 2006), and in a cohort of ischemic stroke patients higher plasma CX_3CL1 levels were associated with better survival outcome at a six month assessment point (Donohue et al., 2012). Peripherally this interaction is critical for many homeostatic processes including the survival of CX_3CR1^{high}

monocyte/macrophages, wound healing and cell transmigration for immune surveillance, thus when developing analgesics that target this interaction it might be worth considering either a centrally acting compound or a compound such as a CatS inhibitor that targets the shedding of soluble CX_3CL1 leaving the membrane bound CX_3CL1 intact.

1.2. The endothelium, adhesion molecules and the transmigration of leukocytes

1.2.1. Endothelial function and the transmigration of leukocytes

The endothelium lines the entire vascular system and is composed of a monolayer of endothelial cells linked together by adhesive structures or cell to cell junctions (tight junctions, adheren junction and gap junctions (Michiels, 2003). A versatile and multifunctional organ, the endothelium acts as a semi-permeable barrier as well as having many synthetic and metabolic functions, including the regulation of thrombosis and thrombolysis, regulation of platelet adhesion, modulation of vascular tone and regulation of immune and inflammatory responses (via the control of immune cell trafficking). Endothelial cells produce and release several vaso-active substances (e.g. prostacyclin and NO) that cause vasodilation and inhibit the adhesion and aggregation of platelets; these substances are released in response to a range of chemical stimuli as well as changes in hemodynamic forces such as alterations in blood pressure. Additionally these cells can be activated by stimuli, including thrombin and histamine, which cause a shift towards a pro-thrombotic/pro-proliferative/vasoconstricting phenotype (Sumpio et al., 2002).

The rapid migration of leukocytes from the vasculature to a target tissue is an essential process in the normal function of the immune system. The migration of these cells is commonly initiated

through the local generation of inflammatory mediators, such as chemokines, that induce circulating cells to being the process of leukocyte-endothelial adhesion. The process, shown in figure 4.2, begins with the adhesion of leukocytes to the endothelium; a process that involves tethering and rolling of leukocytes captured from the blood stream. This leads to firm attachment of leukocytes and subsequent transmigration.

Whilst leukocytes are able to migrate under both physiological and pathophysiological conditions, the interaction of resting endothelial cells with leukocytes is minimal, as under these conditions endothelial cells sequester leukocyte interactive proteins such as P-selectin (and chemokines) in specialised secretory vesicles (Weibel-Palade bodies), and the transcription of several important adhesion molecules such as E-selectin, VCAM-1 and ICAM-1 is suppressed (Pober and Sessa, 2007). The activation of the endothelium can occur in two ways: type I activation, a rapid process occurring independently of changes in gene expression, and type II activation, a slower response that is dependent on the alteration of gene expression. Type I activation is typically mediated by ligand-dependent activation of G-protein coupled receptors, such as histamine receptors (H1), typically coupled to G-α_q proteins (Pober and Cotran, 1990), the activation of which leads to the activation of phospholipase C (PLC) and subsequent release of Ca^{2+} from intracellular stores (Pober and Sessa, 2007). A rise in intracellular calcium in endothelial cells in this way contributes to a number of functions of the cells, but plays an especially important role in leukocyte recruitment. Calcium dependent activation of myosin light chain initiates the exocytosis of Weibel-Palade bodies, thus moving leukocyte interactive proteins (e.g. P-selectin) to the luminal surface of the cell (Birch et al., 1994;Birch et al., 1992). Type II activation is a more persistent form of endothelial

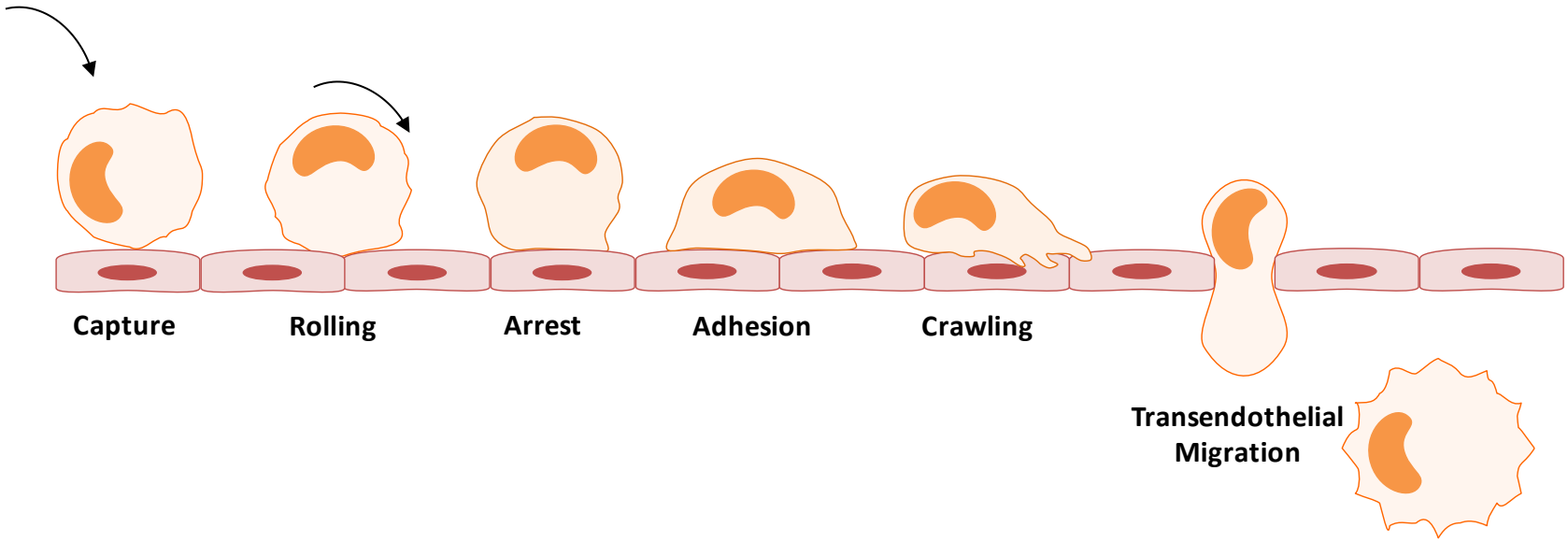

Figure 4.2. The leukocyte transendothelial migration pathway. This simplified schematic shows the various stages of leukocyte migration through the endothelium. The capture and rolling of leukocytes is mediated by selectins; during this time the cells are activated by chemokines expressed on the endothelial surface. The leukocytes then undergo an arrest step and subsequent firm adhesion to the endothelium which is mediated by integrins and supersedes crawling before the final process of migration occurs (adapted from (Ley et al., 2007)).

activation than type I, and is typically mediated by TNFα or IL-1β derived from activated leukocytes. The activation of TNF receptor 1 (TNFR1) and the IL-1 receptor (IL-1R) by these cytokines results in the activation of downstream signalling pathways that ultimately lead to the activation of transcription factors that stimulate the transcription and translation of new genes/proteins. As with type I activation, type II activation of endothelial cells contributes to many of the functions of these cells, but in terms of leukocyte recruitment it triggers the increased expression of a number chemokines and leukocyte adhesion molecules, such as E-selectin, ICAM-1 and VCAM-1, on the luminal surface of the cell (Pober and Sessa, 2007;Collins et al., 1995).

The capture, tethering and rolling of leukocytes to the endothelium is mediated by the weak and reversible interactions of selectins (McEver et al., 1995). These adhesive transmembrane glycoproteins are a family of three molecules each with an N-terminal Ca^{2+}-dependent lectin domain, an EGF domain, a transmembrane domain and a cytoplasmic tail. L-selectin is expressed constitutively on the surface of most leukocytes, P-selectin is rapidly mobilised from secretory granules in endothelial cells, and E-selectin is expressed on endothelial cells under the transcriptional regulation of inflammatory mediators. Selectins bind to sialylated and fucosylated oligosaccharides, the terminal components of glycoproteins expressed on both leukocytes and endothelial cells (Cines et al., 1998). E-selectin binds preferentially to ESL-1 (E-selectin ligand-1), whilst L- and P-selectin bind preferentially to PSGL-1 (P-selectin glycoprotein ligand-1). Under inflammatory conditions, when all three selectins are present, they work cooperatively to allow leukocyte rolling by binding reversibly to their ligands; this slows down leukocytes which facilitates the binding of chemokines and lipid autocoids on the surface of endothelial cells with their receptors on leukocytes. These mediators transduce signals that cooperate with those produced

by activated leukocytes interacting with selectins (Weyrich et al., 1995) to enable the expression and activation of integrins on the surface of the cells (Cines et al., 1998).

The firm adhesion of leukocytes to the activated endothelium is primarily mediated by three integrins: LFA-1 ($\alpha_L\beta_2$/CD11a), Mac-1 ($\alpha_M\beta_2$/CD11b) and VLA4 ($\alpha_4\beta_1$); LFA-1 is the predominant integrin for lymphocyte emigration, Mac-1 for neutrophils adhesion and VLA4 is the predominant integrin expressed on monocytes (although they also constitutively express LFA-1) (Hynes, 1992;Stewart et al., 1995). LFA-1 has the highest affinity for the endothelial ligand ICAM-2 (intercellular adhesion molecule-2); however it can also bind ICAM-1 (intercellular adhesion molecule-1) which is the primary endothelial ligand of Mac-1. The constitutive expression of ICAM-1 is low expression but shows significant up-regulation following the exposure of the endothelium to inflammatory cytokines (Klein et al., 1995;Scholz et al., 1996). Similar to the ICAMs is VCAM-1 (vascular cell adhesion molecule-1), an Ig like protein also found on the surface of cytokine-activated endothelial cells, that selectively binds β_1-integrins, i.e. VLA4 (Pober and Cotran, 1990). Additionally the interaction of integrins can cause leukocyte-induced clustering of ICAM-1 and VCAM-1 at the leukocyte-endothelial cell interface that serves as a platform for firm adhesion (Barreiro et al., 2008;Nourshargh et al., 2010). The transendothelial migration of leukocytes is also mediated by integrins. This process requires continuous cycles of adhesion and detachment; new adhesive contacts form at membrane protrusions at the leading edge of the cell, whilst at the rear of the cell integrins are down-regulated. Chemokines and shear stress promote the formation of these membrane protrusions (filopodia); the expression of integrins here is high and it is thought that the cell uses these filopodia to crawl along the endothelial layer in search of emigration sites (Nourshargh et al., 2010). Furthermore, the interaction of integrins with their ligands causes a rise in calcium in endothelial cells, which activates myosin light chain kinase and subsequently causes

contraction of the cell, promoting the passage of the leukocyte (Michiels, 2003). The migration of leukocytes across the endothelium at cell-cell junctions is also in part regulated by platelet/endothelial cell adhesion molecule-1 (PECAM-1/CD31) which is expressed on both leukocytes and endothelial cells. Evidence suggests that a homophilic interaction between leukocyte PECAM-1 and endothelial PECAM-1 guides leukocytes through endothelial junctions (Muller, 2003;Nourshargh et al., 2006) and contributes to the enhanced expression of leukocyte integrins (Dangerfield et al., 2002;Wang et al., 2005). Blockers of PECAM-1 suppress leukocyte transmigration through cytokine stimulated endothelial cells *in vitro* (Muller et al., 1993) and suppress leukocyte accumulation in the inflamed peritoneum of rats (Vaporciyan et al., 1993), suggesting this protein does indeed contribute to leukocyte migration. However observations made in a PECAM-1 knock-out mouse have failed to find a significant deficit in this process (Duncan et al., 1999).

As well as mediating the activation of integrins, some chemokines can also directly mediate the arrest of leukocytes. Soluble chemokines, such as CXCL8 and CCL2, bind to heparin sulphate on the surface of endothelial cells and become immobilised, providing a site for leukocyte adhesion (Weber et al., 1999;Michiels, 2003). Furthermore the membrane bound chemokine CX_3CL1, expressed on endothelial cells, is able to cluster, enhancing this proteins ability to capture leukocytes (Hermand et al., 2008;Proudfoot et al., 2003). CX_3CL1 might aid leukocyte adhesion though VCAM-1, suggesting co-operation between tethering and adhesion molecules (Kerfoot et al., 2003).

1.2.2. Endothelial dysfunction following chemotherapy

The endothelium is a dynamic organ that responds to a variety of stimuli by undergoing activation. This process is critical for the maintenance of homeostasis; but also allows the endothelium to contribute to the pathogenesis of vascular disease. Indeed endothelial dysfunction, the shift towards a chronically activated state, is associated with most forms of cardiovascular disease, including atherosclerosis, coronary artery disease and diabetes (Endemann and Schiffrin, 2004). For example, in atherosclerosis the morphologically abnormal endothelium is dysfunctional and contributes to the propagation of atherosclerotic lesion formation via several mechanisms, including the enhanced recruitment of monocytes that subsequently differentiate into foam cells (Ross, 1993;McGorisk and Treasure, 1996).

Several cardiovascular complications of chemotherapy have been identified; these include acceleration of coronary artery disease, cardiomyopathy and congestive heart failure. Experimental studies have suggested potential mechanisms to account for these complications and include the dysfunction or damage of endothelial cells (Daher and Yeh, 2008). The treatment of patients with 5-fluorouracil, for example, is associated with acute cardiac toxicity and venous thromboembolic disease. It has demonstrated that this chemotherapeutic agent decreases endothelial cell DNA synthesis and increases prostacyclin release in a fashion consistent with endothelial cell injury (Cwikiel et al., 1996) and inhibits VEGF-induced tubule formation in endothelial cells as well as angiogenesis (Basaki et al., 2001;Drevs et al., 2004). Bevacizumab, a monoclonal antibody against VEGF used for the treatment of a variety of solid tumors, is associated with the worsening of hypertension in patients as well as an increased incidence of both arterial and venous thrombosis (Gordon and Cunningham, 2005;Kabbinavar et al., 2003). Indeed, mice specifically deficient in endothelial VEGF show progressive endothelial degeneration

and apoptosis, as well as diffuse vascular thrombosis that led to organ failure and death (Lee et al., 2007). Bevacizumab-associated thrombotic events are hypothesised to occur as a result of this endothelial disruption, which leads to exposure of the extracellular matrix, platelet activation and reduced levels of thrombomodulin and NO (also thought contribute to bevacizumab-associated hypertension) (Verheul and Pinedo, 2007;Kamba and McDonald, 2007). Cisplatin treatment is associated with coronary ischemia, delayed onset hypertension and left ventricular hypertrophy (Berliner et al., 1990;Daher and Yeh, 2008); whilst the mechanism by which this occurs is not yet known, case-reports of coronary spasm suggest abnormal function of cardiovascular tissue contributes (Doll et al., 1986;Daher and Yeh, 2008). Furthermore, in rats the administration of microtubule disrupting agents such as VCR is associated with cardiotoxicity that manifests as development of vascular endothelial lesions comprised of apoptotic cells (Tochinai et al., 2013). In an *in vitro* setting VCR inhibits VEGF secretion and this is hypothesised to contribute to the cardiotoxicity seen *in vivo* (Avramis et al., 2001).

1.3. The TRPA1 Receptor

1.3.1. TRPA1 structure

The TRP (transient receptor potential) group of proteins is a large family of ion channels that share several characteristics: a six transmembrane domain structure with a pore loop between the fifth and sixth transmembrane segments, and permeability to cations. Despite these structural similarities the TRP channels are a diverse family displaying a wide array of cation selectivities and specific activation mechanisms. The TRP channels contribute to responsiveness to all major classes of external stimuli inducing light, sound, chemical, temperature and touch, as well as providing individual cells with the ability to detect changes in the local environment. Within the TRP super-

family, the channels are divided into seven subfamilies that include five group 1 TRP channels: TRPA, TRPC, TRPM, TRPN (not found in mammals) and TRPV, and two group 2 TRP channels: TRPML and TRPP. The separation of the two groups is based on sequence and topological differences and the subfamilies are named based on the name of the original receptor described in that subfamily, i.e. TRPV1 (transient receptor potential vanilloid-1) which is activated by the inflammatory vanilloid compound capsaicin. The mechanism through which a TRP channel is activated generally cannot reliably be predicted based on its subfamily assignment, however the recurring theme amongst the TRP channels is that they are activated through a diverse range of mechanisms, which a single receptor often responding to a variety of stimuli (Venkatachalam and Montell, 2007).

TRPA1 (transient receptor potential ankyrin-repeat-1) is the only known member of the TRPA subfamily and gains its name due to its possession of a series of N-terminal ankyrin repeats, as shown in figure 4.3. It was first identified in a screen for genes down-regulated following the oncogenic transformation of fibroblasts (Jaquemar et al., 1999), although the effects of the classical TRPA1 agonist, mustard oil, were described much earlier than the receptor itself (Koltzenburg and McMahon, 1986). The gene encoding this protein spans 55.7kbp of the human chromosome 8q13 and has been highly conserved across species for around 500 million years (Nilius et al., 2012;Kang et al., 2010). The *trpa1* gene encodes an 1100 amino acid protein of approximately 120kDa that comprises, as expected, six transmembrane segments with a putative ion permeable site located between transmembrane segments five and six. The long N-terminal domain contains up to eighteen ankyrin repeat domains formed of 33 amino acids that are thought to be involved in protein-protein interaction and channel trafficking to the membrane;

deletion of these domains negatively affects insertion of the channel into the membrane (Nilius et al., 2012).

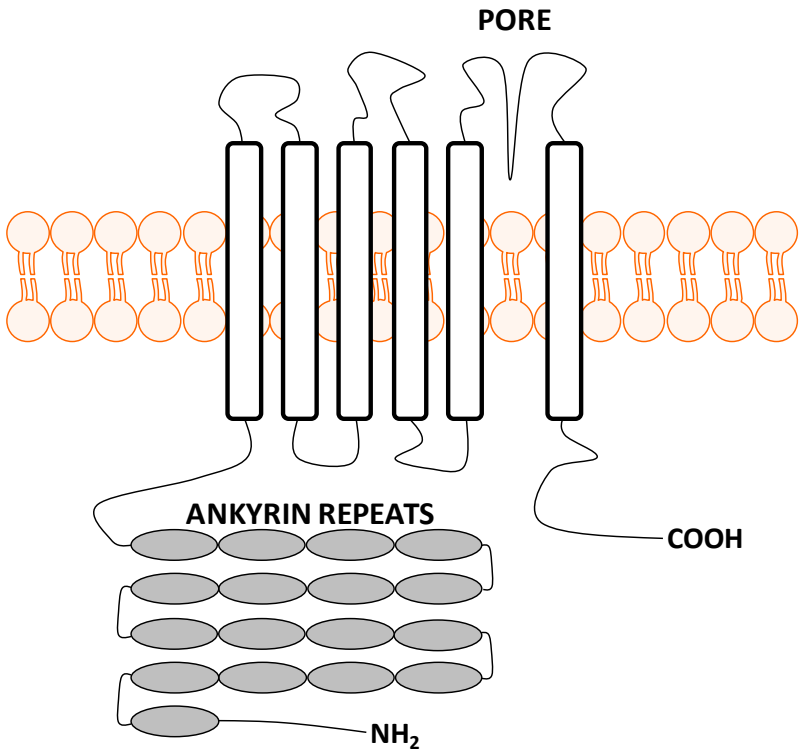

Figure 4.3. Schematic representation of the TRPA1 receptor. The TRPA1 receptor is comprised of six transmembrane domains, represented by the rectangular bars. Between the fifth and sixth transmembrane domains lies the pore domain. At the N-terminal end of the protein are a series of ankyrin repeat domains, represented by the grey ovals; it is these that give the TRPA1 receptor its name.

Site-directed mutagenesis studies have identified cysteine and lysine residues in the N-terminal domain as critical for the covalent bonding of agonists and subsequent activation of the receptor (Hinman et al., 2006;Macpherson et al., 2007). Additionally TRPA1 possesses a number of Ca^{2+} binding sites and an EF hand motif (helix-loop-helix structure) that allow Ca^{2+}-dependent activation of this receptor (Doerner et al., 2007;Zurborg et al., 2007). Whole cell-patch clamp

studies have revealed that TRPA1 activates quite slowly following ligand binding; likely a reflection of the need for the agonist to penetrate the cell membrane to reach the intracellular agonist binding site (Macpherson et al., 2007;Koivisto, 2012). Recently Karashima and colleagues used advanced electrophysological techniques to predict a pore diameter for TRPA1 of at least 11A with a relative basal P_{Ca}/P_{Na} of around 5 that increases to approximately 9 in the presence of an agonist, indicating this ion channel possesses a relatively large pore with higher calcium permeability than most other TRP channels (Karashima et al., 2010).

1.3.2. TRPA1 expression

Within the nervous system TRPA1 activation is associated with pain; TRPA1 was originally described as a nociceptive channel and can be found on small myelinated Aδ and unmyelinated C fibres with their cell bodies in the dorsal root and trigeminal ganglion. Approximately 25% of TRPA1 containing neurons are peptidergic and release substance P and CGRP; however generally TRPA1 is expressed in neurons that also express the nerve growth factor (NGF) receptor TrkA and the heat and capsaicin sensitive ion channel TRPV1 (Story et al., 2003;Bautista et al., 2007;Nagata et al., 2005;Nilius et al., 2012). Quantification of TRPA1 positive neurons indicates that under normal conditions TRPA1 is expressed by approximately 55% of TRPV1 positive neurons, but that this can be increased to approximately 80% by treatment with NGF (Kobayashi et al., 2005;Diogenes et al., 2007). Additionally there is likely a small population of TRPA1 positive neurons that are not TRPV1 positive, as a small population of TRPA1 positive neurons have been identified that do not respond to the TRPV1 agonist capsaicin (Salas et al., 2009). Recent evidence, however, indicates that TRPA1 expression is not confined to sensory neurons. TRPA1 is also found extensively in the brain; it is found in the hippocampus, neurons of the nucleus supraopticus and in the brain stem (Nilius et al., 2012). Furthermore, this ion channel has been found in other

neuronal tissues including sympathetic neurons (Andrade et al., 2008) such as the vagal fibres innovating the heart, where TRPA1 contributes to vasovagal reflexes (Pozsgai et al., 2010) and in the pelvic nerve innovating the colon where activation of TRPA1 contributes to the inhibition of contractility (Poole et al., 2011).

Additionally TRPA1 expression has been observed outside of the nervous system. In the cardiovascular system TRPA1 is found in endothelial cells concentrated at myo-endothelial junctions; here its activation contributes to endothelium-dependent smooth muscle cell hyperpolarization and vasodilatation, thus contributing to the maintenance of vascular tone (Earley et al., 2009;Yanaga et al., 2006;Andrade et al., 2012). TRPA1 is expressed in the epithelial cells of a number of structures in the urinary tract in both rodents and humans (Nagata et al., 2005;Streng et al., 2008;Gratzke et al., 2010), and is up-regulated in patients with outlet obstruction (Du et al., 2007); furthermore the intravesicular administration of TRPA1 agonists can cause urinary bladder over-activity (Du et al., 2007;Streng et al., 2008). The TRPA1 receptor is expressed in synovial cells responsible for maintaining the integrity of synovial tissue (Kochukov et al., 2006), in odontoblasts where it is hypothesised to contribute to the transmission of external stimuli signals to nearby nerves (El Karim et al., 2011;Byers, 1984), and is expressed by endocrine cells of the gastrointestinal (GI) tract where it contributes to serotonin release and subsequent modulation of GI motility (Kellum et al., 1999;Gershon, 2003;Nozawa et al., 2009). As well as being found in the nerves innovating the skin, TRPA1 is also expressed in non-neuronal skin cells such as keratinocytes and fibroblasts, where its activation mediates the secretion of eicosanoids (Jain et al., 2011) and induces an increase in proliferation related growth factors and inflammatory cytokines, suggesting a role in the proliferation of keratinocytes and skin inflammation (Atoyan et al., 2009).

1.3.3. TRPA1 Activation

TRPA1 is primarily activated chemically with a variety of compounds that occur naturally, such as allyl isothiocyanate (AITC; mustard oils), cinnamaldehyde and allicin (garlic oil extract) (Bautista et al., 2013). It should be noted that several of these naturally occurring compounds that are able to activate TRPA1 are also able to activate other TRP channels, mainly members of the TRPV family. For example mustard oil has recently been observed to activate mouse and human recombinant TRPV1 as well as TRPV1 in sensory neurons (Everaerts et al., 2011). Additionally TRPA1 can be activated by menthol and icillin, chemicals that induce a cooling sensation; this has lead to the proposition that TRPA1 is able to act as a cold receptor (Story et al., 2003). Indeed, when exogenously expressed *in vitro* TRPA1 is activated by noxious cold (<17^{o}C) (Story et al., 2003;Bandell et al., 2004), however the examination of the phenotype of TRPA1 knock-out mice regarding noxious cold sensation remains controversial (see below). More recently a number of synthetic drugs were identified as activators of TRPA1; these include the inhalational anaesthetic isoflurane (Matta et al., 2008), the antipsychotic chlorpromazine (Hill and Schaefer, 2007) and antifungal and antiprotozoal drug clioquinol (Andersson et al., 2009). Additionally the TRPA1 receptor can act as a sensor for environmental irritants and pollutants including, but not limited to, acrolein and α,β-unsaturated aldehyde that is present in tear gas, vehicle exhaust and smoke (Andrade et al., 2012). Emerging evidence has implicated that TRPA1 can also be activated by the endogenous products of metabolism and oxidative stress; a large number of reactive oxygen species (ROS) including those that cause cysteine oxidation and/or disulfide formation, reactive nitrogen species (RNS) that cause S-nitrosylation and reactive carbonyl species (RCS) are all potential TRPA1 activators (Takahashi et al., 2008;Nilius et al., 2012;Andersson et al., 2008). These products of oxidative stress directly activate TRPA1 due to their electrophilic properties; the activation of TRPA1 by electrophilic compounds results in large inward currents and the

abolishment of outward currents, whereas following activation with non-electrophilic compounds this receptor demonstrates predominantly outward rectification (Nilius et al., 2012;Andrade et al., 2012). The induction of inward currents is a result of the electrophilic modification of N-terminal cysteine residues of the protein that results in the dilation of the pore. The products of oxidative stress are produced as a result of an imbalance of the production and neutralization of oxidative substances, and the interaction between them and TRPA1 is an important mechanism for detecting tissue damage under inflammatory conditions.

Due to the expression of TRPA1 on sensory neurons, this receptor has been implicated in both mechanotransduction and the transmission of cold sensitivity, especially at noxious thresholds. TRPA1 knock-out mice show deficits in the sensation of noxious punctuate mechanical stimuli (Kwan et al., 2006), as well as deficits in the mechanosensory function of nociceptors in the pelvic and splanchnic nerves which contribute to the maintenance of GI motility (Brierley et al., 2009). In models of gastric distension the up-regulation of TRPA1 is accompanied by visceral hypersensitivity which can be attenuated by the administration of a selective TRPA1 antagonist (Yang et al., 2008;Kondo et al., 2009). The contribution of TRPA1 to the transmission of cold sensitivity is more controversial. Two separate knock-out animals have been developed; whilst in both instances the portion of the gene knocked out was the same (a sequence encoding a region between the fifth and sixth transmembrane domains required for ion conduction), Bautista et al working with one knock-out have reported normal responses to cold temperatures *in vivo* and *in vitro* (Bautista et al., 2006), whilst Kwan et al working with a second knock-out have reported that these mice have a significant deficit in cold sensation (Kwan et al., 2006). This deficit has been confirmed by a second group using this same mouse; $TRPA1^{-/-}$ mice showed longer latencies for

paw withdrawal from a 10°C (noxious) stimulus than wild-type litter mates and cold hypersensitivity induced by methanol was absent in these animals (Gentry et al., 2010).

Due to its role in the transmission of noxious stimuli, and its activation by a number of irritants and products of tissue damage, TRPA1 has been suggested as a viable target for the development of analgesics for both inflammatory and neuropathic pain. Following the induction of an inflammatory injury (intraplantar CFA), TRPA1 mRNA is up-regulated at sites distant to the original injury, such as the DRG; this is associated with increased sensitivity to noxious cold (hyperalgesia) that, interestingly, cesses to occur as TRPA1 expression returns to pre-injury levels (da Costa et al., 2010;Obata et al., 2005). Additionally the development of both cold and mechanical hyperalgesia can be prevented in the CFA inflammatory model by the systemic administration of the selective TRPA1 antagonists AP-18 and HC-030031 (da Costa et al., 2010;Petrus et al., 2007;Eid et al., 2008), and in models of inflammatory arthritis TRPA1 knock-out mice showed a reduction in the development of mechanical hyperalgesia (Fernandes et al., 2011). It should be noted that TRPA1 does not appear to contribute to the inflammatory process itself, rather it contributes to nociceptive transmission; the inflammatory components of these models, such as articular inflammation, mononuclear cell infiltration and bone erosion are not reduced in TRPA1 knock-out mice (Fernandes et al., 2011), but TRPA1 antagonists are able to reduce the response of wide dynamic range neurons to noxious pinch and decrease the spontaneous firing of neurons in arthritis-inflamed rats (McGaraughty et al., 2010). The mechanism by which TRAP1 is upregulated in these inflammatory states is thought to be NGF-p38 MAPK dependent; p38 MAPK is activated by noxious cold and sensitizes TRPA1 causing, in turn, TRPA1-dependent hyperalgesia (Obata et al., 2005). NGF is one of many growth factors found to be upregulated in peripheral tissues in response to injury (Malin et al., 2006;Stucky et al., 2009).

In a similar fashion to that of an inflammatory injury, the expression of TRPA1 is elevated by nerve injuries that result in the development of neuropathic pain, for example spinal nerve ligation, where the over-expression of TRPA1 is essential for the development of cold hyperalgesia (Obata et al., 2005). However rather than occurring in the DRG that corresponds to the damaged nerve, TRPA1 is up-regulated in nearby uninjured DRG, suggesting a compensatory effect (Katsura et al., 2006). The increased expression of TRPA1 mRNA following nerve injury does correspond to an increase in function protein; TRPA1 protein is over-expressed in Aδ fibres and its pharmacological antagonism attenuates cold hyperalgesia caused by nerve injury without altering noxious cold sensitivity in uninjured animals (Chen et al., 2011;Ji et al., 2008).

1.3.4. TRPA1 in chemotherapy pain

Following incubation with cisplatin or oxaliplatin cultured DRG neurons show an increased expression of TRPA1, in a pattern similar to the increase in expression of this receptor observed in the trigeminal ganglia of cisplatin treated mice (Ta et al., 2010). Additionally oxaliplatin is able to induce calcium responses in TRPA1 transfected cells CHO cells (Nassini et al., 2011) and the mechanical and cold allodynia occurring as a result of bortezomib, PTX or oxaliplatin treatment are attenuated in TRPA1 knock-out mice (Trevisan et al., 2013) or by blockade of the receptor with the TRPA1 antagonist HC-030031 (Nassini et al., 2011;Materazzi et al., 2012). Interestingly the ability of chemotherapeutics to activate TRPA1 may not be direct, rather they may occur as a result of an increase in reactive oxygen species that in turn activate the TRPA1 receptor; oxaliplatin or cisplatin induced and increase in intracellular calcium levels in TRPA1 transfected CHO cells are ablated by the addition of the anti-oxidant ROS scavenger glutathione (Nassini et al., 2011). Peroxynitrite is increased in nervous tissues of animals receiving PTX, and the reduction of superoxide production

by the administration of an NADPH-oxidase inhibitor attenuates chemotherapy induced mechanical allodynia (Doyle et al., 2012), as does the administration of the anti-oxidant acetyl-L-carnitine (ALC) (Flatters et al., 2006;Ghirardi et al., 2005a;Ghirardi et al., 2005b) . These studies have led to the suggestion that targeting either TRPA1 or reactive oxygen species are likely to be beneficial in reducing the pain related behaviours that develop following chemotherapy (Materazzi et al., 2012;Nassini et al., 2011;Trevisan et al., 2013;Flatters et al., 2006;Doyle et al., 2012).

1.4. Chapter aims

The attenuation of mechanical allodynia by the CatS inhibitor LHVS and in CX_3CR1 knock-out mice establishes a role for CX_3CL1 signalling in the development and/or maintenance of chronic pain following nerve injury. Additionally an association of this chemokine with leukocyte transendothelial migration has been discussed, and an association between treatment with chemotherapeutic agents and endothelial dysfunction has been suggested. Here we hypothesise that VCR activates endothelial cells, which is associated with the increased expression of adhesion molecules and the chemokine CX_3CL1. Furthermore, we hypothesise that CX_3CL1 activates monocytes as they transmigrate across the endothelium, causing them to release pro-nociceptive mediators; thus, the aims of this chapter are:

- To establish the effect of inhibiting CX_3CL1 cleavage on the development of VCR-induced mechanical allodynia in mice.
- To determine the effect of VCR treatment of the protein expression and morphology of endothelial cells *in vivo* and *in vitro*.
- To determine the effect of CX_3CL1 treatment on the production of pro-nociceptive mediators from monocyte/macrophages.
- To ascertain the suitability of TRPA1 as a therapeutic target for the prevention of VCR-induced painful peripheral neuropathy.

2. Methods

2.1. Induction of vincristine induced painful peripheral neuropathy and drug treatment

2.1.1. Animals

Unless otherwise stated, all experiments were performed using adult male C57Bl/6 mice (22-27g; 10-14 weeks from Harlan UK or bred in house), in accordance with The Animals Scientific Procedures Act (ASPA) 1986, United Kingdom Home Office regulations and institutional guidelines. Animals were individually housed (to prevent aggressive behaviour) on a 12 hour light / 12 hour dark cycle at 21-22^{o}C, with food and water *ad libitum*.

2.1.2. Generation and breeding of CX_3CL1-mCherry mice

To produce experimental CX_3CL1-mCherry heterozygous mice, an original breeding stock of CX_3CL1-mCherry homozygous mice ($CX_3CR1^{mCherry/mCherry}$) was kindly gifted to us by Dr Steffen Jung (Weizmann Institute of Science). The original CX_3CR1-mCherry mice were generated using a RedET recombination system to replace the first exon of the *cx3cl1* gene with a gene encoding a monomeric *mcherry* reporter gene. The desired transgene was extracted and injected into fertilised CB6F1 oocytes to establish transgenic mice. These were then back-crossed onto a C57Bl/6 background for a minimum of 8 generations. $CX_3CL1^{mCherry/mCherry}$ homozygous mice were mated with wild-type C57Bl/6 mice to produce heterozygous ($CX_3CL1^{+/mCherry}$) offspring (Kim et al., 2011). Litters were weaned at 21 days and group housed (up to 5 per cage) in single sex cages. Both male and female animals were used for behavioural studies from ten weeks old, at which time they were singly housed and allowed to acclimatise to their new cage for one week.

2.1.3. Generation and breeding of TRPA1$^{-/-}$ mice

An experimental cohort of TRPA1$^{-/-}$ mice was kindly gifted to us by Professor Stuart Bevan; these mice were breed from heterozygous breeding pairs provided by Dr Kelvin Kwan and Dr David Corey (Harvard Medical School). The original TRPA1$^{-/-}$ mice were generated by the insertion of a targeting vector (containing an internal ribosomal entry site and a placental alkaline phosphatase gene [IRES PLAP]) into the exon encoding the pore domain of TRPA1. To prevent the production of a truncated TRPA1 product an endoplasmic reticulum retention signal and stop codon were inserted upstream of the IRES PLAP cassette; this results in the deletion of the pore-forming region and renders the channel non-conducting. This newly created vector was transfected into murine embryonic stem cells. These were subsequently injected into blastocysts to generate germ-line chimeric mice that were then mated with wild-type C57Bl/6 mice to generate heterozygous (TRPA1$^{+/-}$) offspring (Kwan et al., 2006). Breeding pairs were then established to produce offspring of various genotypes (homozygous wild-type [TRPA1$^{+/+}$], heterozygous [TRPA1$^{+/-}$] and homozygous knock-out [TRPA1$^{-/-}$]) in a ratio of 1:2:1. Litters were weaned at 21 days and group housed (up to 5 per cage) in single sex cages. Animals were used for behavioural studies from ten weeks old, at which time they were singly housed and allowed to acclimatise to their new cage for one week. Both male and female animals were used, with wild-type littermates serving as a control.

2.1.4. Vincristine induced painful peripheral neuropathy

VCR neuropathy was induced as previously described in chapter two; briefly VCR (Sigma, UK) was dissolved in sterile saline and 0.5mg/kg was injected into the peritoneal cavity (intraperitoneally [i.p.]), using a 30G needle, daily for five days per cycle, for one or two cycles, as shown in figure 4.4 below.

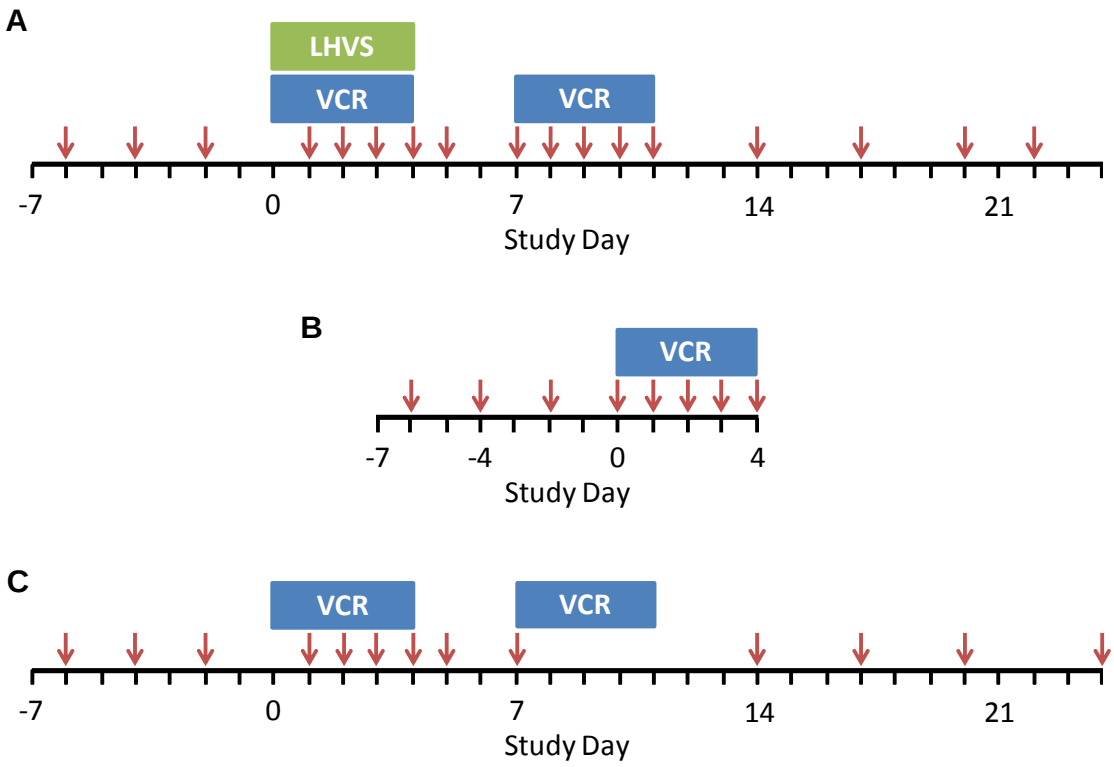

Figure 4.4. Experimental schedule for behavioural assessment and drug dosing. Blue boxes represent cycles of VCR treatment, green boxes represent cycles or LHVS treatment and red arrows represent study days behavioural phenotype was assessed. Behavioural tests were performed approximately 1 hour after dosing. **(A)** LHVS study. **(B)** CX_3CL1-mCherry study. **(C)** $TRPA1^{-/-}$ study.

2.1.5. Cathepsin S inhibitor (LHVS) treatment

The irreversible Cathepsin S inhibitor LHVS (morpholinurea-leucine-homophenylalanine-vinyl sulfone-phenyl [NeoMPS Inc, USA]) was dissolved in sterile saline containing 20% cremophor (v/v) and 30mg/kg was injected into the peritoneal cavity (intraperitoneally[i.p.]), using a 30G needle,

twice daily (am and pm) for five days one hour prior to VCR treatment, as shown in figure 4.4A above. [Performed by Tom Pitcher].

2.2. Behavioural testing

2.2.1. Assessment of mechanical sensitivity

Mechanical sensitivity was assessed as described in chapter two. Data are expressed as 50% paw withdrawal threshold, in grams, calculated using the method described by Dixon (Dixon 1980).

2.2.2. Assessment of cold sensitivity

Cold sensitivity was assessed as described in chapter two. Data are expressed as withdrawal latencies in seconds. [Performed by Clive Gentry].

2.2.3. Statistical analysis of behavioural data

Statistical analysis behavioural data was carried out on raw data, using SigmaPlot 12.0 software (Systat Software Inc, UK). Data are shown as mean ± standard error of the mean (SEM) and analysed by two-repeated measures analysis of variance (ANOVA) followed by Tukey post-hoc test. A p value of less than 0.05 ($P<0.05$) was considered significant (*), less than 0.01 ($P<0.01$) moderately significant (**) and less than 0.001 ($P<0.001$) highly significant (***).

2.3 Genotyping

2.3.1. Ear biopsy and DNA extraction

Ear biopsies and DNA extraction were performed as described in chapter three.

2.3.2. CX3CL1-mCherry PCR

A single PCR reaction was performed for each DNA sample. A PCR reaction master mix was made for each allele (wild-type and knock-out) consisting of 3mM $MgCl_2$ (Promega, UK), 20% (v/v) 5x reaction buffer (Promega, UK), 100µM dNTP (Promega, UK), 50 units/ml Taq DNA polymerase (Promega, UK) and 0.1µM forward and reverse oligonucleotide primer (Sigma, UK). The forward and reverse oligonucleotide primers had the sequences 5'CCAGCCGCGAGTGACTAC 3' and 5' CCCCAGGGAGATGCAGTC 3' respectively. Each reaction consisted of 2µl of 1:10 diluted DNA and 23µl of PCR master mix. The PCR reaction was performed in a TC412 Flexigene thermal cycle (Techne, UK) with an initial denaturation step of 95^{o}C for 5 minutes, followed by 34 cycles with a denaturation at 94^{o}C for 30 seconds, annealing at 60^{o}C for 30 seconds and polymerisation at 120^{o}C for 30 seconds. This was then followed by a final extension step at 72^{o}C for 5 minutes. The expected sizes of the end products were 300bp for the wild-type CX3CL1 gene and 1000bp for the CX3CL1-mCherry gene.

2.3.3. Gel electrophoresis and band visualisation

To visualise the PCR products a gel electrophoresis was performed. Post- PCR samples were loaded onto, and run down, a 2% agarose gel containing 100µg/ml ethidium bromide (Sigma, UK), at 100V for 25 minutes using a Power Pac 200 (BioRad, UK). A 1kb DNA ladder was also run down each gel to allow for the sizes of the products to be easily determined. The gels were viewed using a GeneGenius system (Syngene, UK) and images collected using the GeneSnap programme (Syngene, UK). All samples from experimental and breeding animals underwent a repeat analysis to reduce the likelihood of both false positive and false negative results.

2.4. Assessment of CX_3CL1 in plasma

2.4.1. Blood collection

Approximately one hour after their last dose of VCR (or vehicle) mice were euthanised by exposure to an increasing concentration of CO_2. Using a 25G 25mm (VWR, UK) needle attached to a 1ml syringe (VWR, UK) a cardiac puncture was performed; the needle was inserted into the chest wall, at the approximate level of the diaphragm, through the sternum, and approximately 0.8ml of blood drawn. This was then transferred to a 1.5ml Eppendorf containing heparin coated beads (Sarstedt, Germany) before gently shaking. Samples were stored on ice and then centrifuged at 2000g for 20 minutes to separate plasma from cells. Plasma (supernatant) was transferred to fresh tubes and stored at -20^{o}C.

2.4.2. CX_3CL1 ELISA

CX_3CL1 content of plasma samples was assessed by ELISA using a Quantikine CX_3CL1/fractalkine ELISA kit (RnD Systems, UK) as per manufacturer's instructions. Briefly assay diluents and plasma samples or kit supplied standards (0.62-40ng/ml) or controls were added to the plate and incubated for two hours before washing. Mouse CX_3CL1 conjugate was subsequently incubated in the wells for two hours prior to further washing. Substrate solution was added to the wells and incubated, protected from light, for 30 minutes before a stop solution was added and the optical density analysed at 450nm wavelength (with wavelength correction at 540nm) using a Flexstation plate reader (Molecular Devices, USA). All standards, controls and samples were run in duplicate. Optical density for each sample was calculated by averaging the duplicate values. Statistical analysis was carried out on raw data, using SigmaPlot 12.0 software (Systat Software Inc, UK) and data are shown as mean ± standard error of the mean (SEM). Data was analysed for statistical

significance by one-way analysis of variance (ANOVA) followed by Dunnett post-hoc test. A p value of less than 0.05 ($P<0.05$) was considered significant (*), less than 0.01 ($P<0.01$) moderately significant (**) and less than 0.001 ($P<0.001$) highly significant (***).

2.5. Immunohistochemistry

2.5.1. Tissue preparation

Mice, under pentobarbital anaesthesia (Sodium pentobarbital, 200mg/ml; Euthatal; Merial Animal Health, UK), were transcardially perfused with saline solution (0.9% NaCl [VWR, UK] w/v, 0.1% heparin sodium [5000units/ml, Leo Laboratories Ltd, UK]), followed by 4% paraformaldehyde in 0.1M phosphate buffer (containing 1.5% picric acid [Sigma, UK] v/v). The sciatic nerves were exposed by an incision from knee to hip and a 15-20mm section excised. Nerves were post-fixed for 2 hours in the perfusion fixative before being cryoprotected in 20% sucrose in 0.1M phosphate buffer at $4^{o}C$ for a minimum of 72 hours. Following cryoprotection tissues were embedded in optimum cutting temperature embedding medium (OCT) (VWR, UK) and frozen in liquid nitrogen. Transverse sections of the nerve were cryostat cut (Bright Instruments, UK) at 15µm thick and thaw-mounted onto glass microscope slides (VWR, UK). Slides were stored in cryoprotectant (PBS containing 20% w/v sucrose [VWR, UK] and 30% v/v ethylene glycol [VWR, UK]) at $-20^{o}C$ until use.

2.5.2. Immunohistochemical staining

Slides were washed six times for 5 minutes in PBS and incubated over night at room temperature with a primary antibody, mouse anti-mCherry (1:500, Abcam [UK]) or goat anti-CD31 (1:500, R&D Systems [UK]), in PBS-Tx-Az. Slides were then washed three times for 5 minutes in PBS and incubated at room temperature, in the dark, with an appropriate secondary antibody (1:1000

donkey anti-mouse IgG-conjugated Alexa Fluor 546™, Molecular Probes [USA] or donkey anti-goat IgG-conjugated Alexa Fluor 488™, Molecular Probes [USA]) for 2.5-3 hours. Following three further PBS washes slides were cover-slipped with Vectashield mounting media with DAPI (Vector Laboratories, USA) and visualised under a Zeiss Axioplan 2 fluorescent microscope (Zeiss, UK).

2.5.3. Quantification of immunohistochemistry

The number of positive cells for each immunohistochemical marker was determined. Three tissue sections per animal were selected at random with experimental group blinded. The number of cells positive for the given marker was counted in the total nerve area.

2.5.4. Statistical analysis of immunohistochemical data

Statistical analysis for immunohistochemistry was carried out on raw data, using SigmaPlot 12.0 software (Systat Software Inc, UK). An average cell number per animal was calculated and subsequently a mean value for each experimental group. The groups compared to one another using a one-way analysis of variance (ANOVA) followed by Tukey post-hoc test. Group difference with a P value of less than 0.05 ($P<0.05$) was considered significant.

2.6. Culture of endothelial cells

2.6.1. Endothelial cell culture

A primary HUVEC (human umbilical vein endothelial cells) line was obtained from HPA culture collections and cultured in accordance to their guidelines. Briefly cells were maintained in endothelial cell culture media (40% DMEM, 40% HAM-12, 20% FBS [Invitrogen, UK] containing 50mg/L endothelial growth supplement [AbD Serotec, UK], 100mg/L heparin sodium [Sigma, UK]

and 1% penicillin/streptomycin [Invitrogen, UK]) at 37^{o}C and 5% CO_2 until they reached approximately 95% confluency. Cells were then passaged by removal of the media and incubation with 0.25% tyrpsin-EDTA (Invitrogen, UK) for 1 minute. An equal volume of FBS (Invitrogen, UK) was added and the resulting suspension centrifuged at 220g for 5 minutes. The supernatant was removed and the cell pellet resuspended in endothelial media before cells were plated as a 1:4 split.

2.6.2. Endothelial cell treatment

For Western blot experiments cells were plated in 6-well plates (Nunc, UK), for ELISA experiments cells were plated in 24-well plates (Nunc, UK) or for immunocytochemistry cells were plated on glass cover-slips in 24-well plates (Nunc, UK). Cells were grown to approximately 95% confluency for Western blot and ELISA experiments, approximately 90% confluency for immunocytochemistry and 75% confluency for live-dead analysis. A stock solution of VCR (1mg/ml VCR; Sigma, UK) was made by dilution of the salt in sterile PBS (Invitrogen, UK), this was subsequently diluted in endothelial cell culture media to the required concentration and cells incubated in this at 37^{o}C and 5% CO_2.

2.6.3. Live-dead assay

The Live/Dead cell viability assay (Invitrogen, UK) was performed as described in the manufacturer's guidelines. Briefly, following treatment of HUVEC cultures with VCR or 70% methanol as a positive 'dead' control, culture media was removed and the cells washed once with sterile PBS. Cells were incubated in PBS containing 1µm calcein (green) and 2µm EthD-1 (red) dyes at room temperature for 30 minutes whilst protected from light. Following incubation cell cover-

slips were mounted onto glass microscope slides, using the assay solution as a mounting medium, and the cells visualised using a Zeiss Axioplan 2 fluorescent microscope (Zeiss, UK). Five areas of the cover-slip were selected at random and an image taken at x20 magnification; these images were used for quantification by counting the total number of cells stained red (dead) and green (live). Statistical analysis of the data was performed on raw data using SigmaPlot 12.0 software (Systat Software Inc, UK). An average percentage of live cells per cover-slip (equal to one well) was calculated and subsequently an average for the treatment group per experiment. Five cover-slips per group were analysed in each culture experiment and the experiment repeated in triplicate. Data presented are mean ± SEM of each experiment; groups are compared to one another using a one-way analysis of variance (ANOVA) followed by Tukey post-hoc test. Group difference with a P value of less than 0.05 ($P<0.05$) was considered significant.

2.6.4. Endothelial cell morphology assessment

Following treatment with VCR, cells were fixed by incubation in 4% PFA solution (4% paraformaldehyde [Sigma, UK] in 0.1M phosphate buffer) for 30 minutes followed by 3 minutes in cold methanol (Sigma, UK). Following 3 washes with PBS cells were incubated in a primary antibody solution (goat anti-β-tubulin 1:200 [Sigma, UK]) for 2.5 hours followed by a 45 minute incubation in secondary antibody solution (anti-goat IgG-conjugated Alexa Fluor 488™ 1:1000 [Molecular Probes, USA]). Cover-slips were mounted onto glass microscope slides with Vectashield mounting media with DAPI (Vector Laboratories, USA) and visualised under a Zeiss Axioplan 2 fluorescent microscope (Zeiss, UK).

2.6.5. CX_3CL1 ELISA

Cells were treated with vehicle or VCR when they reached approximately 95% confluency in a total volume of 210µl. CX_3CL1 content of media samples was assessed by ELISA using a Quantikine CX_3CL1/fractalkine ELISA kit (RnD Systems, UK) as per manufacturer's instructions, and as described above. Statistical analysis was carried out on raw data, using SigmaPlot 12.0 software (Systat Software Inc, UK) and data are shown as mean ± standard error of the mean (SEM). Data was analysed for statistical significance by one-way analysis of variance (ANOVA) followed by Dunnett post-hoc test. A p value of less than 0.05 ($P<0.05$) was considered significant (*), less than 0.01 ($P<0.01$) moderately significant (**) and less than 0.001 ($P<0.001$) highly significant (***).

2.6.6. HUCEV phenotyping FACs

For these experiments use of primary HUVEC was approved by the East London & The City Research Ethics Committee (REC Ref 06/Q0605/40 ELCHA, UK). Cells were seeded into 12-well plates coated with gelatin and incubated in DMEM (Invitrogen, UK) containing 10% FBS (Invitrogen, UK) overnight until confluency was reached. HUVEC were then treated with either 10ng/ml human TNFα (R & D Systems Ltd, UK) or 10nM VCR (Sigma, UK) for 18 hours. Cells were then gently trypsinised (0.25% trypsin-EDTA [Invitrogen, UK] 1-2 minutes), re-suspended in complete Medium-199 (GE Healthcare, UK), washed and stained with either PE-conjugated ICAM-1 (clone HA58; eBioscience, UK), FITC-conjugated VCAM-1 (clone 1.G11B1; AbD Serotech, UK) or PE-conjugated CD31 (clone WB59; Biolegend, UK). Cells were incubated on ice for 30 minutes then washed twice with PBS containing 1.5% BSA (Sigma, UK) and re-suspended before analysis on a BD FACS calibur flow cytometer (Becton Dickenson, UK). [Performed by Dr Suchita Nadkarni].

2.7. Primary macrophage culture

2.7.1. Primary macrophage culture

To encourage monocyte/macrophage infiltration of the peritoneal cavity 1ml of polyacrylamide biogel beads (BioRad, UK) was injected into the peritoneal cavity of CX_3CR1 wild-type ($CX_3CR1^{+/+}$) or knock-out ($CX_3CR1^{-/-}$) mice to induced a sterile inflammation. After four days the cell infiltrate was collected by peritoneal lavage; the peritoneal cavity was flushed with 8ml of cold sterile PBS (Invitrogen, UK) containing 3mM EDTA (Invitrogen, UK) by injection into the cavity with a 25G needle, avoiding perforation of the bowel. The abdomen was gently massaged and the fluid aspirated, filtered through a 75µm nylon mesh and the cells collected on ice. Cell suspensions were centrifuged at 220g for 10 minutes and resuspended in macrophage culture medium (DMEM [Invitrogen, UK] containing 10% FBS [Invitrogen, UK] and 1% penicillin/streptomycin [Invitrogen, UK]) for seeding onto culture plates.

2.7.2. ROS Production

Macrophages from both CX_3CR1 wild-type ($CX_3CR1^{+/+}$) and knock-out ($CX_3CR1^{-/-}$) mice were seeded at 2 x 10^5 cells/well in 96-well plates (Nunc, UK) and left to adhere in RPMI-1640 media (GE Healthcare, UK) containing 10% FBS (Invitrogen, UK) at 37^{o}C for 1 hour. Cells were washed with warm PBS and incubated with freshly prepared RPMI-1640 media supplemented with 10% FBS and 60µM luminol (Sigma, UK). Macrophages were then treated with either phorbol-12-myristate-13-acetate (PMA 100ng/ml; Sigma, UK) or CX_3CL1 (recombinant mouse CX_3CL1 chemokine domain aa25-105; R&D Systems, UK). ROS production was monitored on a Novostar plate reader (BMG Labtech) at 37^{o}C. [Performed by Dr Suchita Nadkarni].

2.8. Western Blotting

2.8.1. Sample preparation

Following treatment, media was removed from cells and 130µl of lysis buffer consisting of 20 mM tris(hydroxymethyl)aminomethane (Tris- HCl [Sigma, UK]) pH 7.5; 10 mM NaF (Sigma, UK); 150 mM NaCl (VWR, UK); 1% nonyl-phenoxylpolyethoxylethanol (NP-40, Sigma, UK); 1 mM Phenylmethanesulfonyl fluoride (PMSF, Sigma, UK); 1 mM Na_3VO_4 (Sigma, UK); 10 mg/ml proteinase inhibitor (Roche, UK), was added to each well and the plates incubated on ice for 30 minutes. Using a cell scraper lysates were removed from the wells and the supernatants collected following centrifugation at 100,000g for 15 minutes at 4^{o}C. Samples were stored at -80^{o}C until use.

2.8.2. BCA protein assay

The protein concentrations of cell lysates were determined using the Pierce bicinchoninic acid (BCA) protein assay kit (Thermo Scientific, UK), performed in accordance to the instructions provided by the manufacturer and using bovine serum albumin (BSA 2mg/ml, Sigma, UK) as a standard. Briefly the two provided reagents, A (Na_2CO_3, $NaHCO_3$, BCA and $Na_2C_4H_4O_6$ in 0.1M NaOH) and B ($CuSO_4$) are mixed together in a ratio of 50:1, 200µl of the resulting solution are added to 10µl of each sample, in duplicate, in a 96-well culture plate (Nunc, Germany). Following a 30 minute incubation in the absence of light, light absorbance at 563nm was measure using a Flexstation (Molecular Devices, USA). A standard curve was generated from the BSA standards and the protein concentrations of samples calculated from this.

2.8.3. Gel electrophoresis

Equal amounts of protein were mixed with loading buffer (10% w/v SDS [Sigma, UK], 10mM β-mercaptoethanol [Sigma, UK], 20% v/v glycerol [VWR, UK], 200mM Tris-HCL [Sigma, UK] and 0.05%

w/v bromophenol blue [Sigma, UK]) in a 5:1 ratio and the protein denatured by heating to 95^{o}C for 5 minutes. Protein samples were separated on 8-12% SDS-polyacrylamide gels, alongside a complete protein marker (Fermentas, UK), in running buffer (25mM Tris-HCl [Sigma, UK], 200mM glycine [Sigma, UK], 10% w/v SDS [Sigma, UK]) at 90-100V for approximately 70-100 minutes using a PowerPac 200 (BioRad, UK).

2.8.4. Visualisation of proteins

To allow visualisation, proteins were transferred to PVDF membranes (Immobilon 0.45µm, Millipore, UK) in ice cold transfer buffer (25mM Tris-HCl [Sigma, UK], 200mM glycine [Sigma, UK], 20% v/v methanol [VWR, UK], pH7.4) at 100V for 60 minutes. Membranes were then blocked in TBS-T (tris buffered saline) containing 5% w/v non-fat dried milk at room temperature for 60 minutes, before being incubated overnight at 4^{o}C in the presence of a primary antibody, goat anti-human CX_3CL1 (1:500, R&D Systems, UK). Membranes were then incubated with the appropriate horseradish peroxidase-conjugated secondary antibody (1:2000, anti-goat HRP conjugate [Dako, UK]) at room temperature for 60 minutes. Blots were washed three times with TBS-T and twice with PBS before being developed using Amersham ECL Plus western blotting detection system (GE Healthcare, UK) and exposed to Amersham Hyperfilm ECL (GE Healthcare, UK). Blots were then scanned and the density of the protein bands quantified using Quantity-One 1D Analysis Software (BioRad, UK).

2.8.5. Membrane stripping

To allow re-probing of a loading control, western blot membranes were stripped of their initial primary/secondary/ECL complex. Membranes were incubated in stripping buffer (TBS-T containing 1% SDS and 0.1% β-mercaptoethanol) at 60^{o}C for 30 minutes before being washed under running

dH_20 for 5 minutes, washed three times in TBS-T, blocked for 60 minutes in TBS-T containing 10% non-fat dried milk and incubated in a primary antibody against GAPDH (1:500 rabbit anti-GAPDH [Sigma, UK]) and secondary antibody (1:2000, anti-rabbit HRP conjugate [Dako, UK]) as above.

2.8.6. Statistical analysis of western blot data

All densometric values were normalised to GAPDH bands, which was used to adjust for any uneven protein loading. Statistical analysis for western blots was carried out on this normalised data, using SigmaPlot 12.0 software (Systat Software Inc, UK). A mean value for each experimental group was then calculated, and the groups compared to one another using a Student's t-test. Group difference with a P value of less than 0.05 ($P<0.05$) was considered significant. Data shown are mean ± SEM.

3. Results

In chapter three we established a role for the chemokine receptor CX_3CR1 in the development of VCR-induced painful peripheral neuropathy; mice lacking this receptor show a delayed onset of pain. Here we have performed a series of experiments to determine the expression profile and role in the development of pain of this receptors ligand, CX_3CL1.

3.1. Inhibiting the cleavage of CX_3CL1's chemokine domain prevents the development of mechanical allodynia induced by VCR

A wealth of literature exists describing the relationship of membrane bound CX_3CL1 with its receptor CX_3CR1 and their role in the transmigration of monocyte/macrophage; indeed we have shown that this relationship is essential for the development of pain following VCR treatment. However it is in its cleaved form that CX_3CL1 is able to activate intracellular signalling pathways downstream of CX_3CR1. To determine the necessity for this cleavage on the development of VCR-induced mechanical allodynia we blocked this process with the irreversible CatS inhibitor LHVS. To determine the potential of this inhibitor as a prophylactic, LHVS was administered one hour prior to VCR (and again approximately 12 hours later).

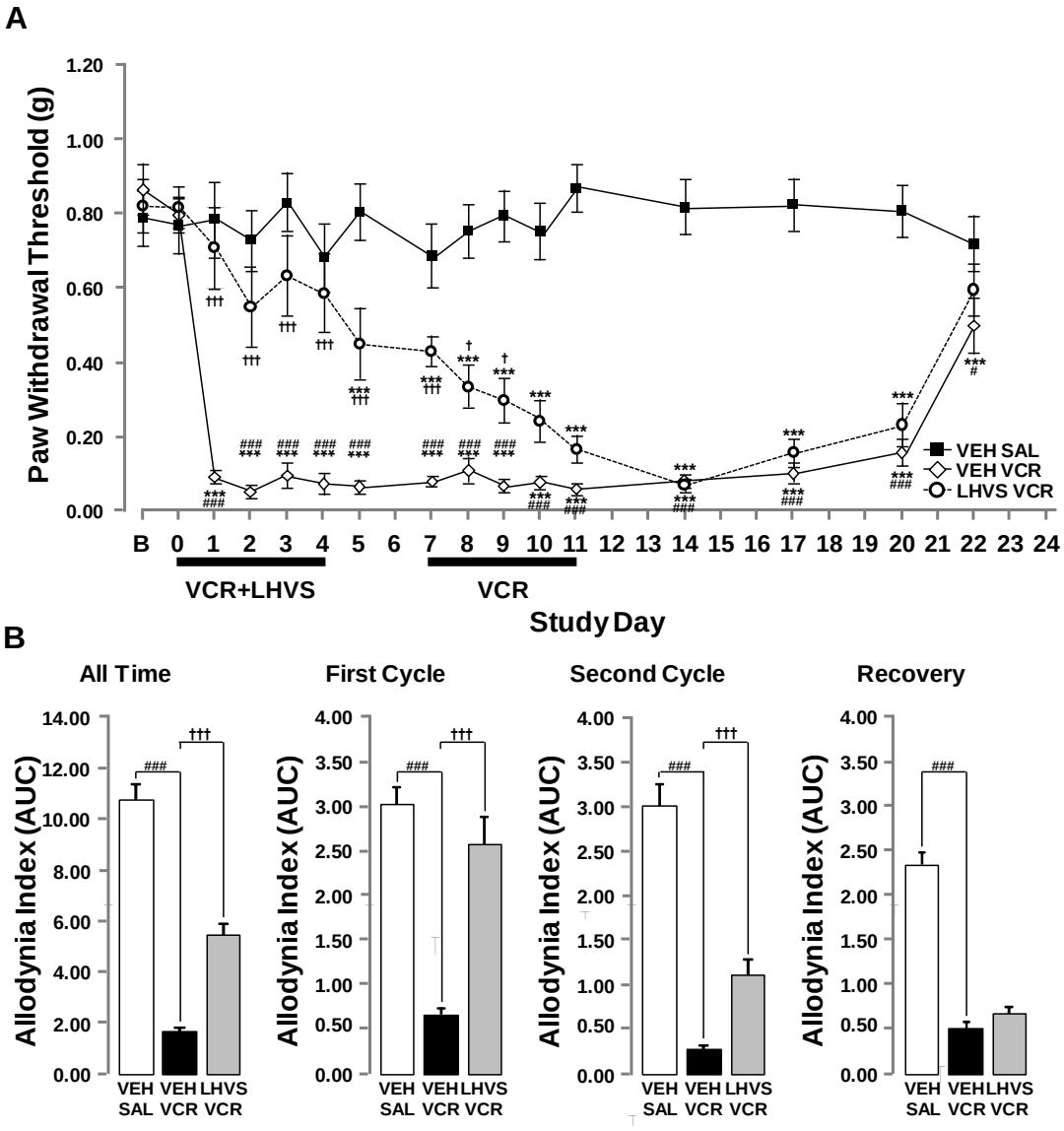

Figure 4.5. Chronic administration of a Cathepsin S inhibitor (LHVS) delays the onset of VCR-induced mechanical allodynia. Development of mechanical allodynia following *i.p.* VCR (0.5mg/kg/day; 0-4 and 7-11; black horizontal bars), when administered with twice daily *i.p.* LHVS (or vehicle). **(A)** Time course of the development of mechanical allodynia shown as 50% paw withdrawal threshold (PWT), data are mean ± SEM. N=8 per group, ***P<0.001 vs baseline threshold, ### P<0.001 vs saline threshold, ††† P<0.001 vs vehicle threshold, two-way repeated measures ANOVA with post-hoc Holm-Sidak test. **(B)** Area under the curve (AUC) analysis with data expressed as allodynia index. All time is the analysis of AUC for baseline-day 24, first cycle baseline-day 4, second cycle day 7-day 11 and recovery day 11-day 24. Data shown are mean ± SEM. N=8 per group, ### P<0.001 compared to saline threshold, ††† P<0.001 compared to vehicle threshold with One-way ANOVA analysis and Holm-Sidak post-hoc.

The data presented in figure 4.5 confirms that administration of VCR (0.5mg/kg i.p.) for five consecutive days (days 0-4; first cycle, cumulative dose 2.5mg/kg), followed by a two day pause and second subsequent cycle of treatment (five consecutive days; 7-11, cumulative dose 5.0mg/kg) was associated with significant and severe hind-paw mechanical hypersensitivity (figure 4.5A; VEH-VCR). However, mice receiving twice daily LHVS (LHVS-VCR) failed to develop significant allodynia for the first cycle of chemotherapy (figure 4.5A; LHVS-VCR), exhibiting only a 14.8% (±10.9) reduction in allodynia index (figure 4.5B; first cycle) compared to a 76.9% (±2.1) reduction in vehicle-VCR treated animals. It should be noted that the mechanical thresholds of LHVS-VCR mice are not statistically significant from those of saline-treated control animals during this first cycle.

Following the cessation of LHVS treatment, during the administration of a second cycle of VCR, these mice (LHVS-VCR) went on to develop mechanical allodynia comparable to the same extent as vehicle treated animals (figure 4.5A day 14). However the decline in mechanical threshold they experience was much more gradual than that which occurred in vehicle treated animals during the first VCR cycle, and the allodynia index of LHVS-VCR animals remains significantly higher than that of VEH-VCR mice during the second cycle; this is demonstrated by the area under the curve analysis of the second VCR cycle time-points, where a significant difference is seen in the allodynia indices of VEH-VCR and LHVS-VCR mice (figure 4.5B; second cycle). No difference between the rates of recovery was seen between these two groups. These data show that the systemic administration of a CatS inhibitor prevents the development of VCR-induced mechanical allodynia.

3.2. VCR treatment does not alter CX_3CL1 expression *in vivo*

In the periphery CX_3CL1 is constitutively expressed on endothelial cells. It has been established that spinal CX_3CL1 plays a key role in the development of neuropathic pain; inhibiting its cleavage or neutralising its action with an antibody attenuates pain behaviours in models of peripheral nerve injury. We set out to determine whether or not VCR treatment alters the level of expression of this protein on endothelial cells within the nerve, using a mouse expressing CX_3CL1 with an mCherry tag.

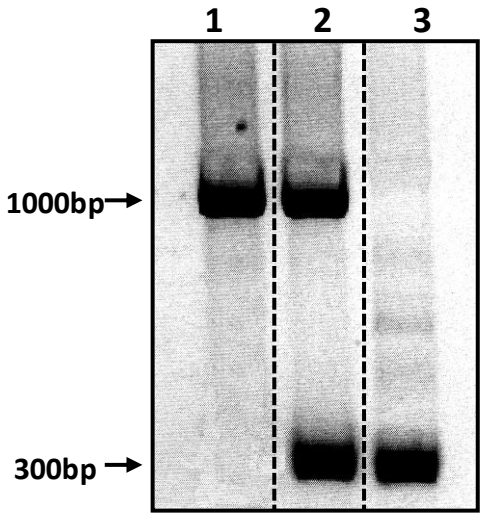

Figure 4.6. Genotyping electrophoresis of PCR samples from CX_3CL1-mCherry mice. Representative image of agarose gel following electrophoresis of PCR products with homozygous knock-in mice (lane 1) and wild-type mice (lane 3) yielding a 300bp product, yielding a 1000bp product and heterozygous mice yielding both (lane 2).

Prior to all experiments, mice were genotyped to confirm expression of wild-type CX_3CL1 protein and CX_3CL1-mCherry protein. As figure 4.6 demonstrates wild-type mice ($CX_3CL1^{+/+}$) express a

single transcript of approximately 300bp and homozygous mCherry ($CX_3CR1^{mCherry/mCherry}$) mice express a single, larger transcript of approximately 1000bp, whilst heterozygous $CX_3CR1^{+/mCherry}$ mice express one wild-type (300bp) and one mCherry transcript (1000bp). Genotyping was performed twice (to remove false positives) and only heterozygous mice selected for experimentation.

Whilst previous assessment of the function of CX_3CL1 in these mice has suggested that the mCherry tag does not affect function, we have demonstrated that the normal interaction between this protein and its receptor CX_3CR1 is critical for the development of pain in our model. Thus we first assessed the mechanical thresholds in $CX_3CR1^{+/mCherry}$ mice to ensure the mCherry expression was not influencing the function of this protein. This was indeed the case; the systemic administration of multiple VCR cycles to CX_3CL1-mCherry mice was associated with the development of severe and sustained hind-paw mechanical allodynia (figure 4.7A) with mechanical thresholds and allodynia indexes (area under curve analysis; figure 4.7B) being comparable to those of all previously tested wild-type mice (see chapter two). The maximum reduction in thresholds was also comparable to the reductions shown in wild-type ($CX_3CR1^{+/+}$) mice ($CX_3CR1^{+/mCherry}$ 98.20% ± 0.27, $CX_3CR1^{+/+}$ 98.00% ± 0.21 reduction in PWT).

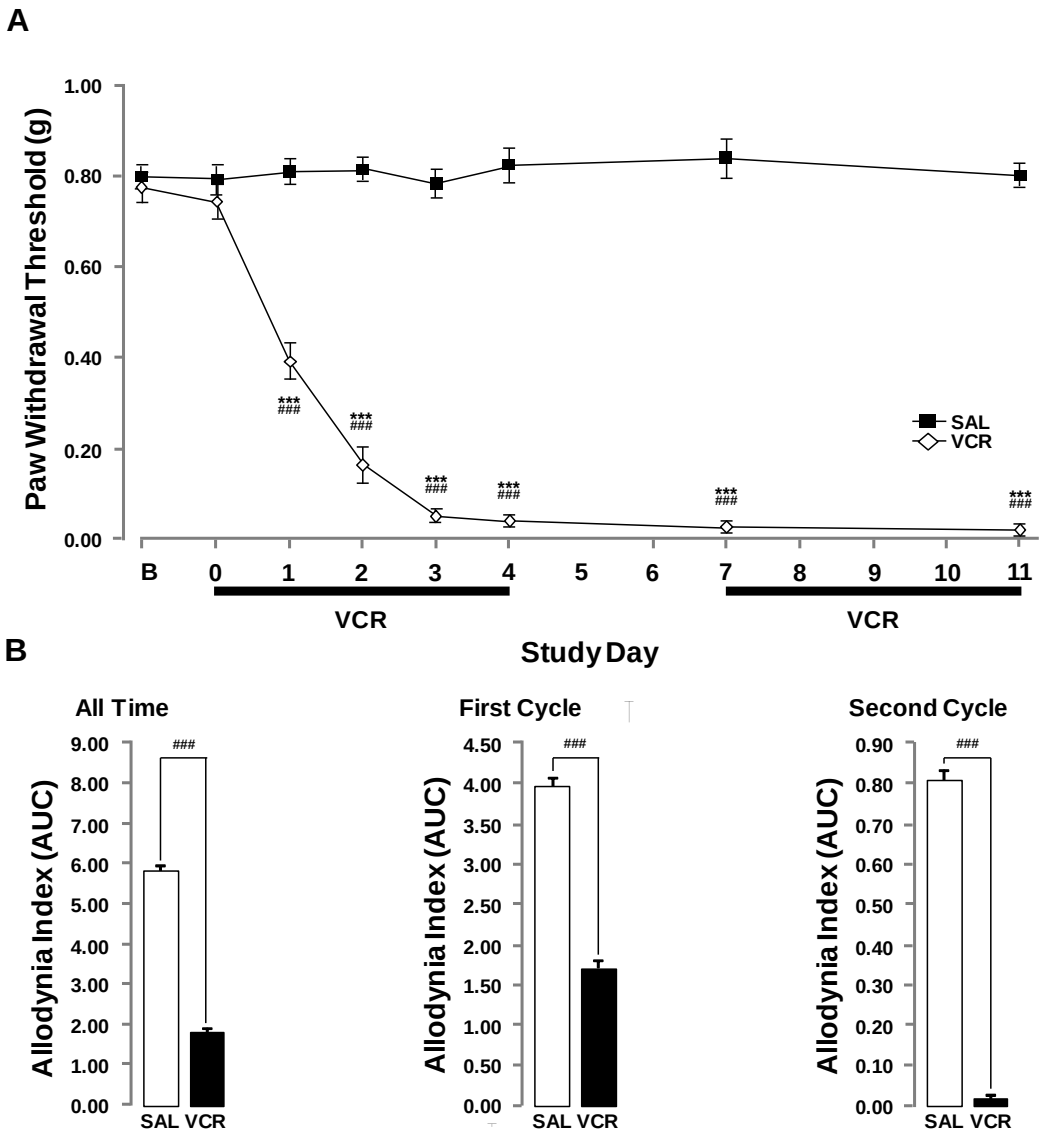

Figure 4.7. Heterozygous CX_3CL1-mCherry mice develop severe sustained mechanical allodynia following VCR treatment. Development of mechanical allodynia following *i.p.* VCR (0.5mg/kg/day; days 0-4 and 7-11; black horizontal bars). **(A)** Time course of the development of mechanical allodynia shown as 50% paw withdrawal threshold (PWT), data shown as mean ± SEM. N=8 per group, ***P<0.001 vs baseline threshold, ### P<0.001 vs saline threshold, two-way repeated measures ANOVA with post-hoc Holm-Sidak test. **(B)** Area under the curve (AUC) analysis showing data expressed as allodynia index. All time = BL-day 11, first cycle = Bl-day 4, second cycle = day 7-11. Data shown are mean ± SEM. N=8 per group, ### P<0.001 compared to saline threshold with Student's t-test.

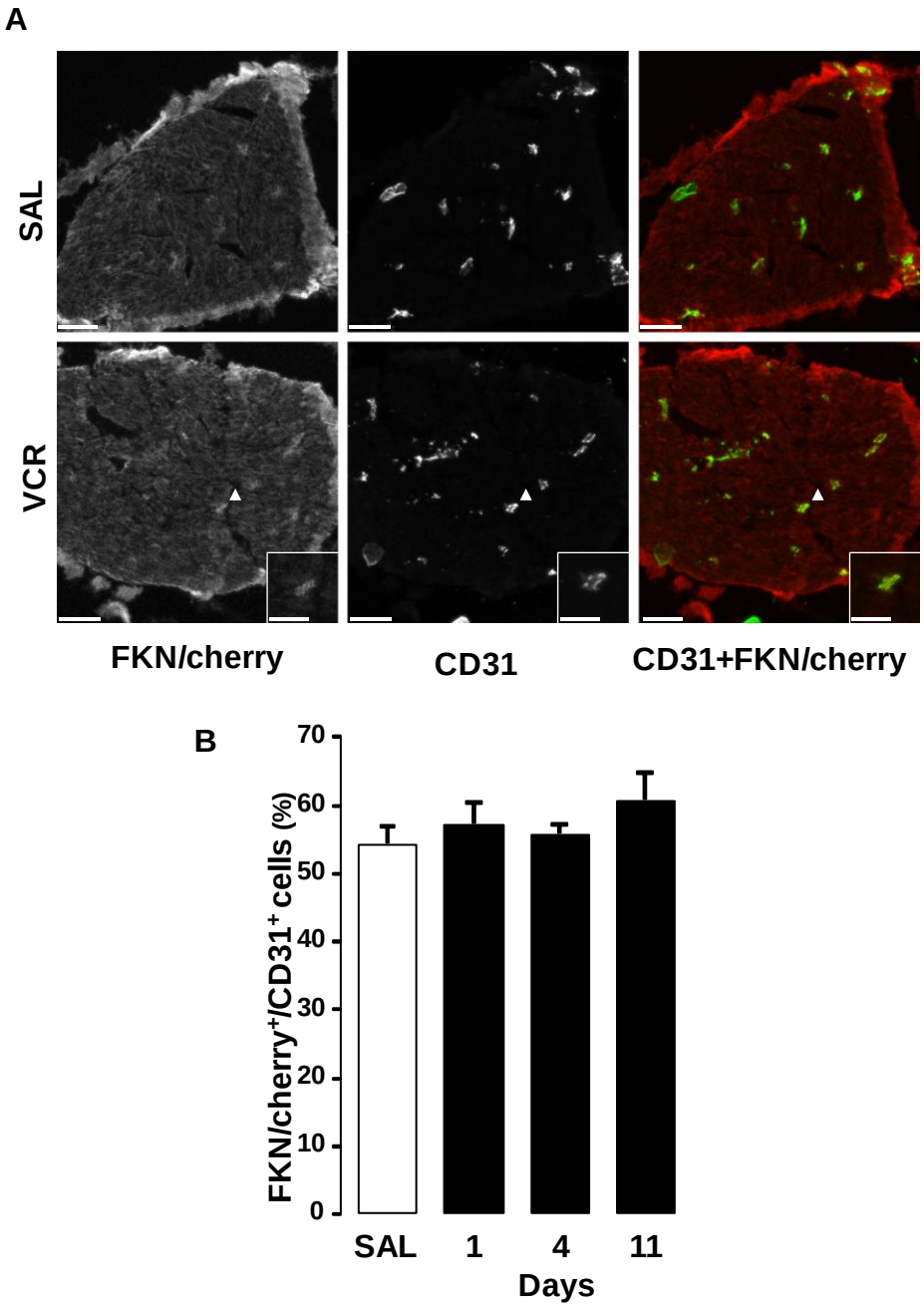

Figure 4.8. VCR administration does not alter the number of endothelial cells expressing CX_3CL1 in the nerve. (A) Representative images showing $CD31^+$ (green) and $mCherry^+$ / CX_3CL1^+ (red) cells in the (transverse) sciatic nerve in vehicle (SAL) and VCR (day 11) treated animals. Scale bars equal 100µm and 50µm in inserts. **(B)** Quantification of the number of $CD31^+$ cells that are $mCherry^+$ (CX_3CL1^+) in the whole nerve section. Data shown are mean ± SEM and N=4 per group. No significant difference found (one-way ANOVA with post-hoc Tukey test).

Using mice expressing CX_3CL1-mCherry we set out to test the hypothesis that VCR administration causes an increase in CX_3CL1 expression on endothelial cells which allows increased monocyte/macrophage transmigration; however the null hypothesis is in fact true. As figure 4.8 demonstrates, under normal physiological conditions CX_3CL1 is expressed by approximately 54% (54.07% ± 2.64) of endothelial cells found in the nerve, and whilst this trends slightly towards an increase following two cycles of VCR (Day 11; 60.62% ± 3.63) it is far from significant (P=0.319), indicating that VCR does not increase CX_3CL1 expression.

We next hypothesised that an increase in CX_3CL1 was occurring but that the protein was being subjected to an increased rate of cleavage, so was subsequently released into the blood stream, where it would act as a chemoattractant to monocyte/macrophages. Thus we used a CX_3CL1 ELISA to determine the blood plasma concentrations of CX_3CL1 in vehicle treated animals (saline) and compared this to CX_3CL1 plasma concentrations of mice following a single injection, a single cycle or two cycles of VCR (day 1,4 and 11 respectively). As figure 4.9 demonstrates no increase in plasma CX_3CL1 concentration was observed at any time point tested, confirming the observation made in endothelial cells *in vivo*, that VCR treatment does not increase CX_3CL1 expression.

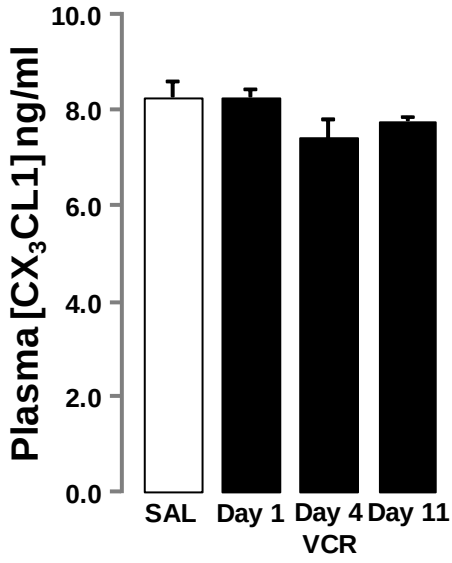

Figure 4.9. VCR administration does not alter plasma concentration of CX_3CL1. Plasma concentration of CX_3CL1 as determined by ELISA following *i.p.* VCR (0.5mg/kg/day; days0-4 and 7-11). Data shown are mean ± SEM. N=8 per group, no significant difference found (one-way ANOVA).

3.3. VCR treatment alters endothelial cell morphology and expression of adhesion molecules, but not CX_3CL1, *in vitro*

To further assess changes to endothelial cells caused by VCR we established a culture system using a primary HUVEC line. We first assessed the viability of cells treated with varying concentrations of VCR over increasing incubation times. As figure 4.9A/B demonstrates, no concentration of VCR tested had a significant impact of the viability of cells, however a reduction in the number of cells present was seen at the highest concentration tested (1000nm; figure 4.10C), albeit without a significant reduction in protein concentration of the cell lysates (figure 4.11); thus this concentration was not utilised for further experiments.

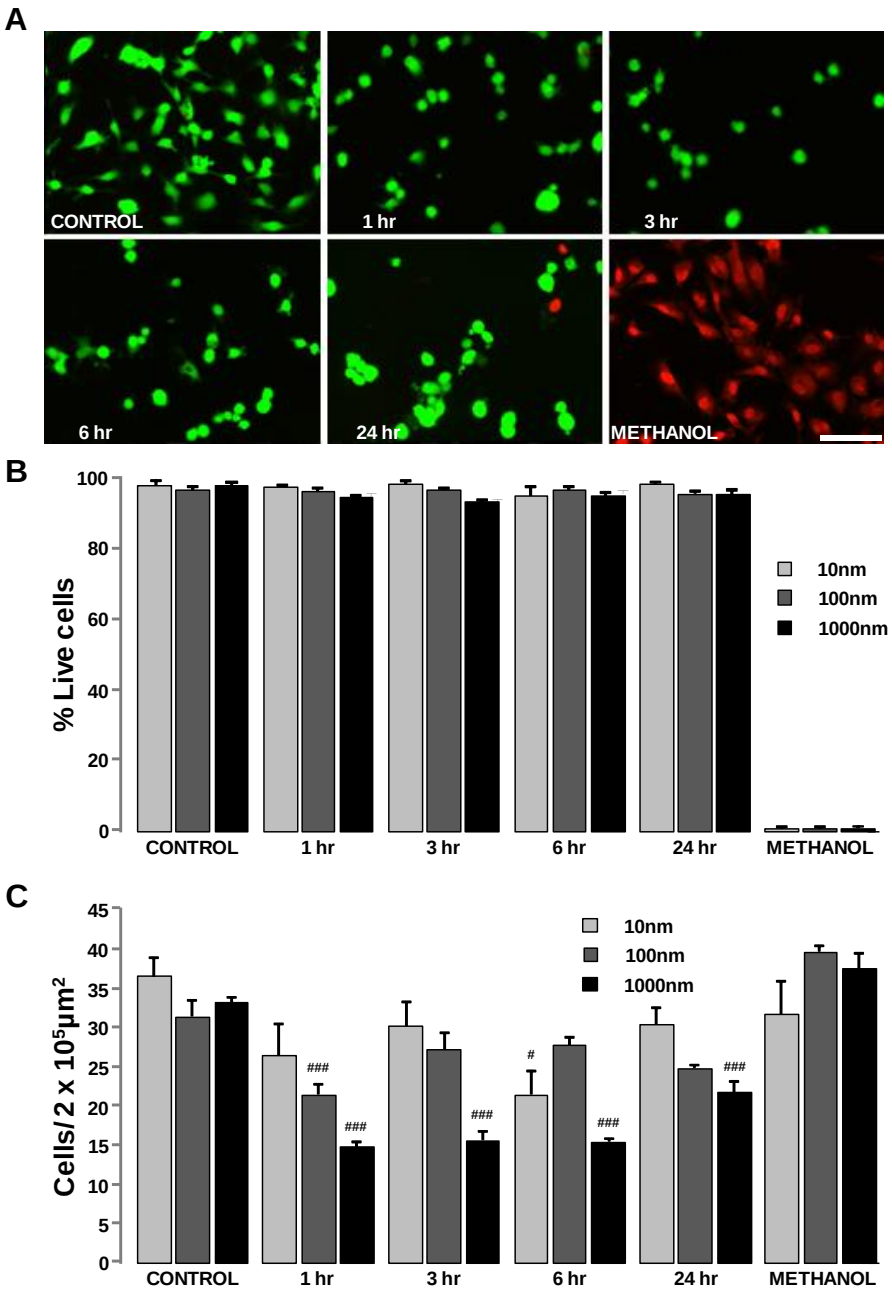

Figure 4.10. Incubation with VCR does not affect viability of endothelial cells *in vitro*. (A) Representative images showing live (green) and dead (red) HUVEC/endothelial cells following incubation in 1000nM VCR for 1-24 hours or 70% methanol (positive control). Scale bar equal 100µm. **(B)** Quantification of the percentage of live cells in each condition. Data shown are mean ± SEM and N=4 cultures. No significant difference found between VCR groups. **(C)** Quantification of the number of cells in each condition. Data shown are mean ± SEM per 2 x $10^5 \mu m^2$. N=4 cultures, two way ANOVA followed by Holm-Sidak post-hoc. ***P<0.001, *P<0.05 vs. control condition.

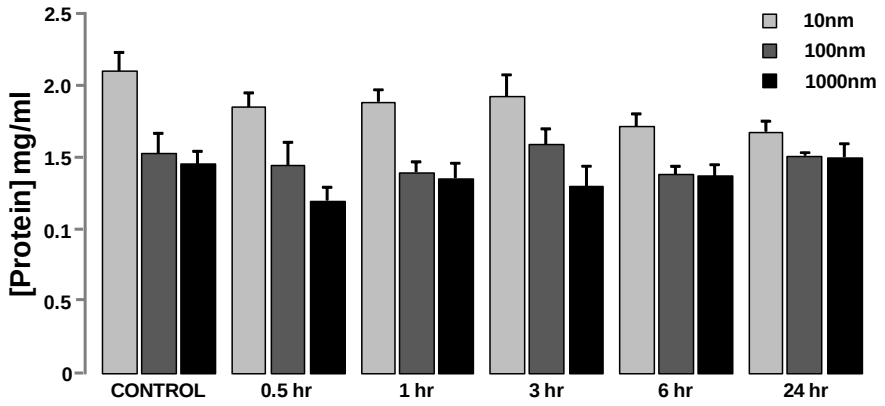

Figure 4.11. Incubation with VCR does not affect protein concentrations of HUVEC lysates. Protein concentrations of HUVEC lysates following incubation with VCR (1000nm, 100nm, 10nm) for varying times (shown in hours), assessed by BCA protein assay. Data shown are mean ± SEM and N=5 culture. No significant difference found (two way ANOVA).

Whilst not an accurate marker of cell morphology, the live/dead assay appeared to demonstrate that incubation with VCR caused endothelial cells to take on a more hypertrophied morphology than they possessed under control conditions. To further examine this change, endothelial cells that had been incubated with either 10nm or 100nm of VCR were stained for the structural protein β-tubulin. As figure 4.12 demonstrates, under control conditions endothelial cells associate closely with one another, forming a confluent monolayer, and under high magnification (figure 4.12C) the β-tubulin itself appears quite evenly distributed throughout the cell. However following incubation with VCR (in particular for 24 hours at a concentration of 100nm), cells take on a hypertrophied appearance and the β-tubulin appears less well defined and more disorganised. In fact when cells are treated with 100nm VCR for 24 hours the tubulin structure collapsed completely.

A

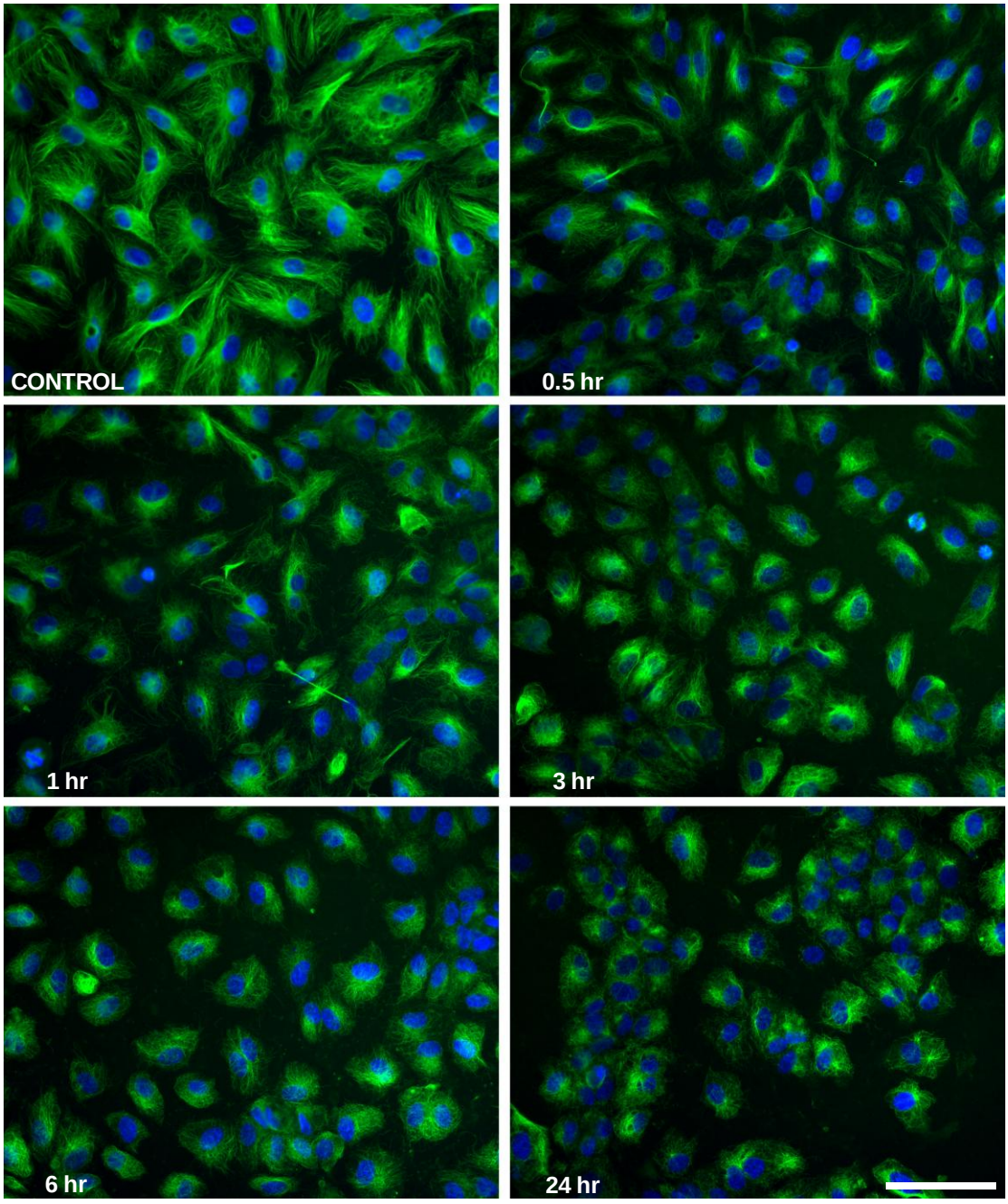

Figure legend to follow.

B

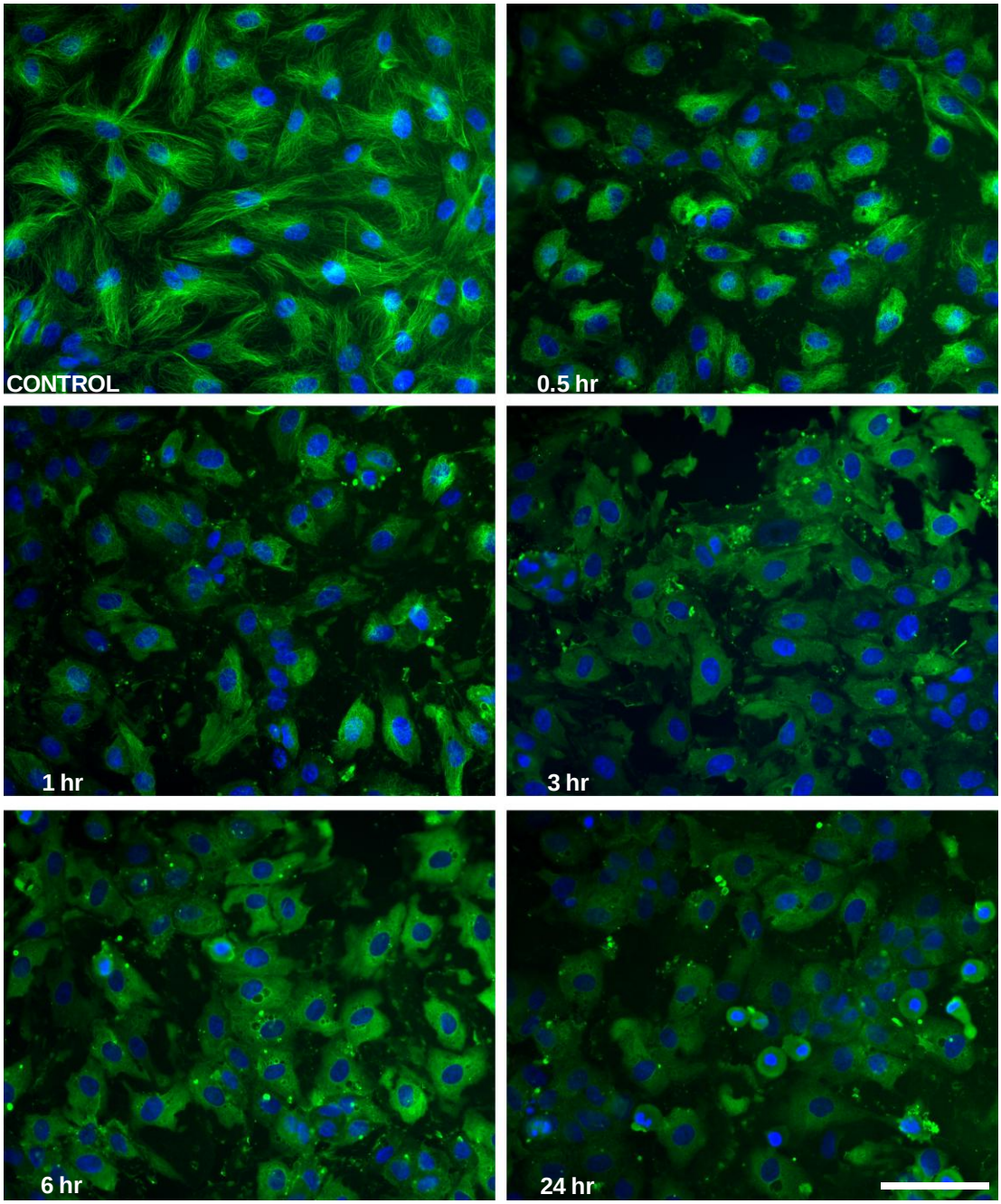

Figure legend to follow.

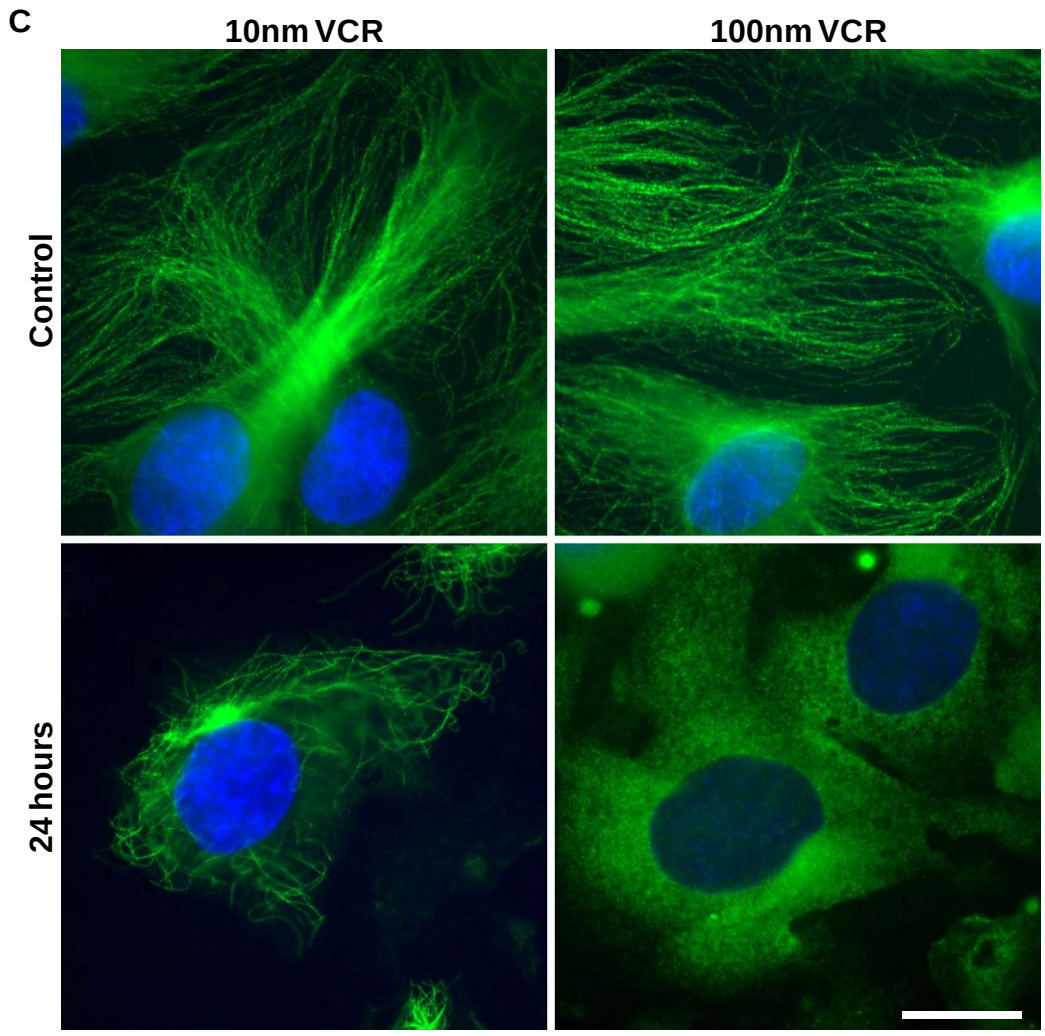

Figure 4.12. Incubation with VCR alters tubulin organisation and morphology of HUVEC *in vitro*. Representative images showing β-tubulin in HUVEC/endothelial cells following incubation in VCR for 0.5-24 hours. **(A)** Low magnification images of 10nm VCR treated cells. Scale bar equal to 100µm **(B)** Low magnification images of 100nm VCR treated cells. Scale bar equal to 100µm **(C)** High magnification images of cells treated with 10nm and 100nm VCR or control media for 24 hours Scale bar equal to 20µm.

Western blot analysis of the protein content of endothelial cells treated with either 10nm or 100nm VCR has demonstrated that, as *in vivo*, VCR does not increase the expression of CX_3CL1 (figure 4.13); these data are supported by FACS analysis of VCR treated primary HUVEC in which very little expression of CX_3CL1 was almost undetectable under all conditions examined (figure 4.15). Additionally, CX_3CL1 could not be detected (by ELISA) in the media of these cells, indicating this VCR does not cause significant shedding of this protein from the cell membrane. What FACS analysis did reveal, however, is that incubation with VCR (10nm for 18 hours) significantly increased the number of endothelial cells expressing the adhesion molecule VCAM-1 (figure 4.14C). As virtually all HUVECs express CD31 and ICAM-1, we measured the expression of these adhesion molecules on the single cell level, looking for changes in the degree of expression. Incubation of HUVEC with VCR (10nm, 18hours) produced a trend towards an increase in ICAM-1 expression of the cell surface (figure 4.15C), and was associated with a moderate but significant decrease in CD31 expression (figure 4.14D). The positive control, TNFα, produced a marked increase in the number of VCAM-1^+ cells and in the expression of ICAM-1 as well as a substantial reduction in CD31 expression (figure 4.14C/D and 4.15C).

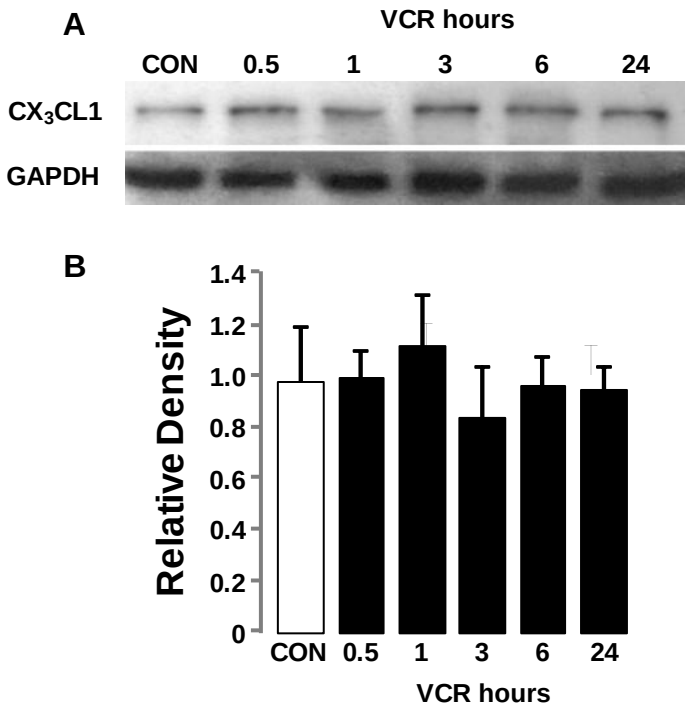

Figure 4.13. Incubation with VCR does not alter CX_3CL1 protein levels in endothelial cells *in vitro*. (A) Representative blot showing CX3CL1 expression (chemokine domain) in HUVEC/endothelial cell lysates following incubation with 10nM VCR. CX3CL1 band size 90kDa; GAPDH band size 37kDa. **(B)** Quantification of protein expression normalised to GAPDH loading control. Data shown are mean ± SEM. N=3 cultures, no significant difference found (one way ANOVA).

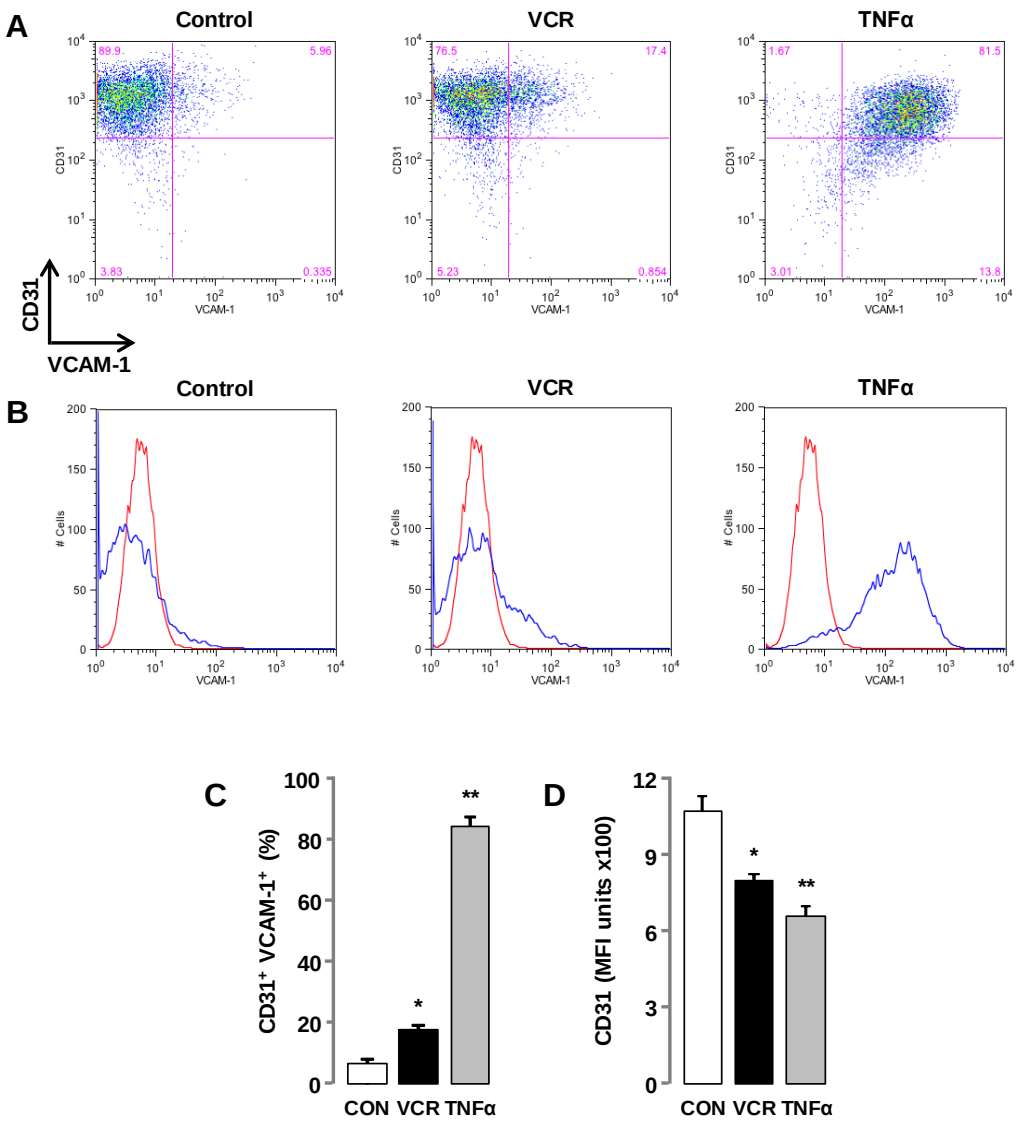

Figure 4.14. Incubation with VCR alters adhesion molecule expression in endothelial cells *in vitro*. (A/B) Representative FACS and frequency plots of cells stained for CD31 and VCAM-1 following incubation with VCR (10nM) or TNFα (10ng/ml; positive control). **(C)** Quantification of VCAM-1 levels on endothelial cells (CD31+). Data shown are mean ± SEM, N=3 mice per group, one way ANOVA with Tukey post-hoc. **(D)** Quantification of CD31 levels on endothelial cells. Data shown are mean ± SEM, N=3 mice per group, one way ANOVA with Tukey post-hoc

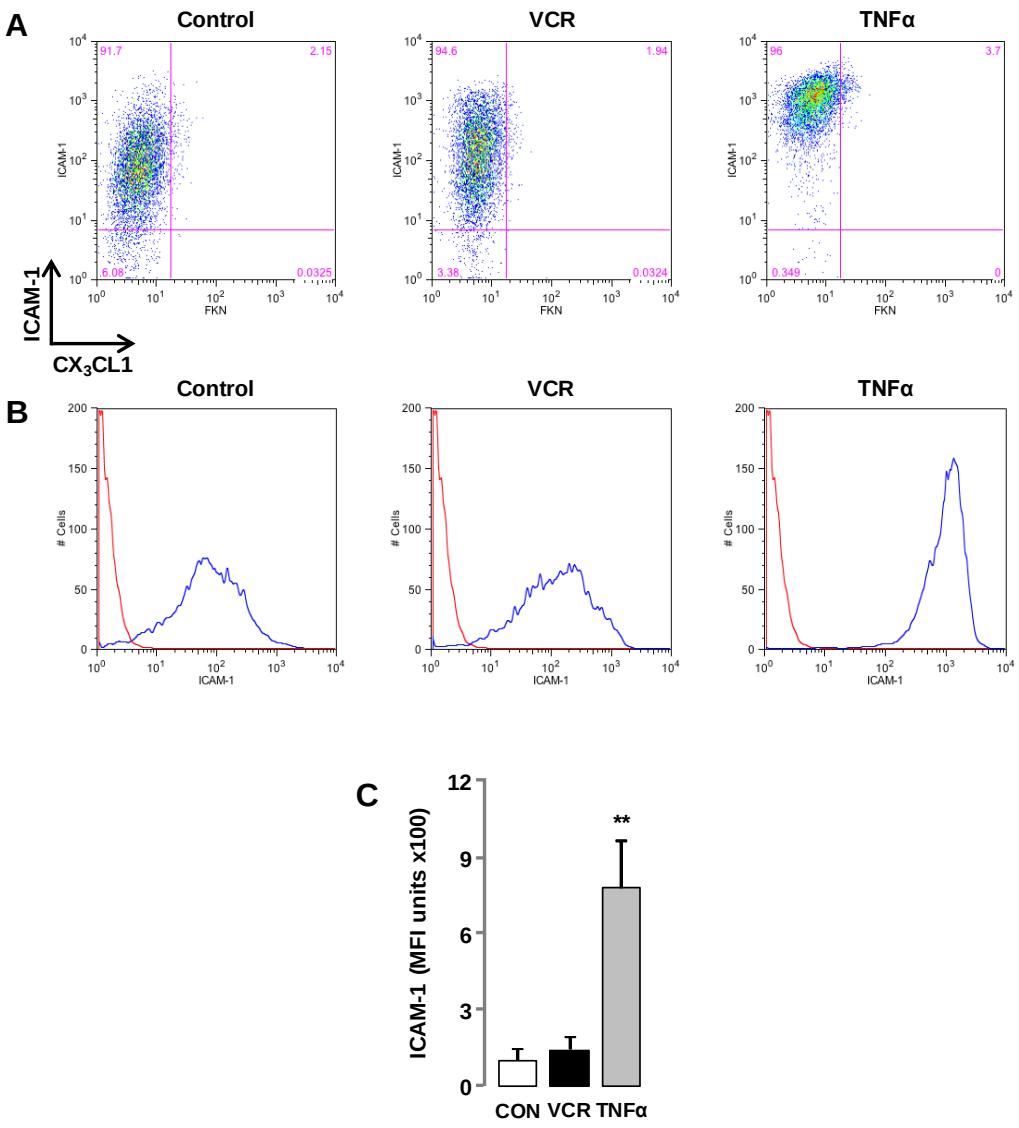

Figure 4.15. Incubation with VCR does not alter ICAM-1 expression in endothelial cells *in vitro*. (A/B) Representative FACS and frequency plots of cells stained for FKN (CX_3CL1; not detected) and ICAM-1 following incubation with VCR (10nM) or TNFα (10ng/ml; positive control). **(C)** Quantification of ICAM-1 levels on endothelial cells. Data shown are mean ± SEM, N=3 mice per group, one way ANOVA with Tukey post-hoc.

3.4. CX_3CR1-mediates ROS production in macrophages

The data above demonstrates that although its expression is not altered by VCR treatment, CX_3CL1 is expressed by endothelial cells *in vitro* and *in vivo*, and we have demonstrated in chapter three that infiltrating monocyte/macrophages express CX_3CR1, the receptor for this ligand. But is CX_3CL1 able to activate CX_3CR1 in a pro-nociceptive fashion following transmigration? In order the test the hypothesis that monocyte/macrophages do indeed produce pro-nociceptive mediators following exposure to CX_3CL1, we evaluated the production of reactive oxygen species (ROS) in these cells. Oxidative stress is known to occur as a result of chemotherapy treatment, and it has been demonstrated that ROS are able to activate TRPA1 receptors, a receptor known to contribute significantly to the aberrant transmission of pain.

Here we show that treatment of peritoneal monocyte/macrophages, with the chemokine domain of CX_3CL1 (200ng/ml, amino acids 25-100 mouse-recombinant protein) induces the rapid production of ROS which reaches significance after 12 minutes of incubation (figure 4.16; $CX_3CR1^{+/+}$). This response was absent in monocyte/macrophages lacking CX_3CR1 (taken from the peritoneal cavity of $CX_3CR1^{-/-}$ mice), demonstrating that this effect of CX_3CL1 is CX_3CR1 mediated.

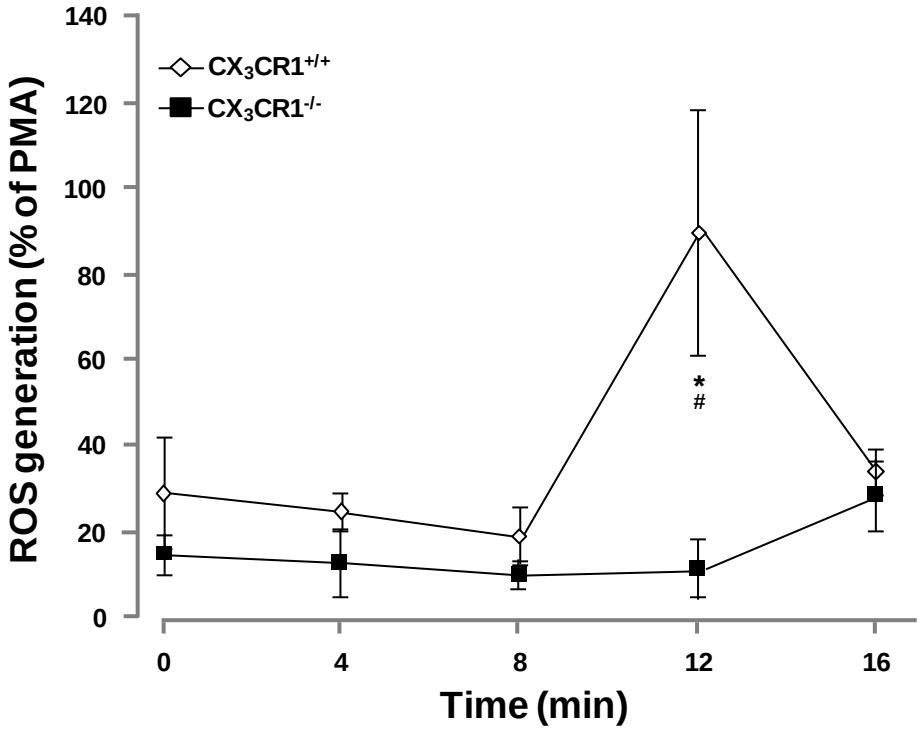

Figure 4.16. Treatment with CX_3CL1 stimulates the production of ROS in macrophages *in vitro*. ROS production by peritoneal macrophages ($CX_3CR1^{+/+}$ and $CX_3CR1^{-/-}$) induced by CX_3CL1 (recombinant mouse chemokine domain 200ng/ml) as determined by change in luminol bioluminescence over time expressed as a percentage of positive control response (PMA 100ng/ml). Data shown are mean ± SEM, N=3 animals per group,*P<0.05 two-way ANOVA with Tukey post-hoc.

3.5. TRPA1-deficiency reduces the severity of and aids recovery of VCR-induced mechanical allodynia

ROS are known to activate TRPA1 receptor channels located on the terminals and axons of sensory neurons on the peripheral nerves, resulting in the generation of action potentials and contributing to the generation of pain. To determine whether or not this mechanism may contribute to the development of pain in VCR-induced painful peripheral neuropathy we evaluated the profile of the development of allodynia in $TRPA1^{-/-}$ mice following the administration of VCR. As figure 4.17A demonstrates, the mechanical thresholds of TRPA1-deficient mice decrease following the daily administration of VCR, however this was to a lesser extent than that occurring in wild-type mice ($TRPA1^{+/+}$) during the first cycle of treatment (days 0-4); during the first cycle wild-type mice experience a decrease in allodynia index of 57.10% (±2.07; figure 4.17B) whilst knock-outs experience a decrease of 32.79% (±3.19; figure 4.17B). Furthermore, during the break between treatment cycles (figure 4.17A; day 7) $TRPA1^{-/-}$ mice exhibited significant signs of recovery; the mechanical thresholds of $TRPA1^{-/-}$ mice, whilst still significantly lower than those of saline-treated animals, were more than double their thresholds from day 4 at the end of the first VCR cycle previous (day 4; figure 4.17A). This effect is not seen in wild-type mice. The thresholds of $TRPA1^{-/-}$ mice during the second cycle of chemotherapy follow a similar pattern to those seen in the first cycle; a substantial reduction ($TRPA1^{-/-}$ 83.62% ±1.44 vs. $TRPA1^{+/+}$ 98.87% ± 0.07) in threshold is observed, however these mice do not show allodynia as severe as wild-type mice (figure 4.17B allodynia index second cycle: $TRPA1^{-/-}$ 55.68% ±5.69 reduction, $TRPA1^{+/+}$ 98.73% ±0.07 reduction). Following the cessation of treatment, $TRPA1^{-/-}$ mice show marked acceleration of recovery in comparison to $TRPA1^{+/+}$ mice; their mechanical thresholds return to baseline levels four day earlier than those of wild-type mice.

Conversely, TRPA1-deficiency appears to offer no protection from the development of VCR-induced cold allodynia; in both $TRPA1^{-/-}$ and $TRPA1^{+/+}$ mice cold-induced withdrawal latency is reduced by VCR treatment to approximately 5.5 seconds (figure 4.18A). However $TRPA1^{-/-}$ mice have a significantly higher baseline withdrawal threshold than $TRPA1^{+/+}$, and as such, they reduction in allodynia index they experience during the second cycle of VCR treatment is considerably greater (figure 4.18B; $TRPA1^{-/-}$ 58.60% ±1.86 reduction vs. $TRPA1^{+/+}$ 41.03% ±3.97). Thus due to their higher baseline withdrawal latencies (to cold), TRPA1 knock-out mice show more pronounced cold allodynia as a result of VCR treatment than wild-type mice.

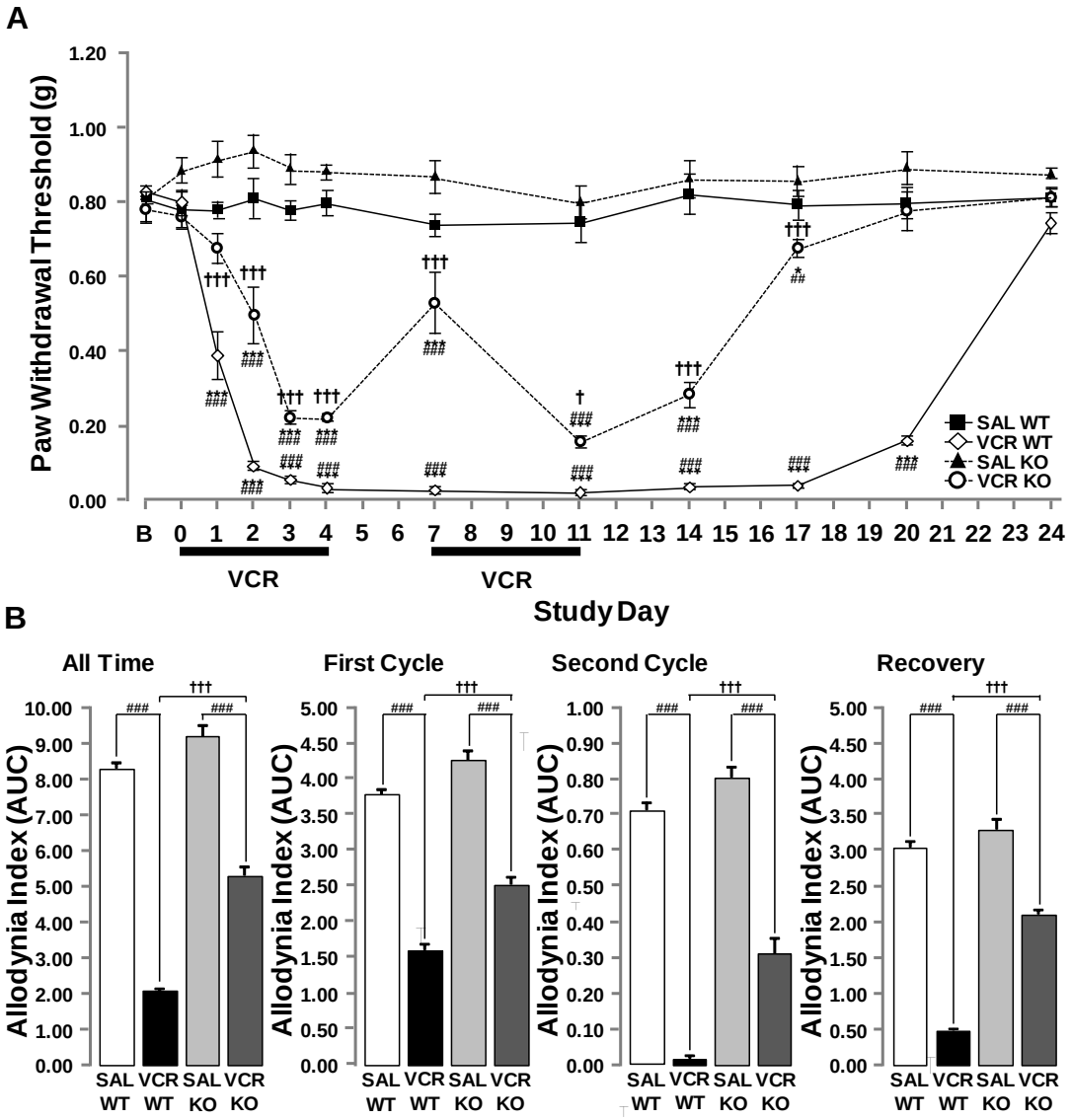

Figure 4.17. TRPA1-deficiency reduces the severity and aids recovery of mechanical allodynia induced by repeated systemic administration of VCR. Development of mechanical allodynia in TRPA1$^{-/-}$ (KO) mice or TRPA1$^{+/+}$ (WT) control receiving *i.p.* VCR (0.5mg/kg/day), days 0-4 and 7-11; black horizontal bars (or vehicle [SA]). **(A)** Temporal profile of mechanical allodynia development shown as 50% PWT, data shown as mean ± SEM. N=8 per group, *P<0.05 / ***P<0.001 vs baseline threshold, ## P<0.01 / ### P<0.001 vs saline threshold, † P<0.05 / ††† P<0.001 vs WT threshold, two-way RM ANOVA with post-hoc Holm-Sidak test. **(B)** Area under the curve (AUC) analysis data expressed as allodynia index. All time = BL-day 24, first cycle= BL-day 4, second cycle = 7-11, recovery = 11-24. Data shown are mean ± SEM. N=8 per group, ### P<0.001 vs saline index, ††† P<0.001 VCR WT vs VCR KO index with one way ANOVA and post-hoc Holm-Sidak.

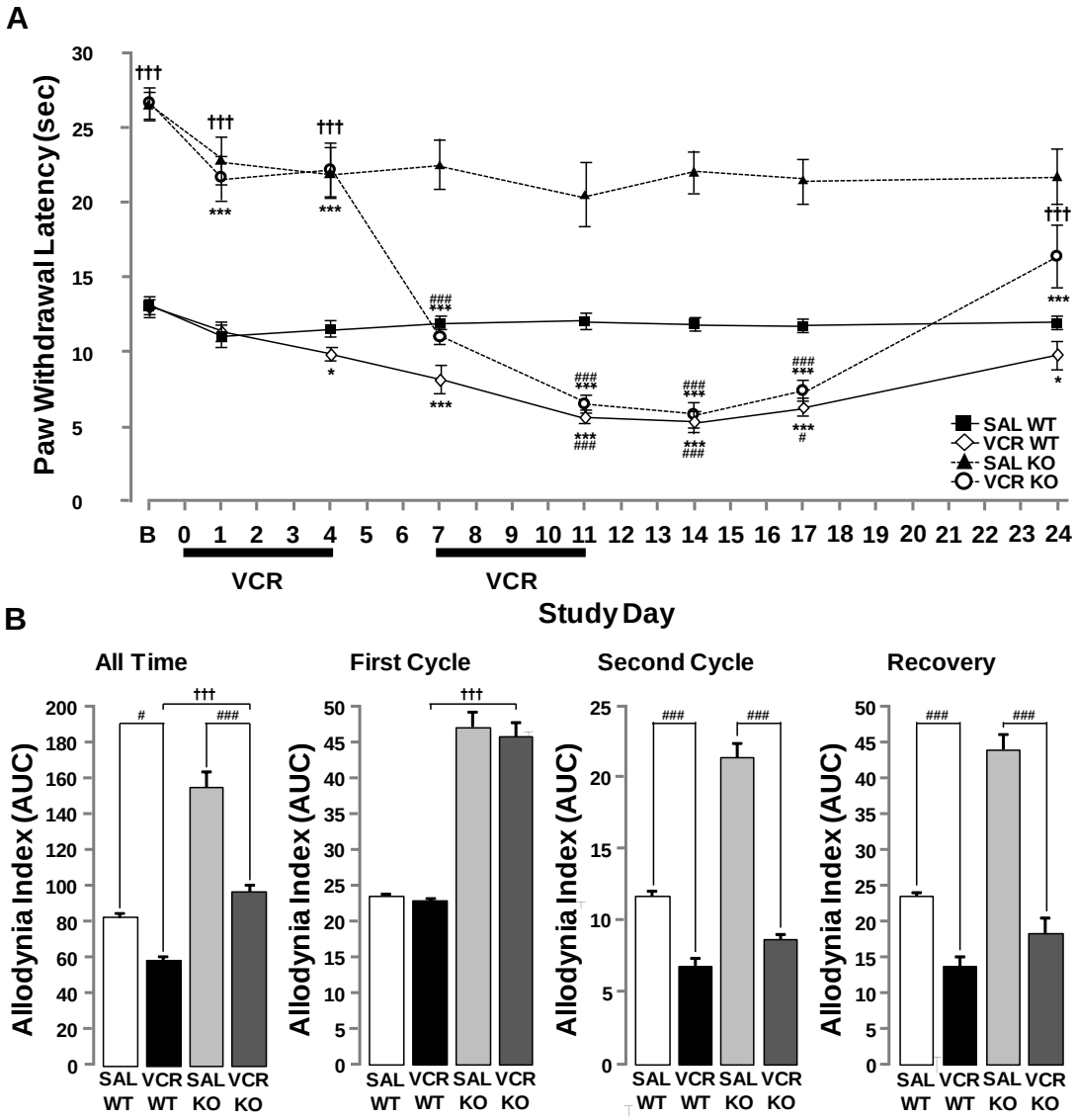

Figure 4.18. TRPA1 knock-out mice have a more pronounced cold hypersensitivity than wild-type mice following repeated systemic administration of VCR due to their higher baseline withdrawal latency. Development of cold allodynia in TRPA1$^{-/-}$ (KO) mice or TRPA1$^{+/+}$ (WT) control receiving *i.p.* VCR (0.5mg/kg/day), days 0-4 and 7-11; black horizontal bars (or vehicle [SAL]). **(A)** Temporal profile of cold allodynia development shown as paw withdrawal latency (seconds), data shown as mean ± SEM. N=8 per group, *P<0.05 / ***P<0.001 vs baseline threshold, # P<0.05 / ### P<0.001 vs saline threshold, ††† P<0.001 vs WT threshold, two-way RM ANOVA with post-hoc Holm-Sidak test. **(B)** Area under the curve (AUC) analysis data expressed as allodynia index. All time = BL-day 24, first cycle= BL-day 4, second cycle = 7-11, recovery = 11-24. Data shown are mean ± SEM. N=8 per group, ### P<0.001 vs saline index, ††† P<0.001 VCR WT vs VCR KO index with one way ANOVA and post-hoc Holm-Sidak.

4. Discussion

Here, in this chapter, we set out to test the hypothesis that VCR reacts with endothelial cells to push the endothelium towards an activated state, which is associated with the increased expression of adhesion molecules, including the transmembrane chemokine CX_3CL1. Furthermore, we hypothesise that soluble CX_3CL1 activates monocytes as they transmigrate across the endothelium, causing them to produce factors (ROS) that act upon the nerve (via TRPA1) to enhance nociceptive transmission. The principle finding of the work described here is that treatment VCR does indeed activate endothelial cells; altering the expression of some of the adhesion molecules required for the adhesion and transmigration of leukocytes. Additionally these data demonstrate that whilst the expression of CX_3CL1 is not altered by VCR treatment, it is expressed by endothelial cells both *in vivo* and *in vitro*, and inhibition of the solubilisation of this protein remains a viable therapeutic target for the treatment of VCR-induced painful peripheral neuropathy. Moreover, we demonstrate that a soluble form of CX_3CL1 (aa25-100), such as that arising from the cleavage of the membrane bound chemokine, is able to activate monocyte/macrophages, causing them to produce ROS. ROS are known to activate TRPA1 receptors along the axons of sensory neurons. Finally, we demonstrate that this TRPA1-dependent mechanism does indeed contribute to the development and maintenance of mechanical allodynia arising as a result of VCR treatment, as mice deficient in this receptor-channel protein show a significant attenuation of mechanical allodynia.

The treatment of pain arising as the result of chronic treatment with chemotherapeutic agents such as VCR represents a major unmet clinical need. However without fully understanding the mechanism by which this neuropathy occurs, we have been unable to provide suitable targets for

the development of preventative agents. Following evidence described in chapter three, which indicates a prevalent role for the CX_3CR1^+ monocyte/macrophage in the development of VCR-induced neuropathy, here, we delineated the cellular and molecular players mediating VCR-pain mechanisms. A series of elegant experiments have established that whilst full length membrane bound CX_3CL1 is able to mediate the adhesion of CX_3CR1^+ monocyte/macrophages to the endothelial surface, the activation of these cells, demonstrated by calcium fluxes within the cell, requires binding of a soluble form of the protein to the receptor (Schwarz et al., 2010). This indicates that the solubilisation of transmembrane CX_3CL1 is an essential process in the CX_3CL1-CX3CR1 dependent activation of leukocytes. Previous work in our laboratory has focused extensively on the role of the cysteine protease Cathepsin S (CatS) in the cleavage of neuronal CX_3CL1, and contribution of CatS to the development of pain in a number of neuropathic and inflammatory disease models. We have demonstrated that inhibition of CX_3CL1 cleavage by this enzyme, with the irreversible CatS inhibitor LHVS, is sufficient to attenuate mechanical allodynia in both models of inflammatory arthritis (Clark et al., 2012) and peripheral nerve injury (Clark et al., 2007b) . In both of these chronic pain models significant immune cell infiltration/proliferation and activation is observed within the spinal cord. These cells can be activated by soluble forms of CX_3CL1; CatS inhibitors significantly reduce microglial activation, and it has been demonstrated several times that microglial activation contributes to the development of a pain phenotype in neuropathic and inflammatory models (Ledeboer et al., 2005;Lin et al., 2007;Raghavendra et al., 2003;Hua et al., 2005). As well as being expressed in the microglia of the CNS, CatS is expressed in monocyte/macrophages in the periphery. In the peripheral nerve and DRG CatS co-localises with the macrophage marker OX6 and is upregulated following nerve injury (Barclay et al., 2007). Furthermore, expression of CatS has been demonstrated in cultured primary monocyte/macrophages and is substantially upregulated by exposure of the cells to the

inflammatory cytokine IFNγ (Geraghty et al., 2007). Expression of CatS has also been reported in F4/80$^+$ macrophages in the inflamed intestine, where the secretion of active CatS is associated with neuronal hyperexcitability and the development of visceral hyperalgesia (Cattaruzza et al., 2011). In line with this evidence, we observed that the development of mechanical allodynia occurring as a result of VCR treatment was prevented by the CatS inhibitor LHVS. Therefore, our data support the possibility that the CatS-dependent cleavage of CX_3CL1 is critical for the development of VCR-pain and indicate that the inhibition of CatS is a viable therapeutic option for the prophylaxis of this condition. It should be noted that endothelial CX_3CL1 can also be cleaved by ADAM10 and ADAM17, which are constitutively expressed by endothelial cells; the effect of the inhibition of these proteases on the development of VCR-induced allodynia remains to be assessed.

Within the CNS, CX_3CL1 is expressed primarily on neurons, and it is the cleavage of this that has been shown to contribute to the development of pain in several neuropathic and inflammatory pain models (albeit in rats not mice); intrathecally administered LHVS attenuates pain (Clark et al., 2012;Clark et al., 2007b). However, the reduction in pain seen observed in the VCR model arises as a result of the inhibition of peripheral CatS found in macrophages, as LHVS administered systemically does not reach the CNS (Barclay et al., 2007). Peripherally CX_3CL1 is expressed predominantly on endothelial cells; here its expression is constitutive, but it can be substantially increased by inflammatory stimuli such as exposure to LPS or inflammatory cytokines (Harrison et al., 1999;Pan et al., 1997;Muehlhoefer et al., 2000). Thus we next hypothesised that treatment with VCR provides an inflammatory stimulus that induces the upregulation of CX_3CL1 on endothelial cells. We first assessed the expression of CX_3CL1 on endothelial cells *in vivo* using a genetically manipulated mouse that co-expresses the mCherry reporter protein with CX_3CL1. Using

this mouse we visualised CX_3CL1 in the small blood vessels of the sciatic nerve by co-staining transverse sections with the endothelial marker CD31. As the literature suggested, there was almost complete co-localization of CX_3CL1 (mCherry) with CD31, however in control vehicle treated animals, not all CD31+ cells expressed CX_3CL1. Analysis of the expression of these proteins revealed no difference in the immunoreactivity of CX_3CL1-mCherry between vehicle and VCR treated tissue; thus to establish whether or not a there was a difference in CX_3CL1 expression we assessed the number of $CD31^+$ endothelial cells that expressed CX_3CL1-mCherry. No increase in the number of CX_3CL1-mCherry expression $CD31^+$ cells was observed in animals treated with VCR when assessed after a single dose, a single cycle or two full cycles of treatment. In this mouse the sequence encoding the mCherry reporter is inserted into the first exon of the *cx3cl1* gene (Kim et al., 2011); this corresponds to the N-terminal region of the translated protein (Pan et al., 1997;Bazan et al., 1997), which forms part of the soluble protein cleaved from the membrane tether by CatS (and ADAM-10/17). To assess the possibility that upregulation of CX_3CL1-mCherry might not be detected due to enhanced cleavage of the protein, we determined the plasma concentration of CX_3CL1 in vehicle and VCR treated mice, hypothesizing that if there was indeed enhanced expression and cleavage of CX_3CL1 this would be reflected in the plasma concentration of soluble CX_3CL1. This was not the case, the plasma concentration of CX_3CL1, as determined by ELISA, was not altered by VCR treatment when assessed after a single dose, a single cycle or two cycles of treatment. To evaluate the endothelial expression of CX_3CL1 in a more controlled environment, the effect of VCR on CX_3CL1 expression and cell morphology was examined *in vitro* using a primary HUVEC (human umbilical vascular endothelial cell) line.

Due to the know toxicity of VCR, prior to assessing the effect of VCR on CX_3CL1 *in vitro*, we assessed the viability of HUVEC incubated with VCR. Our data demonstrate that whilst incubation

with VCR for increasing times does not alter the ratio of live to dead cells, at the highest concentration tested (1000nM) it does significantly reduce the number of cells in culture; thus the highest concentration was not used in further experiments. VCR exerts its cytotoxic effects via the binding to and disruption of the cytoskeleton protein tubulin. To determine whether or not VCR was able to exert this effect on HUVECs at the concentrations tested, we stained the cells with a pan β-tubulin antibody and observed their morphology after incubation with VCR for increasing times; VCR does indeed affect the tubulin structure in cultured HUVECs. Whilst this was not an affect that could be suitably quantified, a distinct qualitative difference can be observed between VCR and vehicle treated cells. Incubation with VCR causes a dramatic collapse in the tubulin structure of HUVECs, and was associated with the development of a hypertrophied appearance and reduction in cell to cell contact; however it did not alter the expression of CX_3CL1 in these cells, and no soluble CX_3CL1 was detected in the culture media in which these cells were treated.

Overall our data indicate that exposure to VCR does not alter the CX_3CL1 expression in endothelial cells; nonetheless VCR has a dramatic effect on the morphology of the cells, suggesting VCR may be able to induce endothelial activation. To assess this possibility we returned to our hypothesis that VCR provided an inflammatory stimulus to endothelial cells, thus pushing them towards an activated (type II) state. To address this hypothesis we phenotyped primary HUVEC cells using the expression of two key adhesion molecules: ICAM-1 and VCAM-1. These molecules play a critical role in the adhesion and transendothelial migration of leukocytes, however in the resting endothelium the transcription of many endothelial molecules, including VCAM-1, is suppressed (Pober and Sessa, 2007), and it is not until the endothelium undergoes prolonged activation, such as that triggered by the release of pro-inflammatory cytokines from leukocytes, that these proteins are upregulated on the luminal surface of the endothelium (Hadad et al., 2011;Kjaergaard

et al., 2013;Collins et al., 1995). As counter-receptors for the leukocyte β_2 integrins the upregulation of ICAM-1 and VCAM-1 on inflammatory cytokine activated endothelial cells plays a critical role in the targeting of leukocyte transmigration to areas of inflammation (Min et al., 2005); thus the enhanced expression of these adhesion molecules can be used as a surrogate marker for 'pro-inflammatory' activation of endothelial cells. FACS analysis of the expression of ICAM-1 and VCAM-1 on VCR treated HUVECs demonstrated that whilst constitutively expressed on all cells, there was a trend towards an increase in the expression of ICAM-1. Although this was not a significant increase, the increase in VCAM-1 expression observed was; incubation of HUVEC with VCR significantly increased the number of cells expressing VCAM-1, and together, these data suggest that the endothelial cells are indeed becoming activated.

Whilst based on these data we must accept the null hypothesis, that VCR does not cause an increase in the expression of CX_3CL1 on endothelial cells, our FACS analysis does provide evidence that VCR induces activation of endothelial cells. Despite the lack of increase in CX_3CL1 on endothelial cells, its constitutive expression means that it may still be able to promote the transmigration of and activate monocyte/macrophages as they adhere to the endothelium via VCAM-1 (and ICAM-1) which, as a result of VCR acting upon the endothelium, is now expressed on the cells. We can hypothesise that CX_3CL1 is able to activate these cells in a way that contributes to the development of pain, despite needing to be solubilised to activate the CX_3CR1 receptor; we have demonstrated that inhibiting the solubilisation of this protein prevents the development of mechanical allodynia arising as a result of VCR chemotherapy. Furthermore, we provide evidence that soluble CX_3CL1, at a concentration similar to those shown previously in our laboratory to activate the CX_3CR1 receptor in microglia (Staniland et al., 2010), is able to activate monocyte/macrophages in a CX_3CR1-dependent manner. In this instance assessed

monocyte/macrophage activation in terms of the production of reactive oxygen species (ROS). ROS are produced as a consequence of oxidative stress, which is known to occur as a result of chemotherapy; ROS scavengers are able to ablate cellular calcium fluxes induced by oxaliplatin (Nassini et al., 2011), and the reduction of superoxide production by the administration of an NADPH-oxidase inhibitor attenuates chemotherapy induced mechanical allodynia (Doyle et al., 2012), as does the administration of the anti-oxidant acetyl-L-carnitine (Flatters et al., 2006;Ghirardi et al., 2005a;Ghirardi et al., 2005b;Pisano et al., 2003).

But how does an increase in ROS production equate to the development of pain following VCR chemotherapy? Recent evidence has demonstrated that ROS are able to activate the TRPA1 receptor found on the axons and terminals of sensory neurons (Takahashi et al., 2008;Nilius et al., 2012;Andersson et al., 2008;Weller et al., 2011). The expression of TRPA1 is upregulated in a number of models of chronic pain and inflammation, and is associated with the development of hyperalgesia; both cold and mechanical hyperalgesia occurring as a result of CFA-induced inflammation are reduced by the systemic administration of selective TRPA1 antagonists (Obata et al., 2005;da Costa et al., 2010;Petrus et al., 2007;Eid et al., 2008). Chemotherapeutic pain models are no exception to this; TRPA1 upregulation has been demonstrated following exposure of cultured DRG neurons to cisplatin or oxaliplatin in a similar pattern to that seen *in vivo* in the trigeminal ganglia of cisplatin treated mice (Windebank and Grisold, 2008;Ta et al., 2010). Furthermore the calcium currents induced in cells by ROS are TRPA1 dependent (Materazzi et al., 2012;Nassini et al., 2011), and oxaliplatin and cisplatin induced pain behaviours are attenuated by the administration of TRPA1 antagonists (Materazzi et al., 2012;Nassini et al., 2011;Barriere et al., 2012). This evidence led us to develop the hypothesis that ROS generated by monocyte/macrophages that have infiltrated the peripheral nerve are able to induce mechanical

allodynia via the activation of TRPA1, thus TRPA1 deficient mice should exhibit attenuated pain behaviours following the induction of VCR-neuropathy.

As our data demonstrate, TRPA1 knock-out mice exhibit a reduction in the development of mechanical allodynia occurring as a result of VCR chemotherapy; whilst the mechanical thresholds in these mice do decline following treatment, it is to a lesser extent than that observed in wild-type mice. Furthermore, we provide evidence of both earlier and more rapid recovery of mechanical thresholds in TRPA1 deficient mice in comparison to their wild-type littermate controls. Conversely, TRPA1-deficiency appears to offer no protection from the development of VCR-induced cold allodynia; due to higher baseline withdrawal latencies to a cold stimulus, TRPA1 knock-out mice show more pronounced cold allodynia as a result of VCR treatment than wild-type mice. These data indicate that the development and maintenance of cold and mechanical hypersensitivity in VCR treated mice may occur via different mechanisms, and that whilst TRPA1 is a viable target for the development of analgesics for this condition, these drugs may not alleviate all symptoms of the neuropathy. Additionally, it should be noted that the attenuation of mechanical allodynia seen as a result of TRPA1 absence is only partial and does not prevent the development of pain in these animals, thus TRPA1 antagonists might have limited efficacy in this model.

Chapter 5:

General Discussion

1. Thesis aims and summary of findings

The treatment of pain arising as the result of chronic treatment with chemotherapeutic agents such as vincristine sulphate (VCR) represents a major unmet clinical need. Thus, the aim of the work presented in this thesis was to investigate possible mechanisms by which repeated cycles of chemotherapy with the anti-neoplastic drug VCR causes enhanced nociception, with the secondary aim of identify novel therapeutic targets for the prevention of this condition.

Establishing a murine model of VCR-induced neuropathic pain, we used several *in vivo* and *in vitro* approaches to assess the pathological changes occurring as the result of two cycles of VCR treatment at both a gross behavioural and more detailed cellular level. The main findings of this work are summarised below:

1. The systemic administration of two five day cycles of VCR results rapid in the development of severe mechanical allodynia and mild cold hypersensitivity. This behavioural phenotype is fully established by the end of the first cycle of treatment and is sustained throughout the second, but recovers approximately two weeks after the cessation of treatment.
2. Whilst not associated with signs of sensory neuron damage, the development of allodynia is associated with astrogliosis in the spinal cord and significant monocyte/macrophage infiltration in the peripheral nerve. Astrogliosis is evident at the end of the first cycle of VCR treatment, peaks at the end of the second cycle, and is no longer observable once allodynia has recovered. Monocyte/macrophage infiltration is evident twenty-four hours after the first administration of VCR and continues to increase throughout the duration of

the treatment cycles, before returning to baseline levels by the time allodynia has recovered.

3. Monocyte/macrophage infiltration of the peripheral nerve represents a critical and early step in the development of enhanced nociception, occurring within twenty-hour hours of the first VCR administration; depletion of these cells prevents the development of allodynia. Infiltrating monocyte/macrophages display a shift towards pro-inflammatory phenotype; the percentage of monocyte/macrophages that are $Gr1^+$ increases following the administration of a cycle of VCR. Furthermore, we suggest that the expression of the CX_3CR1 receptor is critical for monocyte/macrophage infiltration of the peripheral nerve as in the absence of this protein, this infiltration does not occur and the development of allodynia is delayed.
4. VCR treatment has a substantial impact on the integrity of endothelial cells; VCR dramatically disrupts the tubulin cytoskeleton and morphology of these cells and induces an up-regulation of the adhesion molecule VCAM-1, indicative of a shift towards a type II activated state.
5. CX_3CR1 mediates the activation of monocyte/macrophages by CX_3CL1, which results in the production of reactive oxygen species (ROS); ROS are known to evoke pain by activating neuronal TRPA1 channels, and indeed TRPA1-deficiency attenuates allodynia in this model. TRPA1-/- mice exhibit a reduction in the severity of allodynia experienced following the first cycle of VCR. Partial recovery is observed between treatment cycles and these animals recover at an accelerated rate, compared to wild-types, following cessation of the second cycle of VCR.

Here we demonstrate that VCR-induced neuropathic allodynia is the result of a cascade of events in the peripheral nerve (figure 5.1) that begins with an alteration in endothelial cell adhesion properties as a consequence of a shift towards a type II activated state; this promotes the recruitment and trafficking of CX_3CR1-expressing monocyte/macrophages. The CX_3CR1-dependent activation of monocyte/macrophage by endothelial CX_3CL1 results in pro-nociceptive effects mediated by the production of ROS and the activation of TRPA1 receptors on the axons of sensory neurons, which enhances nociceptive transmission. Due to their involvement in this mechanism the following targets may offer viable therapeutic targets for the prevention of VCR-induced painful peripheral neuropathy:

1. Peripheral CX_3CR1 (in monocyte/macrophages)
2. Enzymes capable of solubilizing CX_3CL1 (e.g. CatS in macrophages or endothelial ADAM10/17)
3. Anti-oxidants or ROS scavengers (targeting ROS released from macrophages)
4. TRPA1 channels in sensory neurons

This pathway is, to the best of our knowledge, the first detailed description of the molecular mechanisms that cause the important treatment-limiting painful peripheral neuropathy associated with chemotherapy for haematological malignancy.

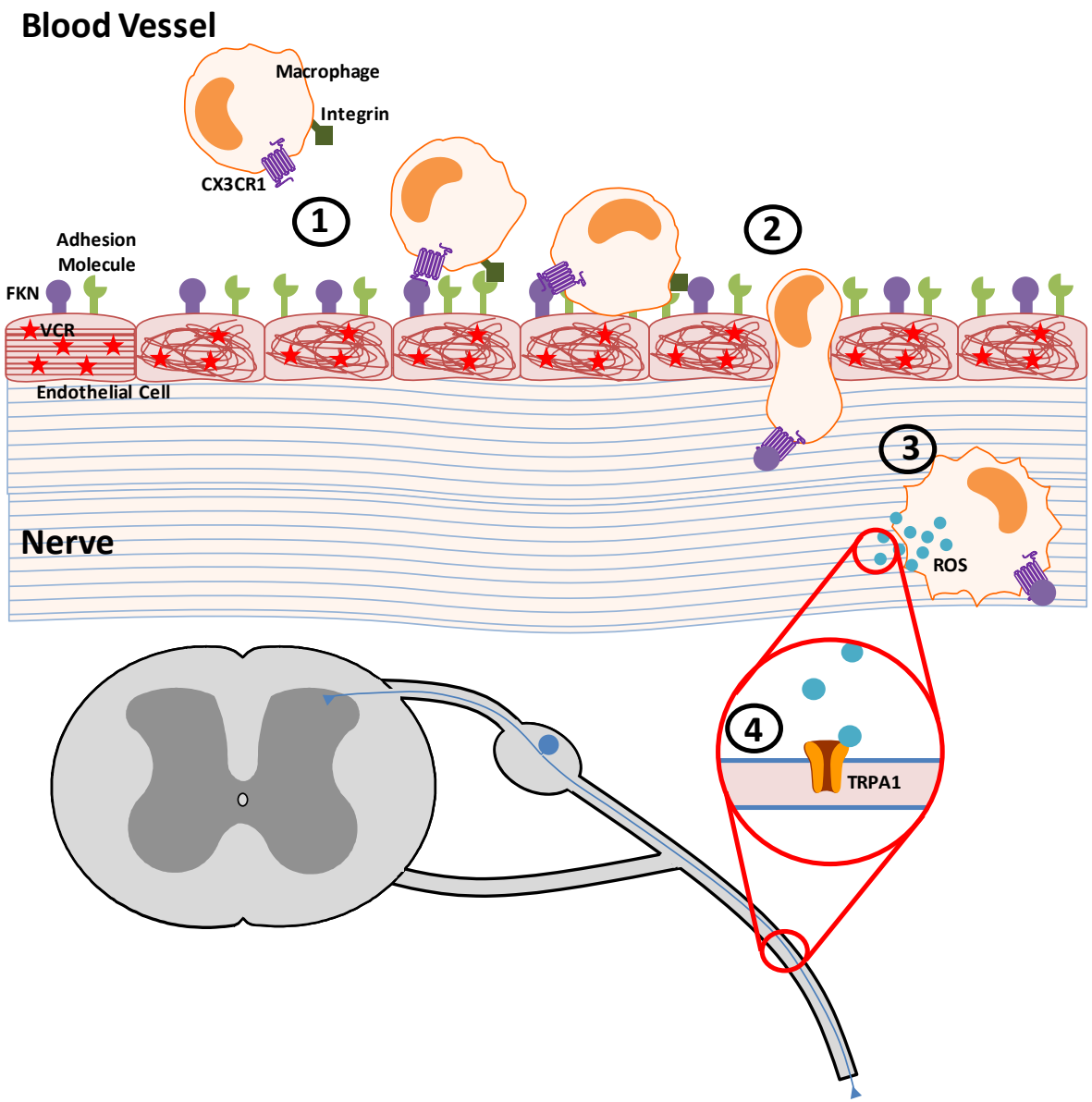

Figure 5.1. A novel pathway for VCR-induced neuropathy. (1) VCR causes binds tubulin in endothelial cells, including those lining the small blood vessels within the peripheral nerve, causing activation and dysfunction that enhances the expression of selected adhesion molecules. **(2)** These, in turn, mediate transendothelial migration of monocytes. As monocytes undergo this process CX_3CR1 on their surface binds its ligand, CX_3CL1 on the endothelium, resulting in the activation of the cells as they migrate into the nerve. **(3)** The activation of monocyte/macrophages triggers the synthesis and release of a number of pro-inflammatory and pro-nociceptive mediators, including ROS. **(4)** ROS activate TRPA1 receptors on the axon of primary afferent fibers, resulting in enhanced nociceptive transmission that manifests behaviourally as mechanical and cold hypersensitivity,

2. General Discussion

Chemotherapy-induced painful peripheral neuropathy is the dose-limited side-effect of several classes of chemotherapeutic agents, including the vinca alkaloids, taxanes and platinum-containing compounds. Depending on the agent and regimen used, this side-effect occurs in up to 97% of patients (Tanabe et al., 2013), is dose-limiting in an excess of 70% (Postma et al., 1995) and results in treatment cessation in between 20% and 40% of patients (Briani et al., 2013;Dougherty et al., 2007;Bennett et al., 2012). Symptoms of the neuropathy are almost exclusively sensory (suggesting it is the sensory neurons that are prone to this neuropathy) and most severe in the hands and feet. Currently chemotherapy-induced neuropathy is primarily managed in the clinic by way of symptomatic treatment with classical analgesics; however the efficacy of this approach is quite varied and often leaves many patients continuing to report pain severe enough to interfere with the activities of daily living. It has recently been reported that the average pain score of patients suffering from vinca alkaloid induced neuropathy receiving doses of morphine in excess of 85mg/day only declines to three out of ten; in some individuals this score is as high as eight out of ten. Patients prescribed gabapentin, codeine, paracetamol, tramadol and/or fentanyl report maximum daily pain scores as high as ten out of ten (average 8.2 ± 1.7) (Dougherty et al., 2007). Furthermore, only 75% of patients with bortezomib-induced neuropathy report any decrease in pain intensity at all with ongoing oxycodone treatment (Cartoni et al., 2012). Not only is this pain management approach ineffective, it does nothing to prevent or treat the underlying cause of pain, the development of peripheral neuropathy.

In the last two decades basic scientists, working alongside clinicians, have established a set of animal models of chemotherapy-induced neuropathy that mimic the human condition and allow

the mechanisms that underlie this condition to be investigated. Early research focused on the changes occurring to the properties of neurons as a consequence of chemotherapy; repeatedly patients report pain and mechanical and cold hypersensitivity that correlates with electrophysiological changes. For example, symptomatic VCR-neuropathy patients show abnormal amplitudes of sural sensory nerve action potentials and a decrease in sensory nerve conduction velocity; these electrophysiological changes are not observed in patients with no symptoms of neuropathy (Krishnan et al., 2005). These changes are a common finding across chemotherapeutic regimens (Krarup-Hansen et al., 2007) and it has been demonstrated that they persist, along with pain, beyond the cessation of the chemotherapy (Argyriou et al., 2007;Ramchandren et al., 2009). The same electrophysiological abnormalities are reproduced in rodent models of this chemotherapy-induced pain; the (single) administration of PTX, oxaliplatin, cisplatin and VCR is associated with the development of both mechanical and cold hypersensitivity in the extremities (hind paw), a decrease in sensory nerve conduction velocities and hyper-responsitivity of subsets of C-fibres in the tail, digital, saphenous and sciatic nerves (Polomano et al., 2001;Gilardini et al., 2012;Wozniak et al., 2011;Guindon et al., 2013;Aley et al., 1996;Tanner et al., 2003). Interestingly the neuropathy arising as a result of chemotherapy is predominantly sensory; motor symptoms occur rarely and tend to be associated with extended periods of treatment and more advanced cancers. As a result a series of electrophysiological observations (see above) and chemotherapeutics tropism for sensory neurons, most of the early research in this field was based on the assumption that it was in these cells that the initial damage was occurring. Certainly there is evidence for damage to primary afferent fibres occurring as a result of treatment with chemotherapeutic agents; an increase in the expression of ATF-3 in the cell bodies in the DRG, a classical marker of neuronal stress/damage, has been observed in several laboratories (Hansen et al., 2011;Khasabova et al., 2012). Additionally evidence has been presented demonstrating

disruption of tubulin structure in sensory neurons in the saphenous nerve (Tanner et al., 2003), a decrease in the density of myelinated fibres in the sciatic nerve (Kawashiri et al., 2009;Callizot et al., 2008) and a decrease in intra-epidermal nerve fibre density in the glabrous skin of the hind paw (Siau et al., 2006) in several models of chemotherapy-pain. However, these changes are not observed concomitantly with the generation of pain, rather they are observed between 1 and 3 weeks after the start of chemotherapy treatment, when pain (hypersensitivity) is well established. Specifically when we examined neuronal stress, by assessment of ATF-3 expression in the DRG, we were unable to observe a significant increase at an early time point (day 4) despite the severe mechanical allodynia observed in these animals. Furthermore, no microglial response was observed in the dorsal horn of the spinal cord at this time, or any later time points examined. This data indicates that neuronal damage is unlikely to be the initial step in the development of chemotherapy-induced neuropathy, and VCR may cause neuronal damage via an indirect mechanism. Indeed we demonstrate here that significant infiltration of monocyte/macrophages occurs rapidly in the sciatic nerve within the first cycle of VCR treatment, with a temporal profile similar to that of the development of mechanical allodynia. Furthermore, the prevention of this infiltration substantially delays the onset of this pain behaviour. In light of this, we suggest that the first step in the development VCR-induced pain is an inflammatory reaction; monocyte/macrophages infiltrate in response to damage to the endothelial cells that line the blood vessels within the nerve. Certainly our data show that VCR induces the activation of endothelial cells, which we propose to be the first site of action of VCR; the upregulation of adhesion molecules demonstrated here is indicative of type II endothelial activation in response to an inflammatory stimulus. Furthermore, our data indicate that immune cell infiltration of the nerve is critical for the development of allodynia in this model; retarding infiltration by reducing the circulating population of monocyte/macrophages or by knocking out the CX_3CR1 receptor

prevents the development of mechanical allodynia. Additionally the onset of mechanical allodynia can be delayed by the administration of the cathepsin S inhibitor LHVS, which we hypothesise inhibits CX_3CR1-dependent monocyte/macrophage activation by soluble forms of CX_3CL1 by preventing the liberation of these soluble forms from membrane bound CX_3CL1. The activation of immune cells by CX_3CL1 has been shown, in other models and in an *in vitro* setting, to cause the upregulation of pro-inflammatory mediators (e.g. IL-1β and TNFα (Ishida et al., 2008b)). These, in turn, are able to activate their neuronally expressed receptors and sensitise peripheral nociceptors; this is observed behaviorally as mechanical hypersensitivity (Reeve et al., 2000;Kawasaki et al., 2008;Gruber-Schoffnegger et al., 2013;Liu et al., 2013b).

As we propose that one of the initial processes in the development of VCR-induced mechanical allodynia is the infiltration of monocyte/macrophages we must consider the biological importance of the infiltration we observe. In our model the number of monocyte/macrophages in the sciatic nerve increases from 1.6 (± 0.1) to 3.0 (± 0.2) cells per $10^4\mu m^2$ after the first 24 hours and to 4.7 (± 0.1) at its peak (this represents a 3 fold increase). Certainly data obtained from the study whereby we depleted these cells indicate that this infiltration is highly biologically significant; if we prevent infiltration by depleting monocyte/macrophages we substantially delay the onset of mechanical allodynia. Additionally, the degree of monocyte/macrophage infiltration that we demonstrate is consistent with observations previously published in this model; Uceyler et al report an approximate threefold increase in macrophages in the sciatic nerve of mice treated with two cycles of VCR. Furthermore, this degree of monocyte/macrophage infiltration is comparable to that previously reported in a model of chronic nerve compression; Gray et al observe approximately 3.5 macrophages per $10^4\mu m^2$ in the sciatic nerve four weeks after injury (Gray et al., 2007). Whilst this is the first instance in which our laboratory has examined macrophage

infiltration in a model of chemotherapy-neuropathy, we have previously examined this process in a severe surgical injury model; seven days after partial ligation of the sciatic nerve approximately 20 macrophages are seen per $10^4 \mu m^2$. This level of infiltration is substantially greater than we observe in the VCR model; however then mechanism by which it occurs is likely different as, whilst CX3CR1-/- mice exhibit an attenuated mechanical and thermal hypersensitivity following PNL, the number of macrophages in the nerve of these animals is comparable to that of wild-types (Staniland et al., 2010).

In this set of experiments we have examined the contribution to VCR-induced allodynia of infiltrating monocyte/macrophages in the peripheral nerve, and have not yet assessed the contribution of other infiltrating immune cells, in particular neutrophils. Neutrophils respond rapidly to injury or infection and their numbers peak as early as 24 hours after insult (Perkins and Tracey, 2000). Indeed the temporal profile of the development of mechanical allodynia doesn't negate a role for these cells in the development of pain in our model; the involvement of these cells certainly warrants investigation. However, the development of mechanical allodynia following VCR administration is completely prevented by the pre-treatment of mice with liposome clodronate which depletes monocyte/macrophages and not neutrophils, and by the deficiency of the CX_3CR1 receptor which is also exclusively a monocytic effect. Additionally, VCR-chemotherapy is classically associated with the development of neutropenia, a decrease in circulating neutrophils; a reduction in neutrophils has been demonstrated to be anti-nociceptive in models of neuropathic pain, yet pain remains the most prevalent side-effect of VCR in patients. Regardless, a contribution of neutrophils to the development of pain the recruitment of monocyte/macrophage in this model, cannot yet be ruled out and indeed work to investigate this is underway in our laboratory.

The mechanism by which VCR causes allodynia that we describe here indicates that the initial site of action of VCR, rather than the sensory neurons, is the endothelial cells lining the blood vessels of the nerve. We hypothesise that it is this that allows enhanced monocyte/macrophage adhesion and subsequent infiltration of the nerve. Evidence suggests VCR has a tropism for sensory neurons as the blood nerve barrier in peripheral nerve is relatively permeable, and it is likely that this results in preferential accumulation of monocyte/macrophages in the nerve. However as VCR is administered systemically it is possible that endothelial disruption evoked by VCR might affect other organs. Indeed, our data indicate that there is infiltration of monocyte/macrophages into the peritoneal cavity of VCR-treated mice as well as the sciatic nerve; however we would need to assess monocyte/macrophages infiltration into other tissues to draw firm conclusions. A literature search for endothelial disruption following chemotherapy reveals that there is evidence to indicate that VCR-induced endothelial disruption contributes to the development of the non-neuronal side-effects of this drug, specifically cardiovascular toxicity. It has been demonstrated that a number of chemotherapeutic agents are toxic to the cardiovascular system; their administration results in the development of vascular complications such as ischemia, myocardial infarction, thrombosis and hypertension (Daher and Yeh, 2008). The administration of both 5-fluorouracil and bevacizumab to endothelial cells in culture and to rodents have resulted in a number of effects consistent with endothelial cell injury, including endothelial cell specific decreases in DNA synthesis, increased prostacyclin release, inhibition of VEGF-induced tubule formation and reduced cell migration and angiogenesis (Daher and Yeh, 2008). Moreover, in a recent set of experiments Mikaelian and colleagues were able to demonstrate that the mechanism of cardiotoxicity of tubulin binding drugs is primary endothelial damage (Mikaelian et al., 2010); here they assessed endothelial damage induced by both VCR and vinblastine, providing evidence to support this process occurring as a result of vinca alkaloid treatment.

Whilst investigation into endothelial dysfunction as a result of treatment with chemotherapeutic agents (vinca alkaloids, 5-fluorouracil and bevacizumab [anti-VEGF antibody]) is underway, the evidence collected is not yet strong enough to apply this mechanism to chemotherapeutic agents of all classes (which have very varied mechanisms of action). Similarly, the same can be said of our proposed mechanism for the initiation of VCR-induced mechanical allodynia. VCR functions as an anti-neoplastic by disrupting tubulin and causing the disassembly of microtubules. Whilst we have demonstrated here that it is capable of causing severe morphological changes in endothelial cells, not all chemotherapeutic agents exert their anti-cancer effects in this way. The taxane class of compounds are also considered tubulin binders, however rather than causing disassembly of microtubules they promote microtubule stability. Whilst this may indicate that these compounds, the most well known of which is PTX, are unlikely to cause pain via the same mechanism as the vinca alkaloids, monocyte/macrophage infiltration of the peripheral nerve has been demonstrated following intravenous PTX administration (Peters et al., 2007a). The platinum based compounds exert their anti-neoplastic effects by cross-linking DNA strands, thus preventing its replication and RNA and protein synthesis. Whilst both cisplatin and oxaliplatin induce the development of pain in both patients and animal models, enhanced monocyte/macrophage infiltration of the nerve has not yet been reported following the administration of these compounds.

The evidence we provide here to support the hypothesis that VCR treatment causing endothelial damage is in an *in vitro* setting, and further work is required to determine the degree to which this occurs *in vivo*; for example immunohistochemical analysis of adhesion molecule expression in the endothelial cells of VCR-treated animals. However, by comparing the VCR concentrations used *in vitro* to those achieved *in vivo*, we can predict that endothelial damage is likely to be observed *in vivo*. In the studies presented here VCR was administered to mice intraperitoneally; whilst we did

not assess the serum concentration of VCR in our mice this has been reported previously. Using toxicity based assays Dixon et al demonstrated that, in the mouse, the VCR content of the serum is approximately 0.35% of the original quantity given intraperitoneally (Dixon et al., 1969). Using this value we can predict the blood concentration of VCR in our mouse model system; a single administration of 0.5mg/kg of VCR in a 25g mouse results in a blood concentration of VCR of approximately 30nM; this is comparable with the concentrations we have used to investigate the effect of VCR on endothelial cells *in vitro* (10 and 100nM). In the adult human the maximum dose of VCR administered is 2mg, given intravenously into a blood volume of approximately 4.7L; this equates to a blood concentration of VCR in an adult human of approximately 450nM. This value is substantially greater than the predicted blood concentration of VCR in the mouse and the concentrations used *in vitro*, thus provide a basis for the hypothesis that the VCR-induced endothelial damage that we see *in vitro* occurs in man. It should be noted that this dose in humans represents a total cycle over a week, whilst the calculations presented for a mouse represent only a single dose in our study protocol, as an accurate rate of elimination of VCR in the mouse is not known.

The mechanism outlined here proposes that the infiltration of CX_3CR1^+ monocyte/macrophages into the nerve as a result of endothelial dysfunction represent the initiating steps in the development of chemotherapy pain. However, as demonstrated by studies undertaken using the CX_3CR1 knock-out mouse, deficiency of this receptor delays the onset of pain, rather than preventing it altogether, indicating that CX_3CR1-dependent migration of monocyte/macrophages may be important in the development of pain rather than its maintenance. Our data indicate that monocyte/macrophage infiltration remains a critical step in the development of VCR-induced mechanical allodynia, as even in CX_3CR1 knock-out mice after a four day delay in pain onset;

mechanical allodynia develops concomitantly with monocyte/macrophage infiltration of the sciatic nerve. This indicates that the blockade of CX_3CR1 function alone may not be sufficient to prevent the development of VCR-pain after several cycles of chemotherapy, and that a multi-drug approach may be required. The interaction of CX_3CR1 and its ligand CX_3CL1 is vital for the survival of CX_3CR1^{high} resident monocyte/macrophages and for the early infiltration of these cells into the nerve. However a second population of monocyte/macrophages is far less dependent on this mechanism for function: the $CX_3CR^{int}CCR2^{+}$ monocyte/macrophages. Whilst these cells express CX_3CR1, its expression is not critical for survival; the population persists in mice deficient of this protein (Jung et al., 2000). Furthermore, migration of these cells is CCR2 dependent rather than CX_3CR1; thus this later infiltration might be mediated by the interaction between CCR2 and its ligand CCL2 (MCP-1) and that these proteins will provide further targets for the development of analgesics specifically for VCR-induced pain, that will likely be most efficacious when used in combination with inhibitors of CX_3CR1 activation.

Following the first cycle of VCR chemotherapy, CX_3CR1 knock-out mice show an almost complete attenuation of mechanical allodynia; however TRPA1 knock-out mice show only a partial attenuation, and whilst our data indicate that TRPA1-deficiency aids recovery from VCR-induced hypersensitivity, it does not prevent the onset of this condition. We hypothesise that this difference in attenuation arises from TRPA1 having a role in the development of pain in a later stage of the mechanistic pathway than CX_3CR1. Inhibiting monocyte/macrophage infiltration and CX_3CR1 signalling in this model is highly effective at preventing the development of pain occurring as a result of VCR therapy; however these processes, whilst not hypothesised to be causative, occur early in our proposed mechanism. The activation of neuronal TRPA1 by ROS however, is proposed to be the final process in this mechanism, when it is likely that several signalling

pathways have been recruited to enhance nociceptive transmission. For example, once activated monocyte/macrophages are able to synthesise and release a host of pro-nociceptive mediators, including TNF and IL-6 (Niu et al., 2012;Dumitru et al., 2000). The increased expression of these mediators following chemotherapy has been demonstrated (Pusztai et al., 2004;Starkweather, 2010), and antibody neutralisation of these proteins are anti-nociceptive when administered peripherally (Kiguchi et al., 2008b). Additionally, following its release from macrophages, CatS, as well as cleaving CX_3CL1, is able to activate the PAR2 receptor. This receptor is expressed on sciatic nerve and DRG (Liu et al., 2013a) and can be upregulated by pro-inflammatory cytokines including IL-6 (Shinohara et al., 2012). It has been demonstrated that activation of PAR2 can sensitise neurons, contributes to inflammation-induced pain responses (Hoogerwerf et al., 2001) and is critical for the induction of nerve-injury induced neuronal hyperexcitability (Huang et al., 2012). Thus, whilst we have presented here a mechanism by which initial endothelial damage and monocyte/macrophage infiltration of the nerve results in the pro-nociceptive activation of neurons following the administration of VCR, we hypothesise that due to a divergence of signalling pathway subsequent to monocyte/macrophage infiltration, targeting the recruitment of these cells represents the most favourable opportunity to prevent chemotherapy-induced painful peripheral neuropathy.

The model used here examines the consequences of chemotherapy in the absence of cancer; whilst this does not accurately approximate the clinical situation, it does allows the mechanisms by which CX_3CR1 monocyte/macrophages contribute to the development of vincristine-induced painful peripheral neuropathy to be investigated in a controlled manner. What must be considered however is how, in a cancer baring patient, modulation of monocyte/macrophage function would influence tumour burden and/or progression. This can be investigated, in a similar

fashion to the experiments performed here, by administering liposome encapsulate clodronate to deplete monocyte/macrophages in cancer bearing mice. Such experiments have provided evidence that indicates that monocyte/macrophages actually promote tumour progression and the development of metastasis; several groups have reported that liposome encapsulated clodronate has significant anti-tumour activity. For example in a mouse model of colon cancer macrophage depleted animals displayed significantly smaller primary tumours, and did not go on to develop liver or peritoneal metastases which were evident in over 80% of untreated mice (Kruse et al., 2013). Similarly weekly administration of liposome encapsulated clodronate to fibrosarcoma or colon carcinoma bearing mice substantially inhibited tumour growth and significantly increased survival the survival rate of these mice (Guth et al., 2012). This approach to depleting macrophages also reduces tumour growth in models of melanoma (Gazzaniga et al., 2007), ovarian (Robinson-Smith et al., 2007), lung (Kimura et al., 2007), teratocarcinoma (Zeisberger et al., 2006) and prostate (Halin et al., 2009) models of cancers. Additionally the administration of an anti-Gr-1 antibody to otherwise immunocompetent mice, resulting in the depletion of granulocytes and macrophages, reduced the growth of a UV-light induced tumour (Seung et al., 1995).

It is now widely accepted in the oncology field that solid tumours contain a multitude of non-malignant as well as malignant cells; leukocytes were observed within tumours as early as the mid-nineteenth century (Balkwill and Mantovani, 2001). One of the most notable populations of non-malignant cells within the tumour is macrophages. These cells are typically referred to as tumour-associated macrophages (TAMs), however are predominantly derived from peripheral blood monocytes (Stephens et al., 1978) that proliferate locally (McBride, 1986). TAMs are recruited to tumours by chemokines, cytokines and growth factors that are released from the malignant cells

themselves (Pollard, 2004); CCL2 (MCP-1), macrophage colony stimulating factor (M-CSF/CSF-1) and vascular endothelial growth factor (VEGF) are thought to contribute most substantially (Bingle et al., 2002), whilst IL-4 and IL-10 promote differentiation to an M2/alternatively-activated phenotype (Qian and Pollard, 2010). In fact CCL2 is widely expressed in tumours of many types (Scotton et al., 2001;Pollard, 2004) and the role of CCL2-CCR2 signalling in monocyte-macrophage mobilisation and recruitment is well established. Furthermore high levels of this chemokine correlate with poor prognosis (Leek and Harris, 2002;Saji et al., 2001), as does over-expression of CSF-1 (Lin et al., 2002;Scholl et al., 1994;Kacinski, 1995). Experimental over-expression of CSF-1 results in earlier macrophage infiltration, accelerated tumour progression and increased metastasis, whilst the genetic ablation or pharmacological blockade of CSF-1 has opposing effects (Lin et al., 2001;Oguma et al., 2008;Abraham et al., 2010). In patients a correlation is observed between TAM density and poor prognosis; a recent meta-analysis demonstrated this correlation is evident in over 80% of studies (Bingle et al., 2002;Scholl et al., 1994). For example, in non-small cell lung cancer patients there is a positive correlation between intratumoural macrophage density and tumour grade/stage (Bonde et al., 2012). In prostate carcinoma patients a high density of TAMs is associated with shorter survival time (Lissbrant et al., 2000), in breast cancer patients a high TAM density is associated with reduced relapse-free and overall survival time (Leek et al., 1996) and there is a strong association between increased macrophage density and poor survival in lung (Chen et al., 2005), hepatocellular (Zhou et al., 2009) and thyroid cancers (Ryder et al., 2008). Conversely TAM density has been shown to be associated with good prognosis in a small study of colorectal cancer (Nakayama et al., 2002) and contradictory data have been obtained from studies of stomach cancer (Bingle et al., 2002;Scholl et al., 1994). The current understanding of these findings is that it is not just the density of the TAMs that is important in determining prognosis, rather the phenotype of these cells is also critically important. In the majority of

tumours TAMs take on an M2/alternatively-activated phenotype which promotes immunosubversion by the cancer via inhibition of cytotoxic T-cell responses (Zitvogel et al., 2006;Kuang et al., 2009) and results in poor prognosis, whilst in a small number of cancers an M1/classically activated phenotype of TAMs predominates and take on a protective role by activating tumour-killing mechanisms, antagonise the immunosuppressive actions of M2 macrophages and amplify beneficial T-cell responses (Murray and Wynn, 2011;Biswas and Mantovani, 2010;Sica and Bronte, 2007).

So the majority of TAMs are M2-like and contribute to tumour progression, but how do they achieve this? Once within the tumour, TAMs contribute to the local microenvironment in a number of ways, and it is this microenvironment that is responsible for the regulation of tumour growth and the development of metastases. Firstly, TAMs produce a number of trophic factors that directly promote the survival and proliferation of cancer cells, including (but not limited to) endothelial growth factor (EGF), platelet-derived growth factor (PDGF) and transforming growth factor-β (TGF-β) (Richards et al., 2013). Secondly, due to the physiological function of macrophages to initiate and/or support angiogenesis, TAMs promote neovascularisation and angiogenesis of tumours via the synthesis and release angiogenic factors such as VEGF and angiopoietins (Bando and Toi, 2000;Leek and Harris, 2002). Additionally TAMs also increase the bioavailability of constitutively expressed VEGF as they produced matrix metalloprotease-9 (MMP9) which releases VEGF from intracellular stores (Qian and Pollard, 2010). Macrophage depletion reduces angiogenesis in cancer models (Kubota et al., 2009) and inhibits angiogenesis in transplanted tumours (Gazzaniga et al., 2007;Halin et al., 2009;Kimura et al., 2007), conversely over-expression of VEGF in macrophage-depleted mice restores vascularisation capacity and accelerates tumour progression (Lin and Pollard, 2007). Finally TAMs are metastases-promoting;

the ablation of macrophages, both genetic and chemical, indicates that TAMs are required for efficient metastatic growth (Qian et al., 2009). Initially the interaction between TAMs and tumour cells promote the migration of tumours cells out of the primary tumour as TAMs respond to chemotactic gradients of growth factors (Wyckoff et al., 2004). TAMs also produce proteases such as matrix metalloproteases and cathepsins that facilitate the escape of cells from the primary tumour and tissue invasion into secondary sites by breaking down basement membranes (Qian and Pollard, 2010;Condeelis and Pollard, 2006). These cells promote intravasation of tumour cells into blood vessels by clustering on the abluminal side of vessels and releasing TNF-α which impairs the endothelial barrier (Wyckoff et al., 2007;Zervantonakis et al., 2012) and promote extravasation into tissues where CCL2 produced by tumour and target site stromal cells stimulates the release of VEGF (Qian et al., 2011).

Overall the observations made in the above studies indicated that the majority of macrophages do indeed contribute significantly to the progression of tumour growth and that inhibiting their function may be beneficial rather than enhance tumour burden. Thus the modulation of monocyte/macrophage function that here we propose will attenuate the development of chemotherapy-pain is likely to have a favourable effect when examined in models of cancer.

3. Future Directions

Whilst the work presented here provides us with a mechanism by which VCR chemotherapy results in the development of chronic pain, there is much space for further investigation, not only into the precise cellular changes occurring but also into the divergence of pathways that this data hints are important. In addition the mechanism described here provides us with several novel targets for the development of disease specific analgesics that require further attention. These further avenues of investigation are described briefly below:

1. An investigation of VCR-induced endothelial damage and the effect of this on monocyte/macrophage infiltration and activation *in vivo*. This can be achieved with a series of immunohistochemical studies examining the expression of adhesion molecules associated with type II endothelial activation and by assessing the structure of the endothelium *in vivo*. Similarly monocyte/macrophage activation can be assessed immunohistochemically by assessment of the expression of the phosphorylated forms of the MAP kinases known to be activated in these cells and by changes in the expression and release of pro-nociceptive mediators from these cells.
2. An investigation into the role of $CX_3CR^{int}CCR2^{+}$ monocyte/macrophages in a VCR model of chemotherapy pain, and the potential of combined CX_3CR1/CCR2 antagonism as a prophylactic treatment for the development of this condition. This can be achieved using a similar approach that used to establish the role of CX_3CR1^{high} monocyte/macrophages here.
3. Thirdly, an investigation into the contribution to pain made by central sensitisation induced by VCR-treatment. Here we demonstrate astrogliosis in our model in a temporal

profile similar to that of the development of mechanical allodynia, however reversing this with the glial inhibitor fluorocitrate does not impact the behavioural phenotype; do these cells significantly contribute to dysfunctions in nociceptive transmission in this model? Additionally are there changes in dorsal horn neurons as a result of chemotherapy treatment? Is there an increase in expression of glutamate or neuropeptide receptors? Is there a decrease in inhibitory input such as that seen in nerve injury models of neuropathic pain? Alternatively, could the astrogliosis seen here be anti- rather than pro-nociceptive or inflammatory phenotype? If so could this phenotype be enhanced to assist recovery in patients in whom this pain is already well established?

4. Finally it is important to assess how translational this proposed mechanism is. This can be achieved by first assessing the contribution to pain of endothelial damage, monocyte/macrophage infiltration and activation, and TRPA1 activation in models of pain induced by chemotherapeutic agents with differing mechanisms of action (i.e. not tubulin disrupters). Additionally the contribution of this proposed mechanism could be assessed humans; however this would require either the identification of surrogate markers for endothelial damage/macrophage recruitment or the examination of post-mortem tissue.

Reference List

Abbadie C, Lindia JA, Cumiskey AM, Peterson LB, Mudgett JS, Bayne EK, DeMartino JA, MacIntyre DE, Forrest MJ (2003) Impaired neuropathic pain responses in mice lacking the chemokine receptor CCR2. Proc Natl Acad Sci U S A 100:7947-7952.

Abbott NJ, Ronnback L, Hansson E (2006) Astrocyte-endothelial interactions at the blood-brain barrier. Nat Rev Neurosci 7:41-53.

Abraham D, Zins K, Sioud M, Lucas T, Schafer R, Stanley ER, Aharinejad S (2010) Stromal cell-derived CSF-1 blockade prolongs xenograft survival of CSF-1-negative neuroblastoma. Int J Cancer 126:1339-1352.

Afonseca SO, Cruz FM, Cubero D, I, Lera AT, Schindler F, Okawara M, Souza LF, Rodrigues NP, Giglio A (2013) Vitamin E for prevention of oxaliplatin-induced peripheral neuropathy: a pilot randomized clinical trial. Sao Paulo Med J 131:35-38.

Agarwal SK (2011) Core management principles in rheumatoid arthritis to help guide managed care professionals. J Manag Care Pharm 17:S03-S08.

Ajami B, Bennett JL, Krieger C, McNagny KM, Rossi FM (2011) Infiltrating monocytes trigger EAE progression, but do not contribute to the resident microglia pool. Nat Neurosci 14:1142-1149.

Akaneya Y, Takahashi M, Hatanaka H (1995) Interleukin-1 beta enhances survival and interleukin-6 protects against MPP+ neurotoxicity in cultures of fetal rat dopaminergic neurons. Exp Neurol 136:44-52.

Akopian AN, Souslova V, England S, Okuse K, Ogata N, Ure J, Smith A, Kerr BJ, McMahon SB, Boyce S, Hill R, Stanfa LC, Dickenson AH, Wood JN (1999) The tetrodotoxin-resistant sodium channel SNS has a specialized function in pain pathways. Nat Neurosci 2:541-548.

Albers JW, Chaudhry V, Cavaletti G, Donehower RC (2011) Interventions for preventing neuropathy caused by cisplatin and related compounds. Cochrane Database Syst RevCD005228.

Aldskogius H, Kozlova EN (1998) Central neuron-glial and glial-glial interactions following axon injury. Prog Neurobiol 55:1-26.

Alessandri-Haber N, Dina OA, Joseph EK, Reichling DB, Levine JD (2008) Interaction of transient receptor potential vanilloid 4, integrin, and SRC tyrosine kinase in mechanical hyperalgesia. J Neurosci 28:1046-1057.

Aley KO, Reichling DB, Levine JD (1996) Vincristine hyperalgesia in the rat: a model of painful vincristine neuropathy in humans. Neuroscience 73:259-265.

Alimoradi H, Pourmohammadi N, Mehr SE, Hassanzadeh G, Hadian MR, Sharifzadeh M, Bakhtiarian A, Dehpour AR (2012) Effects of lithium on peripheral neuropathy induced by vincristine in rats. Acta Med Iran 50:373-379.

Allchorne AJ, Gooding HL, Mitchell R, Fleetwood-Walker SM (2012) A novel model of combined neuropathic and inflammatory pain displaying long-lasting allodynia and spontaneous pain-like behaviour. Neurosci Res 74:230-238.

Allodi I, Udina E, Navarro X (2012) Specificity of peripheral nerve regeneration: interactions at the axon level. Prog Neurobiol 98:16-37.

Anand U, Otto WR, Anand P (2010) Sensitization of capsaicin and icilin responses in oxaliplatin treated adult rat DRG neurons. Mol Pain 6:82.

Andersson DA, Gentry C, Moss S, Bevan S (2008) Transient receptor potential A1 is a sensory receptor for multiple products of oxidative stress. J Neurosci 28:2485-2494.

Andersson DA, Gentry C, Moss S, Bevan S (2009) Clioquinol and pyrithione activate TRPA1 by increasing intracellular Zn2+. Proc Natl Acad Sci U S A 106:8374-8379.

Andrade EL, Luiz AP, Ferreira J, Calixto JB (2008) Pronociceptive response elicited by TRPA1 receptor activation in mice. Neuroscience 152:511-520.

Andrade EL, Meotti FC, Calixto JB (2012) TRPA1 antagonists as potential analgesic drugs. Pharmacol Ther 133:189-204.

Andrew D, Greenspan JD (1999) Mechanical and heat sensitization of cutaneous nociceptors after peripheral inflammation in the rat. J Neurophysiol 82:2649-2656.

Andriambeloson E, Baillet C, Vitte PA, Garotta G, Dreano M, Callizot N (2006) Interleukin-6 attenuates the development of experimental diabetes-related neuropathy. Neuropathology 26:32-42.

Araque A, Li N, Doyle RT, Haydon PG (2000) SNARE protein-dependent glutamate release from astrocytes. J Neurosci 20:666-673.

Argyriou AA, Briani C, Cavaletti G, Bruna J, Alberti P, Velasco R, Lonardi S, Cortinovis D, Cazzaniga M, Campagnolo M, Santos C, Kalofonos HP (2013a) Advanced age and liability to oxaliplatin-induced peripheral neuropathy: post hoc analysis of a prospective study. Eur J Neurol 20:788-794.

Argyriou AA, Cavaletti G, Briani C, Velasco R, Bruna J, Campagnolo M, Alberti P, Bergamo F, Cortinovis D, Cazzaniga M, Santos C, Papadimitriou K, Kalofonos HP (2013b) Clinical pattern and associations of oxaliplatin acute neurotoxicity: a prospective study in 170 patients with colorectal cancer. Cancer 119:438-444.

Argyriou AA, Chroni E, Koutras A, Ellul J, Papapetropoulos S, Katsoulas G, Iconomou G, Kalofonos HP (2005a) Vitamin E for prophylaxis against chemotherapy-induced neuropathy: a randomized controlled trial. Neurology 64:26-31.

Argyriou AA, Chroni E, Polychronopoulos P, Iconomou G, Koutras A, Makatsoris T, Gerolymos MK, Gourzis P, Assimakopoulos K, Kalofonos HP (2006) Efficacy of oxcarbazepine for prophylaxis against cumulative oxaliplatin-induced neuropathy. Neurology 67:2253-2255.

Argyriou AA, Koutras A, Polychronopoulos P, Papapetropoulos S, Iconomou G, Katsoulas G, Makatsoris T, Kalofonos HP, Chroni E (2005b) The impact of paclitaxel or cisplatin-based chemotherapy on sympathetic skin response: a prospective study. Eur J Neurol 12:858-861.

Argyriou AA, Polychronopoulos P, Koutras A, Xiros N, Petsas T, Argyriou K, Kalofonos HP, Chroni E (2007) Clinical and electrophysiological features of peripheral neuropathy induced by administration of cisplatin plus paclitaxel-based chemotherapy. Eur J Cancer Care (Engl) 16:231-237.

Armstrong D, Dry RM, Keele CA, Markham JW (1953) Observations on chemical excitants of cutaneous pain in man. J Physiol 120:326-351.

Arrieta O, Michel Ortega RM, Villanueva-Rodriguez G, Serna-Thome MG, Flores-Estrada D, Diaz-Romero C, Rodriguez CM, Martinez L, Sanchez-Lara K (2010) Association of nutritional status and serum albumin levels with development of toxicity in patients with advanced non-small cell lung cancer treated with paclitaxel-cisplatin chemotherapy: a prospective study. BMC Cancer 10:50.

Aspinall AI, Curbishley SM, Lalor PF, Weston CJ, Liaskou E, Adams RM, Holt AP, Adams DH (2010) CX(3)CR1 and vascular adhesion protein-1-dependent recruitment of CD16(+) monocytes across human liver sinusoidal endothelium. Hepatology 51:2030-2039.

Atoyan R, Shander D, Botchkareva NV (2009) Non-neuronal expression of transient receptor potential type A1 (TRPA1) in human skin. J Invest Dermatol 129:2312-2315.

Attal N, Bouhassira D, Gautron M, Vaillant JN, Mitry E, Lepere C, Rougier P, Guirimand F (2009) Thermal hyperalgesia as a marker of oxaliplatin neurotoxicity: a prospective quantified sensory assessment study. Pain 144:245-252.

Auffray C, Fogg D, Garfa M, Elain G, Join-Lambert O, Kayal S, Sarnacki S, Cumano A, Lauvau G, Geissmann F (2007) Monitoring of blood vessels and tissues by a population of monocytes with patrolling behavior. Science 317:666-670.

Auffray C, Sieweke MH, Geissmann F (2009) Blood monocytes: development, heterogeneity, and relationship with dendritic cells. Annu Rev Immunol 27:669-692.

Augusto C, Pietro M, Cinzia M, Sergio C, Sara C, Luca G, Scaioli V (2008) Peripheral neuropathy due to paclitaxel: study of the temporal relationships between the therapeutic schedule and the clinical quantitative score (QST) and comparison with neurophysiological findings. J Neurooncol 86:89-99.

Authier N, Gillet JP, Fialip J, Eschalier A, Coudore F (2003) A new animal model of vincristine-induced nociceptive peripheral neuropathy. Neurotoxicology 24:797-805.

Averill S, McMahon SB, Clary DO, Reichardt LF, Priestley JV (1995) Immunocytochemical localization of trkA receptors in chemically identified subgroups of adult rat sensory neurons. Eur J Neurosci 7:1484-1494.

Avramis IA, Kwock R, Avramis VI (2001) Taxotere and vincristine inhibit the secretion of the angiogenesis inducing vascular endothelial growth factor (VEGF) by wild-type and drug-resistant human leukemia T-cell lines. Anticancer Res 21:2281-2286.

Baguley BC, Holdaway KM, Thomsen LL, Zhuang L, Zwi LJ (1991) Inhibition of growth of colon 38 adenocarcinoma by vinblastine and colchicine: evidence for a vascular mechanism. Eur J Cancer 27:482-487.

Baliki M, Al-Amin HA, Atweh SF, Jaber M, Hawwa N, Jabbur SJ, Apkarian AV, Saade NE (2003) Attenuation of neuropathic manifestations by local block of the activities of the ventrolateral orbito-frontal area in the rat. Neuroscience 120:1093-1104.

Balkwill F, Mantovani A (2001) Inflammation and cancer: back to Virchow? Lancet 357:539-545.

Bandell M, Story GM, Hwang SW, Viswanath V, Eid SR, Petrus MJ, Earley TJ, Patapoutian A (2004) Noxious cold ion channel TRPA1 is activated by pungent compounds and bradykinin. Neuron 41:849-857.

Bando H, Toi M (2000) Tumor angiogenesis, macrophages, and cytokines. Adv Exp Med Biol 476:267-284.

Bangham AD, Horne RW (1964) Negative staining of phospholipids and their structural modifcation by surface-active agents as observed in the electron microscope. J Mol Biol 8:660-668.

Bangham AD, Horne RW, Glauert AM, Dingle JT, Lucy JA (1962) Action of saponin on biological cell membranes. Nature 196:952-955.

Barclay J, Clark AK, Ganju P, Gentry C, Patel S, Wotherspoon G, Buxton F, Song C, Ullah J, Winter J, Fox A, Bevan S, Malcangio M (2007) Role of the cysteine protease cathepsin S in neuropathic hyperalgesia. Pain 130:225-234.

Baron R, Binder A, Wasner G (2010) Neuropathic pain: diagnosis, pathophysiological mechanisms, and treatment. Lancet Neurol 9:807-819.

Barreiro O, Zamai M, Yanez-Mo M, Tejera E, Lopez-Romero P, Monk PN, Gratton E, Caiolfa VR, Sanchez-Madrid F (2008) Endothelial adhesion receptors are recruited to adherent leukocytes by inclusion in preformed tetraspanin nanoplatforms. J Cell Biol 183:527-542.

Barriere DA, Rieusset J, Chanteranne D, Busserolles J, Chauvin MA, Chapuis L, Salles J, Dubray C, Morio B (2012) Paclitaxel therapy potentiates cold hyperalgesia in streptozotocin-induced diabetic rats through enhanced mitochondrial reactive oxygen species production and TRPA1 sensitization. Pain 153:553-561.

Barron L, Wynn TA (2011) Fibrosis is regulated by Th2 and Th17 responses and by dynamic interactions between fibroblasts and macrophages. Am J Physiol Gastrointest Liver Physiol 300:G723-G728.

Bartley EJ, Fillingim RB (2013) Sex differences in pain: a brief review of clinical and experimental findings. Br J Anaesth 111:52-58.

Bas DB, Su J, Sandor K, Agalave NM, Lundberg J, Codeluppi S, Baharpoor A, Nandakumar KS, Holmdahl R, Svensson CI (2012) Collagen antibody-induced arthritis evokes persistent pain with spinal glial involvement and transient prostaglandin dependency. Arthritis Rheum 64:3886-3896.

Basaki Y, Chikahisa L, Aoyagi K, Miyadera K, Yonekura K, Hashimoto A, Okabe S, Wierzba K, Yamada Y (2001) gamma-Hydroxybutyric acid and 5-fluorouracil, metabolites of UFT, inhibit the angiogenesis induced by vascular endothelial growth factor. Angiogenesis 4:163-173.

Bautista DM, Jordt SE, Nikai T, Tsuruda PR, Read AJ, Poblete J, Yamoah EN, Basbaum AI, Julius D (2006) TRPA1 mediates the inflammatory actions of environmental irritants and proalgesic agents. Cell 124:1269-1282.

Bautista DM, Pellegrino M, Tsunozaki M (2013) TRPA1: A gatekeeper for inflammation. Annu Rev Physiol 75:181-200.

Bautista DM, Siemens J, Glazer JM, Tsuruda PR, Basbaum AI, Stucky CL, Jordt SE, Julius D (2007) The menthol receptor TRPM8 is the principal detector of environmental cold. Nature 448:204-208.

Bazan JF, Bacon KB, Hardiman G, Wang W, Soo K, Rossi D, Greaves DR, Zlotnik A, Schall TJ (1997) A new class of membrane-bound chemokine with a CX3C motif. Nature 385:640-644.

Bee LA, Dickenson AH (2007) Rostral ventromedial medulla control of spinal sensory processing in normal and pathophysiological states. Neuroscience 147:786-793.

Beers C, Burich A, Kleijmeer MJ, Griffith JM, Wong P, Rudensky AY (2005) Cathepsin S controls MHC class II-mediated antigen presentation by epithelial cells in vivo. J Immunol 174:1205-1212.

Beers DR, Henkel JS, Xiao Q, Zhao W, Wang J, Yen AA, Siklos L, McKercher SR, Appel SH (2006) Wild-type microglia extend survival in PU.1 knockout mice with familial amyotrophic lateral sclerosis. Proc Natl Acad Sci U S A 103:16021-16026.

Beggs S, Salter MW (2007) Stereological and somatotopic analysis of the spinal microglial response to peripheral nerve injury. Brain Behav Immun 21:624-633.

Belkouch M, Dansereau MA, Reaux-Le GA, Van SJ, Beaudet N, Chraibi A, Melik-Parsadaniantz S, Sarret P (2011) The chemokine CCL2 increases Nav1.8 sodium channel activity in primary sensory neurons through a Gbetagamma-dependent mechanism. J Neurosci 31:18381-18390.

Bellelis P, Barbeiro DF, Rizzo LV, Baracat EC, Abrao MS, Podgaec S (2013) Transcriptional changes in the expression of chemokines related to natural killer and T-regulatory cells in patients with deep infiltrative endometriosis. Fertil Steril 99:1987-1993.

Beltramo M, Bernardini N, Bertorelli R, Campanella M, Nicolussi E, Fredduzzi S, Reggiani A (2006) CB2 receptor-mediated antihyperalgesia: possible direct involvement of neural mechanisms. Eur J Neurosci 23:1530-1538.

Bennett BK, Park SB, Lin CS, Friedlander ML, Kiernan MC, Goldstein D (2012) Impact of oxaliplatin-induced neuropathy: a patient perspective. Support Care Cancer 20:2959-2967.

Bennett GJ, Xie YK (1988) A peripheral mononeuropathy in rat that produces disorders of pain sensation like those seen in man. Pain 33:87-107.

Benson AB, III, Ajani JA, Catalano RB, Engelking C, Kornblau SM, Martenson JA, Jr., McCallum R, Mitchell EP, O'Dorisio TM, Vokes EE, Wadler S (2004) Recommended guidelines for the treatment of cancer treatment-induced diarrhea. J Clin Oncol 22:2918-2926.

Berger T, Malayeri R, Doppelbauer A, Krajnik G, Huber H, Auff E, Pirker R (1997) Neurological monitoring of neurotoxicity induced by paclitaxel/cisplatin chemotherapy. Eur J Cancer 33:1393-1399.

Bergsteinsdottir K, Kingston A, Mirsky R, Jessen KR (1991) Rat Schwann cells produce interleukin-1. J Neuroimmunol 34:15-23.

Berliner S, Rahima M, Sidi Y, Teplitsky Y, Zohar Y, Nussbaum B, Pinkhas J (1990) Acute coronary events following cisplatin-based chemotherapy. Cancer Invest 8:583-586.

Bianchi G, Vitali G, Caraceni A, Ravaglia S, Capri G, Cundari S, Zanna C, Gianni L (2005) Symptomatic and neurophysiological responses of paclitaxel- or cisplatin-induced neuropathy to oral acetyl-L-carnitine. Eur J Cancer 41:1746-1750.

Binder A, Stengel M, Maag R, Wasner G, Schoch R, Moosig F, Schommer B, Baron R (2007) Pain in oxaliplatin-induced neuropathy--sensitisation in the peripheral and central nociceptive system. Eur J Cancer 43:2658-2663.

Bingle L, Brown NJ, Lewis CE (2002) The role of tumour-associated macrophages in tumour progression: implications for new anticancer therapies. J Pathol 196:254-265.

Birch KA, Ewenstein BM, Golan DE, Pober JS (1994) Prolonged peak elevations in cytoplasmic free calcium ions, derived from intracellular stores, correlate with the extent of thrombin-stimulated exocytosis in single human umbilical vein endothelial cells. J Cell Physiol 160:545-554.

Birch KA, Pober JS, Zavoico GB, Means AR, Ewenstein BM (1992) Calcium/calmodulin transduces thrombin-stimulated secretion: studies in intact and minimally permeabilized human umbilical vein endothelial cells. J Cell Biol 118:1501-1510.

Biswas SK, Mantovani A (2010) Macrophage plasticity and interaction with lymphocyte subsets: cancer as a paradigm. Nat Immunol 11:889-896.

Blankman JL, Simon GM, Cravatt BF (2007) A comprehensive profile of brain enzymes that hydrolyze the endocannabinoid 2-arachidonoylglycerol. Chem Biol 14:1347-1356.

Blom AB, van Lent PL, Holthuysen AE, van der Kraan PM, Roth J, Van RN, van den Berg WB (2004) Synovial lining macrophages mediate osteophyte formation during experimental osteoarthritis. Osteoarthritis Cartilage 12:627-635.

Boivin N, Menasria R, Gosselin D, Rivest S, Boivin G (2012) Impact of deficiency in CCR2 and CX3CR1 receptors on monocytes trafficking in herpes simplex virus encephalitis. J Gen Virol 93:1294-1304.

Bolcskei K, Helyes Z, Szabo A, Sandor K, Elekes K, Nemeth J, Almasi R, Pinter E, Petho G, Szolcsanyi J (2005) Investigation of the role of TRPV1 receptors in acute and chronic nociceptive processes using gene-deficient mice. Pain 117:368-376.

Bolin LM, Verity AN, Silver JE, Shooter EM, Abrams JS (1995) Interleukin-6 production by Schwann cells and induction in sciatic nerve injury. J Neurochem 64:850-858.

Bonde AK, Tischler V, Kumar S, Soltermann A, Schwendener RA (2012) Intratumoral macrophages contribute to epithelial-mesenchymal transition in solid tumors. BMC Cancer 12:35.

Bonduelle O, Duffy D, Verrier B, Combadiere C, Combadiere B (2012) Cutting edge: Protective effect of CX3CR1+ dendritic cells in a vaccinia virus pulmonary infection model. J Immunol 188:952-956.

Booker L, Kinsey SG, Abdullah RA, Blankman JL, Long JZ, Ezzili C, Boger DL, Cravatt BF, Lichtman AH (2012) The fatty acid amide hydrolase (FAAH) inhibitor PF-3845 acts in the nervous system to reverse LPS-induced tactile allodynia in mice. Br J Pharmacol 165:2485-2496.

Boyette-Davis J, Dougherty PM (2011) Protection against oxaliplatin-induced mechanical hyperalgesia and intraepidermal nerve fiber loss by minocycline. Exp Neurol 229:353-357.

Bradbury EJ, Burnstock G, McMahon SB (1998) The expression of P2X3 purinoreceptors in sensory neurons: effects of axotomy and glial-derived neurotrophic factor. Mol Cell Neurosci 12:256-268.

Braz JM, Ackerman L, Basbaum AI (2011) Sciatic nerve transection triggers release and intercellular transfer of a genetically expressed macromolecular tracer in dorsal root ganglia. J Comp Neurol 519:2648-2657.

Breedveld FC (2002) Current and future management approaches for rheumatoid arthritis. Arthritis Res 4 Suppl 2:S16-S21.

Briani C, Campagnolo M, Lucchetta M, Cacciavillani M, Dalla TC, Granata G, Bergamo F, Lonardi S, Zagonel V, Cavaletti G, Ermani M, Padua L (2013) Ultrasound assessment of oxaliplatin-induced neuropathy and correlations with neurophysiologic findings. Eur J Neurol 20:188-192.

Brierley SM, Hughes PA, Page AJ, Kwan KY, Martin CM, O'Donnell TA, Cooper NJ, Harrington AM, Adam B, Liebregts T, Holtmann G, Corey DP, Rychkov GY, Blackshaw LA (2009) The ion channel TRPA1 is required for normal mechanosensation and is modulated by algesic stimuli. Gastroenterology 137:2084-2095.

Brouwers EE, Huitema AD, Boogerd W, Beijnen JH, Schellens JH (2009) Persistent neuropathy after treatment with cisplatin and oxaliplatin. Acta Oncol 48:832-841.

Brunello A, Kapoor R, Extermann M (2011) Hyperglycemia during chemotherapy for hematologic and solid tumors is correlated with increased toxicity. Am J Clin Oncol 34:292-296.

Budai D, Larson AA (1996) Role of substance P in the modulation of C-fiber-evoked responses of spinal dorsal horn neurons. Brain Res 710:197-203.

Bujalska M, Arazna M, Makulska-Nowak H, Gumulka SW (2008a) Alpha(1) and alpha(2)-adrenoreceptor antagonists in streptozotocin- and vincristine-induced hyperalgesia. Pharmacol Rep 60:499-507.

Bujalska M, Makulska-Nowak H, Gumulka SW (2009) Magnesium ions and opioid agonists in vincristine-induced neuropathy. Pharmacol Rep 61:1096-1104.

Bujalska M, Tatarkiewicz J, Gumulka SW (2008b) Effect of bradykinin receptor antagonists on vincristine- and streptozotocin-induced hyperalgesia in a rat model of chemotherapy-induced and diabetic neuropathy. Pharmacology 81:158-163.

Buldyrev I, Tanner NM, Hsieh HY, Dodd EG, Nguyen LT, Balkowiec A (2006) Calcitonin gene-related peptide enhances release of native brain-derived neurotrophic factor from trigeminal ganglion neurons. J Neurochem 99:1338-1350.

Burakgazi AZ, Messersmith W, Vaidya D, Hauer P, Hoke A, Polydefkis M (2011) Longitudinal assessment of oxaliplatin-induced neuropathy. Neurology 77:980-986.

Burgos E, Gomez-Nicola D, Pascual D, Martin MI, Nieto-Sampedro M, Goicoechea C (2012) Cannabinoid agonist WIN 55,212-2 prevents the development of paclitaxel-induced peripheral neuropathy in rats. Possible involvement of spinal glial cells. Eur J Pharmacol 682:62-72.

Byers MR (1984) Dental sensory receptors. Int Rev Neurobiol 25:39-94.

Cahoy JD, Emery B, Kaushal A, Foo LC, Zamanian JL, Christopherson KS, Xing Y, Lubischer JL, Krieg PA, Krupenko SA, Thompson WJ, Barres BA (2008) A transcriptome database for astrocytes, neurons, and oligodendrocytes: a new resource for understanding brain development and function. J Neurosci 28:264-278.

Callizot N, Andriambeloson E, Glass J, Revel M, Ferro P, Cirillo R, Vitte PA, Dreano M (2008) Interleukin-6 protects against paclitaxel, cisplatin and vincristine-induced neuropathies without impairing chemotherapeutic activity. Cancer Chemother Pharmacol 62:995-1007.

Calvo M, Bennett DL (2012) The mechanisms of microgliosis and pain following peripheral nerve injury. Exp Neurol 234:271-282.

Cambien B, Pomeranz M, Schmid-Antomarchi H, Millet MA, Breittmayer V, Rossi B, Schmid-Alliana A (2001) Signal transduction pathways involved in soluble fractalkine-induced monocytic cell adhesion. Blood 97:2031-2037.

Campbell JN, Meyer RA (2006) Mechanisms of neuropathic pain. Neuron 52:77-92.

Caprioli A, Coccurello R, Rapino C, Di SS, Di TM, Vertechy M, Vacca V, Battista N, Pavone F, Maccarrone M, Borsini F (2012) The novel reversible fatty acid amide hydrolase inhibitor ST4070 increases endocannabinoid brain levels and counteracts neuropathic pain in different animal models. J Pharmacol Exp Ther 342:188-195.

Cardona AE, Pioro EP, Sasse ME, Kostenko V, Cardona SM, Dijkstra IM, Huang D, Kidd G, Dombrowski S, Dutta R, Lee JC, Cook DN, Jung S, Lira SA, Littman DR, Ransohoff RM (2006) Control of microglial neurotoxicity by the fractalkine receptor. Nat Neurosci 9:917-924.

Carlson JD, Maire JJ, Martenson ME, Heinricher MM (2007) Sensitization of pain-modulating neurons in the rostral ventromedial medulla after peripheral nerve injury. J Neurosci 27:13222-13231.

Cartoni C, Brunetti GA, Federico V, Efficace F, Grammatico S, Tendas A, Scaramucci L, Cupelli L, D'Elia GM, Truini A, Niscola P, Petrucci MT (2012) Controlled-release oxycodone for the treatment of bortezomib-induced neuropathic pain in patients with multiple myeloma. Support Care Cancer 20:2621-2626.

Cascinu S, Catalano V, Cordella L, Labianca R, Giordani P, Baldelli AM, Beretta GD, Ubiali E, Catalano G (2002) Neuroprotective effect of reduced glutathione on oxaliplatin-based chemotherapy in advanced colorectal cancer: a randomized, double-blind, placebo-controlled trial. J Clin Oncol 20:3478-3483.

Casey EB, Jellife AM, Le Quesne PM, Millett YL (1973) Vincristine neuropathy. Clinical and electrophysiological observations. Brain 96:69-86.

Cata JP, Weng HR, Dougherty PM (2008) Behavioral and electrophysiological studies in rats with cisplatin-induced chemoneuropathy. Brain Res 1230:91-98.

Caterina MJ, Leffler A, Malmberg AB, Martin WJ, Trafton J, Petersen-Zeitz KR, Koltzenburg M, Basbaum AI, Julius D (2000) Impaired nociception and pain sensation in mice lacking the capsaicin receptor. Science 288:306-313.

Caterina MJ, Schumacher MA, Tominaga M, Rosen TA, Levine JD, Julius D (1997) The capsaicin receptor: a heat-activated ion channel in the pain pathway. Nature 389:816-824.

Cattaruzza F, Lyo V, Jones E, Pham D, Hawkins J, Kirkwood K, Valdez-Morales E, Ibeakanma C, Vanner SJ, Bogyo M, Bunnett NW (2011) Cathepsin S is activated during colitis and causes visceral hyperalgesia by a PAR2-dependent mechanism in mice. Gastroenterology 141:1864-1874.

Cen P, Liu C, Du XL (2012) Comparison of toxicity profiles of fluorouracil versus oxaliplatin regimens in a large population-based cohort of elderly patients with colorectal cancer. Ann Oncol 23:1503-1511.

Chacur M, Milligan ED, Gazda LS, Armstrong C, Wang H, Tracey KJ, Maier SF, Watkins LR (2001) A new model of sciatic inflammatory neuritis (SIN): induction of unilateral and bilateral mechanical allodynia following acute unilateral peri-sciatic immune activation in rats. Pain 94:231-244.

Chaplan SR, Bach FW, Pogrel JW, Chung JM, Yaksh TL (1994) Quantitative assessment of tactile allodynia in the rat paw. J Neurosci Methods 53:55-63.

Chen JJ, Lin YC, Yao PL, Yuan A, Chen HY, Shun CT, Tsai MF, Chen CH, Yang PC (2005) Tumor-associated macrophages: the double-edged sword in cancer progression. J Clin Oncol 23:953-964.

Chen MJ, Kress B, Han X, Moll K, Peng W, Ji RR, Nedergaard M (2012) Astrocytic CX43 hemichannels and gap junctions play a crucial role in development of chronic neuropathic pain following spinal cord injury. Glia 60:1660-1670.

Chen Y, Green SR, Almazan F, Quehenberger O (2006) The amino terminus and the third extracellular loop of CX3CR1 contain determinants critical for distinct receptor functions. Mol Pharmacol 69:857-865.

Chen Y, Yang C, Wang ZJ (2011) Proteinase-activated receptor 2 sensitizes transient receptor potential vanilloid 1, transient receptor potential vanilloid 4, and transient receptor potential ankyrin 1 in paclitaxel-induced neuropathic pain. Neuroscience 193:440-451.

Chen X, Geller EB, Rogers TJ, Adler MW (2007) The chemokine CX3CL1/fractalkine interferes with the antinociceptive effect induced by opioid agonists in the periaqueductal grey of rats. Brain Res 1153: 52-57.

Chessell IP, Hatcher JP, Bountra C, Michel AD, Hughes JP, Green P, Egerton J, Murfin M, Richardson J, Peck WL, Grahames CB, Casula MA, Yiangou Y, Birch R, Anand P, Buell GN (2005) Disruption of the P2X7 purinoceptor gene abolishes chronic inflammatory and neuropathic pain. Pain 114:386-396.

Cheunsuang O, Morris R (2000) Spinal lamina I neurons that express neurokinin 1 receptors: morphological analysis. Neuroscience 97:335-345.

Chien LY, Cheng JK, Chu D, Cheng CF, Tsaur ML (2007) Reduced expression of A-type potassium channels in primary sensory neurons induces mechanical hypersensitivity. J Neurosci 27:9855-9865.

Chinnery HR, McLenachan S, Humphries T, Kezic JM, Chen X, Ruitenberg MJ, McMenamin PG (2012) Accumulation of murine subretinal macrophages: effects of age, pigmentation and CX3CR1. Neurobiol Aging 33:1769-1776.

Cho HJ, Kim JK, Park HC, Kim JK, Kim DS, Ha SO, Hong HS (1998) Changes in brain-derived neurotrophic factor immunoreactivity in rat dorsal root ganglia, spinal cord, and gracile nuclei following cut or crush injuries. Exp Neurol 154:224-230.

Choi S, Na HS, Kim J, Lee J, Lee S, Kim D, Park J, Chen CC, Campbell KP, Shin HS (2007) Attenuated pain responses in mice lacking Ca(V)3.2 T-type channels. Genes Brain Behav 6:425-431.

Christoph T, Grunweller A, Mika J, Schafer MK, Wade EJ, Weihe E, Erdmann VA, Frank R, Gillen C, Kurreck J (2006) Silencing of vanilloid receptor TRPV1 by RNAi reduces neuropathic and visceral pain in vivo. Biochem Biophys Res Commun 350:238-243.

Cines DB, Pollak ES, Buck CA, Loscalzo J, Zimmerman GA, McEver RP, Pober JS, Wick TM, Konkle BA, Schwartz BS, Barnathan ES, McCrae KR, Hug BA, Schmidt AM, Stern DM (1998) Endothelial cells in physiology and in the pathophysiology of vascular disorders. Blood 91:3527-3561.

Claassen I, Van RN, Claassen E (1990) A new method for removal of mononuclear phagocytes from heterogeneous cell populations in vitro, using the liposome-mediated macrophage 'suicide' technique. J Immunol Methods 134:153-161.

Clapham DE, Montell C, Schultz G, Julius D (2003) International Union of Pharmacology. XLIII. Compendium of voltage-gated ion channels: transient receptor potential channels. Pharmacol Rev 55:591-596.

Clark AK, Gentry C, Bradbury EJ, McMahon SB, Malcangio M (2007a) Role of spinal microglia in rat models of peripheral nerve injury and inflammation. Eur J Pain 11:223-230.

Clark AK, Grist J, Al-Kashi A, Perretti M, Malcangio M (2012) Spinal cathepsin S and fractalkine contribute to chronic pain in the collagen-induced arthritis model. Arthritis Rheum 64:2038-2047.

Clark AK, Staniland AA, Malcangio M (2011) Fractalkine/CX3CR1 signalling in chronic pain and inflammation. Curr Pharm Biotechnol 12:1707-1714.

Clark AK, Staniland AA, Marchand F, Kaan TK, McMahon SB, Malcangio M (2010) P2X7-dependent release of interleukin-1beta and nociception in the spinal cord following lipopolysaccharide. J Neurosci 30:573-582.

Clark AK, Yip PK, Grist J, Gentry C, Staniland AA, Marchand F, Dehvari M, Wotherspoon G, Winter J, Ullah J, Bevan S, Malcangio M (2007b) Inhibition of spinal microglial cathepsin S for the reversal of neuropathic pain. Proc Natl Acad Sci U S A 104:10655-10660.

Clark AK, Yip PK, Malcangio M (2009) The liberation of fractalkine in the dorsal horn requires microglial cathepsin S. J Neurosci 29:6945-6954.

Clatworthy AL, Illich PA, Castro GA, Walters ET (1995) Role of peri-axonal inflammation in the development of thermal hyperalgesia and guarding behavior in a rat model of neuropathic pain. Neurosci Lett 184:5-8.

Clover AJ, Kumar AH, Caplice NM (2011) Deficiency of CX3CR1 delays burn wound healing and is associated with reduced myeloid cell recruitment and decreased sub-dermal angiogenesis. Burns 37:1386-1393.

Coffeen U, Lopez-Avila A, Ortega-Legaspi JM, del AR, Lopez-Munoz FJ, Pellicer F (2008) Dopamine receptors in the anterior insular cortex modulate long-term nociception in the rat. Eur J Pain 12:535-543.

Colburn RW, DeLeo JA, Rickman AJ, Yeager MP, Kwon P, Hickey WF (1997) Dissociation of microglial activation and neuropathic pain behaviors following peripheral nerve injury in the rat. J Neuroimmunol 79:163-175.

Colburn RW, Rickman AJ, DeLeo JA (1999) The effect of site and type of nerve injury on spinal glial activation and neuropathic pain behavior. Exp Neurol 157:289-304.

Collingridge GL, Isaac JT, Wang YT (2004) Receptor trafficking and synaptic plasticity. Nat Rev Neurosci 5:952-962.

Collins T, Read MA, Neish AS, Whitley MZ, Thanos D, Maniatis T (1995) Transcriptional regulation of endothelial cell adhesion molecules: NF-kappa B and cytokine-inducible enhancers. FASEB J 9:899-909.

Combadiere C, Feumi C, Raoul W, Keller N, Rodero M, Pezard A, Lavalette S, Houssier M, Jonet L, Picard E, Debre P, Sirinyan M, Deterre P, Ferroukhi T, Cohen SY, Chauvaud D, Jeanny JC, Chemtob S, Behar-Cohen F, Sennlaub F (2007) CX3CR1-dependent subretinal microglia cell accumulation is associated with cardinal features of age-related macular degeneration. J Clin Invest 117:2920-2928.

Combadiere C, Potteaux S, Gao JL, Esposito B, Casanova S, Lee EJ, Debre P, Tedgui A, Murphy PM, Mallat Z (2003) Decreased atherosclerotic lesion formation in CX3CR1/apolipoprotein E double knockout mice. Circulation 107:1009-1016.

Condeelis J, Pollard JW (2006) Macrophages: obligate partners for tumor cell migration, invasion, and metastasis. Cell 124:263-266.

Corcione A, Ferretti E, Bertolotto M, Fais F, Raffaghello L, Gregorio A, Tenca C, Ottonello L, Gambini C, Furtado G, Lira S, Pistoia V (2009) CX3CR1 is expressed by human B lymphocytes and mediates [corrected] CX3CL1 driven chemotaxis of tonsil centrocytes. PLoS One 4:e8485.

Costa G, Hreshchyhyn MM, Holland JF (1962) Initial clinical studies with vincristine. Cancer Chemother Rep 24:39-44.

Costa R, Motta EM, Dutra RC, Manjavachi MN, Bento AF, Malinsky FR, Pesquero JB, Calixto JB (2011) Anti-nociceptive effect of kinin B(1) and B(2) receptor antagonists on peripheral neuropathy induced by paclitaxel in mice. Br J Pharmacol 164:681-693.

Costigan M, Befort K, Karchewski L, Griffin RS, D'Urso D, Allchorne A, Sitarski J, Mannion JW, Pratt RE, Woolf CJ (2002) Replicate high-density rat genome oligonucleotide microarrays reveal hundreds of regulated genes in the dorsal root ganglion after peripheral nerve injury. BMC Neurosci 3:16.

Costigan M, et al. (2010) Multiple chronic pain states are associated with a common amino acid-changing allele in KCNS1. Brain 133:2519-2527.

Coull JA, Beggs S, Boudreau D, Boivin D, Tsuda M, Inoue K, Gravel C, Salter MW, De KY (2005) BDNF from microglia causes the shift in neuronal anion gradient underlying neuropathic pain. Nature 438:1017-1021.

Coull JA, Boudreau D, Bachand K, Prescott SA, Nault F, Sik A, De KP, De KY (2003) Trans-synaptic shift in anion gradient in spinal lamina I neurons as a mechanism of neuropathic pain. Nature 424:938-942.

Coulter DA, Eid T (2012) Astrocytic regulation of glutamate homeostasis in epilepsy. Glia 60:1215-1226.

Cox JJ, Reimann F, Nicholas AK, Thornton G, Roberts E, Springell K, Karbani G, Jafri H, Mannan J, Raashid Y, Al-Gazali L, Hamamy H, Valente EM, Gorman S, Williams R, McHale DP, Wood JN, Gribble FM, Woods CG (2006) An SCN9A channelopathy causes congenital inability to experience pain. Nature 444:894-898.

Coyle DE (1998) Partial peripheral nerve injury leads to activation of astroglia and microglia which parallels the development of allodynic behavior. Glia 23:75-83.

Coyle VM, Lungulescu D, Toganel C, Niculescu A, Pop S, Ciuleanu T, Cebotaru C, Devane J, Martin M, Wilson RH (2013) A randomised double-blind placebo-controlled phase II study of AGI004 for control of chemotherapy-induced diarrhoea. Br J Cancer 108:1027-1033.

Cravatt BF, Giang DK, Mayfield SP, Boger DL, Lerner RA, Gilula NB (1996) Molecular characterization of an enzyme that degrades neuromodulatory fatty-acid amides. Nature 384:83-87.

Cwikiel M, Eskilsson J, Albertsson M, Stavenow L (1996) The influence of 5-fluorouracil and methotrexate on vascular endothelium. An experimental study using endothelial cells in the culture. Ann Oncol 7:731-737.

D'Haese JG, Demir IE, Friess H, Ceyhan GO (2010) Fractalkine/CX3CR1: why a single chemokine-receptor duo bears a major and unique therapeutic potential. Expert Opin Ther Targets 14:207-219.

D'Haese JG, Friess H, Ceyhan GO (2012) Therapeutic potential of the chemokine-receptor duo fractalkine/CX3CR1: an update. Expert Opin Ther Targets 16:613-618.

D'Mello R, Dickenson AH (2008) Spinal cord mechanisms of pain. Br J Anaesth 101:8-16.

da Costa DS, Meotti FC, Andrade EL, Leal PC, Motta EM, Calixto JB (2010) The involvement of the transient receptor potential A1 (TRPA1) in the maintenance of mechanical and cold hyperalgesia in persistent inflammation. Pain 148:431-437.

Dagkalis A, Wallace C, Hing B, Liversidge J, Crane IJ (2009) CX3CR1-deficiency is associated with increased severity of disease in experimental autoimmune uveitis. Immunology 128:25-33.

Dagouassat M, Gagliolo JM, Chrusciel S, Bourin MC, Duprez C, Caramelle P, Boyer L, Hue S, Stern JB, Validire P, Longrois D, Norel X, Dubois-Rande JL, Le GS, Adnot S, Boczkowski J (2013) The cyclooxygenase-2-prostaglandin E2 pathway maintains senescence of chronic obstructive pulmonary disease fibroblasts. Am J Respir Crit Care Med 187:703-714.

Daher IN, Yeh ET (2008) Vascular complications of selected cancer therapies. Nat Clin Pract Cardiovasc Med 5:797-805.

Dahl E, Cohen SP (2008) Perineural injection of etanercept as a treatment for postamputation pain. Clin J Pain 24:172-175.

Dale DC, Boxer L, Liles WC (2008) The phagocytes: neutrophils and monocytes. Blood 112:935-945.

Damas JK, Boullier A, Waehre T, Smith C, Sandberg WJ, Green S, Aukrust P, Quehenberger O (2005) Expression of fractalkine (CX3CL1) and its receptor, CX3CR1, is elevated in coronary artery disease and is reduced during statin therapy. Arterioscler Thromb Vasc Biol 25:2567-2572.

Dangerfield J, Larbi KY, Huang MT, Dewar A, Nourshargh S (2002) PECAM-1 (CD31) homophilic interaction up-regulates alpha6beta1 on transmigrated neutrophils in vivo and plays a functional

role in the ability of alpha6 integrins to mediate leukocyte migration through the perivascular basement membrane. J Exp Med 196:1201-1211.

Daniele CA, Macdermott AB (2009) Low-threshold primary afferent drive onto GABAergic interneurons in the superficial dorsal horn of the mouse. J Neurosci 29:686-695.

Dansereau MA, Gosselin RD, Pohl M, Pommier B, Mechighel P, Mauborgne A, Rostene W, Kitabgi P, Beaudet N, Sarret P, Melik-Parsadaniantz S (2008) Spinal CCL2 pronociceptive action is no longer effective in CCR2 receptor antagonist-treated rats. J Neurochem 106:757-769.

Daulhac L, Mallet C, Courteix C, Etienne M, Duroux E, Privat AM, Eschalier A, Fialip J (2006) Diabetes-induced mechanical hyperalgesia involves spinal mitogen-activated protein kinase activation in neurons and microglia via N-methyl-D-aspartate-dependent mechanisms. Mol Pharmacol 70:1246-1254.

Davalos D, Grutzendler J, Yang G, Kim JV, Zuo Y, Jung S, Littman DR, Dustin ML, Gan WB (2005) ATP mediates rapid microglial response to local brain injury in vivo. Nat Neurosci 8:752-758.

Decosterd I, Woolf CJ (2000) Spared nerve injury: an animal model of persistent peripheral neuropathic pain. Pain 87:149-158.

Denes A, Ferenczi S, Halasz J, Kornyei Z, Kovacs KJ (2008) Role of CX3CR1 (fractalkine receptor) in brain damage and inflammation induced by focal cerebral ischemia in mouse. J Cereb Blood Flow Metab 28:1707-1721.

Deng L, Guindon J, Vemuri VK, Thakur GA, White FA, Makriyannis A, Hohmann AG (2012) The maintenance of cisplatin- and paclitaxel-induced mechanical and cold allodynia is suppressed by cannabinoid CB(2) receptor activation and independent of CXCR4 signaling in models of chemotherapy-induced peripheral neuropathy. Mol Pain 8:71.

Denoyer A, Godefroy D, Celerier I, Frugier J, Riancho L, Baudouin F, Rostene W, Baudouin C (2012) CX3CL1 expression in the conjunctiva is involved in immune cell trafficking during toxic ocular surface inflammation. Mucosal Immunol 5:702-711.

Dermietzel R, Hertberg EL, Kessler JA, Spray DC (1991) Gap junctions between cultured astrocytes: immunocytochemical, molecular, and electrophysiological analysis. J Neurosci 11:1421-1432.

Devor M (2001) Neuropathic pain: what do we do with all these theories? Acta Anaesthesiol Scand 45:1121-1127.

Di Cesare ML, Zanardelli M, Failli P, Ghelardini C (2012) Oxaliplatin-induced neuropathy: oxidative stress as pathological mechanism. Protective effect of silibinin. J Pain 13:276-284.

Dib-Hajj SD, Cummins TR, Black JA, Waxman SG (2007) From genes to pain: Na v 1.7 and human pain disorders. Trends Neurosci 30:555-563.

Dib-Hajj SD, Rush AM, Cummins TR, Hisama FM, Novella S, Tyrrell L, Marshall L, Waxman SG (2005) Gain-of-function mutation in Nav1.7 in familial erythromelalgia induces bursting of sensory neurons. Brain 128:1847-1854.

Dichmann S, Herouy Y, Purlis D, Rheinen H, Gebicke-Harter P, Norgauer J (2001) Fractalkine induces chemotaxis and actin polymerization in human dendritic cells. Inflamm Res 50:529-533.

Dickenson A (1983) The inhibitory effects of thalamic stimulation on the spinal transmission of nociceptive information in the rat. Pain 17:213-224.

Dina OA, Chen X, Reichling D, Levine JD (2001) Role of protein kinase Cepsilon and protein kinase A in a model of paclitaxel-induced painful peripheral neuropathy in the rat. Neuroscience 108:507-515.

Diogenes A, Akopian AN, Hargreaves KM (2007) NGF up-regulates TRPA1: implications for orofacial pain. J Dent Res 86:550-555.

Dixon GJ, Dulmadge EA, Mulligan LT, Mellett LB (1969) Cell culture bioassay for vincristine sulfate in sera from mice, rats, dogs, and monkeys. Cancer Res 29:1810-1813.

Dixon W (1980) Efficient analysis of experimental observations. Annu Rev Pharmacol Toxicol 20:441-462.

Docherty RJ, Farmer CE (2009) The pharmacology of voltage-gated sodium channels in sensory neurones. Handb Exp Pharmacol519-561.

Doerner JF, Gisselmann G, Hatt H, Wetzel CH (2007) Transient receptor potential channel A1 is directly gated by calcium ions. J Biol Chem 282:13180-13189.

Doll DC, List AF, Greco FA, Hainsworth JD, Hande KR, Johnson DH (1986) Acute vascular ischemic events after cisplatin-based combination chemotherapy for germ-cell tumors of the testis. Ann Intern Med 105:48-51.

Donnelly DJ, Longbrake EE, Shawler TM, Kigerl KA, Lai W, Tovar CA, Ransohoff RM, Popovich PG (2011) Deficient CX3CR1 signaling promotes recovery after mouse spinal cord injury by limiting the recruitment and activation of Ly6Clo/iNOS+ macrophages. J Neurosci 31:9910-9922.

Donohue MM, Cain K, Zierath D, Shibata D, Tanzi PM, Becker KJ (2012) Higher plasma fractalkine is associated with better 6-month outcome from ischemic stroke. Stroke 43:2300-2306.

Donoso JA, Green LS, Heller-Bettinger IE, Samson FE (1977) Action of the vinca alkaloids vincristine, vinblastine, and desacetyl vinblastine amide on axonal fibrillar organelles in vitro. Cancer Res 37:1401-1407.

Dougherty PM, Cata JP, Burton AW, Vu K, Weng HR (2007) Dysfunction in multiple primary afferent fiber subtypes revealed by quantitative sensory testing in patients with chronic vincristine-induced pain. J Pain Symptom Manage 33:166-179.

Dougherty PM, Cata JP, Cordella JV, Burton A, Weng HR (2004) Taxol-induced sensory disturbance is characterized by preferential impairment of myelinated fiber function in cancer patients. Pain 109:132-142.

Doyle T, Chen Z, Muscoli C, Bryant L, Esposito E, Cuzzocrea S, Dagostino C, Ryerse J, Rausaria S, Kamadulski A, Neumann WL, Salvemini D (2012) Targeting the overproduction of peroxynitrite for the prevention and reversal of paclitaxel-induced neuropathic pain. J Neurosci 32:6149-6160.

Drenth JP, Waxman SG (2007) Mutations in sodium-channel gene SCN9A cause a spectrum of human genetic pain disorders. J Clin Invest 117:3603-3609.

Drevs J, Fakler J, Eisele S, Medinger M, Bing G, Esser N, Marme D, Unger C (2004) Antiangiogenic potency of various chemotherapeutic drugs for metronomic chemotherapy. Anticancer Res 24:1759-1763.

Driessen CM, de Kleine-Bolt KM, Vingerhoets AJ, Mols F, Vreugdenhil G (2012) Assessing the impact of chemotherapy-induced peripheral neurotoxicity on the quality of life of cancer patients: the introduction of a new measure. Support Care Cancer 20:877-881.

Du S, Araki I, Yoshiyama M, Nomura T, Takeda M (2007) Transient receptor potential channel A1 involved in sensory transduction of rat urinary bladder through C-fiber pathway. Urology 70:826-831.

Dubuisson D, Dennis SG (1977) The formalin test: a quantitative study of the analgesic effects of morphine, meperidine, and brain stem stimulation in rats and cats. Pain 4:161-174.

Dumitru CD, Ceci JD, Tsatsanis C, Kontoyiannis D, Stamatakis K, Lin JH, Patriotis C, Jenkins NA, Copeland NG, Kollias G, Tsichlis PN (2000) TNF-alpha induction by LPS is regulated posttranscriptionally via a Tpl2/ERK-dependent pathway. Cell 103:1071-1083.

Duncan GS, Andrew DP, Takimoto H, Kaufman SA, Yoshida H, Spellberg J, de la Pompa JL, Elia A, Wakeham A, Karan-Tamir B, Muller WA, Senaldi G, Zukowski MM, Mak TW (1999) Genetic evidence for functional redundancy of Platelet/Endothelial cell adhesion molecule-1 (PECAM-1): CD31-deficient mice reveal PECAM-1-dependent and PECAM-1-independent functions. J Immunol 162:3022-3030.

Durrenberger PF, Facer P, Casula MA, Yiangou Y, Gray RA, Chessell IP, Day NC, Collins SD, Bingham S, Wilson AW, Elliot D, Birch R, Anand P (2006) Prostanoid receptor EP1 and Cox-2 in injured human nerves and a rat model of nerve injury: a time-course study. BMC Neurol 6:1.

Durrenberger PF, Facer P, Gray RA, Chessell IP, Naylor A, Bountra C, Banati RB, Birch R, Anand P (2004) Cyclooxygenase-2 (Cox-2) in injured human nerve and a rat model of nerve injury. J Peripher Nerv Syst 9:15-25.

Dworkin RH, O'Connor AB, Backonja M, Farrar JT, Finnerup NB, Jensen TS, Kalso EA, Loeser JD, Miaskowski C, Nurmikko TJ, Portenoy RK, Rice AS, Stacey BR, Treede RD, Turk DC, Wallace MS (2007) Pharmacologic management of neuropathic pain: evidence-based recommendations. Pain 132:237-251.

Earley S, Gonzales AL, Crnich R (2009) Endothelium-dependent cerebral artery dilation mediated by TRPA1 and Ca2+-Activated K+ channels. Circ Res 104:987-994.

Echeverry S, Shi XQ, Zhang J (2008) Characterization of cell proliferation in rat spinal cord following peripheral nerve injury and the relationship with neuropathic pain. Pain 135:37-47.

Echeverry S, Wu Y, Zhang J (2013) Selectively reducing cytokine/chemokine expressing macrophages in injured nerves impairs the development of neuropathic pain. Exp Neurol 240:205-218.

Eckhoff L, Nielsen M, Moeller S, Knoop A (2011) TAX. Acta Oncol 50:1075-1082.

Egashira N, Hirakawa S, Kawashiri T, Yano T, Ikesue H, Oishi R (2010) Mexiletine reverses oxaliplatin-induced neuropathic pain in rats. J Pharmacol Sci 112:473-476.

Eid SR, Crown ED, Moore EL, Liang HA, Choong KC, Dima S, Henze DA, Kane SA, Urban MO (2008) HC-030031, a TRPA1 selective antagonist, attenuates inflammatory- and neuropathy-induced mechanical hypersensitivity. Mol Pain 4:48.

El Karim IA, Linden GJ, Curtis TM, About I, McGahon MK, Irwin CR, Lundy FT (2011) Human odontoblasts express functional thermo-sensitive TRP channels: implications for dentin sensitivity. Pain 152:2211-2223.

El-Shazly AE, Doloriert HC, Bisig B, Lefebvre PP, Delvenne P, Jacobs N (2013) Novel cooperation between CX3CL1 and CCL26 inducing NK cell chemotaxis via CX3CR1: a possible mechanism for NK cell infiltration of the allergic nasal tissue. Clin Exp Allergy 43:322-331.

Eliav E, Herzberg U, Ruda MA, Bennett GJ (1999) Neuropathic pain from an experimental neuritis of the rat sciatic nerve. Pain 83:169-182.

Ellis A, Bennett DL (2013) Neuroinflammation and the generation of neuropathic pain. Br J Anaesth 111:26-37.

Emery EC, Young GT, Berrocoso EM, Chen L, McNaughton PA (2011) HCN2 ion channels play a central role in inflammatory and neuropathic pain. Science 333:1462-1466.

Endemann DH, Schiffrin EL (2004) Endothelial dysfunction. J Am Soc Nephrol 15:1983-1992.

Esfahani A, Ghoreishi Z, Nikanfar A, Sanaat Z, Ghorbanihaghjo A (2012) Influence of chemotherapy on the lipid peroxidation and antioxidant status in patients with acute myeloid leukemia. Acta Med Iran 50:454-458.

Everaerts W, Gees M, Alpizar YA, Farre R, Leten C, Apetrei A, Dewachter I, van LF, Vennekens R, De RD, Nilius B, Voets T, Talavera K (2011) The capsaicin receptor TRPV1 is a crucial mediator of the noxious effects of mustard oil. Curr Biol 21:316-321.

Falk S, Uldall M, Appel C, Ding M, Heegaard AM (2013) Influence of sex differences on the progression of cancer-induced bone pain. Anticancer Res 33:1963-1969.

Falsig J, Porzgen P, Lotharius J, Leist M (2004) Specific modulation of astrocyte inflammation by inhibition of mixed lineage kinases with CEP-1347. J Immunol 173:2762-2770.

Faure S, Meyer L, Costagliola D, Vaneensberghe C, Genin E, Autran B, Delfraissy JF, McDermott DH, Murphy PM, Debre P, Theodorou I, Combadiere C (2000) Rapid progression to AIDS in HIV+ individuals with a structural variant of the chemokine receptor CX3CR1. Science 287:2274-2277.

Feng L, Chen S, Garcia GE, Xia Y, Siani MA, Botti P, Wilson CB, Harrison JK, Bacon KB (1999) Prevention of crescentic glomerulonephritis by immunoneutralization of the fractalkine receptor CX3CR1 rapid communication. Kidney Int 56:612-620.

Ferlay J, Shin HR, Bray F, Forman D, Mathers C, Parkin DM (2010) Estimates of worldwide burden of cancer in 2008: GLOBOCAN 2008. Int J Cancer 127:2893-2917.

Fernandes ES, Russell FA, Spina D, McDougall JJ, Graepel R, Gentry C, Staniland AA, Mountford DM, Keeble JE, Malcangio M, Bevan S, Brain SD (2011) A distinct role for transient receptor potential ankyrin 1, in addition to transient receptor potential vanilloid 1, in tumor necrosis factor alpha-induced inflammatory hyperalgesia and Freund's complete adjuvant-induced monarthritis. Arthritis Rheum 63:819-829.

Fernyhough P, Calcutt NA (2010) Abnormal calcium homeostasis in peripheral neuropathies. Cell Calcium 47:130-139.

Fidanboylu M, Griffiths LA, Flatters SJ (2011) Global inhibition of reactive oxygen species (ROS) inhibits paclitaxel-induced painful peripheral neuropathy. PLoS One 6:e25212.

Fields HL, Heinricher MM (1989) Brainstem modulation of nociceptor-driven withdrawal reflexes. Ann N Y Acad Sci 563:34-44.

Fields HL, Malick A, Burstein R (1995) Dorsal horn projection targets of ON and OFF cells in the rostral ventromedial medulla. J Neurophysiol 74:1742-1759.

Fields HL, Vanegas H, Hentall ID, Zorman G (1983) Evidence that disinhibition of brain stem neurones contributes to morphine analgesia. Nature 306:684-686.

Fischer S, Kleinschnitz C, Muller M, Kobsar I, Ip CW, Rollins B, Martini R (2008a) Monocyte chemoattractant protein-1 is a pathogenic component in a model for a hereditary peripheral neuropathy. Mol Cell Neurosci 37:359-366.

Fischer S, Weishaupt A, Troppmair J, Martini R (2008b) Increase of MCP-1 (CCL2) in myelin mutant Schwann cells is mediated by MEK-ERK signaling pathway. Glia 56:836-843.

Flatters SJ, Bennett GJ (2004) Ethosuximide reverses paclitaxel- and vincristine-induced painful peripheral neuropathy. Pain 109:150-161.

Flatters SJ, Bennett GJ (2006) Studies of peripheral sensory nerves in paclitaxel-induced painful peripheral neuropathy: evidence for mitochondrial dysfunction. Pain 122:245-257.

Flatters SJ, Fox AJ, Dickenson AH (2003) Spinal interleukin-6 (IL-6) inhibits nociceptive transmission following neuropathy. Brain Res 984:54-62.

Flatters SJ, Fox AJ, Dickenson AH (2004) Nerve injury alters the effects of interleukin-6 on nociceptive transmission in peripheral afferents. Eur J Pharmacol 484:183-191.

Flatters SJ, Xiao WH, Bennett GJ (2006) Acetyl-L-carnitine prevents and reduces paclitaxel-induced painful peripheral neuropathy. Neurosci Lett 397:219-223.

Fong AM, Erickson HP, Zachariah JP, Poon S, Schamberg NJ, Imai T, Patel DD (2000) Ultrastructure and function of the fractalkine mucin domain in CX(3)C chemokine domain presentation. J Biol Chem 275:3781-3786.

Fong AM, Robinson LA, Steeber DA, Tedder TF, Yoshie O, Imai T, Patel DD (1998) Fractalkine and CX3CR1 mediate a novel mechanism of leukocyte capture, firm adhesion, and activation under physiologic flow. J Exp Med 188:1413-1419.

Foussat A, Coulomb-L'Hermine A, Gosling J, Krzysiek R, Durand-Gasselin I, Schall T, Balian A, Richard Y, Galanaud P, Emilie D (2000) Fractalkine receptor expression by T lymphocyte subpopulations and in vivo production of fractalkine in human. Eur J Immunol 30:87-97.

Freund J (1947) Some Aspects of Active Immunization. pp 291-308.

Frith JC, Monkkonen J, Auriola S, Monkkonen H, Rogers MJ (2001) The molecular mechanism of action of the antiresorptive and antiinflammatory drug clodronate: evidence for the formation in vivo of a metabolite that inhibits bone resorption and causes osteoclast and macrophage apoptosis. Arthritis Rheum 44:2201-2210.

Frith JC, Monkkonen J, Blackburn GM, Russell RG, Rogers MJ (1997) Clodronate and liposome-encapsulated clodronate are metabolized to a toxic ATP analog, adenosine 5'-(beta, gamma-dichloromethylene) triphosphate, by mammalian cells in vitro. J Bone Miner Res 12:1358-1367.

Fukuizumi T, Ohkubo T, Kitamura K (2003) Spinal sensitization mechanism in vincristine-induced hyperalgesia in mice. Neurosci Lett 343:89-92.

Furuyama T, Kiyama H, Sato K, Park HT, Maeno H, Takagi H, Tohyama M (1993) Region-specific expression of subunits of ionotropic glutamate receptors (AMPA-type, KA-type and NMDA receptors) in the rat spinal cord with special reference to nociception. Brain Res Mol Brain Res 18:141-151.

Gabay E, Wolf G, Shavit Y, Yirmiya R, Tal M (2011) Chronic blockade of interleukin-1 (IL-1) prevents and attenuates neuropathic pain behavior and spontaneous ectopic neuronal activity following nerve injury. Eur J Pain 15:242-248.

Galli SJ, Nakae S, Tsai M (2005) Mast cells in the development of adaptive immune responses. Nat Immunol 6:135-142.

Gamelin L, Boisdron-Celle M, Delva R, Guerin-Meyer V, Ifrah N, Morel A, Gamelin E (2004) Prevention of oxaliplatin-related neurotoxicity by calcium and magnesium infusions: a retrospective study of 161 patients receiving oxaliplatin combined with 5-Fluorouracil and leucovorin for advanced colorectal cancer. Clin Cancer Res 10:4055-4061.

Gan AM, Butoi ED, Manea A, Simion V, Stan D, Parvulescu MM, Calin M, Manduteanu I, Simionescu M (2013) Inflammatory effects of resistin on human smooth muscle cells: up-regulation of fractalkine and its receptor, CX3CR1 expression by TLR4 and Gi-protein pathways. Cell Tissue Res 351:161-174.

Gao YJ, Ji RR (2010a) Light touch induces ERK activation in superficial dorsal horn neurons after inflammation: involvement of spinal astrocytes and JNK signaling in touch-evoked central sensitization and mechanical allodynia. J Neurochem 115:505-514.

Gao YJ, Ji RR (2010b) Targeting astrocyte signaling for chronic pain. Neurotherapeutics 7:482-493.

Gao YJ, Xu ZZ, Liu YC, Wen YR, Decosterd I, Ji RR (2010a) The c-Jun N-terminal kinase 1 (JNK1) in spinal astrocytes is required for the maintenance of bilateral mechanical allodynia under a persistent inflammatory pain condition. Pain 148:309-319.

Gao YJ, Zhang L, Ji RR (2010b) Spinal injection of TNF-alpha-activated astrocytes produces persistent pain symptom mechanical allodynia by releasing monocyte chemoattractant protein-1. Glia 58:1871-1880.

Gao YJ, Zhang L, Samad OA, Suter MR, Yasuhiko K, Xu ZZ, Park JY, Lind AL, Ma Q, Ji RR (2009) JNK-induced MCP-1 production in spinal cord astrocytes contributes to central sensitization and neuropathic pain. J Neurosci 29:4096-4108.

Garrison CJ, Dougherty PM, Carlton SM (1994) GFAP expression in lumbar spinal cord of naive and neuropathic rats treated with MK-801. Exp Neurol 129:237-243.

Garrison CJ, Dougherty PM, Kajander KC, Carlton SM (1991) Staining of glial fibrillary acidic protein (GFAP) in lumbar spinal cord increases following a sciatic nerve constriction injury. Brain Res 565:1-7.

Garton KJ, Gough PJ, Blobel CP, Murphy G, Greaves DR, Dempsey PJ, Raines EW (2001) Tumor necrosis factor-alpha-converting enzyme (ADAM17) mediates the cleavage and shedding of fractalkine (CX3CL1). J Biol Chem 276:37993-38001.

Gauchan P, Andoh T, Kato A, Kuraishi Y (2009) Involvement of increased expression of transient receptor potential melastatin 8 in oxaliplatin-induced cold allodynia in mice. Neurosci Lett 458:93-95.

Gauer RL, Braun MM (2012) Thrombocytopenia. Am Fam Physician 85:612-622.

Gazzaniga S, Bravo AI, Guglielmotti A, Van RN, Maschi F, Vecchi A, Mantovani A, Mordoh J, Wainstok R (2007) Targeting tumor-associated macrophages and inhibition of MCP-1 reduce angiogenesis and tumor growth in a human melanoma xenograft. J Invest Dermatol 127:2031-2041.

Geis C, Beyreuther BK, Stohr T, Sommer C (2011) Lacosamide has protective disease modifying properties in experimental vincristine neuropathy. Neuropharmacology 61:600-607.

Geissmann F, Jung S, Littman DR (2003) Blood monocytes consist of two principal subsets with distinct migratory properties. Immunity 19:71-82.

Geissmann F, Manz MG, Jung S, Sieweke MH, Merad M, Ley K (2010) Development of monocytes, macrophages, and dendritic cells. Science 327:656-661.

Gentry C, Stoakley N, Andersson DA, Bevan S (2010) The roles of iPLA2, TRPM8 and TRPA1 in chemically induced cold hypersensitivity. Mol Pain 6:4.

Geraghty P, Greene CM, O'Mahony M, O'Neill SJ, Taggart CC, McElvaney NG (2007) Secretory leucocyte protease inhibitor inhibits interferon-gamma-induced cathepsin S expression. J Biol Chem 282:33389-33395.

Gershon MD (2003) Plasticity in serotonin control mechanisms in the gut. Curr Opin Pharmacol 3:600-607.

Geske FJ, Monks J, Lehman L, Fadok VA (2002) The role of the macrophage in apoptosis: hunter, gatherer, and regulator. Int J Hematol 76:16-26.

Ghilardi G, Biondi ML, Turri O, Guagnellini E, Scorza R (2004) Internal carotid artery occlusive disease and polymorphisms of fractalkine receptor CX3CR1: a genetic risk factor. Stroke 35:1276-1279.

Ghirardi O, Lo GP, Pisano C, Vertechy M, Bellucci A, Vesci L, Cundari S, Miloso M, Rigamonti LM, Nicolini G, Zanna C, Carminati P (2005a) Acetyl-L-Carnitine prevents and reverts experimental chronic neurotoxicity induced by oxaliplatin, without altering its antitumor properties. Anticancer Res 25:2681-2687.

Ghirardi O, Vertechy M, Vesci L, Canta A, Nicolini G, Galbiati S, Ciogli C, Quattrini G, Pisano C, Cundari S, Rigamonti LM (2005b) Chemotherapy-induced allodinia: neuroprotective effect of acetyl-L-carnitine. In Vivo 19:631-637.

Ghosh S, Wise LE, Chen Y, Gujjar R, Mahadevan A, Cravatt BF, Lichtman AH (2013) The monoacylglycerol lipase inhibitor JZL184 suppresses inflammatory pain in the mouse carrageenan model. Life Sci 92:498-505.

Giaume C, Fromaget C, el AA, Cordier J, Glowinski J, Gros D (1991) Gap junctions in cultured astrocytes: single-channel currents and characterization of channel-forming protein. Neuron 6:133-143.

Gidding CE, Kellie SJ, Kamps WA, de Graaf SS (1999) Vincristine revisited. Crit Rev Oncol Hematol 29:267-287.

Gilardini A, Avila RL, Oggioni N, Rodriguez-Menendez V, Bossi M, Canta A, Cavaletti G, Kirschner DA (2012) Myelin structure is unaltered in chemotherapy-induced peripheral neuropathy. Neurotoxicology 33:1-7.

Gilchrist M, Thorsson V, Li B, Rust AG, Korb M, Roach JC, Kennedy K, Hai T, Bolouri H, Aderem A (2006) Systems biology approaches identify ATF3 as a negative regulator of Toll-like receptor 4. Nature 441:173-178.

Go VL, Yaksh TL (1987) Release of substance P from the cat spinal cord. J Physiol 391:141-167.

Goda S, Imai T, Yoshie O, Yoneda O, Inoue H, Nagano Y, Okazaki T, Imai H, Bloom ET, Domae N, Umehara H (2000) CX3C-chemokine, fractalkine-enhanced adhesion of THP-1 cells to endothelial cells through integrin-dependent and -independent mechanisms. J Immunol 164:4313-4320.

Gogas KR (2006) Glutamate-based therapeutic approaches: NR2B receptor antagonists. Curr Opin Pharmacol 6:68-74.

Gordon MS, Cunningham D (2005) Managing patients treated with bevacizumab combination therapy. Oncology 69 Suppl 3:25-33.

Gordon S, Taylor PR (2005) Monocyte and macrophage heterogeneity. Nat Rev Immunol 5:953-964.

Gosselin RD, Varela C, Banisadr G, Mechighel P, Rostene W, Kitabgi P, Melik-Parsadaniantz S (2005) Constitutive expression of CCR2 chemokine receptor and inhibition by MCP-1/CCL2 of GABA-induced currents in spinal cord neurones. J Neurochem 95:1023-1034.

Gow DJ, Sester DP, Hume DA (2010) CSF-1, IGF-1, and the control of postnatal growth and development. J Leukoc Biol 88:475-481.

Graeber MB, Christie MJ (2012) Multiple mechanisms of microglia: a gatekeeper's contribution to pain states. Exp Neurol 234:255-261.

Gratzke C, Weinhold P, Reich O, Seitz M, Schlenker B, Stief CG, Andersson KE, Hedlund P (2010) Transient receptor potential A1 and cannabinoid receptor activity in human normal and hyperplastic prostate: relation to nerves and interstitial cells. Eur Urol 57:902-910.

Gray M, Palispis W, Popovich PG, Van RN, Gupta R (2007) Macrophage depletion alters the blood-nerve barrier without affecting Schwann cell function after neural injury. J Neurosci Res 85:766-777.

Groopman JE, Itri LM (1999) Chemotherapy-induced anemia in adults: incidence and treatment. J Natl Cancer Inst 91:1616-1634.

Gruber-Schoffnegger D, Drdla-Schutting R, Honigsperger C, Wunderbaldinger G, Gassner M, Sandkuhler J (2013) Induction of thermal hyperalgesia and synaptic long-term potentiation in the spinal cord lamina I by TNF-alpha and IL-1beta is mediated by glial cells. J Neurosci 33:6540-6551.

Guillouet M, Gueret G, Rannou F, Giroux-Metges MA, Gioux M, Arvieux CC, Pennec JP (2011) Tumor necrosis factor-alpha downregulates sodium current in skeletal muscle by protein kinase C activation: involvement in critical illness polyneuromyopathy. Am J Physiol Cell Physiol 301:C1057-C1063.

Guindon J, Hohmann AG (2009) The endocannabinoid system and pain. CNS Neurol Disord Drug Targets 8:403-421.

Guindon J, Lai Y, Takacs SM, Bradshaw HB, Hohmann AG (2013) Alterations in endocannabinoid tone following chemotherapy-induced peripheral neuropathy: effects of endocannabinoid deactivation inhibitors targeting fatty-acid amide hydrolase and monoacylglycerol lipase in comparison to reference analgesics following cisplatin treatment. Pharmacol Res 67:94-109.

Guo W, Wang H, Watanabe M, Shimizu K, Zou S, LaGraize SC, Wei F, Dubner R, Ren K (2007) Glial-cytokine-neuronal interactions underlying the mechanisms of persistent pain. J Neurosci 27:6006-6018.

Guptarak J, Wanchoo S, Durham-Lee J, Wu Y, Zivadinovic D, Paulucci-Holthauzen A, Nesic O (2013) Inhibition of IL-6 signaling: A novel therapeutic approach to treating spinal cord injury pain. Pain.

Guth AM, Hafeman SD, Dow SW (2012) Depletion of phagocytic myeloid cells triggers spontaneous T cell- and NK cell-dependent antitumor activity. Oncoimmunology 1:1248-1257.

Gwak YS, Hassler SE, Hulsebosch CE (2013) Reactive oxygen species contribute to neuropathic pain and locomotor dysfunction via activation of CamKII in remote segments following spinal cord contusion injury in rats. Pain 154:1699-1708.

Hadad N, Tuval L, Elgazar-Carmom V, Levy R, Levy R (2011) Endothelial ICAM-1 protein induction is regulated by cytosolic phospholipase A2alpha via both NF-kappaB and CREB transcription factors. J Immunol 186:1816-1827.

Hai T, Wolfgang CD, Marsee DK, Allen AE, Sivaprasad U (1999) ATF3 and stress responses. Gene Expr 7:321-335.

Halassa MM, Fellin T, Takano H, Dong JH, Haydon PG (2007) Synaptic islands defined by the territory of a single astrocyte. J Neurosci 27:6473-6477.

Halin S, Rudolfsson SH, Van RN, Bergh A (2009) Extratumoral macrophages promote tumor and vascular growth in an orthotopic rat prostate tumor model. Neoplasia 11:177-186.

Hamers FP, Brakkee JH, Cavalletti E, Tedeschi M, Marmonti L, Pezzoni G, Neijt JP, Gispen WH (1993) Reduced glutathione protects against cisplatin-induced neurotoxicity in rats. Cancer Res 53:544-549.

Hamers FP, van der Hoop RG, Steerenburg PA, Neijt JP, Gispen WH (1991) Putative neurotrophic factors in the protection of cisplatin-induced peripheral neuropathy in rats. Toxicol Appl Pharmacol 111:514-522.

Hamilton NB, Attwell D (2010) Do astrocytes really exocytose neurotransmitters? Nat Rev Neurosci 11:227-238.

Hanisch UK, Kettenmann H (2007) Microglia: active sensor and versatile effector cells in the normal and pathologic brain. Nat Neurosci 10:1387-1394.

Hansen N, Uceyler N, Palm F, Zelenka M, Biko L, Lesch KP, Gerlach M, Sommer C (2011) Serotonin transporter deficiency protects mice from mechanical allodynia and heat hyperalgesia in vincristine neuropathy. Neurosci Lett 495:93-97.

Hansen RR, Malcangio M (2013) Astrocytes-Multitaskers in chronic pain. Eur J Pharmacol.

Hargreaves K, Dubner R, Brown F, Flores C, Joris J (1988) A new and sensitive method for measuring thermal nociception in cutaneous hyperalgesia. Pain 32:77-88.

Harrison JK, Fong AM, Swain PA, Chen S, Yu YR, Salafranca MN, Greenleaf WB, Imai T, Patel DD (2001) Mutational analysis of the fractalkine chemokine domain. Basic amino acid residues differentially contribute to CX3CR1 binding, signaling, and cell adhesion. J Biol Chem 276:21632-21641.

Harrison JK, Jiang Y, Chen S, Xia Y, Maciejewski D, McNamara RK, Streit WJ, Salafranca MN, Adhikari S, Thompson DA, Botti P, Bacon KB, Feng L (1998) Role for neuronally derived fractalkine in mediating interactions between neurons and CX3CR1-expressing microglia. Proc Natl Acad Sci U S A 95:10896-10901.

Harrison JK, Jiang Y, Wees EA, Salafranca MN, Liang HX, Feng L, Belardinelli L (1999) Inflammatory agents regulate in vivo expression of fractalkine in endothelial cells of the rat heart. J Leukoc Biol 66:937-944.

Hartmann B, Ahmadi S, Heppenstall PA, Lewin GR, Schott C, Borchardt T, Seeburg PH, Zeilhofer HU, Sprengel R, Kuner R (2004) The AMPA receptor subunits GluR-A and GluR-B reciprocally modulate spinal synaptic plasticity and inflammatory pain. Neuron 44:637-650.

Haskell CA, Cleary MD, Charo IF (2000) Unique role of the chemokine domain of fractalkine in cell capture. Kinetics of receptor dissociation correlate with cell adhesion. J Biol Chem 275:34183-34189.

Hassel B, Paulsen RE, Johnsen A, Fonnum F (1992) Selective inhibition of glial cell metabolism in vivo by fluorocitrate. Brain Res 576:120-124.

Hathway GJ, Vega-Avelaira D, Moss A, Ingram R, Fitzgerald M (2009) Brief, low frequency stimulation of rat peripheral C-fibres evokes prolonged microglial-induced central sensitization in adults but not in neonates. Pain 144:110-118.

Haydon PG (2001) GLIA: listening and talking to the synapse. Nat Rev Neurosci 2:185-193.

Heinricher MM, Martenson ME, Neubert MJ (2004) Prostaglandin E2 in the midbrain periaqueductal gray produces hyperalgesia and activates pain-modulating circuitry in the rostral ventromedial medulla. Pain 110:419-426.

Heinricher MM, Tavares I, Leith JL, Lumb BM (2009) Descending control of nociception: Specificity, recruitment and plasticity. Brain Res Rev 60:214-225.

Henley JM, Jenkins R, Hunt SP (1993) Localisation of glutamate receptor binding sites and mRNAs to the dorsal horn of the rat spinal cord. Neuropharmacology 32:37-41.

Herbert MK, Just H, Schmidt RF (2001) Histamine excites groups III and IV afferents from the cat knee joint depending on their resting activity. Neurosci Lett 305:95-98.

Herkenham M, Lynn AB, Johnson MR, Melvin LS, de Costa BR, Rice KC (1991) Characterization and localization of cannabinoid receptors in rat brain: a quantitative in vitro autoradiographic study. J Neurosci 11:563-583.

Hermand P, Pincet F, Carvalho S, Ansanay H, Trinquet E, Daoudi M, Combadiere C, Deterre P (2008) Functional adhesiveness of the CX3CL1 chemokine requires its aggregation. Role of the transmembrane domain. J Biol Chem 283:30225-30234.

Herrero JF, Laird JM, Lopez-Garcia JA (2000) Wind-up of spinal cord neurones and pain sensation: much ado about something? Prog Neurobiol 61:169-203.

Hill K, Schaefer M (2007) TRPA1 is differentially modulated by the amphipathic molecules trinitrophenol and chlorpromazine. J Biol Chem 282:7145-7153.

Hill SA, Lonergan SJ, Denekamp J, Chaplin DJ (1993) Vinca alkaloids: anti-vascular effects in a murine tumour. Eur J Cancer 29A:1320-1324.

Himes RH, Kersey RN, Heller-Bettinger I, Samson FE (1976) Action of the vinca alkaloids vincristine, vinblastine, and desacetyl vinblastine amide on microtubules in vitro. Cancer Res 36:3798-3802.

Hinman A, Chuang HH, Bautista DM, Julius D (2006) TRP channel activation by reversible covalent modification. Proc Natl Acad Sci U S A 103:19564-19568.

Hohmann AG, Herkenham M (1999) Localization of central cannabinoid CB1 receptor messenger RNA in neuronal subpopulations of rat dorsal root ganglia: a double-label in situ hybridization study. Neuroscience 90:923-931.

Hollmann M, Heinemann S (1994) Cloned glutamate receptors. Annu Rev Neurosci 17:31-108.

Holmes FE, Arnott N, Vanderplank P, Kerr NC, Longbrake EE, Popovich PG, Imai T, Combadiere C, Murphy PM, Wynick D (2008) Intra-neural administration of fractalkine attenuates neuropathic pain-related behaviour. J Neurochem 106:640-649.

Holness CL, Simmons DL (1993) Molecular cloning of CD68, a human macrophage marker related to lysosomal glycoproteins. Blood 81:1607-1613.

Hong S, Wiley JW (2006) Altered expression and function of sodium channels in large DRG neurons and myelinated A-fibers in early diabetic neuropathy in the rat. Biochem Biophys Res Commun 339:652-660.

Hoogerwerf WA, Zou L, Shenoy M, Sun D, Micci MA, Lee-Hellmich H, Xiao SY, Winston JH, Pasricha PJ (2001) The proteinase-activated receptor 2 is involved in nociception. J Neurosci 21:9036-9042.

Horne RW, Bangham AD, Whittaker VP (1963) Negatively stained lipoprotein membranes. Nature 200:1340.

Hosobuchi Y, Adams JE, Rutkin B (1973) Chronic thalamic stimulation for the control of facial anesthesia dolorosa. Arch Neurol 29:158-161.

Howlett AC, Breivogel CS, Childers SR, Deadwyler SA, Hampson RE, Porrino LJ (2004) Cannabinoid physiology and pharmacology: 30 years of progress. Neuropharmacology 47 Suppl 1:345-358.

Hu JH, Yang JP, Liu L, Li CF, Wang LN, Ji FH, Cheng H (2012) Involvement of CX3CR1 in bone cancer pain through the activation of microglia p38 MAPK pathway in the spinal cord. Brain Res 1465:1-9.

Hu P, McLachlan EM (2002) Macrophage and lymphocyte invasion of dorsal root ganglia after peripheral nerve lesions in the rat. Neuroscience 112:23-38.

Hua XY, Svensson CI, Matsui T, Fitzsimmons B, Yaksh TL, Webb M (2005) Intrathecal minocycline attenuates peripheral inflammation-induced hyperalgesia by inhibiting p38 MAPK in spinal microglia. Eur J Neurosci 22:2431-2440.

Huang YW, Su P, Liu GY, Crow MR, Chaukos D, Yan H, Robinson LA (2009) Constitutive endocytosis of the chemokine CX3CL1 prevents its degradation by cell surface metalloproteases. J Biol Chem 284:29644-29653.

Huang ZJ, Li HC, Cowan AA, Liu S, Zhang YK, Song XJ (2012) Chronic compression or acute dissociation of dorsal root ganglion induces cAMP-dependent neuronal hyperexcitability through activation of PAR2. Pain 153:1426-1437.

Hudson LJ, Bevan S, Wotherspoon G, Gentry C, Fox A, Winter J (2001) VR1 protein expression increases in undamaged DRG neurons after partial nerve injury. Eur J Neurosci 13:2105-2114.

Hughes PM, Botham MS, Frentzel S, Mir A, Perry VH (2002) Expression of fractalkine (CX3CL1) and its receptor, CX3CR1, during acute and chronic inflammation in the rodent CNS. Glia 37:314-327.

Huitinga I, Damoiseaux JG, Van RN, Dopp EA, Dijkstra CD (1992) Liposome mediated affection of monocytes. Immunobiology 185:11-19.

Hundhausen C, Misztela D, Berkhout TA, Broadway N, Saftig P, Reiss K, Hartmann D, Fahrenholz F, Postina R, Matthews V, Kallen KJ, Rose-John S, Ludwig A (2003) The disintegrin-like metalloproteinase ADAM10 is involved in constitutive cleavage of CX3CL1 (fractalkine) and regulates CX3CL1-mediated cell-cell adhesion. Blood 102:1186-1195.

Hundhausen C, Schulte A, Schulz B, Andrzejewski MG, Schwarz N, von HP, Winter U, Paliga K, Reiss K, Saftig P, Weber C, Ludwig A (2007) Regulated shedding of transmembrane chemokines by the disintegrin and metalloproteinase 10 facilitates detachment of adherent leukocytes. J Immunol 178:8064-8072.

Hynes RO (1992) Integrins: versatility, modulation, and signaling in cell adhesion. Cell 69:11-25.

Iftinca MC, Zamponi GW (2009) Regulation of neuronal T-type calcium channels. Trends Pharmacol Sci 30:32-40.

Ikejima H, Imanishi T, Tsujioka H, Kashiwagi M, Kuroi A, Tanimoto T, Kitabata H, Ishibashi K, Komukai K, Takeshita T, Akasaka T (2010) Upregulation of fractalkine and its receptor, CX3CR1, is associated with coronary plaque rupture in patients with unstable angina pectoris. Circ J 74:337-345.

Ikuno N, Soda H, Watanabe M, Oka M (1995) Irinotecan (CPT-11) and characteristic mucosal changes in the mouse ileum and cecum. J Natl Cancer Inst 87:1876-1883.

Imai T, Hieshima K, Haskell C, Baba M, Nagira M, Nishimura M, Kakizaki M, Takagi S, Nomiyama H, Schall TJ, Yoshie O (1997) Identification and molecular characterization of fractalkine receptor CX3CR1, which mediates both leukocyte migration and adhesion. Cell 91:521-530.

Inoue K, Tsuda M (2009) Microglia and neuropathic pain. Glia 57:1469-1479.

Inquimbert P, Rodeau JL, Schlichter R (2007) Differential contribution of GABAergic and glycinergic components to inhibitory synaptic transmission in lamina II and laminae III-IV of the young rat spinal cord. Eur J Neurosci 26:2940-2949.

Ishida Y, Gao JL, Murphy PM (2008a) Chemokine receptor CX3CR1 mediates skin wound healing by promoting macrophage and fibroblast accumulation and function. J Immunol 180:569-579.

Ishida Y, Hayashi T, Goto T, Kimura A, Akimoto S, Mukaida N, Kondo T (2008b) Essential involvement of CX3CR1-mediated signals in the bactericidal host defense during septic peritonitis. J Immunol 181:4208-4218.

Iwamoto T, Ishibashi M, Fujieda A, Masuya M, Katayama N, Okuda M (2010) Drug interaction between itraconazole and bortezomib: exacerbation of peripheral neuropathy and thrombocytopenia induced by bortezomib. Pharmacotherapy 30:661-665.

Ja'afer FM, Hamdan FB, Mohammed FH (2006) Vincristine-induced neuropathy in rat: electrophysiological and histological study. Exp Brain Res 173:334-345.

Jain A, Bronneke S, Kolbe L, Stab F, Wenck H, Neufang G (2011) TRP-channel-specific cutaneous eicosanoid release patterns. Pain 152:2765-2772.

Jakowec MW, Yen L, Kalb RG (1995) In situ hybridization analysis of AMPA receptor subunit gene expression in the developing rat spinal cord. Neuroscience 67:909-920.

James SE, Dunham M, Carrion-Jones M, Murashov A, Lu Q (2010) Rho kinase inhibitor Y-27632 facilitates recovery from experimental peripheral neuropathy induced by anti-cancer drug cisplatin. Neurotoxicology 31:188-194.

Jamieson SM, Liu JJ, Connor B, Dragunow M, McKeage MJ (2007) Nucleolar enlargement, nuclear eccentricity and altered cell body immunostaining characteristics of large-sized sensory neurons following treatment of rats with paclitaxel. Neurotoxicology 28:1092-1098.

Janssen SP, Truin M, Van KM, Joosten EA (2011) Differential GABAergic disinhibition during the development of painful peripheral neuropathy. Neuroscience 184:183-194.

Jaquemar D, Schenker T, Trueb B (1999) An ankyrin-like protein with transmembrane domains is specifically lost after oncogenic transformation of human fibroblasts. J Biol Chem 274:7325-7333.

Jardim DL, Rodrigues CA, Novis YA, Rocha VG, Hoff PM (2012) Oxaliplatin-related thrombocytopenia. Ann Oncol 23:1937-1942.

Jasmin L, Boudah A, Ohara PT (2003a) Long-term effects of decreased noradrenergic central nervous system innervation on pain behavior and opioid antinociception. J Comp Neurol 460:38-55.

Jasmin L, Rabkin SD, Granato A, Boudah A, Ohara PT (2003b) Analgesia and hyperalgesia from GABA-mediated modulation of the cerebral cortex. Nature 424:316-320.

Ji G, Zhou S, Carlton SM (2008) Intact Adelta-fibers up-regulate transient receptor potential A1 and contribute to cold hypersensitivity in neuropathic rats. Neuroscience 154:1054-1066.

Ji RR, Samad TA, Jin SX, Schmoll R, Woolf CJ (2002) p38 MAPK activation by NGF in primary sensory neurons after inflammation increases TRPV1 levels and maintains heat hyperalgesia. Neuron 36:57-68.

Ji XT, Qian NS, Zhang T, Li JM, Li XK, Wang P, Zhao DS, Huang G, Zhang L, Fei Z, Jia D, Niu L (2013) Spinal astrocytic activation contributes to mechanical allodynia in a rat chemotherapy-induced neuropathic pain model. PLoS One 8:e60733.

Jimenez-Andrade JM, Peters CM, Mejia NA, Ghilardi JR, Kuskowski MA, Mantyh PW (2006) Sensory neurons and their supporting cells located in the trigeminal, thoracic and lumbar ganglia differentially express markers of injury following intravenous administration of paclitaxel in the rat. Neurosci Lett 405:62-67.

Jin SX, Zhuang ZY, Woolf CJ, Ji RR (2003) p38 mitogen-activated protein kinase is activated after a spinal nerve ligation in spinal cord microglia and dorsal root ganglion neurons and contributes to the generation of neuropathic pain. J Neurosci 23:4017-4022.

Johnson DC, Corthals SL, Walker BA, Ross FM, Gregory WM, Dickens NJ, Lokhorst HM, Goldschmidt H, Davies FE, Durie BG, Van NB, Child JA, Sonneveld P, Morgan GJ (2011) Genetic factors underlying the risk of thalidomide-related neuropathy in patients with multiple myeloma. J Clin Oncol 29:797-804.

Jones BA, Riegsecker S, Rahman A, Beamer M, Aboualaiwi W, Khuder SA, Ahmed S (2013) Role of ADAM17, p38 MAPK, cathepsins, and proteasome pathway in the synthesis and shedding of fractalkine/CX3CL1 in rheumatoid arthritis. Arthritis Rheum.

Joseph EK, Levine JD (2006) Mitochondrial electron transport in models of neuropathic and inflammatory pain. Pain 121:105-114.

Jung S, Aliberti J, Graemmel P, Sunshine MJ, Kreutzberg GW, Sher A, Littman DR (2000) Analysis of fractalkine receptor CX(3)CR1 function by targeted deletion and green fluorescent protein reporter gene insertion. Mol Cell Biol 20:4106-4114.

Kabbinavar F, Hurwitz HI, Fehrenbacher L, Meropol NJ, Novotny WF, Lieberman G, Griffing S, Bergsland E (2003) Phase II, randomized trial comparing bevacizumab plus fluorouracil (FU)/leucovorin (LV) with FU/LV alone in patients with metastatic colorectal cancer. J Clin Oncol 21:60-65.

Kacinski BM (1995) CSF-1 and its receptor in ovarian, endometrial and breast cancer. Ann Med 27:79-85.

Kamba T, McDonald DM (2007) Mechanisms of adverse effects of anti-VEGF therapy for cancer. Br J Cancer 96:1788-1795.

Kanbayashi Y, Hosokawa T, Kitawaki J, Taguchi T (2013) Statistical identification of predictors for paclitaxel-induced peripheral neuropathy in patients with breast or gynaecological cancer. Anticancer Res 33:1153-1156.

Kang K, Pulver SR, Panzano VC, Chang EC, Griffith LC, Theobald DL, Garrity PA (2010) Analysis of Drosophila TRPA1 reveals an ancient origin for human chemical nociception. Nature 464:597-600.

Karashima Y, Prenen J, Talavera K, Janssens A, Voets T, Nilius B (2010) Agonist-induced changes in Ca(2+) permeation through the nociceptor cation channel TRPA1. Biophys J 98:773-783.

Kashiba H, Fukui H, Morikawa Y, Senba E (1999) Gene expression of histamine H1 receptor in guinea pig primary sensory neurons: a relationship between H1 receptor mRNA-expressing neurons and peptidergic neurons. Brain Res Mol Brain Res 66:24-34.

Kato K, Kikuchi S, Shubayev VI, Myers RR (2009) Distribution and tumor necrosis factor-alpha isoform binding specificity of locally administered etanercept into injured and uninjured rat sciatic nerve. Neuroscience 160:492-500.

Katsura H, Obata K, Mizushima T, Yamanaka H, Kobayashi K, Dai Y, Fukuoka T, Tokunaga A, Sakagami M, Noguchi K (2006) Antisense knock down of TRPA1, but not TRPM8, alleviates cold hyperalgesia after spinal nerve ligation in rats. Exp Neurol 200:112-123.

Katsuyama S, Sato K, Yagi T, Kishikawa Y, Nakamura H (2013) Effects of repeated milnacipran and fluvoxamine treatment on mechanical allodynia in a mouse paclitaxel-induced neuropathic pain model. Biomed Res 34:105-111.

Kautio AL, Haanpaa M, Kautiainen H, Kalso E, Saarto T (2011) Burden of chemotherapy-induced neuropathy--a cross-sectional study. Support Care Cancer 19:1991-1996.

Kautio AL, Haanpaa M, Saarto T, Kalso E (2008) Amitriptyline in the treatment of chemotherapy-induced neuropathic symptoms. J Pain Symptom Manage 35:31-39.

Kawasaki Y, Zhang L, Cheng JK, Ji RR (2008) Cytokine mechanisms of central sensitization: distinct and overlapping role of interleukin-1beta, interleukin-6, and tumor necrosis factor-alpha in regulating synaptic and neuronal activity in the superficial spinal cord. J Neurosci 28:5189-5194.

Kawashiri T, Egashira N, Itoh Y, Shimazoe T, Ikegami Y, Yano T, Yoshimura M, Oishi R (2009) Neurotropin reverses paclitaxel-induced neuropathy without affecting anti-tumour efficacy. Eur J Cancer 45:154-163.

Kellum JM, Albuquerque FC, Stoner MC, Harris RP (1999) Stroking human jejunal mucosa induces 5-HT release and Cl- secretion via afferent neurons and 5-HT4 receptors. Am J Physiol 277:G515-G520.

Kenney B, Stack G (2009) Drug-induced thrombocytopenia. Arch Pathol Lab Med 133:309-314.

Kerfoot SM, Lord SE, Bell RB, Gill V, Robbins SM, Kubes P (2003) Human fractalkine mediates leukocyte adhesion but not capture under physiological shear conditions; a mechanism for selective monocyte recruitment. Eur J Immunol 33:729-739.

Kerr BJ, Bradbury EJ, Bennett DL, Trivedi PM, Dassan P, French J, Shelton DB, McMahon SB, Thompson SW (1999) Brain-derived neurotrophic factor modulates nociceptive sensory inputs and NMDA-evoked responses in the rat spinal cord. J Neurosci 19:5138-5148.

Kew JN, Kemp JA (2005) Ionotropic and metabotropic glutamate receptor structure and pharmacology. Psychopharmacology (Berl) 179:4-29.

Khan B, Rangasamy S, McGuire PG, Howdieshell TR (2013) The role of monocyte subsets in myocutaneous revascularization. J Surg Res 183:963-975.

Khasabova IA, Khasabov S, Paz J, Harding-Rose C, Simone DA, Seybold VS (2012) Cannabinoid type-1 receptor reduces pain and neurotoxicity produced by chemotherapy. J Neurosci 32:7091-7101.

Kigerl KA, McGaughy VM, Popovich PG (2006) Comparative analysis of lesion development and intraspinal inflammation in four strains of mice following spinal contusion injury. J Comp Neurol 494:578-594.

Kiguchi N, Maeda T, Kobayashi Y, Kishioka S (2008a) Up-regulation of tumor necrosis factor-alpha in spinal cord contributes to vincristine-induced mechanical allodynia in mice. Neurosci Lett 445:140-143.

Kiguchi N, Maeda T, Kobayashi Y, Kondo T, Ozaki M, Kishioka S (2008b) The critical role of invading peripheral macrophage-derived interleukin-6 in vincristine-induced mechanical allodynia in mice. Eur J Pharmacol 592:87-92.

Kim BJ, Park HR, Roh HJ, Jeong DS, Kim BS, Park KW, Cho SC, So YT, Oh SY, Kim SJ (2010) Chemotherapy-related polyneuropathy may deteriorate quality of life in patients with B-cell lymphoma. Qual Life Res 19:1097-1103.

Kim CF, Moalem-Taylor G (2011) Detailed characterization of neuro-immune responses following neuropathic injury in mice. Brain Res 1405:95-108.

Kim DS, Figueroa KW, Li KW, Boroujerdi A, Yolo T, Luo ZD (2009) Profiling of dynamically changed gene expression in dorsal root ganglia post peripheral nerve injury and a critical role of injury-induced glial fibrillary acidic protein in maintenance of pain behaviors [corrected]. Pain 143:114-122.

Kim KW, Vallon-Eberhard A, Zigmond E, Farache J, Shezen E, Shakhar G, Ludwig A, Lira SA, Jung S (2011) In vivo structure/function and expression analysis of the CX3C chemokine fractalkine. Blood 118:e156-e167.

Kim S, Seiryu M, Okada S, Kuroishi T, Takano-Yamamoto T, Sugawara S, Endo Y (2013) Analgesic effects of the non-nitrogen-containing bisphosphonates etidronate and clodronate, independent of anti-resorptive effects on bone. Eur J Pharmacol 699:14-22.

Kim SH, Chung JM (1992) An experimental model for peripheral neuropathy produced by segmental spinal nerve ligation in the rat. Pain 50:355-363.

Kimura YN, Watari K, Fotovati A, Hosoi F, Yasumoto K, Izumi H, Kohno K, Umezawa K, Iguchi H, Shirouzu K, Takamori S, Kuwano M, Ono M (2007) Inflammatory stimuli from macrophages and cancer cells synergistically promote tumor growth and angiogenesis. Cancer Sci 98:2009-2018.

King IL, Dickendesher TL, Segal BM (2009) Circulating Ly-6C+ myeloid precursors migrate to the CNS and play a pathogenic role during autoimmune demyelinating disease. Blood 113:3190-3197.

Kinsey SG, Long JZ, Cravatt BF, Lichtman AH (2010) Fatty acid amide hydrolase and monoacylglycerol lipase inhibitors produce anti-allodynic effects in mice through distinct cannabinoid receptor mechanisms. J Pain 11:1420-1428.

Kirschke H, Schmidt I, Wiederanders B (1986) Cathepsin S. The cysteine proteinase from bovine lymphoid tissue is distinct from cathepsin L (EC 3.4.22.15). Biochem J 240:455-459.

Kjaergaard AG, Dige A, Krog J, Tonnesen E, Wogensen L (2013) Soluble Adhesion Molecules Correlate with Surface Expression in an In Vitro Model of Endothelial Activation. Basic Clin Pharmacol Toxicol.

Klein CL, Bittinger F, Skarke CC, Wagner M, Kohler H, Walgenbach S, Kirkpatrick CJ (1995) Effects of cytokines on the expression of cell adhesion molecules by cultured human omental mesothelial cells. Pathobiology 63:204-212.

Knight K, Wade S, Balducci L (2004) Prevalence and outcomes of anemia in cancer: a systematic review of the literature. Am J Med 116 Suppl 7A:11S-26S.

Kobayashi K, Fukuoka T, Obata K, Yamanaka H, Dai Y, Tokunaga A, Noguchi K (2005) Distinct expression of TRPM8, TRPA1, and TRPV1 mRNAs in rat primary afferent neurons with adelta/c-fibers and colocalization with trk receptors. J Comp Neurol 493:596-606.

Kocher L, Anton F, Reeh PW, Handwerker HO (1987) The effect of carrageenan-induced inflammation on the sensitivity of unmyelinated skin nociceptors in the rat. Pain 29:363-373.

Kochukov MY, McNearney TA, Fu Y, Westlund KN (2006) Thermosensitive TRP ion channels mediate cytosolic calcium response in human synoviocytes. Am J Physiol Cell Physiol 291:C424-C432.

Kofuji P, Newman EA (2004) Potassium buffering in the central nervous system. Neuroscience 129:1045-1056.

Koivisto A (2012) Sustained TRPA1 activation in vivo. Acta Physiol (Oxf) 204:248-254.

Koizumi K, Saitoh Y, Minami T, Takeno N, Tsuneyama K, Miyahara T, Nakayama T, Sakurai H, Takano Y, Nishimura M, Imai T, Yoshie O, Saiki I (2009) Role of CX3CL1/fractalkine in osteoclast differentiation and bone resorption. J Immunol 183:7825-7831.

Koltzenburg M, Bennett DL, Shelton DL, McMahon SB (1999) Neutralization of endogenous NGF prevents the sensitization of nociceptors supplying inflamed skin. Eur J Neurosci 11:1698-1704.

Koltzenburg M, McMahon SB (1986) Plasma extravasation in the rat urinary bladder following mechanical, electrical and chemical stimuli: evidence for a new population of chemosensitive primary sensory afferents. Neurosci Lett 72:352-356.

Kondo T, Obata K, Miyoshi K, Sakurai J, Tanaka J, Miwa H, Noguchi K (2009) Transient receptor potential A1 mediates gastric distention-induced visceral pain in rats. Gut 58:1342-1352.

Kono H, Rock KL (2008) How dying cells alert the immune system to danger. Nat Rev Immunol 8:279-289.

Kottschade LA, Sloan JA, Mazurczak MA, Johnson DB, Murphy BP, Rowland KM, Smith DA, Berg AR, Stella PJ, Loprinzi CL (2011) The use of vitamin E for the prevention of chemotherapy-induced peripheral neuropathy: results of a randomized phase III clinical trial. Support Care Cancer 19:1769-1777.

Koury MJ, Bondurant MC (1990) Control of red cell production: the roles of programmed cell death (apoptosis) and erythropoietin. Transfusion 30:673-674.

Koury ST, Bondurant MC, Koury MJ (1988) Localization of erythropoietin synthesizing cells in murine kidneys by in situ hybridization. Blood 71:524-527.

Krarup-Hansen A, Helweg-Larsen S, Schmalbruch H, Rorth M, Krarup C (2007) Neuronal involvement in cisplatin neuropathy: prospective clinical and neurophysiological studies. Brain 130:1076-1088.

Kreider T, Anthony RM, Urban JF, Jr., Gause WC (2007) Alternatively activated macrophages in helminth infections. Curr Opin Immunol 19:448-453.

Kris MG, Gralla RJ, Clark RA, Tyson LB, O'Connell JP, Wertheim MS, Kelsen DP (1985) Incidence, course, and severity of delayed nausea and vomiting following the administration of high-dose cisplatin. J Clin Oncol 3:1379-1384.

Krishnan AV, Goldstein D, Friedlander M, Kiernan MC (2005) Oxaliplatin-induced neurotoxicity and the development of neuropathy. Muscle Nerve 32:51-60.

Krishnan AV, Goldstein D, Friedlander M, Kiernan MC (2006) Oxaliplatin and axonal Na+ channel function in vivo. Clin Cancer Res 12:4481-4484.

Kruse J, von BW, Evert K, Albers N, Hadlich S, Hagemann S, Gunther C, Van RN, Heidecke CD, Partecke LI (2013) Macrophages promote tumour growth and liver metastasis in an orthotopic syngeneic mouse model of colon cancer. Int J Colorectal Dis 28:1337-1349.

Kuang DM, Zhao Q, Peng C, Xu J, Zhang JP, Wu C, Zheng L (2009) Activated monocytes in peritumoral stroma of hepatocellular carcinoma foster immune privilege and disease progression through PD-L1. J Exp Med 206:1327-1337.

Kubo T, Yamashita T, Yamaguchi A, Hosokawa K, Tohyama M (2002) Analysis of genes induced in peripheral nerve after axotomy using cDNA microarrays. J Neurochem 82:1129-1136.

Kubota Y, Takubo K, Shimizu T, Ohno H, Kishi K, Shibuya M, Saya H, Suda T (2009) M-CSF inhibition selectively targets pathological angiogenesis and lymphangiogenesis. J Exp Med 206:1089-1102.

Kupers RC, Gybels JM (1993) Electrical stimulation of the ventroposterolateral thalamic nucleus (VPL) reduces mechanical allodynia in a rat model of neuropathic pain. Neurosci Lett 150:95-98.

Kurihara T, Warr G, Loy J, Bravo R (1997) Defects in macrophage recruitment and host defense in mice lacking the CCR2 chemokine receptor. J Exp Med 186:1757-1762.

Kwan KY, Allchorne AJ, Vollrath MA, Christensen AP, Zhang DS, Woolf CJ, Corey DP (2006) TRPA1 contributes to cold, mechanical, and chemical nociception but is not essential for hair-cell transduction. Neuron 50:277-289.

Lai J, Gold MS, Kim CS, Bian D, Ossipov MH, Hunter JC, Porreca F (2002) Inhibition of neuropathic pain by decreased expression of the tetrodotoxin-resistant sodium channel, NaV1.8. Pain 95:143-152.

Landsman L, Bar-On L, Zernecke A, Kim KW, Krauthgamer R, Shagdarsuren E, Lira SA, Weissman IL, Weber C, Jung S (2009) CX3CR1 is required for monocyte homeostasis and atherogenesis by promoting cell survival. Blood 113:963-972.

Lawson LJ, Perry VH, Gordon S (1992) Turnover of resident microglia in the normal adult mouse brain. Neuroscience 48:405-415.

Lawson SN (2002) Phenotype and function of somatic primary afferent nociceptive neurones with C-, Adelta- or Aalpha/beta-fibres. Exp Physiol 87:239-244.

Lawson SN, Crepps B, Perl ER (2002) Calcitonin gene-related peptide immunoreactivity and afferent receptive properties of dorsal root ganglion neurones in guinea-pigs. J Physiol 540:989-1002.

Le GP, Nyberg F, Terenius L, Hokfelt T (1985) Calcitonin gene-related peptide is a potent inhibitor of substance P degradation. Eur J Pharmacol 115:309-311.

Leandri M, Ghignotti M, Emionite L, Leandri S, Cilli M (2012) Electrophysiological features of the mouse tail nerves and their changes in chemotherapy induced peripheral neuropathy (CIPN). J Neurosci Methods 209:403-409.

Ledeboer A, Jekich BM, Sloane EM, Mahoney JH, Langer SJ, Milligan ED, Martin D, Maier SF, Johnson KW, Leinwand LA, Chavez RA, Watkins LR (2007) Intrathecal interleukin-10 gene therapy attenuates paclitaxel-induced mechanical allodynia and proinflammatory cytokine expression in dorsal root ganglia in rats. Brain Behav Immun 21:686-698.

Ledeboer A, Sloane EM, Milligan ED, Frank MG, Mahony JH, Maier SF, Watkins LR (2005) Minocycline attenuates mechanical allodynia and proinflammatory cytokine expression in rat models of pain facilitation. Pain 115:71-83.

Lee DH, Chang L, Sorkin LS, Chaplan SR (2005) Hyperpolarization-activated, cation-nonselective, cyclic nucleotide-modulated channel blockade alleviates mechanical allodynia and suppresses ectopic discharge in spinal nerve ligated rats. J Pain 6:417-424.

Lee S, Chen TT, Barber CL, Jordan MC, Murdock J, Desai S, Ferrara N, Nagy A, Roos KP, Iruela-Arispe ML (2007) Autocrine VEGF signaling is required for vascular homeostasis. Cell 130:691-703.

Leek RD, Harris AL (2002) Tumor-associated macrophages in breast cancer. J Mammary Gland Biol Neoplasia 7:177-189.

Leek RD, Lewis CE, Whitehouse R, Greenall M, Clarke J, Harris AL (1996) Association of macrophage infiltration with angiogenesis and prognosis in invasive breast carcinoma. Cancer Res 56:4625-4629.

Legha SS (1986) Vincristine neurotoxicity. Pathophysiology and management. Med Toxicol 1:421-427.

Lesnik P, Haskell CA, Charo IF (2003) Decreased atherosclerosis in CX3CR1-/- mice reveals a role for fractalkine in atherogenesis. J Clin Invest 111:333-340.

Lever IJ, Grant AD, Pezet S, Gerard NP, Brain SD, Malcangio M (2003) Basal and activity-induced release of substance P from primary afferent fibres in NK1 receptor knockout mice: evidence for negative feedback. Neuropharmacology 45:1101-1110.

Levinson SR, Luo S, Henry MA (2012) The role of sodium channels in chronic pain. Muscle Nerve 46:155-165.

Lewin GR, Rueff A, Mendell LM (1994) Peripheral and central mechanisms of NGF-induced hyperalgesia. Eur J Neurosci 6:1903-1912.

Ley K, Laudanna C, Cybulsky MI, Nourshargh S (2007) Getting to the site of inflammation: the leukocyte adhesion cascade updated. Nat Rev Immunol 7:678-689.

Li L, Huang L, Sung SS, Vergis AL, Rosin DL, Rose CE, Jr., Lobo PI, Okusa MD (2008) The chemokine receptors CCR2 and CX3CR1 mediate monocyte/macrophage trafficking in kidney ischemia-reperfusion injury. Kidney Int 74:1526-1537.

Li P, Wilding TJ, Kim SJ, Calejesan AA, Huettner JE, Zhuo M (1999) Kainate-receptor-mediated sensory synaptic transmission in mammalian spinal cord. Nature 397:161-164.

Liao YH, Zhang GH, Jia D, Wang P, Qian NS, He F, Zeng XT, He Y, Yang YL, Cao DY, Zhang Y, Wang DS, Tao KS, Gao CJ, Dou KF (2011) Spinal astrocytic activation contributes to mechanical allodynia in a mouse model of type 2 diabetes. Brain Res 1368:324-335.

Liaw WJ, Stephens RL, Jr., Binns BC, Chu Y, Sepkuty JP, Johns RA, Rothstein JD, Tao YX (2005) Spinal glutamate uptake is critical for maintaining normal sensory transmission in rat spinal cord. Pain 115:60-70.

Light AR, Trevino DL, Perl ER (1979) Morphological features of functionally defined neurons in the marginal zone and substantia gelatinosa of the spinal dorsal horn. J Comp Neurol 186:151-171.

Lin CS, Tsaur ML, Chen CC, Wang TY, Lin CF, Lai YL, Hsu TC, Pan YY, Yang CH, Cheng JK (2007) Chronic intrathecal infusion of minocycline prevents the development of spinal-nerve ligation-induced pain in rats. Reg Anesth Pain Med 32:209-216.

Lin EY, Gouon-Evans V, Nguyen AV, Pollard JW (2002) The macrophage growth factor CSF-1 in mammary gland development and tumor progression. J Mammary Gland Biol Neoplasia 7:147-162.

Lin EY, Nguyen AV, Russell RG, Pollard JW (2001) Colony-stimulating factor 1 promotes progression of mammary tumors to malignancy. J Exp Med 193:727-740.

Lin EY, Pollard JW (2007) Tumor-associated macrophages press the angiogenic switch in breast cancer. Cancer Res 67:5064-5066.

Lin PC, Lee MY, Wang WS, Yen CC, Chao TC, Hsiao LT, Yang MH, Chen PM, Lin KP, Chiou TJ (2006) N-acetylcysteine has neuroprotective effects against oxaliplatin-based adjuvant chemotherapy in colon cancer patients: preliminary data. Support Care Cancer 14:484-487.

Lindenlaub T, Sommer C (2000) Partial sciatic nerve transection as a model of neuropathic pain: a qualitative and quantitative neuropathological study. Pain 89:97-106.

Lindia JA, McGowan E, Jochnowitz N, Abbadie C (2005) Induction of CX3CL1 expression in astrocytes and CX3CR1 in microglia in the spinal cord of a rat model of neuropathic pain. J Pain 6:434-438.

Lissbrant IF, Stattin P, Wikstrom P, Damber JE, Egevad L, Bergh A (2000) Tumor associated macrophages in human prostate cancer: relation to clinicopathological variables and survival. Int J Oncol 17:445-451.

Liu GY, Kulasingam V, Alexander RT, Touret N, Fong AM, Patel DD, Robinson LA (2005) Recycling of the membrane-anchored chemokine, CX3CL1. J Biol Chem 280:19858-19866.

Liu S, Liu YP, Yue DM, Liu GJ (2013a) Protease-activated receptor 2 in dorsal root ganglion contributes to peripheral sensitization of bone cancer pain. Eur J Pain.

Liu T, Jiang CY, Fujita T, Luo SW, Kumamoto E (2013b) Enhancement by interleukin-1beta of AMPA and NMDA receptor-mediated currents in adult rat spinal superficial dorsal horn neurons. Mol Pain 9:16.

Liu T, Van RN, Tracey DJ (2000) Depletion of macrophages reduces axonal degeneration and hyperalgesia following nerve injury. Pain 86:25-32.

Liuzzo JP, Petanceska SS, Devi LA (1999a) Neurotrophic factors regulate cathepsin S in macrophages and microglia: A role in the degradation of myelin basic protein and amyloid beta peptide. Mol Med 5:334-343.

Liuzzo JP, Petanceska SS, Moscatelli D, Devi LA (1999b) Inflammatory mediators regulate cathepsin S in macrophages and microglia: A role in attenuating heparan sulfate interactions. Mol Med 5:320-333.

Loprinzi CL, Reeves BN, Dakhil SR, Sloan JA, Wolf SL, Burger KN, Kamal A, Le-Lindqwister NA, Soori GS, Jaslowski AJ, Novotny PJ, Lachance DH (2011) Natural history of paclitaxel-associated acute pain syndrome: prospective cohort study NCCTG N08C1. J Clin Oncol 29:1472-1478.

Lovick TA (2008) Pro-nociceptive action of cholecystokinin in the periaqueductal grey: a role in neuropathic and anxiety-induced hyperalgesic states. Neurosci Biobehav Rev 32:852-862.

Lucas AD, Bursill C, Guzik TJ, Sadowski J, Channon KM, Greaves DR (2003) Smooth muscle cells in human atherosclerotic plaques express the fractalkine receptor CX3CR1 and undergo chemotaxis to the CX3C chemokine fractalkine (CX3CL1). Circulation 108:2498-2504.

Lucas DR, Newhouse JP (1957) The toxic effect of sodium L-glutamate on the inner layers of the retina. AMA Arch Ophthalmol 58:193-201.

Luhmann UF, Carvalho LS, Robbie SJ, Bainbridge JW, Ali RR (2013a) Reply to comment on "Ccl2, Cx3cr1 and Ccl2/Cx3cr1 chemokine deficiencies are not sufficient to cause age-related retinal degeneration" by Luhmann et al. (Exp. Eye Res. 107, February 2013, 80-87). Exp Eye Res 111:136.

Luhmann UF, Carvalho LS, Robbie SJ, Cowing JA, Duran Y, Munro PM, Bainbridge JW, Ali RR (2013b) Ccl2, Cx3cr1 and Ccl2/Cx3cr1 chemokine deficiencies are not sufficient to cause age-related retinal degeneration. Exp Eye Res 107:80-87.

Lyons A, Lynch AM, Downer EJ, Hanley R, O'Sullivan JB, Smith A, Lynch MA (2009) Fractalkine-induced activation of the phosphatidylinositol-3 kinase pathway attentuates microglial activation in vivo and in vitro. J Neurochem 110:1547-1556.

Lyszkiewicz M, Witzlau K, Pommerencke J, Krueger A (2011) Chemokine receptor CX3CR1 promotes dendritic cell development under steady-state conditions. Eur J Immunol 41:1256-1265.

Ma W, Quirion R (2002) Partial sciatic nerve ligation induces increase in the phosphorylation of extracellular signal-regulated kinase (ERK) and c-Jun N-terminal kinase (JNK) in astrocytes in the lumbar spinal dorsal horn and the gracile nucleus. Pain 99:175-184.

Maciejewski-Lenoir D, Chen S, Feng L, Maki R, Bacon KB (1999) Characterization of fractalkine in rat brain cells: migratory and activation signals for CX3CR-1-expressing microglia. J Immunol 163:1628-1635.

Macpherson LJ, Dubin AE, Evans MJ, Marr F, Schultz PG, Cravatt BF, Patapoutian A (2007) Noxious compounds activate TRPA1 ion channels through covalent modification of cysteines. Nature 445:541-545.

Maho A, Bensimon A, Vassart G, Parmentier M (1999) Mapping of the CCXCR1, CX3CR1, CCBP2 and CCR9 genes to the CCR cluster within the 3p21.3 region of the human genome. Cytogenet Cell Genet 87:265-268.

Malawista SE, Sato H, Bensch KG (1968) Vinblastine and griseofulvin reversibly disrupt the living mitotic spindle. Science 160:770-772.

Malcangio M, Bowery NG (1994) Spinal cord SP release and hyperalgesia in monoarthritic rats: involvement of the GABAB receptor system. Br J Pharmacol 113:1561-1566.

Malcangio M, Tomlinson DR (1998) A pharmacologic analysis of mechanical hyperalgesia in streptozotocin/diabetic rats. Pain 76:151-157.

Malin SA, Molliver DC, Koerber HR, Cornuet P, Frye R, Albers KM, Davis BM (2006) Glial cell line-derived neurotrophic factor family members sensitize nociceptors in vitro and produce thermal hyperalgesia in vivo. J Neurosci 26:8588-8599.

Malinow R, Schulman H, Tsien RW (1989) Inhibition of postsynaptic PKC or CaMKII blocks induction but not expression of LTP. Science 245:862-866.

Maljevic S, Lerche H (2012) Potassium channels: a review of broadening therapeutic possibilities for neurological diseases. J Neurol.

Mantyh PW, Rogers SD, Honore P, Allen BJ, Ghilardi JR, Li J, Daughters RS, Lappi DA, Wiley RG, Simone DA (1997) Inhibition of hyperalgesia by ablation of lamina I spinal neurons expressing the substance P receptor. Science 278:275-279.

Marchand F, Perretti M, McMahon SB (2005) Role of the immune system in chronic pain. Nat Rev Neurosci 6:521-532.

Marchand JE, Wurm WH, Kato T, Kream RM (1994) Altered tachykinin expression by dorsal root ganglion neurons in a rat model of neuropathic pain. Pain 58:219-231.

Materazzi S, Fusi C, Benemei S, Pedretti P, Patacchini R, Nilius B, Prenen J, Creminon C, Geppetti P, Nassini R (2012) TRPA1 and TRPV4 mediate paclitaxel-induced peripheral neuropathy in mice via a glutathione-sensitive mechanism. Pflugers Arch 463:561-569.

Matsuda LA, Bonner TI, Lolait SJ (1993) Localization of cannabinoid receptor mRNA in rat brain. J Comp Neurol 327:535-550.

Matta JA, Cornett PM, Miyares RL, Abe K, Sahibzada N, Ahern GP (2008) General anesthetics activate a nociceptive ion channel to enhance pain and inflammation. Proc Natl Acad Sci U S A 105:8784-8789.

Mauri FA, Pinato DJ, Trivedi P, Sharma R, Shiner RJ (2012) Isogeneic comparison of primary and metastatic lung cancer identifies CX3CR1 as a molecular determinant of site-specific metastatic diffusion. Oncol Rep 28:647-653.

Mayer ML, Westbrook GL, Guthrie PB (1984) Voltage-dependent block by Mg2+ of NMDA responses in spinal cord neurones. Nature 309:261-263.

Mazars GJ (1975) Intermittent stimulation of nucleus ventralis posterolateralis for intractable pain. Surg Neurol 4:93-95.

McBride WH (1986) Phenotype and functions of intratumoral macrophages. Biochim Biophys Acta 865:27-41.

McCarthy PW, Lawson SN (1989) Cell type and conduction velocity of rat primary sensory neurons with substance P-like immunoreactivity. Neuroscience 28:745-753.

McDermott DH, Fong AM, Yang Q, Sechler JM, Cupples LA, Merrell MN, Wilson PW, D'Agostino RB, O'Donnell CJ, Patel DD, Murphy PM (2003) Chemokine receptor mutant CX3CR1-M280 has impaired adhesive function and correlates with protection from cardiovascular disease in humans. J Clin Invest 111:1241-1250.

McDermott DH, Halcox JP, Schenke WH, Waclawiw MA, Merrell MN, Epstein N, Quyyumi AA, Murphy PM (2001) Association between polymorphism in the chemokine receptor CX3CR1 and coronary vascular endothelial dysfunction and atherosclerosis. Circ Res 89:401-407.

McEver RP, Moore KL, Cummings RD (1995) Leukocyte trafficking mediated by selectin-carbohydrate interactions. J Biol Chem 270:11025-11028.

McGaraughty S, Chu KL, Perner RJ, Didomenico S, Kort ME, Kym PR (2010) TRPA1 modulation of spontaneous and mechanically evoked firing of spinal neurons in uninjured, osteoarthritic, and inflamed rats. Mol Pain 6:14.

McGorisk GM, Treasure CB (1996) Endothelial dysfunction in coronary heart disease. Curr Opin Cardiol 11:341-350.

McKercher SR, Torbett BE, Anderson KL, Henkel GW, Vestal DJ, Baribault H, Klemsz M, Feeney AJ, Wu GE, Paige CJ, Maki RA (1996) Targeted disruption of the PU.1 gene results in multiple hematopoietic abnormalities. EMBO J 15:5647-5658.

McMahon SB, Bennett DL, Priestley JV, Shelton DL (1995) The biological effects of endogenous nerve growth factor on adult sensory neurons revealed by a trkA-IgG fusion molecule. Nat Med 1:774-780.

McMahon SB, Malcangio M (2009) Current challenges in glia-pain biology. Neuron 64:46-54.

Mehta NN, Heffron SP, Patel PN, Ferguson J, Shah RD, Hinkle CC, Krishnamoorthy P, Shah R, Tabita-Martinez J, Terembula K, Master SR, Rickels MR, Reilly MP (2012) A human model of inflammatory cardio-metabolic dysfunction; a double blind placebo-controlled crossover trial. J Transl Med 10:124.

Melli G, Taiana M, Camozzi F, Triolo D, Podini P, Quattrini A, Taroni F, Lauria G (2008) Alpha-lipoic acid prevents mitochondrial damage and neurotoxicity in experimental chemotherapy neuropathy. Exp Neurol 214:276-284.

Merighi A, Polak JM, Theodosis DT (1991) Ultrastructural visualization of glutamate and aspartate immunoreactivities in the rat dorsal horn, with special reference to the co-localization of glutamate, substance P and calcitonin-gene related peptide. Neuroscience 40:67-80.

Mert T, Gunay I, Ocal I, Guzel AI, Inal TC, Sencar L, Polat S (2009) Macrophage depletion delays progression of neuropathic pain in diabetic animals. Naunyn Schmiedebergs Arch Pharmacol 379:445-452.

Mertens M, Singh JA (2009) Anakinra for rheumatoid arthritis: a systematic review. J Rheumatol 36:1118-1125.

Michael GJ, Averill S, Shortland PJ, Yan Q, Priestley JV (1999) Axotomy results in major changes in BDNF expression by dorsal root ganglion cells: BDNF expression in large trkB and trkC cells, in pericellular baskets, and in projections to deep dorsal horn and dorsal column nuclei. Eur J Neurosci 11:3539-3551.

Michiels C (2003) Endothelial cell functions. J Cell Physiol 196:430-443.

Mikaelian I, Buness A, de Vera-Mudry MC, Kanwal C, Coluccio D, Rasmussen E, Char HW, Carvajal V, Hilton H, Funk J, Hoflack JC, Fielden M, Herting F, Dunn M, Suter-Dick L (2010) Primary endothelial damage is the mechanism of cardiotoxicity of tubulin-binding drugs. Toxicol Sci 117:144-151.

Miletic G, Miletic V (2008) Loose ligation of the sciatic nerve is associated with TrkB receptor-dependent decreases in KCC2 protein levels in the ipsilateral spinal dorsal horn. Pain 137:532-539.

Millan MJ (1999) The induction of pain: an integrative review. Prog Neurobiol 57:1-164.

Milligan E, Zapata V, Schoeniger D, Chacur M, Green P, Poole S, Martin D, Maier SF, Watkins LR (2005a) An initial investigation of spinal mechanisms underlying pain enhancement induced by fractalkine, a neuronally released chemokine. Eur J Neurosci 22:2775-2782.

Milligan ED, Langer SJ, Sloane EM, He L, Wieseler-Frank J, O'Connor K, Martin D, Forsayeth JR, Maier SF, Johnson K, Chavez RA, Leinwand LA, Watkins LR (2005b) Controlling pathological pain by adenovirally driven spinal production of the anti-inflammatory cytokine, interleukin-10. Eur J Neurosci 21:2136-2148.

Milligan ED, O'Connor KA, Nguyen KT, Armstrong CB, Twining C, Gaykema RP, Holguin A, Martin D, Maier SF, Watkins LR (2001) Intrathecal HIV-1 envelope glycoprotein gp120 induces enhanced pain states mediated by spinal cord proinflammatory cytokines. J Neurosci 21:2808-2819.

Milligan ED, Twining C, Chacur M, Biedenkapp J, O'Connor K, Poole S, Tracey K, Martin D, Maier SF, Watkins LR (2003) Spinal glia and proinflammatory cytokines mediate mirror-image neuropathic pain in rats. J Neurosci 23:1026-1040.

Milligan ED, Zapata V, Chacur M, Schoeniger D, Biedenkapp J, O'Connor KA, Verge GM, Chapman G, Green P, Foster AC, Naeve GS, Maier SF, Watkins LR (2004) Evidence that exogenous and endogenous fractalkine can induce spinal nociceptive facilitation in rats. Eur J Neurosci 20:2294-2302.

Min JK, Kim YM, Kim SW, Kwon MC, Kong YY, Hwang IK, Won MH, Rho J, Kwon YG (2005) TNF-related activation-induced cytokine enhances leukocyte adhesiveness: induction of ICAM-1 and

VCAM-1 via TNF receptor-associated factor and protein kinase C-dependent NF-kappaB activation in endothelial cells. J Immunol 175:531-540.

Miyoshi K, Obata K, Kondo T, Okamura H, Noguchi K (2008) Interleukin-18-mediated microglia/astrocyte interaction in the spinal cord enhances neuropathic pain processing after nerve injury. J Neurosci 28:12775-12787.

Mizoue LS, Bazan JF, Johnson EC, Handel TM (1999) Solution structure and dynamics of the CX3C chemokine domain of fractalkine and its interaction with an N-terminal fragment of CX3CR1. Biochemistry 38:1402-1414.

Mizoue LS, Sullivan SK, King DS, Kledal TN, Schwartz TW, Bacon KB, Handel TM (2001) Molecular determinants of receptor binding and signaling by the CX3C chemokine fractalkine. J Biol Chem 276:33906-33914.

Mizumura K, Koda H, Kumazawa T (2000) Possible contribution of protein kinase C in the effects of histamine on the visceral nociceptor activities in vitro. Neurosci Res 37:183-190.

Mizuno T, Kawanokuchi J, Numata K, Suzumura A (2003) Production and neuroprotective functions of fractalkine in the central nervous system. Brain Res 979:65-70.

Moalem G, Tracey DJ (2006) Immune and inflammatory mechanisms in neuropathic pain. Brain Res Rev 51:240-264.

Moatti D, Faure S, Fumeron F, Amara M, Seknadji P, McDermott DH, Debre P, Aumont MC, Murphy PM, de PD, Combadiere C (2001) Polymorphism in the fractalkine receptor CX3CR1 as a genetic risk factor for coronary artery disease. Blood 97:1925-1928.

Mogil JS, Wilson SG, Bon K, Lee SE, Chung K, Raber P, Pieper JO, Hain HS, Belknap JK, Hubert L, Elmer GI, Chung JM, Devor M (1999a) Heritability of nociception I: responses of 11 inbred mouse strains on 12 measures of nociception. Pain 80:67-82.

Mogil JS, Wilson SG, Bon K, Lee SE, Chung K, Raber P, Pieper JO, Hain HS, Belknap JK, Hubert L, Elmer GI, Chung JM, Devor M (1999b) Heritability of nociception II. 'Types' of nociception revealed by genetic correlation analysis. Pain 80:83-93.

Montell C, Birnbaumer L, Flockerzi V, Bindels RJ, Bruford EA, Caterina MJ, Clapham DE, Harteneck C, Heller S, Julius D, Kojima I, Mori Y, Penner R, Prawitt D, Scharenberg AM, Schultz G, Shimizu N, Zhu MX (2002) A unified nomenclature for the superfamily of TRP cation channels. Mol Cell 9:229-231.

Moore KA, Kohno T, Karchewski LA, Scholz J, Baba H, Woolf CJ (2002) Partial peripheral nerve injury promotes a selective loss of GABAergic inhibition in the superficial dorsal horn of the spinal cord. J Neurosci 22:6724-6731.

Morgan MM, Fields HL (1994) Pronounced changes in the activity of nociceptive modulatory neurons in the rostral ventromedial medulla in response to prolonged thermal noxious stimuli. J Neurophysiol 72:1161-1170.

Morgan MM, Heinricher MM, Fields HL (1994) Inhibition and facilitation of different nocifensor reflexes by spatially remote noxious stimuli. J Neurophysiol 72:1152-1160.

Morioka N, Sugimoto T, Tokuhara M, Nakamura Y, Abe H, Hisaoka K, Dohi T, Nakata Y (2012) Spinal astrocytes contribute to the circadian oscillation of glutamine synthase, cyclooxygenase-1 and clock genes in the lumbar spinal cord of mice. Neurochem Int 60:817-826.

Mosser DM, Edwards JP (2008) Exploring the full spectrum of macrophage activation. Nat Rev Immunol 8:958-969.

Mross K, Niemann B, Massing U, Drevs J, Unger C, Bhamra R, Swenson CE (2004) Pharmacokinetics of liposomal doxorubicin (TLC-D99; Myocet) in patients with solid tumors: an open-label, single-dose study. Cancer Chemother Pharmacol 54:514-524.

Muehlhoefer A, Saubermann LJ, Gu X, Luedtke-Heckenkamp K, Xavier R, Blumberg RS, Podolsky DK, MacDermott RP, Reinecker HC (2000) Fractalkine is an epithelial and endothelial cell-derived chemoattractant for intraepithelial lymphocytes in the small intestinal mucosa. J Immunol 164:3368-3376.

Muller WA (2003) Leukocyte-endothelial-cell interactions in leukocyte transmigration and the inflammatory response. Trends Immunol 24:327-334.

Muller WA, Weigl SA, Deng X, Phillips DM (1993) PECAM-1 is required for transendothelial migration of leukocytes. J Exp Med 178:449-460.

Murray PJ, Wynn TA (2011) Protective and pathogenic functions of macrophage subsets. Nat Rev Immunol 11:723-737.

Murwani R, Hodgkinson S, Armati P (1996) Tumor necrosis factor alpha and interleukin-6 mRNA expression in neonatal Lewis rat Schwann cells and a neonatal rat Schwann cell line following interferon gamma stimulation. J Neuroimmunol 71:65-71.

Muthuraman A, Jaggi AS, Singh N, Singh D (2008) Ameliorative effects of amiloride and pralidoxime in chronic constriction injury and vincristine induced painful neuropathy in rats. Eur J Pharmacol 587:104-111.

Myers RR, Heckman HM, Rodriguez M (1996) Reduced hyperalgesia in nerve-injured WLD mice: relationship to nerve fiber phagocytosis, axonal degeneration, and regeneration in normal mice. Exp Neurol 141:94-101.

Nagata K, Duggan A, Kumar G, Garcia-Anoveros J (2005) Nociceptor and hair cell transducer properties of TRPA1, a channel for pain and hearing. J Neurosci 25:4052-4061.

Naguib M, Diaz P, Xu JJ, Astruc-Diaz F, Craig S, Vivas-Mejia P, Brown DL (2008) MDA7: a novel selective agonist for CB2 receptors that prevents allodynia in rat neuropathic pain models. Br J Pharmacol 155:1104-1116.

Naguib M, Xu JJ, Diaz P, Brown DL, Cogdell D, Bie B, Hu J, Craig S, Hittelman WN (2012) Prevention of paclitaxel-induced neuropathy through activation of the central cannabinoid type 2 receptor system. Anesth Analg 114:1104-1120.

Nagy GG, Al-Ayyan M, Andrew D, Fukaya M, Watanabe M, Todd AJ (2004) Widespread expression of the AMPA receptor GluR2 subunit at glutamatergic synapses in the rat spinal cord and phosphorylation of GluR1 in response to noxious stimulation revealed with an antigen-unmasking method. J Neurosci 24:5766-5777.

Nagy JI, Rash JE (2000) Connexins and gap junctions of astrocytes and oligodendrocytes in the CNS. Brain Res Brain Res Rev 32:29-44.

Nakayama Y, Nagashima N, Minagawa N, Inoue Y, Katsuki T, Onitsuka K, Sako T, Hirata K, Nagata N, Itoh H (2002) Relationships between tumor-associated macrophages and clinicopathological factors in patients with colorectal cancer. Anticancer Res 22:4291-4296.

Nanki T, Urasaki Y, Imai T, Nishimura M, Muramoto K, Kubota T, Miyasaka N (2004) Inhibition of fractalkine ameliorates murine collagen-induced arthritis. J Immunol 173:7010-7016.

Nassar MA, Stirling LC, Forlani G, Baker MD, Matthews EA, Dickenson AH, Wood JN (2004) Nociceptor-specific gene deletion reveals a major role for Nav1.7 (PN1) in acute and inflammatory pain. Proc Natl Acad Sci U S A 101:12706-12711.

Nassini R, Gees M, Harrison S, De SG, Materazzi S, Moretto N, Failli P, Preti D, Marchetti N, Cavazzini A, Mancini F, Pedretti P, Nilius B, Patacchini R, Geppetti P (2011) Oxaliplatin elicits mechanical and cold allodynia in rodents via TRPA1 receptor stimulation. Pain 152:1621-1631.

Nilius B, Appendino G, Owsianik G (2012) The transient receptor potential channel TRPA1: from gene to pathophysiology. Pflugers Arch 464:425-458.

Nimmerjahn A, Kirchhoff F, Helmchen F (2005) Resting microglial cells are highly dynamic surveillants of brain parenchyma in vivo. Science 308:1314-1318.

Nishiyori A, Minami M, Ohtani Y, Takami S, Yamamoto J, Kawaguchi N, Kume T, Akaike A, Satoh M (1998) Localization of fractalkine and CX3CR1 mRNAs in rat brain: does fractalkine play a role in signaling from neuron to microglia? FEBS Lett 429:167-172.

Niu X, Xing W, Li W, Fan T, Hu H, Li Y (2012) Isofraxidin exhibited anti-inflammatory effects in vivo and inhibited TNF-alpha production in LPS-induced mouse peritoneal macrophages in vitro via the MAPK pathway. Int Immunopharmacol 14:164-171.

Noble RL, Beer CT, Cutts JH (1958) Role of chance observations in chemotherapy: Vinca rosea. Ann N Y Acad Sci 76:882-894.

Nodera H, Spieker A, Sung M, Rutkove S (2011) Neuroprotective effects of Kv7 channel agonist, retigabine, for cisplatin-induced peripheral neuropathy. Neurosci Lett 505:223-227.

Noguchi K, Dubner R, De LM, Senba E, Ruda MA (1994) Axotomy induces preprotachykinin gene expression in a subpopulation of dorsal root ganglion neurons. J Neurosci Res 37:596-603.

Norcini M, Vivoli E, Galeotti N, Bianchi E, Bartolini A, Ghelardini C (2009) Supraspinal role of protein kinase C in oxaliplatin-induced neuropathy in rat. Pain 146:141-147.

Nourshargh S, Hordijk PL, Sixt M (2010) Breaching multiple barriers: leukocyte motility through venular walls and the interstitium. Nat Rev Mol Cell Biol 11:366-378.

Nourshargh S, Krombach F, Dejana E (2006) The role of JAM-A and PECAM-1 in modulating leukocyte infiltration in inflamed and ischemic tissues. J Leukoc Biol 80:714-718.

Novakova-Tousova K, Vyklicky L, Susankova K, Benedikt J, Samad A, Teisinger J, Vlachova V (2007) Functional changes in the vanilloid receptor subtype 1 channel during and after acute desensitization. Neuroscience 149:144-154.

Novakovic SD, Tzoumaka E, McGivern JG, Haraguchi M, Sangameswaran L, Gogas KR, Eglen RM, Hunter JC (1998) Distribution of the tetrodotoxin-resistant sodium channel PN3 in rat sensory neurons in normal and neuropathic conditions. J Neurosci 18:2174-2187.

Nozaki-Taguchi N, Chaplan SR, Higuera ES, Ajakwe RC, Yaksh TL (2001) Vincristine-induced allodynia in the rat. Pain 93:69-76.

Nozawa K, Kawabata-Shoda E, Doihara H, Kojima R, Okada H, Mochizuki S, Sano Y, Inamura K, Matsushime H, Koizumi T, Yokoyama T, Ito H (2009) TRPA1 regulates gastrointestinal motility through serotonin release from enterochromaffin cells. Proc Natl Acad Sci U S A 106:3408-3413.

O'Brien S, et al. (2013) High-dose vincristine sulfate liposome injection for advanced, relapsed, and refractory adult Philadelphia chromosome-negative acute lymphoblastic leukemia. J Clin Oncol 31:676-683.

O'Connor AB, Dworkin RH (2009) Treatment of neuropathic pain: an overview of recent guidelines. Am J Med 122:S22-S32.

O'Shea JJ, Murray PJ (2008) Cytokine signaling modules in inflammatory responses. Immunity 28:477-487.

Obata K, Katsura H, Mizushima T, Yamanaka H, Kobayashi K, Dai Y, Fukuoka T, Tokunaga A, Tominaga M, Noguchi K (2005) TRPA1 induced in sensory neurons contributes to cold hyperalgesia after inflammation and nerve injury. J Clin Invest 115:2393-2401.

Ogbonna AC, Clark AK, Gentry C, Hobbs C, Malcangio M (2013) Pain-like behaviour and spinal changes in the monosodium iodoacetate model of osteoarthritis in C57Bl/6 mice. Eur J Pain 17:514-526.

Oguma K, Oshima H, Aoki M, Uchio R, Naka K, Nakamura S, Hirao A, Saya H, Taketo MM, Oshima M (2008) Activated macrophages promote Wnt signalling through tumour necrosis factor-alpha in gastric tumour cells. EMBO J 27:1671-1681.

Oh DJ, Dursun B, He Z, Lu L, Hoke TS, Ljubanovic D, Faubel S, Edelstein CL (2008) Fractalkine receptor (CX3CR1) inhibition is protective against ischemic acute renal failure in mice. Am J Physiol Renal Physiol 294:F264-F271.

Ohara PT, Granato A, Moallem TM, Wang BR, Tillet Y, Jasmin L (2003) Dopaminergic input to GABAergic neurons in the rostral agranular insular cortex of the rat. J Neurocytol 32:131-141.

Oka T, Aou S, Hori T (1993) Intracerebroventricular injection of interleukin-1 beta induces hyperalgesia in rats. Brain Res 624:61-68.

Okada-Ogawa A, Suzuki I, Sessle BJ, Chiang CY, Salter MW, Dostrovsky JO, Tsuboi Y, Kondo M, Kitagawa J, Kobayashi A, Noma N, Imamura Y, Iwata K (2009) Astroglia in medullary dorsal horn (trigeminal spinal subnucleus caudalis) are involved in trigeminal neuropathic pain mechanisms. J Neurosci 29:11161-11171.

Oku R, Satoh M, Fujii N, Otaka A, Yajima H, Takagi H (1987) Calcitonin gene-related peptide promotes mechanical nociception by potentiating release of substance P from the spinal dorsal horn in rats. Brain Res 403:350-354.

Okuno T, Nakatsuji Y, Kumanogoh A, Koguchi K, Moriya M, Fujimura H, Kikutani H, Sakoda S (2004) Induction of cyclooxygenase-2 in reactive glial cells by the CD40 pathway: relevance to amyotrophic lateral sclerosis. J Neurochem 91:404-412.

Old EA, Malcangio M (2012) Chemokine mediated neuron-glia communication and aberrant signalling in neuropathic pain states. Curr Opin Pharmacol 12:67-73.

Olechowski CJ, Truong JJ, Kerr BJ (2009) Neuropathic pain behaviours in a chronic-relapsing model of experimental autoimmune encephalomyelitis (EAE). Pain 141:156-164.

Oliva AA, Jr., Jiang M, Lam T, Smith KL, Swann JW (2000) Novel hippocampal interneuronal subtypes identified using transgenic mice that express green fluorescent protein in GABAergic interneurons. J Neurosci 20:3354-3368.

Olney JW, Sharpe LG (1969) Brain lesions in an infant rhesus monkey treated with monsodium glutamate. Science 166:386-388.

Owellen RJ, Hartke CA, Dickerson RM, Hains FO (1976) Inhibition of tubulin-microtubule polymerization by drugs of the Vinca alkaloid class. Cancer Res 36:1499-1502.

Owolabi SA, Saab CY (2006) Fractalkine and minocycline alter neuronal activity in the spinal cord dorsal horn. FEBS Lett 580:4306-4310.

Pabbidi RM, Yu SQ, Peng S, Khardori R, Pauza ME, Premkumar LS (2008) Influence of TRPV1 on diabetes-induced alterations in thermal pain sensitivity. Mol Pain 4:9.

Pace A, Giannarelli D, Galie E, Savarese A, Carpano S, Della GM, Pozzi A, Silvani A, Gaviani P, Scaioli V, Jandolo B, Bove L, Cognetti F (2010) Vitamin E neuroprotection for cisplatin neuropathy: a randomized, placebo-controlled trial. Neurology 74:762-766.

Pachman DR, Barton DL, Watson JC, Loprinzi CL (2011) Chemotherapy-induced peripheral neuropathy: prevention and treatment. Clin Pharmacol Ther 90:377-387.

Pal PK (1999) Clinical and electrophysiological studies in vincristine induced neuropathy. Electromyogr Clin Neurophysiol 39:323-330.

Pan Y, Lloyd C, Zhou H, Dolich S, Deeds J, Gonzalo JA, Vath J, Gosselin M, Ma J, Dussault B, Woolf E, Alperin G, Culpepper J, Gutierrez-Ramos JC, Gearing D (1997) Neurotactin, a membrane-anchored chemokine upregulated in brain inflammation. Nature 387:611-617.

Papadopoulos EJ, Fitzhugh DJ, Tkaczyk C, Gilfillan AM, Sassetti C, Metcalfe DD, Hwang ST (2000) Mast cells migrate, but do not degranulate, in response to fractalkine, a membrane-bound chemokine expressed constitutively in diverse cells of the skin. Eur J Immunol 30:2355-2361.

Papadopoulos EJ, Sassetti C, Saeki H, Yamada N, Kawamura T, Fitzhugh DJ, Saraf MA, Schall T, Blauvelt A, Rosen SD, Hwang ST (1999) Fractalkine, a CX3C chemokine, is expressed by dendritic cells and is up-regulated upon dendritic cell maturation. Eur J Immunol 29:2551-2559.

Park HJ, Kim YH, Koh HJ, Park CS, Kang SH, Choi JH, Moon DE (2012) Analgesic effects of dexmedetomidine in vincristine-evoked painful neuropathic rats. J Korean Med Sci 27:1411-1417.

Park HJ, Stokes JA, Pirie E, Skahen J, Shtaerman Y, Yaksh TL (2013) Persistent hyperalgesia in the cisplatin-treated mouse as defined by threshold measures, the conditioned place preference paradigm, and changes in dorsal root ganglia activated transcription factor 3: the effects of gabapentin, ketorolac, and etanercept. Anesth Analg 116:224-231.

Park JS, Yaster M, Guan X, Xu JT, Shih MH, Guan Y, Raja SN, Tao YX (2008) Role of spinal cord alpha-amino-3-hydroxy-5-methyl-4-isoxazolepropionic acid receptors in complete Freund's adjuvant-induced inflammatory pain. Mol Pain 4:67.

Park SB, Lin CS, Krishnan AV, Goldstein D, Friedlander ML, Kiernan MC (2011) Dose effects of oxaliplatin on persistent and transient Na+ conductances and the development of neurotoxicity. PLoS One 6:e18469.

Parvathy SS, Masocha W (2013) Matrix metalloproteinase inhibitor COL-3 prevents the development of paclitaxel-induced hyperalgesia in mice. Med Princ Pract 22:35-41.

Passlick B, Flieger D, Ziegler-Heitbrock HW (1989) Identification and characterization of a novel monocyte subpopulation in human peripheral blood. Blood 74:2527-2534.

Patapoutian A, Tate S, Woolf CJ (2009) Transient receptor potential channels: targeting pain at the source. Nat Rev Drug Discov 8:55-68.

Pekny M, Nilsson M (2005) Astrocyte activation and reactive gliosis. Glia 50:427-434.

Perkins NM, Tracey DJ (2000) Hyperalgesia due to nerve injury: role of neutrophils. Neuroscience 101:745-757.

Perrin FE, Lacroix S, Aviles-Trigueros M, David S (2005) Involvement of monocyte chemoattractant protein-1, macrophage inflammatory protein-1alpha and interleukin-1beta in Wallerian degeneration. Brain 128:854-866.

Perry VH, Hume DA, Gordon S (1985) Immunohistochemical localization of macrophages and microglia in the adult and developing mouse brain. Neuroscience 15:313-326.

Pertovaara A, Kontinen VK, Kalso EA (1997) Chronic spinal nerve ligation induces changes in response characteristics of nociceptive spinal dorsal horn neurons and in their descending regulation originating in the periaqueductal gray in the rat. Exp Neurol 147:428-436.

Pertovaara A, Wei H, Hamalainen MM (1996) Lidocaine in the rostroventromedial medulla and the periaqueductal gray attenuates allodynia in neuropathic rats. Neurosci Lett 218:127-130.

Peters CM, Jimenez-Andrade JM, Jonas BM, Sevcik MA, Koewler NJ, Ghilardi JR, Wong GY, Mantyh PW (2007a) Intravenous paclitaxel administration in the rat induces a peripheral sensory neuropathy characterized by macrophage infiltration and injury to sensory neurons and their supporting cells. Exp Neurol 203:42-54.

Peters CM, Jimenez-Andrade JM, Kuskowski MA, Ghilardi JR, Mantyh PW (2007b) An evolving cellular pathology occurs in dorsal root ganglia, peripheral nerve and spinal cord following intravenous administration of paclitaxel in the rat. Brain Res 1168:46-59.

Petrus M, Peier AM, Bandell M, Hwang SW, Huynh T, Olney N, Jegla T, Patapoutian A (2007) A role of TRPA1 in mechanical hyperalgesia is revealed by pharmacological inhibition. Mol Pain 3:40.

Pevida M, Lastra A, Hidalgo A, Baamonde A, Menendez L (2013) Spinal CCL2 and microglial activation are involved in paclitaxel-evoked cold hyperalgesia. Brain Res Bull 95:21-27.

Pezet S, Malcangio M, Lever IJ, Perkinton MS, Thompson SW, Williams RJ, McMahon SB (2002a) Noxious stimulation induces Trk receptor and downstream ERK phosphorylation in spinal dorsal horn. Mol Cell Neurosci 21:684-695.

Pezet S, Malcangio M, McMahon SB (2002b) BDNF: a neuromodulator in nociceptive pathways? Brain Res Brain Res Rev 40:240-249.

Picozzi VJ, Abrams RA, Decker PA, Traverso W, O'Reilly EM, Greeno E, Martin RC, Wilfong LS, Rothenberg ML, Posner MC, Pisters PW (2011) Multicenter phase II trial of adjuvant therapy for resected pancreatic cancer using cisplatin, 5-fluorouracil, and interferon-alfa-2b-based chemoradiation: ACOSOG Trial Z05031. Ann Oncol 22:348-354.

Piller L, Ecker E (1941) Anticomplementary Factor in Fresh Yeast. pp 139-142.

Pisano C, Pratesi G, Laccabue D, Zunino F, Lo GP, Bellucci A, Pacifici L, Camerini B, Vesci L, Castorina M, Cicuzza S, Tredici G, Marmiroli P, Nicolini G, Galbiati S, Calvani M, Carminati P, Cavaletti G (2003) Paclitaxel and Cisplatin-induced neurotoxicity: a protective role of acetyl-L-carnitine. Clin Cancer Res 9:5756-5767.

Pittman SM, Strickland D, Ireland CM (1994) Polymerization of tubulin in apoptotic cells is not cell cycle dependent. Exp Cell Res 215:263-272.

Pober JS, Cotran RS (1990) The role of endothelial cells in inflammation. Transplantation 50:537-544.

Pober JS, Sessa WC (2007) Evolving functions of endothelial cells in inflammation. Nat Rev Immunol 7:803-815.

Pollard JW (2009) Trophic macrophages in development and disease. Nat Rev Immunol 9:259-270.

Pollard JW (2004) Tumour-educated macrophages promote tumour progression and metastasis. Nat Rev Cancer 4:71-78.

Pollock J, McFarlane SM, Connell MC, Zehavi U, Vandenabeele P, MacEwan DJ, Scott RH (2002) TNF-alpha receptors simultaneously activate Ca2+ mobilisation and stress kinases in cultured sensory neurones. Neuropharmacology 42:93-106.

Polomano RC, Mannes AJ, Clark US, Bennett GJ (2001) A painful peripheral neuropathy in the rat produced by the chemotherapeutic drug, paclitaxel. Pain 94:293-304.

Poole DP, Pelayo JC, Cattaruzza F, Kuo YM, Gai G, Chiu JV, Bron R, Furness JB, Grady EF, Bunnett NW (2011) Transient receptor potential ankyrin 1 is expressed by inhibitory motoneurons of the mouse intestine. Gastroenterology 141:565-75, 575.

Popovich PG, Guan Z, Wei P, Huitinga I, Van RN, Stokes BT (1999) Depletion of hematogenous macrophages promotes partial hindlimb recovery and neuroanatomical repair after experimental spinal cord injury. Exp Neurol 158:351-365.

Porter JT, McCarthy KD (1997) Astrocytic neurotransmitter receptors in situ and in vivo. Prog Neurobiol 51:439-455.

Postma TJ, Heimans JJ (2000) Grading of chemotherapy-induced peripheral neuropathy. Ann Oncol 11:509-513.

Postma TJ, Vermorken JB, Liefting AJ, Pinedo HM, Heimans JJ (1995) Paclitaxel-induced neuropathy. Ann Oncol 6:489-494.

Pozsgai G, Bodkin JV, Graepel R, Bevan S, Andersson DA, Brain SD (2010) Evidence for the pathophysiological relevance of TRPA1 receptors in the cardiovascular system in vivo. Cardiovasc Res 87:760-768.

Proudfoot AE, Handel TM, Johnson Z, Lau EK, LiWang P, Clark-Lewis I, Borlat F, Wells TN, Kosco-Vilbois MH (2003) Glycosaminoglycan binding and oligomerization are essential for the in vivo activity of certain chemokines. Proc Natl Acad Sci U S A 100:1885-1890.

Pusztai L, Mendoza TR, Reuben JM, Martinez MM, Willey JS, Lara J, Syed A, Fritsche HA, Bruera E, Booser D, Valero V, Arun B, Ibrahim N, Rivera E, Royce M, Cleeland CS, Hortobagyi GN (2004) Changes in plasma levels of inflammatory cytokines in response to paclitaxel chemotherapy. Cytokine 25:94-102.

Qian B, Deng Y, Im JH, Muschel RJ, Zou Y, Li J, Lang RA, Pollard JW (2009) A distinct macrophage population mediates metastatic breast cancer cell extravasation, establishment and growth. PLoS One 4:e6562.

Qian BZ, Li J, Zhang H, Kitamura T, Zhang J, Campion LR, Kaiser EA, Snyder LA, Pollard JW (2011) CCL2 recruits inflammatory monocytes to facilitate breast-tumour metastasis. Nature 475:222-225.

Qian BZ, Pollard JW (2010) Macrophage diversity enhances tumor progression and metastasis. Cell 141:39-51.

Qian Q, Jutila MA, Van RN, Cutler JE (1994) Elimination of mouse splenic macrophages correlates with increased susceptibility to experimental disseminated candidiasis. J Immunol 152:5000-5008.

Raghavendra V, Tanga F, DeLeo JA (2003) Inhibition of microglial activation attenuates the development but not existing hypersensitivity in a rat model of neuropathy. J Pharmacol Exp Ther 306:624-630.

Rahn EJ, Hohmann AG (2009) Cannabinoids as pharmacotherapies for neuropathic pain: from the bench to the bedside. Neurotherapeutics 6:713-737.

Rahn EJ, Makriyannis A, Hohmann AG (2007) Activation of cannabinoid CB1 and CB2 receptors suppresses neuropathic nociception evoked by the chemotherapeutic agent vincristine in rats. Br J Pharmacol 152:765-777.

Ramchandren S, Leonard M, Mody RJ, Donohue JE, Moyer J, Hutchinson R, Gurney JG (2009) Peripheral neuropathy in survivors of childhood acute lymphoblastic leukemia. J Peripher Nerv Syst 14:184-189.

Ramsey IS, Delling M, Clapham DE (2006) An introduction to TRP channels. Annu Rev Physiol 68:619-647.

Randolph GJ, Sanchez-Schmitz G, Liebman RM, Schakel K (2002) The CD16(+) (FcgammaRIII(+)) subset of human monocytes preferentially becomes migratory dendritic cells in a model tissue setting. J Exp Med 196:517-527.

Ransohoff RM, Cardona AE (2010) The myeloid cells of the central nervous system parenchyma. Nature 468:253-262.

Ransohoff RM, Perry VH (2009) Microglial physiology: unique stimuli, specialized responses. Annu Rev Immunol 27:119-145.

Rao RD, Flynn PJ, Sloan JA, Wong GY, Novotny P, Johnson DB, Gross HM, Renno SI, Nashawaty M, Loprinzi CL (2008) Efficacy of lamotrigine in the management of chemotherapy-induced peripheral neuropathy: a phase 3 randomized, double-blind, placebo-controlled trial, N01C3. Cancer 112:2802-2808.

Rao RD, Michalak JC, Sloan JA, Loprinzi CL, Soori GS, Nikcevich DA, Warner DO, Novotny P, Kutteh LA, Wong GY (2007) Efficacy of gabapentin in the management of chemotherapy-induced peripheral neuropathy: a phase 3 randomized, double-blind, placebo-controlled, crossover trial (N00C3). Cancer 110:2110-2118.

Raoul W, Keller N, Rodero M, Behar-Cohen F, Sennlaub F, Combadiere C (2008) Role of the chemokine receptor CX3CR1 in the mobilization of phagocytic retinal microglial cells. J Neuroimmunol 198:56-61.

Raport CJ, Schweickart VL, Eddy RL, Jr., Shows TB, Gray PW (1995) The orphan G-protein-coupled receptor-encoding gene V28 is closely related to genes for chemokine receptors and is expressed in lymphoid and neural tissues. Gene 163:295-299.

Rasley A, Bost KL, Olson JK, Miller SD, Marriott I (2002) Expression of functional NK-1 receptors in murine microglia. Glia 37:258-267.

Raspe C, Hocherl K, Rath S, Sauvant C, Bucher M (2013) NF-kappaB-mediated inverse regulation of fractalkine and CX3CR1 during CLP-induced sepsis. Cytokine 61:97-103.

Rebouche CJ (2004) Kinetics, pharmacokinetics, and regulation of L-carnitine and acetyl-L-carnitine metabolism. Ann N Y Acad Sci 1033:30-41.

Reeve AJ, Patel S, Fox A, Walker K, Urban L (2000) Intrathecally administered endotoxin or cytokines produce allodynia, hyperalgesia and changes in spinal cord neuronal responses to nociceptive stimuli in the rat. Eur J Pain 4:247-257.

Renn CL, Carozzi VA, Rhee P, Gallop D, Dorsey SG, Cavaletti G (2011) Multimodal assessment of painful peripheral neuropathy induced by chronic oxaliplatin-based chemotherapy in mice. Mol Pain 7:29.

Renner P, Milazzo S, Liu JP, Zwahlen M, Birkmann J, Horneber M (2012) Primary prophylactic colony-stimulating factors for the prevention of chemotherapy-induced febrile neutropenia in breast cancer patients. Cochrane Database Syst Rev 10:CD007913.

Rexed B (1952) The cytoarchitectonic organization of the spinal cord in the cat. J Comp Neurol 96:414-495.

Reynolds DV (1969) Surgery in the rat during electrical analgesia induced by focal brain stimulation. Science 164:444-445.

Richards DM, Hettinger J, Feuerer M (2013) Monocytes and macrophages in cancer: development and functions. Cancer Microenviron 6:179-191.

Ridet JL, Malhotra SK, Privat A, Gage FH (1997) Reactive astrocytes: cellular and molecular cues to biological function. Trends Neurosci 20:570-577.

Rimaniol AC, Till SJ, Garcia G, Capel F, Godot V, Balabanian K, Durand-Gasselin I, Varga EM, Simonneau G, Emilie D, Durham SR, Humbert M (2003) The CX3C chemokine fractalkine in allergic asthma and rhinitis. J Allergy Clin Immunol 112:1139-1146.

Rius C, Piqueras L, Gonzalez-Navarro H, Albertos F, Company C, Lopez-Gines C, Ludwig A, Blanes JI, Morcillo EJ, Sanz MJ (2013) Arterial and venous endothelia display differential functional fractalkine (CX3CL1) expression by angiotensin-II. Arterioscler Thromb Vasc Biol 33:96-104.

Robinson-Smith TM, Isaacsohn I, Mercer CA, Zhou M, Van RN, Husseinzadeh N, McFarland-Mancini MM, Drew AF (2007) Macrophages mediate inflammation-enhanced metastasis of ovarian tumors in mice. Cancer Res 67:5708-5716.

Rodriguez-Menendez V, Gilardini A, Bossi M, Canta A, Oggioni N, Carozzi V, Tremolizzo L, Cavaletti G (2008) Valproate protective effects on cisplatin-induced peripheral neuropathy: an in vitro and in vivo study. Anticancer Res 28:335-342.

Roelofs RI, Hrushesky W, Rogin J, Rosenberg L (1984) Peripheral sensory neuropathy and cisplatin chemotherapy. Neurology 34:934-938.

Rogers JT, Morganti JM, Bachstetter AD, Hudson CE, Peters MM, Grimmig BA, Weeber EJ, Bickford PC, Gemma C (2011) CX3CR1 deficiency leads to impairment of hippocampal cognitive function and synaptic plasticity. J Neurosci 31:16241-16250.

Rogers MJ, Gordon S, Benford HL, Coxon FP, Luckman SP, Monkkonen J, Frith JC (2000) Cellular and molecular mechanisms of action of bisphosphonates. Cancer 88:2961-2978.

Rojas C, Slusher BS (2012) Pharmacological mechanisms of 5-HT(3) and tachykinin NK(1) receptor antagonism to prevent chemotherapy-induced nausea and vomiting. Eur J Pharmacol 684:1-7.

Romero TR, Resende LC, Guzzo LS, Duarte ID (2013) CB1 and CB2 cannabinoid receptor agonists induce peripheral antinociception by activation of the endogenous noradrenergic system. Anesth Analg 116:463-472.

Romero-Sandoval A, Chai N, Nutile-McMenemy N, DeLeo JA (2008) A comparison of spinal Iba1 and GFAP expression in rodent models of acute and chronic pain. Brain Res 1219:116-126.

Ross R (1993) The pathogenesis of atherosclerosis: a perspective for the 1990s. Nature 362:801-809.

Rouach N, Koulakoff A, Abudara V, Willecke K, Giaume C (2008) Astroglial metabolic networks sustain hippocampal synaptic transmission. Science 322:1551-1555.

Ruiz-Medina J, Baulies A, Bura SA, Valverde O (2013) Paclitaxel-induced neuropathic pain is age dependent and devolves on glial response. Eur J Pain 17:75-85.

Ruth JH, Volin MV, Haines GK, III, Woodruff DC, Katschke KJ, Jr., Woods JM, Park CC, Morel JC, Koch AE (2001) Fractalkine, a novel chemokine in rheumatoid arthritis and in rat adjuvant-induced arthritis. Arthritis Rheum 44:1568-1581.

Ryder M, Ghossein RA, Ricarte-Filho JC, Knauf JA, Fagin JA (2008) Increased density of tumor-associated macrophages is associated with decreased survival in advanced thyroid cancer. Endocr Relat Cancer 15:1069-1074.

Saade NE, Jabbur SJ (2008) Nociceptive behavior in animal models for peripheral neuropathy: spinal and supraspinal mechanisms. Prog Neurobiol 86:22-47.

Sabino MC, Ghilardi JR, Feia KJ, Jongen JL, Keyser CP, Luger NM, Mach DB, Peters CM, Rogers SD, Schwei MJ, De FC, Mantyh PW (2002) The involvement of prostaglandins in tumorigenesis, tumor-induced osteolysis and bone cancer pain. J Musculoskelet Neuronal Interact 2:561-562.

Sachs D, Coelho FM, Costa VV, Lopes F, Pinho V, Amaral FA, Silva TA, Teixeira AL, Souza DG, Teixeira MM (2011) Cooperative role of tumour necrosis factor-alpha, interleukin-1beta and neutrophils in a novel behavioural model that concomitantly demonstrates articular inflammation and hypernociception in mice. Br J Pharmacol 162:72-83.

Saederup N, Cardona AE, Croft K, Mizutani M, Cotleur AC, Tsou CL, Ransohoff RM, Charo IF (2010) Selective chemokine receptor usage by central nervous system myeloid cells in CCR2-red fluorescent protein knock-in mice. PLoS One 5:e13693.

Saif MW, Syrigos K, Kaley K, Isufi I (2010) Role of pregabalin in treatment of oxaliplatin-induced sensory neuropathy. Anticancer Res 30:2927-2933.

Saijo K, Glass CK (2011) Microglial cell origin and phenotypes in health and disease. Nat Rev Immunol 11:775-787.

Saji H, Koike M, Yamori T, Saji S, Seiki M, Matsushima K, Toi M (2001) Significant correlation of monocyte chemoattractant protein-1 expression with neovascularization and progression of breast carcinoma. Cancer 92:1085-1091.

Salas MM, Hargreaves KM, Akopian AN (2009) TRPA1-mediated responses in trigeminal sensory neurons: interaction between TRPA1 and TRPV1. Eur J Neurosci 29:1568-1578.

Saloustros E, Tryfonidis K, Georgoulias V (2011) Prophylactic and therapeutic strategies in chemotherapy-induced neutropenia. Expert Opin Pharmacother 12:851-863.

Samad TA, Moore KA, Sapirstein A, Billet S, Allchorne A, Poole S, Bonventre JV, Woolf CJ (2001) Interleukin-1beta-mediated induction of Cox-2 in the CNS contributes to inflammatory pain hypersensitivity. Nature 410:471-475.

Samson M, Soularue P, Vassart G, Parmentier M (1996) The genes encoding the human CC-chemokine receptors CC-CKR1 to CC-CKR5 (CMKBR1-CMKBR5) are clustered in the p21.3-p24 region of chromosome 3. Genomics 36:522-526.

Sandler SG, Tobin W, Henderson ES (1969) Vincristine-induced neuropathy. A clinical study of fifty leukemic patients. Neurology 19:367-374.

Santello M, Bezzi P, Volterra A (2011) TNFalpha controls glutamatergic gliotransmission in the hippocampal dentate gyrus. Neuron 69:988-1001.

Scemes E, Spray DC (2012) Extracellular K(+) and astrocyte signaling via connexin and pannexin channels. Neurochem Res 37:2310-2316.

Schaible HG, von Banchet GS, Boettger MK, Brauer R, Gajda M, Richter F, Hensellek S, Brenn D, Natura G (2010) The role of proinflammatory cytokines in the generation and maintenance of joint pain. Ann N Y Acad Sci 1193:60-69.

Schapira AH, Cooper JM (1992) Mitochondrial function in neurodegeneration and ageing. Mutat Res 275:133-143.

Scholl SM, Pallud C, Beuvon F, Hacene K, Stanley ER, Rohrschneider L, Tang R, Pouillart P, Lidereau R (1994) Anti-colony-stimulating factor-1 antibody staining in primary breast adenocarcinomas correlates with marked inflammatory cell infiltrates and prognosis. J Natl Cancer Inst 86:120-126.

Scholz D, Devaux B, Hirche A, Potzsch B, Kropp B, Schaper W, Schaper J (1996) Expression of adhesion molecules is specific and time-dependent in cytokine-stimulated endothelial cells in culture. Cell Tissue Res 284:415-423.

Scholz J, Broom DC, Youn DH, Mills CD, Kohno T, Suter MR, Moore KA, Decosterd I, Coggeshall RE, Woolf CJ (2005) Blocking caspase activity prevents transsynaptic neuronal apoptosis and the loss of inhibition in lamina II of the dorsal horn after peripheral nerve injury. J Neurosci 25:7317-7323.

Scholz J, Woolf CJ (2007) The neuropathic pain triad: neurons, immune cells and glia. Nat Neurosci 10:1361-1368.

Schomberg D, Olson JK (2012) Immune responses of microglia in the spinal cord: contribution to pain states. Exp Neurol 234:262-270.

Schulz C, Schafer A, Stolla M, Kerstan S, Lorenz M, von Bruhl ML, Schiemann M, Bauersachs J, Gloe T, Busch DH, Gawaz M, Massberg S (2007) Chemokine fractalkine mediates leukocyte recruitment to inflammatory endothelial cells in flowing whole blood: a critical role for P-selectin expressed on activated platelets. Circulation 116:764-773.

Schwaeble WJ, Stover CM, Schall TJ, Dairaghi DJ, Trinder PK, Linington C, Iglesias A, Schubart A, Lynch NJ, Weihe E, Schafer MK (1998) Neuronal expression of fractalkine in the presence and absence of inflammation. FEBS Lett 439:203-207.

Schwarz N, Pruessmeyer J, Hess FM, Dreymueller D, Pantaler E, Koelsch A, Windoffer R, Voss M, Sarabi A, Weber C, Sechi AS, Uhlig S, Ludwig A (2010) Requirements for leukocyte transmigration via the transmembrane chemokine CX3CL1. Cell Mol Life Sci 67:4233-4248.

Schwei MJ, Honore P, Rogers SD, Salak-Johnson JL, Finke MP, Ramnaraine ML, Clohisy DR, Mantyh PW (1999) Neurochemical and cellular reorganization of the spinal cord in a murine model of bone cancer pain. J Neurosci 19:10886-10897.

Scianni M, Antonilli L, Chece G, Cristalli G, Di Castro MA, Limatola C, Maggi L (2013) Fractalkine (CX3CL1) enhances hippocampal N-methyl-d-aspartate receptor (NMDAR) function via d-serine and adenosine receptor type A2 (A2AR) activity. J Neuroinflammation 10:108.

Scotton C, Milliken D, Wilson J, Raju S, Balkwill F (2001) Analysis of CC chemokine and chemokine receptor expression in solid ovarian tumours. Br J Cancer 85:891-897.

Scuteri A, Galimberti A, Maggioni D, Ravasi M, Pasini S, Nicolini G, Bossi M, Miloso M, Cavaletti G, Tredici G (2009) Role of MAPKs in platinum-induced neuronal apoptosis. Neurotoxicology 30:312-319.

Seidler S, Zimmermann HW, Bartneck M, Trautwein C, Tacke F (2010) Age-dependent alterations of monocyte subsets and monocyte-related chemokine pathways in healthy adults. BMC Immunol 11:30.

Seltzer Z, Dubner R, Shir Y (1990) A novel behavioral model of neuropathic pain disorders produced in rats by partial sciatic nerve injury. Pain 43:205-218.

Serbina NV, Pamer EG (2006) Monocyte emigration from bone marrow during bacterial infection requires signals mediated by chemokine receptor CCR2. Nat Immunol 7:311-317.

Seung LP, Rowley DA, Dubey P, Schreiber H (1995) Synergy between T-cell immunity and inhibition of paracrine stimulation causes tumor rejection. Proc Natl Acad Sci U S A 92:6254-6258.

Seybold VS, McCarson KE, Mermelstein PG, Groth RD, Abrahams LG (2003) Calcitonin gene-related peptide regulates expression of neurokinin1 receptors by rat spinal neurons. J Neurosci 23:1816-1824.

Shan S, Hong-Min T, Yi F, Jun-Peng G, Yue F, Yan-Hong T, Yun-Ke Y, Wen-Wei L, Xiang-Yu W, Jun M, Guo-Hua W, Ya-Ling H, Hua-Wei L, Ding-Fang C (2011) New evidences for fractalkine/CX3CL1 involved in substantia nigral microglial activation and behavioral changes in a rat model of Parkinson's disease. Neurobiol Aging 32:443-458.

Shinohara A, Kutsukake M, Takahashi M, Kyo S, Tachikawa E, Tamura K (2012) Protease-activated receptor-stimulated interleukin-6 expression in endometriosis-like lesions in an experimental mouse model of endometriosis. J Pharmacol Sci 119:40-51.

Shirahama M, Ushio S, Egashira N, Yamamoto S, Sada H, Masuguchi K, Kawashiri T, Oishi R (2012) Inhibition of Ca2+/calmodulin-dependent protein kinase II reverses oxaliplatin-induced mechanical allodynia in rats. Mol Pain 8:26.

Siau C, Xiao W, Bennett GJ (2006) Paclitaxel- and vincristine-evoked painful peripheral neuropathies: loss of epidermal innervation and activation of Langerhans cells. Exp Neurol 201:507-514.

Sica A, Bronte V (2007) Altered macrophage differentiation and immune dysfunction in tumor development. J Clin Invest 117:1155-1166.

Sima AA (2007) Acetyl-L-carnitine in diabetic polyneuropathy: experimental and clinical data. CNS Drugs 21 Suppl 1:13-23.

Simpson DM, Brown S, Tobias J (2008) Controlled trial of high-concentration capsaicin patch for treatment of painful HIV neuropathy. Neurology 70:2305-2313.

Smith EM, Pang H, Cirrincione C, Fleishman S, Paskett ED, Ahles T, Bressler LR, Fadul CE, Knox C, Le-Lindqwister N, Gilman PB, Shapiro CL (2013) Effect of duloxetine on pain, function, and quality of life among patients with chemotherapy-induced painful peripheral neuropathy: a randomized clinical trial. JAMA 309:1359-1367.

Sommer C, Schafers M (1998) Painful mononeuropathy in C57BL/Wld mice with delayed wallerian degeneration: differential effects of cytokine production and nerve regeneration on thermal and mechanical hypersensitivity. Brain Res 784:154-162.

Song KH, Park J, Park JH, Natarajan R, Ha H (2013) Fractalkine and its receptor mediate extracellular matrix accumulation in diabetic nephropathy in mice. Diabetologia 56:1661-1669.

Sorge RE, Lacroix-Fralish ML, Tuttle AH, Sotocinal SG, Austin JS, Ritchie J, Chanda ML, Graham AC, Topham L, Beggs S, Salter MW, Mogil JS (2011) Spinal cord Toll-like receptor 4 mediates inflammatory and neuropathic hypersensitivity in male but not female mice. J Neurosci 31:15450-15454.

Souza GR, Talbot J, Lotufo CM, Cunha FQ, Cunha TM, Ferreira SH (2013) Fractalkine mediates inflammatory pain through activation of satellite glial cells. Proc Natl Acad Sci U S A 110:11193-11198.

Spike RC, Puskar Z, Andrew D, Todd AJ (2003) A quantitative and morphological study of projection neurons in lamina I of the rat lumbar spinal cord. Eur J Neurosci 18:2433-2448.

Staniland AA, Clark AK, Wodarski R, Sasso O, Maione F, D'Acquisto F, Malcangio M (2010) Reduced inflammatory and neuropathic pain and decreased spinal microglial response in fractalkine receptor (CX3CR1) knockout mice. J Neurochem 114:1143-1157.

Starkweather A (2010) Increased interleukin-6 activity associated with painful chemotherapy-induced peripheral neuropathy in women after breast cancer treatment. Nurs Res Pract 2010:281531.

Stephens TC, Currie GA, Peacock JH (1978) Repopulation of gamma-irradiated Lewis lung carcinoma by malignant cells and host macrophage progenitors. Br J Cancer 38:573-582.

Stewart M, Thiel M, Hogg N (1995) Leukocyte integrins. Curr Opin Cell Biol 7:690-696.

Story GM, Peier AM, Reeve AJ, Eid SR, Mosbacher J, Hricik TR, Earley TJ, Hergarden AC, Andersson DA, Hwang SW, McIntyre P, Jegla T, Bevan S, Patapoutian A (2003) ANKTM1, a TRP-like channel expressed in nociceptive neurons, is activated by cold temperatures. Cell 112:819-829.

Strasser F, Demmer R, Bohme C, Schmitz SF, Thuerlimann B, Cerny T, Gillessen S (2008) Prevention of docetaxel- or paclitaxel-associated taste alterations in cancer patients with oral glutamine: a randomized, placebo-controlled, double-blind study. Oncologist 13:337-346.

Streng T, Axelsson HE, Hedlund P, Andersson DA, Jordt SE, Bevan S, Andersson KE, Hogestatt ED, Zygmunt PM (2008) Distribution and function of the hydrogen sulfide-sensitive TRPA1 ion channel in rat urinary bladder. Eur Urol 53:391-399.

Stucky CL, Dubin AE, Jeske NA, Malin SA, McKemy DD, Story GM (2009) Roles of transient receptor potential channels in pain. Brain Res Rev 60:2-23.

Subbarao KV, Stolzenburg JU, Hertz L (1995) Pharmacological characteristics of potassium-induced, glycogenolysis in astrocytes. Neurosci Lett 196:45-48.

Sumpio BE, Riley JT, Dardik A (2002) Cells in focus: endothelial cell. Int J Biochem Cell Biol 34:1508-1512.

Sun JL, Xiao C, Lu B, Zhang J, Yuan XZ, Chen W, Yu LN, Zhang FJ, Chen G, Yan M (2013) CX3CL1/CX3CR1 regulates nerve injury-induced pain hypersensitivity through the ERK5 signaling pathway. J Neurosci Res 91:545-553.

Sun RQ, Lawand NB, Willis WD (2003) The role of calcitonin gene-related peptide (CGRP) in the generation and maintenance of mechanical allodynia and hyperalgesia in rats after intradermal injection of capsaicin. Pain 104:201-208.

Sun S, Cao H, Han M, Li TT, Pan HL, Zhao ZQ, Zhang YQ (2007) New evidence for the involvement of spinal fractalkine receptor in pain facilitation and spinal glial activation in rat model of monoarthritis. Pain 129:64-75.

Sung B, Lim G, Mao J (2003) Altered expression and uptake activity of spinal glutamate transporters after nerve injury contribute to the pathogenesis of neuropathic pain in rats. J Neurosci 23:2899-2910.

Suter MR, Berta T, Gao YJ, Decosterd I, Ji RR (2009) Large A-fiber activity is required for microglial proliferation and p38 MAPK activation in the spinal cord: different effects of resiniferatoxin and bupivacaine on spinal microglial changes after spared nerve injury. Mol Pain 5:53.

Svensson CI, Zattoni M, Serhan CN (2007) Lipoxins and aspirin-triggered lipoxin inhibit inflammatory pain processing. J Exp Med 204:245-252.

Svoboda GH (1958) A note on several new alkaloids from Vinca rosea Linn. I. Leurosine, virosine, perivine. J Am Pharm Assoc Am Pharm Assoc (Baltim) 47:834.

Svoboda GH, Johnson IS, Gorman M, Neuss N (1962) Current status of research on the alkaloids of Vinca rosea Linn. (Catharanthus roseus G. Don). J Pharm Sci 51:707-720.

Sweet MJ, Hume DA (2003) CSF-1 as a regulator of macrophage activation and immune responses. Arch Immunol Ther Exp (Warsz) 51:169-177.

Sweitzer SM, Colburn RW, Rutkowski M, DeLeo JA (1999) Acute peripheral inflammation induces moderate glial activation and spinal IL-1beta expression that correlates with pain behavior in the rat. Brain Res 829:209-221.

Sweitzer SM, Pahl JL, DeLeo JA (2006) Propentofylline attenuates vincristine-induced peripheral neuropathy in the rat. Neurosci Lett 400:258-261.

Sweitzer SM, Schubert P, DeLeo JA (2001) Propentofylline, a glial modulating agent, exhibits antiallodynic properties in a rat model of neuropathic pain. J Pharmacol Exp Ther 297:1210-1217.

Ta LE, Bieber AJ, Carlton SM, Loprinzi CL, Low PA, Windebank AJ (2010) Transient Receptor Potential Vanilloid 1 is essential for cisplatin-induced heat hyperalgesia in mice. Mol Pain 6:15.

Tack J (2011) Current and future therapies for chronic constipation. Best Pract Res Clin Gastroenterol 25:151-158.

Takahashi N, Mizuno Y, Kozai D, Yamamoto S, Kiyonaka S, Shibata T, Uchida K, Mori Y (2008) Molecular characterization of TRPA1 channel activation by cysteine-reactive inflammatory mediators. Channels (Austin) 2:287-298.

Takano Y, Okudaira M, Harmon BV (1993) Apoptosis induced by microtubule disrupting drugs in cultured human lymphoma cells. Inhibitory effects of phorbol ester and zinc sulphate. Pathol Res Pract 189:197-203.

Takeda M, Kitagawa J, Takahashi M, Matsumoto S (2008) Activation of interleukin-1beta receptor suppresses the voltage-gated potassium currents in the small-diameter trigeminal ganglion neurons following peripheral inflammation. Pain 139:594-602.

Takeda M, Tanimoto T, Ikeda M, Nasu M, Kadoi J, Yoshida S, Matsumoto S (2006) Enhanced excitability of rat trigeminal root ganglion neurons via decrease in A-type potassium currents following temporomandibular joint inflammation. Neuroscience 138:621-630.

Tanabe Y, Hashimoto K, Shimizu C, Hirakawa A, Harano K, Yunokawa M, Yonemori K, Katsumata N, Tamura K, Ando M, Kinoshita T, Fujiwara Y (2013) Paclitaxel-induced peripheral neuropathy in patients receiving adjuvant chemotherapy for breast cancer. Int J Clin Oncol 18:132-138.

Tanga FY, Nutile-McMenemy N, DeLeo JA (2005) The CNS role of Toll-like receptor 4 in innate neuroimmunity and painful neuropathy. Proc Natl Acad Sci U S A 102:5856-5861.

Tanga FY, Raghavendra V, DeLeo JA (2004) Quantitative real-time RT-PCR assessment of spinal microglial and astrocytic activation markers in a rat model of neuropathic pain. Neurochem Int 45:397-407.

Tanner KD, Reichling DB, Gear RW, Paul SM, Levine JD (2003) Altered temporal pattern of evoked afferent activity in a rat model of vincristine-induced painful peripheral neuropathy. Neuroscience 118:809-817.

Tao YX (2012) AMPA receptor trafficking in inflammation-induced dorsal horn central sensitization. Neurosci Bull 28:111-120.

Tarozzo G, Bortolazzi S, Crochemore C, Chen SC, Lira AS, Abrams JS, Beltramo M (2003) Fractalkine protein localization and gene expression in mouse brain. J Neurosci Res 73:81-88.

Tarrant TK, Liu P, Rampersad RR, Esserman D, Rothlein LR, Timoshchenko RG, McGinnis MW, Fitzhugh DJ, Patel DD, Fong AM (2012) Decreased Th17 and antigen-specific humoral responses in CX(3) CR1-deficient mice in the collagen-induced arthritis model. Arthritis Rheum 64:1379-1387.

Tatsushima Y, Egashira N, Kawashiri T, Mihara Y, Yano T, Mishima K, Oishi R (2011) Involvement of substance P in peripheral neuropathy induced by paclitaxel but not oxaliplatin. J Pharmacol Exp Ther 337:226-235.

Tatsushima Y, Egashira N, Narishige Y, Fukui S, Kawashiri T, Yamauchi Y, Oishi R (2013) Calcium channel blockers reduce oxaliplatin-induced acute neuropathy: a retrospective study of 69 male patients receiving modified FOLFOX6 therapy. Biomed Pharmacother 67:39-42.

Tawfik VL, Nutile-McMenemy N, Lacroix-Fralish ML, DeLeo JA (2007) Efficacy of propentofylline, a glial modulating agent, on existing mechanical allodynia following peripheral nerve injury. Brain Behav Immun 21:238-246.

Tawfik VL, Regan MR, Haenggeli C, Lacroix-Fralish ML, Nutile-McMenemy N, Perez N, Rothstein JD, DeLeo JA (2008) Propentofylline-induced astrocyte modulation leads to alterations in glial glutamate promoter activation following spinal nerve transection. Neuroscience 152:1086-1092.

Tenorio G, Kulkarni A, Kerr BJ (2013) Resident glial cell activation in response to perispinal inflammation leads to acute changes in nociceptive sensitivity: implications for the generation of neuropathic pain. Pain 154:71-81.

Tenscher K, Metzner B, Hofmann C, Schopf E, Norgauer J (1997) The monocyte chemotactic protein-4 induces oxygen radical production, actin reorganization, and CD11b up-regulation via a pertussis toxin-sensitive G-protein in human eosinophils. Biochem Biophys Res Commun 240:32-35.

Thacker MA, Clark AK, Bishop T, Grist J, Yip PK, Moon LD, Thompson SW, Marchand F, McMahon SB (2009) CCL2 is a key mediator of microglia activation in neuropathic pain states. Eur J Pain 13:263-272.

Thacker MA, Clark AK, Marchand F, McMahon SB (2007) Pathophysiology of peripheral neuropathic pain: immune cells and molecules. Anesth Analg 105:838-847.

Thibault K, Elisabeth B, Sophie D, Claude FZ, Bernard R, Bernard C (2008) Antinociceptive and anti-allodynic effects of oral PL37, a complete inhibitor of enkephalin-catabolizing enzymes, in a rat model of peripheral neuropathic pain induced by vincristine. Eur J Pharmacol 600:71-77.

Tikka TM, Koistinaho JE (2001) Minocycline provides neuroprotection against N-methyl-D-aspartate neurotoxicity by inhibiting microglia. J Immunol 166:7527-7533.

Tillu DV, Gebhart GF, Sluka KA (2008) Descending facilitatory pathways from the RVM initiate and maintain bilateral hyperalgesia after muscle insult. Pain 136:331-339.

Tochinai R, Ando M, Suzuki T, Suzuki K, Nagata Y, Hata C, Uchida K, Kobayashi T, Kado S, Kaneko K (2013) Histopathological studies of microtubule disassembling agent-induced myocardial lesions in rats. Exp Toxicol Pathol 65:737-743.

Todd AJ (2002) Anatomy of primary afferents and projection neurones in the rat spinal dorsal horn with particular emphasis on substance P and the neurokinin 1 receptor. Exp Physiol 87:245-249.

Todd AJ (2010) Neuronal circuitry for pain processing in the dorsal horn. Nat Rev Neurosci 11:823-836.

Todd AJ, McGill MM, Shehab SA (2000) Neurokinin 1 receptor expression by neurons in laminae I, III and IV of the rat spinal dorsal horn that project to the brainstem. Eur J Neurosci 12:689-700.

Todd AJ, Sullivan AC (1990) Light microscope study of the coexistence of GABA-like and glycine-like immunoreactivities in the spinal cord of the rat. J Comp Neurol 296:496-505.

Todd AJ, Watt C, Spike RC, Sieghart W (1996) Colocalization of GABA, glycine, and their receptors at synapses in the rat spinal cord. J Neurosci 16:974-982.

Todorovic SM, Jevtovic-Todorovic V (2007) Regulation of T-type calcium channels in the peripheral pain pathway. Channels (Austin) 1:238-245.

Tofaris GK, Patterson PH, Jessen KR, Mirsky R (2002) Denervated Schwann cells attract macrophages by secretion of leukemia inhibitory factor (LIF) and monocyte chemoattractant protein-1 in a process regulated by interleukin-6 and LIF. J Neurosci 22:6696-6703.

Tofthagen C (2010) Patient perceptions associated with chemotherapy-induced peripheral neuropathy. Clin J Oncol Nurs 14:E22-E28.

Tong N, Perry SW, Zhang Q, James HJ, Guo H, Brooks A, Bal H, Kinnear SA, Fine S, Epstein LG, Dairaghi D, Schall TJ, Gendelman HE, Dewhurst S, Sharer LR, Gelbard HA (2000) Neuronal fractalkine expression in HIV-1 encephalitis: roles for macrophage recruitment and neuroprotection in the central nervous system. J Immunol 164:1333-1339.

Tonia T, Mettler A, Robert N, Schwarzer G, Seidenfeld J, Weingart O, Hyde C, Engert A, Bohlius J (2012) Erythropoietin or darbepoetin for patients with cancer. Cochrane Database Syst Rev 12:CD003407.

Topp KS, Tanner KD, Levine JD (2000) Damage to the cytoskeleton of large diameter sensory neurons and myelinated axons in vincristine-induced painful peripheral neuropathy in the rat. J Comp Neurol 424:563-576.

Tracey I, Mantyh PW (2007) The cerebral signature for pain perception and its modulation. Neuron 55:377-391.

Trevisan G, Materazzi S, Fusi C, Altomare A, Aldini G, Lodovici M, Patacchini R, Geppetti P, Nassini R (2013) Novel Therapeutic Strategy to Prevent Chemotherapy-Induced Persistent Sensory Neuropathy By TRPA1 Blockade. Cancer Res.

Trombetta ES, Mellman I (2005) Cell biology of antigen processing in vitro and in vivo. Annu Rev Immunol 23:975-1028.

Tsakiri N, Kimber I, Rothwell NJ, Pinteaux E (2008) Interleukin-1-induced interleukin-6 synthesis is mediated by the neutral sphingomyelinase/Src kinase pathway in neurones. Br J Pharmacol 153:775-783.

Tsantoulas C, Zhu L, Shaifta Y, Grist J, Ward JP, Raouf R, Michael GJ, McMahon SB (2012) Sensory neuron downregulation of the Kv9.1 potassium channel subunit mediates neuropathic pain following nerve injury. J Neurosci 32:17502-17513.

Tsou CL, Haskell CA, Charo IF (2001) Tumor necrosis factor-alpha-converting enzyme mediates the inducible cleavage of fractalkine. J Biol Chem 276:44622-44626.

Tsuda M, Masuda T, Kitano J, Shimoyama H, Tozaki-Saitoh H, Inoue K (2009) IFN-gamma receptor signaling mediates spinal microglia activation driving neuropathic pain. Proc Natl Acad Sci U S A 106:8032-8037.

Tsuda M, Mizokoshi A, Shigemoto-Mogami Y, Koizumi S, Inoue K (2004) Activation of p38 mitogen-activated protein kinase in spinal hyperactive microglia contributes to pain hypersensitivity following peripheral nerve injury. Glia 45:89-95.

Tsuda M, Shigemoto-Mogami Y, Koizumi S, Mizokoshi A, Kohsaka S, Salter MW, Inoue K (2003) P2X4 receptors induced in spinal microglia gate tactile allodynia after nerve injury. Nature 424:778-783.

Tsuda M, Ueno H, Kataoka A, Tozaki-Saitoh H, Inoue K (2008) Activation of dorsal horn microglia contributes to diabetes-induced tactile allodynia via extracellular signal-regulated protein kinase signaling. Glia 56:378-386.

Tsujino H, Kondo E, Fukuoka T, Dai Y, Tokunaga A, Miki K, Yonenobu K, Ochi T, Noguchi K (2000) Activating transcription factor 3 (ATF3) induction by axotomy in sensory and motoneurons: A novel neuronal marker of nerve injury. Mol Cell Neurosci 15:170-182.

Tumati S, Largent-Milnes TM, Keresztes A, Ren J, Roeske WR, Vanderah TW, Varga EV (2012) Repeated morphine treatment-mediated hyperalgesia, allodynia and spinal glial activation are blocked by co-administration of a selective cannabinoid receptor type-2 agonist. J Neuroimmunol 244:23-31.

Turnsek T, Kregar I, Lebez D (1975) Acid sulphydryl protease from calf lymph nodes. Biochim Biophys Acta 403:514-520.

Uceyler N, Kobsar I, Biko L, Ulzheimer J, Levinson SR, Martini R, Sommer C (2006) Heterozygous P0 deficiency protects mice from vincristine-induced polyneuropathy. J Neurosci Res 84:37-46.

Uchida M, Ito T, Nakamura T, Igarashi H, Oono T, Fujimori N, Kawabe K, Suzuki K, Jensen RT, Takayanagi R (2013) ERK pathway and sheddases play an essential role in ethanol-induced CX3CL1 release in pancreatic stellate cells. Lab Invest 93:41-53.

Uno Y, Horii A, Uno A, Fuse Y, Fukushima M, Doi K, Kubo T (2002) Quantitative changes in mRNA expression of glutamate receptors in the rat peripheral and central vestibular systems following hypergravity. J Neurochem 81:1308-1317.

Urano H, Ara T, Fujinami Y, Hiraoka BY (2012) Aberrant TRPV1 expression in heat hyperalgesia associated with trigeminal neuropathic pain. Int J Med Sci 9:690-697.

Vallejo R, Tilley D, Vogel L, Benyamin R (2010) The role of glia and the immune system in the development and maintenance of neuropathic pain. Pain Practice 10:167-184.

van Lent PL, Holthuysen AE, van den Bersselaar LA, Van RN, Joosten LA, van de Loo FA, van de Putte LB, van den Berg WB (1996) Phagocytic lining cells determine local expression of inflammation in type II collagen-induced arthritis. Arthritis Rheum 39:1545-1555.

Van RN, Sanders A (1994) Liposome mediated depletion of macrophages: mechanism of action, preparation of liposomes and applications. J Immunol Methods 174:83-93.

Van RN, van Kesteren-Hendrikx E (2002) Clodronate liposomes: perspectives in research and therapeutics. J Liposome Res 12:81-94.

Vaporciyan AA, DeLisser HM, Yan HC, Mendiguren II, Thom SR, Jones ML, Ward PA, Albelda SM (1993) Involvement of platelet-endothelial cell adhesion molecule-1 in neutrophil recruitment in vivo. Science 262:1580-1582.

Venkatachalam K, Montell C (2007) TRP channels. Annu Rev Biochem 76:387-417.

Verge GM, Milligan ED, Maier SF, Watkins LR, Naeve GS, Foster AC (2004) Fractalkine (CX3CL1) and fractalkine receptor (CX3CR1) distribution in spinal cord and dorsal root ganglia under basal and neuropathic pain conditions. Eur J Neurosci 20:1150-1160.

Verge VM, Richardson PM, Wiesenfeld-Hallin Z, Hokfelt T (1995) Differential influence of nerve growth factor on neuropeptide expression in vivo: a novel role in peptide suppression in adult sensory neurons. J Neurosci 15:2081-2096.

Verheul HM, Pinedo HM (2007) Possible molecular mechanisms involved in the toxicity of angiogenesis inhibition. Nat Rev Cancer 7:475-485.

Viana-Cardoso KV, da Silva MT, Junior RC, Peixoto Junior AA, Pinho LG, Santos AA, Ribeiro RA, Rola FH, Gondim FA (2011) Repeated cisplatin treatments inhibit gastrointestinal motility and induces baroreflex changes and mechanical hyperalgesia in rats. Cancer Invest 29:494-500.

Viisanen H, Pertovaara A (2007) Influence of peripheral nerve injury on response properties of locus coeruleus neurons and coeruleospinal antinociception in the rat. Neuroscience 146:1785-1794.

Vilceanu D, Honore P, Hogan QH, Stucky CL (2010) Spinal nerve ligation in mouse upregulates TRPV1 heat function in injured IB4-positive nociceptors. J Pain 11:588-599.

Vinegar R, Truax JF, Selph JL (1976) Quantitative comparison of the analgesic and anti-inflammatory activities of aspirin, phenacetin and acetaminophen in rodents. Eur J Pharmacol 37:23-30.

Visentin GP, Liu CY (2007) Drug-induced thrombocytopenia. Hematol Oncol Clin North Am 21:685-96, vi.

Volterra A, Meldolesi J (2005) Astrocytes, from brain glue to communication elements: the revolution continues. Nat Rev Neurosci 6:626-640.

von Hehn CA, Baron R, Woolf CJ (2012) Deconstructing the neuropathic pain phenotype to reveal neural mechanisms. Neuron 73:638-652.

Vondracek P, Oslejskova H, Kepak T, Mazanek P, Sterba J, Rysava M, Gal P (2009) Efficacy of pregabalin in neuropathic pain in paediatric oncological patients. Eur J Paediatr Neurol 13:332-336.

Vulchanova L, Riedl MS, Shuster SJ, Stone LS, Hargreaves KM, Buell G, Surprenant A, North RA, Elde R (1998) P2X3 is expressed by DRG neurons that terminate in inner lamina II. Eur J Neurosci 10:3470-3478.

Wafai L, Taher M, Jovanovska V, Bornstein JC, Dass CR, Nurgali K (2013) Effects of oxaliplatin on mouse myenteric neurons and colonic motility. Front Neurosci 7:30.

Wagner R, Myers RR (1996) Schwann cells produce tumor necrosis factor alpha: expression in injured and non-injured nerves. Neuroscience 73:625-629.

Wallraff A, Kohling R, Heinemann U, Theis M, Willecke K, Steinhauser C (2006) The impact of astrocytic gap junctional coupling on potassium buffering in the hippocampus. J Neurosci 26:5438-5447.

Wang S, Dangerfield JP, Young RE, Nourshargh S (2005) PECAM-1, alpha6 integrins and neutrophil elastase cooperate in mediating neutrophil transmigration. J Cell Sci 118:2067-2076.

Wang S, Song L, Tan Y, Ma Y, Tian Y, Jin X, Lim G, Zhang S, Chen L, Mao J (2012) A functional relationship between trigeminal astroglial activation and NR1 expression in a rat model of temporomandibular joint inflammation. Pain Med 13:1590-1600.

Wang W, Wang W, Wang Y, Huang J, Wu S, Li YQ (2008) Temporal changes of astrocyte activation and glutamate transporter-1 expression in the spinal cord after spinal nerve ligation-induced neuropathic pain. Anat Rec (Hoboken) 291:513-518.

Wang WS, Lin JK, Lin TC, Chen WS, Jiang JK, Wang HS, Chiou TJ, Liu JH, Yen CC, Chen PM (2007) Oral glutamine is effective for preventing oxaliplatin-induced neuropathy in colorectal cancer patients. Oncologist 12:312-319.

Warwick RA, Hanani M (2013) The contribution of satellite glial cells to chemotherapy-induced neuropathic pain. Eur J Pain 17:571-580.

Watabiki T, Kiso T, Kuramochi T, Yonezawa K, Tsuji N, Kohara A, Kakimoto S, Aoki T, Matsuoka N (2011) Amelioration of neuropathic pain by novel transient receptor potential vanilloid 1 antagonist AS1928370 in rats without hyperthermic effect. J Pharmacol Exp Ther 336:743-750.

Watkins LR, Martin D, Ulrich P, Tracey KJ, Maier SF (1997) Evidence for the involvement of spinal cord glia in subcutaneous formalin induced hyperalgesia in the rat. Pain 71:225-235.

Weber KS, von HP, Clark-Lewis I, Weber PC, Weber C (1999) Differential immobilization and hierarchical involvement of chemokines in monocyte arrest and transmigration on inflamed endothelium in shear flow. Eur J Immunol 29:700-712.

Wei XH, Na XD, Liao GJ, Chen QY, Cui Y, Chen FY, Li YY, Zang Y, Liu XG (2013) The up-regulation of IL-6 in DRG and spinal dorsal horn contributes to neuropathic pain following L5 ventral root transection. Exp Neurol 241:159-168.

Weller K, Reeh PW, Sauer SK (2011) TRPV1, TRPA1, and CB1 in the isolated vagus nerve--axonal chemosensitivity and control of neuropeptide release. Neuropeptides 45:391-400.

Wen F, Zhou Y, Wang W, Hu QC, Liu YT, Zhang PF, Du ZD, Dai J, Li Q (2013) Ca/Mg infusions for the prevention of oxaliplatin-related neurotoxicity in patients with colorectal cancer: a meta-analysis. Ann Oncol 24:171-178.

Wen YR, Suter MR, Kawasaki Y, Huang J, Pertin M, Kohno T, Berde CB, Decosterd I, Ji RR (2007) Nerve conduction blockade in the sciatic nerve prevents but does not reverse the activation of p38 mitogen-activated protein kinase in spinal microglia in the rat spared nerve injury model. Anesthesiology 107:312-321.

Weng HR, Chen JH, Cata JP (2006) Inhibition of glutamate uptake in the spinal cord induces hyperalgesia and increased responses of spinal dorsal horn neurons to peripheral afferent stimulation. Neuroscience 138:1351-1360.

Weyerbacher AR, Xu Q, Tamasdan C, Shin SJ, Inturrisi CE (2010) N-Methyl-D-aspartate receptor (NMDAR) independent maintenance of inflammatory pain. Pain 148:237-246.

Weyrich AS, McIntyre TM, McEver RP, Prescott SM, Zimmerman GA (1995) Monocyte tethering by P-selectin regulates monocyte chemotactic protein-1 and tumor necrosis factor-alpha secretion. Signal integration and NF-kappa B translocation. J Clin Invest 95:2297-2303.

Whitaker-Azmitia PM, Raio M, Raio D, Borella A (1995) A 5-HT3 receptor antagonist fails to prevent cisplatin-induced toxicity in immature rat spinal cord. Eur J Pharmacol 275:139-143.

Wickham R (2012) Evolving treatment paradigms for chemotherapy-induced nausea and vomiting. Cancer Control 19:3-9.

Wilson RH, Lehky T, Thomas RR, Quinn MG, Floeter MK, Grem JL (2002) Acute oxaliplatin-induced peripheral nerve hyperexcitability. J Clin Oncol 20:1767-1774.

Windebank AJ, Grisold W (2008) Chemotherapy-induced neuropathy. J Peripher Nerv Syst 13:27-46.

Witko-Sarsat V, Rieu P, Descamps-Latscha B, Lesavre P, Halbwachs-Mecarelli L (2000) Neutrophils: molecules, functions and pathophysiological aspects. Lab Invest 80:617-653.

Wodarski R, Clark AK, Grist J, Marchand F, Malcangio M (2009) Gabapentin reverses microglial activation in the spinal cord of streptozotocin-induced diabetic rats. Eur J Pain 13:807-811.

Won HH, Lee J, Park JO, Park YS, Lim HY, Kang WK, Kim JW, Lee SY, Park SH (2012) Polymorphic markers associated with severe oxaliplatin-induced, chronic peripheral neuropathy in colon cancer patients. Cancer 118:2828-2836.

Wong BW, Wong D, McManus BM (2002) Characterization of fractalkine (CX3CL1) and CX3CR1 in human coronary arteries with native atherosclerosis, diabetes mellitus, and transplant vascular disease. Cardiovasc Pathol 11:332-338.

Wood JN, Boorman JP, Okuse K, Baker MD (2004) Voltage-gated sodium channels and pain pathways. J Neurobiol 61:55-71.

Woolf C, Wiesenfeld-Hallin Z (1986) Substance P and calcitonin gene-related peptide synergistically modulate the gain of the nociceptive flexor withdrawal reflex in the rat. Neurosci Lett 66:226-230.

Woolf CJ, Mannion RJ (1999) Neuropathic pain: aetiology, symptoms, mechanisms, and management. Lancet 353:1959-1964.

Woolf CJ, Salter MW (2000) Neuronal plasticity: increasing the gain in pain. Science 288:1765-1769.

Wotherspoon G, Fox A, McIntyre P, Colley S, Bevan S, Winter J (2005) Peripheral nerve injury induces cannabinoid receptor 2 protein expression in rat sensory neurons. Neuroscience 135:235-245.

Wozniak KM, Nomoto K, Lapidus RG, Wu Y, Carozzi V, Cavaletti G, Hayakawa K, Hosokawa S, Towle MJ, Littlefield BA, Slusher BS (2011) Comparison of neuropathy-inducing effects of eribulin mesylate, paclitaxel, and ixabepilone in mice. Cancer Res 71:3952-3962.

Wuarin-Bierman L, Zahnd GR, Kaufmann F, Burcklen L, Adler J (1987) Hyperalgesia in spontaneous and experimental animal models of diabetic neuropathy. Diabetologia 30:653-658.

Wyckoff J, Wang W, Lin EY, Wang Y, Pixley F, Stanley ER, Graf T, Pollard JW, Segall J, Condeelis J (2004) A paracrine loop between tumor cells and macrophages is required for tumor cell migration in mammary tumors. Cancer Res 64:7022-7029.

Wyckoff JB, Wang Y, Lin EY, Li JF, Goswami S, Stanley ER, Segall JE, Pollard JW, Condeelis J (2007) Direct visualization of macrophage-assisted tumor cell intravasation in mammary tumors. Cancer Res 67:2649-2656.

Xiao WH, Bennett GJ (2008) Chemotherapy-evoked neuropathic pain: Abnormal spontaneous discharge in A-fiber and C-fiber primary afferent neurons and its suppression by acetyl-L-carnitine. Pain 135:262-270.

Xiao WH, Bennett GJ (2012) Effects of mitochondrial poisons on the neuropathic pain produced by the chemotherapeutic agents, paclitaxel and oxaliplatin. Pain 153:704-709.

Xie JY, Herman DS, Stiller CO, Gardell LR, Ossipov MH, Lai J, Porreca F, Vanderah TW (2005) Cholecystokinin in the rostral ventromedial medulla mediates opioid-induced hyperalgesia and antinociceptive tolerance. J Neurosci 25:409-416.

Xin WJ, Weng HR, Dougherty PM (2009) Plasticity in expression of the glutamate transporters GLT-1 and GLAST in spinal dorsal horn glial cells following partial sciatic nerve ligation. Mol Pain 5:15.

Xu X, Wang Y, Chen J, Ma H, Shao Z, Chen H, Jin G (2012) High expression of CX3CL1/CX3CR1 axis predicts a poor prognosis of pancreatic ductal adenocarcinoma. J Gastrointest Surg 16:1493-1498.

Yanaga A, Goto H, Nakagawa T, Hikiami H, Shibahara N, Shimada Y (2006) Cinnamaldehyde induces endothelium-dependent and -independent vasorelaxant action on isolated rat aorta. Biol Pharm Bull 29:2415-2418.

Yang J, Li Y, Zuo X, Zhen Y, Yu Y, Gao L (2008) Transient receptor potential ankyrin-1 participates in visceral hyperalgesia following experimental colitis. Neurosci Lett 440:237-241.

Yang JL, Xu B, Li SS, Zhang WS, Xu H, Deng XM, Zhang YQ (2012) Gabapentin reduces CX3CL1 signaling and blocks spinal microglial activation in monoarthritic rats. Mol Brain 5:18.

Yang XP, Mattagajasingh S, Su S, Chen G, Cai Z, Fox-Talbot K, Irani K, Becker LC (2007) Fractalkine upregulates intercellular adhesion molecule-1 in endothelial cells through CX3CR1 and the Jak Stat5 pathway. Circ Res 101:1001-1008.

Yang Y, Wang Y, Li S, Xu Z, Li H, Ma L, Fan J, Bu D, Liu B, Fan Z, Wu G, Jin J, Ding B, Zhu X, Shen Y (2004) Mutations in SCN9A, encoding a sodium channel alpha subunit, in patients with primary erythermalgia. J Med Genet 41:171-174.

Yano R, Yamamura M, Sunahori K, Takasugi K, Yamana J, Kawashima M, Makino H (2007) Recruitment of CD16+ monocytes into synovial tissues is mediated by fractalkine and CX3CR1 in rheumatoid arthritis patients. Acta Med Okayama 61:89-98.

Yao K, Lu H, Huang R, Zhang S, Hong X, Shi H, Sun A, Qian J, Zou Y, Ge J (2011) Changes of dendritic cells and fractalkine in type 2 diabetic patients with unstable angina pectoris: a preliminary report. Cardiovasc Diabetol 10:50.

Yao X, Qi L, Chen X, Du J, Zhang Z, Liu S (2013) Expression of CX3CR1 associates with cellular migration, metastasis, and prognosis in human clear cell renal cell carcinoma?>. Urol Oncol.

Ye Z, Wimalawansa SJ, Westlund KN (1999) Receptor for calcitonin gene-related peptide: localization in the dorsal and ventral spinal cord. Neuroscience 92:1389-1397.

Yin Q, Cheng W, Cheng MY, Fan SZ, Shen W (2010) Intrathecal injection of anti-CX3CR1 neutralizing antibody delayed and attenuated pain facilitation in rat tibial bone cancer pain model. Behav Pharmacol 21:595-601.

Yona S, Kim KW, Wolf Y, Mildner A, Varol D, Breker M, Strauss-Ayali D, Viukov S, Guilliams M, Misharin A, Hume DA, Perlman H, Malissen B, Zelzer E, Jung S (2013) Fate mapping reveals origins and dynamics of monocytes and tissue macrophages under homeostasis. Immunity 38:79-91.

Yoon SY, Robinson CR, Zhang H, Dougherty PM (2013) Spinal astrocyte gap junctions contribute to oxaliplatin-induced mechanical hypersensitivity. J Pain 14:205-214.

Yoon YW, Na HS, Chung JM (1996) Contributions of injured and intact afferents to neuropathic pain in an experimental rat model. Pain 64:27-36.

Yoshimura M, Furue H (2006) Mechanisms for the anti-nociceptive actions of the descending noradrenergic and serotonergic systems in the spinal cord. J Pharmacol Sci 101:107-117.

Yoshimura M, Jessell T (1990) Amino acid-mediated EPSPs at primary afferent synapses with substantia gelatinosa neurones in the rat spinal cord. J Physiol 430:315-335.

Yu XH, Cao CQ, Martino G, Puma C, Morinville A, St-Onge S, Lessard E, Perkins MN, Laird JM (2010) A peripherally restricted cannabinoid receptor agonist produces robust anti-nociceptive effects in rodent models of inflammatory and neuropathic pain. Pain 151:337-344.

Zeisberger SM, Odermatt B, Marty C, Zehnder-Fjallman AH, Ballmer-Hofer K, Schwendener RA (2006) Clodronate-liposome-mediated depletion of tumour-associated macrophages: a new and highly effective antiangiogenic therapy approach. Br J Cancer 95:272-281.

Zervantonakis IK, Hughes-Alford SK, Charest JL, Condeelis JS, Gertler FB, Kamm RD (2012) Three-dimensional microfluidic model for tumor cell intravasation and endothelial barrier function. Proc Natl Acad Sci U S A 109:13515-13520.

Zeuner A, Signore M, Martinetti D, Bartucci M, Peschle C, De MR (2007) Chemotherapy-induced thrombocytopenia derives from the selective death of megakaryocyte progenitors and can be rescued by stem cell factor. Cancer Res 67:4767-4773.

Zhang GH, Lv MM, Wang S, Chen L, Qian NS, Tang Y, Zhang XD, Ren PC, Gao CJ, Sun XD, Xu LX (2011a) Spinal astrocytic activation is involved in a virally-induced rat model of neuropathic pain. PLoS One 6:e23059.

Zhang H, Boyette-Davis JA, Kosturakis AK, Li Y, Yoon SY, Walters ET, Dougherty PM (2013) Induction of Monocyte Chemoattractant Protein-1 (MCP-1) and Its Receptor CCR2 in Primary Sensory Neurons Contributes to Paclitaxel-Induced Peripheral Neuropathy. J Pain.

Zhang H, Yoon SY, Zhang H, Dougherty PM (2012) Evidence that spinal astrocytes but not microglia contribute to the pathogenesis of Paclitaxel-induced painful neuropathy. J Pain 13:293-303.

Zhang J, De KY (2006) Spatial and temporal relationship between monocyte chemoattractant protein-1 expression and spinal glial activation following peripheral nerve injury. J Neurochem 97:772-783.

Zhang J, Shi XQ, Echeverry S, Mogil JS, De KY, Rivest S (2007) Expression of CCR2 in both resident and bone marrow-derived microglia plays a critical role in neuropathic pain. J Neurosci 27:12396-12406.

Zhang J, Tuckett RP (2008) Comparison of paclitaxel and cisplatin effects on the slowly adapting type I mechanoreceptor. Brain Res 1214:50-57.

Zhang RX, Liu B, Li A, Wang L, Ren K, Qiao JT, Berman BM, Lao L (2008) Interleukin 1beta facilitates bone cancer pain in rats by enhancing NMDA receptor NR-1 subunit phosphorylation. Neuroscience 154:1533-1538.

Zhang X, Mosser DM (2008) Macrophage activation by endogenous danger signals. J Pathol 214:161-178.

Zhang X, Wang J, Zhou Q, Xu Y, Pu S, Wu J, Xue Y, Tian Y, Lu J, Jiang W, Du D (2011b) Brain-derived neurotrophic factor-activated astrocytes produce mechanical allodynia in neuropathic pain. Neuroscience 199:452-460.

Zhao T, Gao S, Wang X, Liu J, Duan Y, Yuan Z, Sheng J, Li S, Wang F, Yu M, Ren H, Hao J (2012) Hypoxia-inducible factor-1alpha regulates chemotactic migration of pancreatic ductal adenocarcinoma cells through directly transactivating the CX3CR1 gene. PLoS One 7:e43399.

Zheng H, Xiao WH, Bennett GJ (2011) Functional deficits in peripheral nerve mitochondria in rats with paclitaxel- and oxaliplatin-evoked painful peripheral neuropathy. Exp Neurol 232:154-161.

Zheng H, Xiao WH, Bennett GJ (2012) Mitotoxicity and bortezomib-induced chronic painful peripheral neuropathy. Exp Neurol 238:225-234.

Zhou J, Ding T, Pan W, Zhu LY, Li L, Zheng L (2009) Increased intratumoral regulatory T cells are related to intratumoral macrophages and poor prognosis in hepatocellular carcinoma patients. Int J Cancer 125:1640-1648.

Zhuang ZY, Gerner P, Woolf CJ, Ji RR (2005) ERK is sequentially activated in neurons, microglia, and astrocytes by spinal nerve ligation and contributes to mechanical allodynia in this neuropathic pain model. Pain 114:149-159.

Zhuang ZY, Kawasaki Y, Tan PH, Wen YR, Huang J, Ji RR (2007) Role of the CX3CR1/p38 MAPK pathway in spinal microglia for the development of neuropathic pain following nerve injury-induced cleavage of fractalkine. Brain Behav Immun 21:642-651.

Zhuang ZY, Wen YR, Zhang DR, Borsello T, Bonny C, Strichartz GR, Decosterd I, Ji RR (2006) A peptide c-Jun N-terminal kinase (JNK) inhibitor blocks mechanical allodynia after spinal nerve ligation: respective roles of JNK activation in primary sensory neurons and spinal astrocytes for neuropathic pain development and maintenance. J Neurosci 26:3551-3560.

Ziegler-Heitbrock HW, Fingerle G, Strobel M, Schraut W, Stelter F, Schutt C, Passlick B, Pforte A (1993) The novel subset of CD14+/CD16+ blood monocytes exhibits features of tissue macrophages. Eur J Immunol 23:2053-2058.

Zitvogel L, Tesniere A, Kroemer G (2006) Cancer despite immunosurveillance: immunoselection and immunosubversion. Nat Rev Immunol 6:715-727.

Zuo Y, Perkins NM, Tracey DJ, Geczy CL (2003) Inflammation and hyperalgesia induced by nerve injury in the rat: a key role of mast cells. Pain 105:467-479.

Zurborg S, Yurgionas B, Jira JA, Caspani O, Heppenstall PA (2007) Direct activation of the ion channel TRPA1 by Ca2+. Nat Neurosci 10:277-279.